Analyzing and Planning Urban Flood Resilience and Mitigation Strategies: The Case of Adama City, Ethiopia

By: Bikila Merga Leta

A Dissertation Submitted to the Graduate Programs Office of the Ethiopian Institute of Architecture, Building Construction and City Development, Addis Ababa University, for the Fulfillment of the Requirements for the Award of Doctor of Philosophy Degree in Urban and Regional Planning

Advisor: Dr. Dagnachew Adugna (Associate Professor)

Addis Ababa, Ethiopia

July 2024

DECLARATION

I hereby declare that this dissertation is the result of my original work and has not been submitted to any University/Institution for any degree or other purpose. All materials other than my ideas used in this study from other sources have been fully acknowledged and cited properly, following the scientific guidelines of Addis Ababa University.

Name: Bikila Merga Leta

Signature: _____________

Date: _________________

APPROVAL

As a member of the Examiners board of the PhD Dissertation open defense of Bikila Merga Leta, we have read and evaluated the Dissertation prepared by Bikila Merga Leta entitled "**Analyzing and Planning Urban Flood Resilience and Mitigation Strategies: The Case of Adama City, Ethiopia"** and recommended to Ethiopian Institute of Architecture, Building Construction and City Development, Addis Ababa University to accept the Dissertation as it meets the accepted standards to originality and quality for the fulfillment of requirements for the award of Doctor of Philosophy Degree in Urban and Regional Planning.

Board of Examiners:

Dr. Dagnachew Adugna (Associate Professor)	______________	______________
Advisor	**Signature**	**Date**
Prof. Molla Demlie (Professor)	______________	______________
External Examiner	**Signature**	**Date**
Dr. Agizew Nigussie (Associate Professor)	______________	______________
Internal Examiner	**Signature**	**Date**
Dr. Abunu Arega	______________	______________
Chair Person	**Signature**	**Date**
Dr. Dagnachew Adugna (Associate Professor)	______________	______________
Graduate Program Director	**Signature**	**Date**

ACKNOWLEDGMENTS

I would like to begin by expressing my heartfelt gratitude to my advisor, Dr. Dagnachew Adugna, for his unwavering academic support throughout my Ph.D. journey. His valuable time, continuous guidance, and objective feedback from the beginning of the research until the end have been truly inspiring. Without his astute advice and support, I cannot imagine this dissertation reaching its completion.

I would also like to extend my thanks to Prof. Molla Demlie from the University of Kwazulu-Natal and Dr. Agizew Nigussie from the Addis Ababa Institute of Technology for their valuable time and comments on my dissertation. I would like to express my gratitude for the support and insightful discussions from the academic staff at EiABC and AASTU, especially Dr. Solomon Benti, Dr. Alazar Assefa, Dr. Mulugeta Maru, Dr. Abunu Arega from EIABC, Dr. Mulugeta Admas, Dr. Mengistu Addis, Mr. Dawit Adbib, and Mr. Eliyas Bezabeh from AASTU throughout my Ph.D. dissertation study.

Furthermore, I would like to acknowledge the Adama city administration staff, especially Mr. Shimelis Regasa, for providing the necessary data relevant to my study.

Lastly, I am immensely grateful to my wife, Lidiya Kelbesa, and my daughters, Kenake and Melala, for their prayers, patience, and understanding during the highs and lows of my life.

May the almighty God bless you all.

ABSTRACT

This study was conducted in Adama, a rapidly urbanizing city in central Ethiopia which is known to be susceptible to flooding. The study area is located in a low-lying region surrounded by mountains, where frequent flash floods have had a detrimental impact on the local community's well-being. Consequently, this study sought to evaluate the extent of flood vulnerability and devise effective strategies for flood prevention. To achieve this, a Geographic Information System (GIS) approach incorporating multi-criteria decision-making (MCDM) and the analytical hierarchy process (AHP) was utilized to identify and map areas prone to flooding. Various factors, including proximity to drains, topographic wetness index (TWI), elevation, slope, precipitation, land use, normalized difference vegetation index (NDVI), distance from the river and road, drainage density, and soil composition, were Combined and analyzed. The results indicated that 98.69% of the study area faces a moderate to very high risk of flooding, with only 1.31% classified as low risk. The flood susceptibility map produced by the model aligned closely with data gathered from ground control points (GCPs), onsite field observations, Google Earth Satellite Imagery, expert insights, and local community reports. In addition, to characterize flood vulnerability, a Socio-Ecological-Technological Systems (SETS) framework was utilized. Where, each SETS domain identified clusters of flood-prone areas, highlighting the need for urgent adaptive measures to address flood vulnerability in the study area implying adopting holistic approaches to promote sustainable cities. Furthermore, to investigate flood-resistant neighborhoods, a comprehensive analysis of morphological analysis, local community responses, and expert insights was conducted. By considering the current spatial layout and morphology with urban flooding, the city can enhance its flood management strategies for the future. These findings have implications for other flood-prone neighborhoods in similar urban areas, highlighting the importance of spatial arrangement in mitigating urban flood vulnerability. Finally, to quantify and implement strategies for mitigating floods, researchers utilized the Integrated Valuation of Ecosystem Services and Tradeoffs Urban Flood Risk Mitigation (InVEST-UFRM) model as a tool to develop adaptation plans for addressing urban flooding. The InVEST-UFRM model offered a thorough insight into the city's flood situation by effectively analyzing urban watersheds and accurately representing flood risk. Running *the model four times with different rainfall scenarios based on an Intensity-Duration-Frequency curve specific to Adama revealed the impact of varying rainfall depths. In the first scenario, there is a moderate retention capacity of 10.76* m^3 *and a flood volume of 3.34* m^3*. In the second scenario, the retention capacity improved to 11.63* m^3 *with a flood volume of 4.15* m^3*. In the third scenario, there is a further enhancement in retention capacity to 12.21* m^3*, along with a flood volume of 4.76* m^3*. Finally, in the fourth scenario, the retention capacity continues to increase to 12.78* m^3*, with a flood volume of 5.40* m^3*. These simulations produced significant results on runoff retention and flood volume, highlighting the diverse capacities of micro-catchments in the study area to retain runoff and generate floods. The study also emphasized the InVEST-UFRM model's effectiveness in assessing the trade-offs linked to both structural and non-structural flood mitigation strategies. It underscored the significance of incorporating disciplines such as hydrology, remote sensing, geographic information systems, and natural capital assessment tools into urban planning strategies to enhance flood resilience and support sustainable urban development.*

Keywords: Adama, Flooding, Modeling flood, InVEST-UFRM model, Resilience, Social-ecological-technological Systems, Vulnerability.

TABLE OF CONTENTS PAGE

LIST OF TABLES

LIST OF FIGURES

LIST OF ACRONYM AND ABBREVIATIONS

ACA	Adama City Administration
AHP	Analytical Hierarchical Process
CN	Curve Number
CSA	Central Statistical Agency
DEM	Digital Elevation Model
GCP	Ground Control Points
IDF	Intensity-Duration-Frequency
OECD	Economic Co-operation and Development
GIS	Geographic Information System
HSG	Hydrological Soil Group
InVEST	Integrated Valuation of Ecosystem Services and Tradeoffs
LULC	Land use and Land cover
MCDA	Multi-Criteria Decision Analysis
NMA	National Meteorological Agency
NDVI	Normalized Differential Vegetation Index
SCS-CN	Soil Conservation Service Curve Number
SETS	Social-Ecological-Technological Systems
TWI	Topographic Wetness Index
UFRM	Urban Flood Risk Mitigation
USGS	United States Geological Survey
UNDRR	United Nations Office for Disaster Risk Reduction
WLRC	Water and Land Resource Center

LIST OF PAPERS

1. Published Articles

1.1. Leta, B. M., & Adugna, D. (2023). Identification and mapping of flood-prone areas using GIS-based multi-criteria decision-making and analytical hierarchy process: the case of Adama City's watershed, Ethiopia. *Applied Geomatics*, *15*(4), 933-955. https://doi.org/10.1007/s12518-023-00532-9.

1.2. Leta, B. M., & Adugna, D. (2023). Characterizing the level of urban Flood vulnerability using the social-ecological-technological systems framework, the case of Adama city, Ethiopia. *Heliyon*, *9*(10). https://doi.org/10.1016/j.heliyon.2023.e20723.

1.3. Leta, B. M., Adugna, D., & Wondim, A. A. (2024). Comprehensive investigation of flood-resilient neighborhoods: the case of Adama City, Ethiopia. *Applied Water Science*, *14*(2), 14. https://doi.org/10.1007/s13201-023-02053-7.

1.4. Leta, B. M., & Adugna, D. (2024). Quantifying flood risk using InVEST - UFRM model and mitigation strategies: the case of Adama City, Ethiopia. *Model. Earth Syst. Environ.* ***10****, 3257–3277.* https://doi.org/10.1007/s40808-024-01956-x.

Based on the Addis Ababa University ‘Guideline for Dissertation and Thesis Write-up’ (October 2021), this dissertation follows the paper-based Ph.D. dissertation write-up approach.

CHAPTER ONE: INTRODUCTION

1.1 Background of the study

Flooding is a natural occurrence that takes place frequently and extensively, resulting in widespread devastation to the lives, properties, and infrastructure of millions of people worldwide (Amirkhani et al., 2022; Das & Gupta, 2021; EM-DAT, 2015; Vojinovic et al., 2016). Over time, there has been a noticeable rise in both the frequency and intensity of flooding, leading to substantial consequences on the lives of millions of people, as well as on infrastructure and the environment (Das & Gupta, 2021; Hagos et al., 2022; Ozkan & Tarhan, 2016).

Recent studies (have) revealed that approximately 1.81 billion people, accounting for 23% of the global population, are exposed to considerable flood risk (McDermott, 2022; Rentschler et al., 2022). This alarming statistic is a result of various factors, including climate change and environmental degradation caused by inadequate land management (Quan et al., 2021; Wang et al., 2022b; Yue et al., 2021). With the increasing occurrence and severity of extreme weather phenomena such as heavy rainfall and storms, floods have emerged as a prevalent natural disaster globally and are expected to occur more frequently in the future.

The impacts of floods go beyond the physical destruction of infrastructure and property. They also pose a substantial threat to human health, well-being, and the economy, as well as causing harm to ecosystems (Ansah et al., 2020; Rentschler et al., 2022; Talbot et al., 2018). Floods result in more than $40 billion in economic damages every year worldwide (OECD, 2016). Additionally, it is projected that by 2050, an extra two billion people will be at risk of flood disasters (UNESCO, 2012).

From 2000 to 2018, the globe experienced 3798 instances of flash floods, leading to an estimated financial loss of 592 billion USD and causing the deaths of around 0.1 million individuals (NatCatSERVICE, 2020). In 2020 alone, floods across the world tragically took the lives of over six thousand people (Hamidifar & Nones, 2021). This highlights the significant consequences of floods on human lives and the urgent need for effective disaster management strategies.

Flooding can occur in various forms, including urban floods, coastal, and river floods (Balica et al., 2012; Re, 2012). Of these, urban flooding stands out as it is primarily caused by inadequate drainage systems in urban areas (Balica et al., 2012). Many factors contribute to urban floodings, such as increased impervious areas, changes in land cover, excessive urban sprawl, poor urban planning, and flood management (Abebe et al., 2018; Miller & Hutchins, 2017). The rapid growth of cities, changes in natural river channels due to human interventions, and heavy rainfall also play a significant role in urban flooding (Ahmadisharaf et al., 2016; Choubin et al., 2019).

Urban floods have become a significant global issue due to the combined factors of rapid urban growth and climate change (Bibi & Kara, 2023; Manandhar et al., 2023; Yang et al., 2021). The increasing urban population and expanding urbanization put a considerable strain on existing stormwater drain systems, aggravating the risk of flooding. Moreover, urban areas are more severely impacted by floods because of high population density, infrastructure, and properties (Rodríguez et al., 2017). The trends of urbanization further intensify the scale and frequency of floods, posing escalating hazards to communities (Kadaverugu et al., 2021; Konrad, 2003). An alarming issue is the nearly doubled amount of urbanized land situated in floodplains that have a 1 in 100-year chance of experiencing a flood since 1985(Andreadis et al., 2022). It is widely recognized that climate change and human activities, such as uncontrolled land use and land cover change, disrupting major natural drainage, are intensifying the frequency and severity of extreme flood events (Brief, 2021; Kreibich et al., 2015). Additionally, with the ongoing impact of global warming leading to higher sea levels and increasingly severe weather patterns, it is anticipated that the risks linked to floodplains will surge by around 45 percent by the end of the century (Denchak, 2019).

Cities located in flood-prone areas are at a heightened risk of flooding and are more prone to larger flood events due to the amplification of flood magnitudes (Dumedah et al., 2021; Rentschler et al., 2022). This is often due to urbanization in floodplain areas (Al-Zahrani, 2018; Nkwunonwo et al., 2020; Rafiq et al., 2016). As cities grow and populations increase, surface sealing also increases, leading to a rapid rise in surface runoff volume and velocity (Chang et al., 2021; Hemmati et al., 2021). This, combined with changes in land use and development in floodplain areas, can result in higher volume and a shorter time to peak (Feng et al., 2021; Gori et al., 2019; Xu & Zhao, 2016). In contrast, non-urban forested watersheds retain a substantial portion of storm rainfall, while urban watersheds lose most of it to runoff (Sheng & Wilson, 2009).

Various regions across the globe exhibit differing degrees of susceptibility to urban floods, with certain areas proving more exposed than others. The swift urban expansion witnessed in developing nations, notably in Asia and Africa, poses a substantial obstacle in effectively managing flood hazards (Duc, 2013; Kovacs et al., 2017; Wang et al., 2022b). Countries with lower and middle incomes are at risk from flood dangers due to the strong connection between flood vulnerability and poverty. These countries facing challenges with limited social services and insufficient infrastructure are home to 89% of the global population vulnerable to flooding (McDermott, 2022; Rentschler et al., 2022; Rentschler et al., 2022). Additionally, informal settlements in various southern hemisphere nations around the world face immense challenges that contribute to their vulnerability to flooding (Anwana & Owojori, 2023; Tietjen et al., 2023). These settlements frequently face challenges due to inadequate infrastructure, such as a lack of stormwater drain systems, making them more exposed to flooding (Gomez et al., 2023; Peters et al., 2022; Ramiaramanana & Teller, 2021). Conversely, properly designed and formal settlements that have effective drainage systems show lower susceptibility to flooding (Adegun, 2023; Samuel et al., 2019).

In Ethiopia, urban flooding has emerged as a significant problem due to several aspects such as poorly designed drainage systems, inadequate land use planning, absence of an early warning system, and insufficient coordination in flood disaster management efforts (Leta & Adugna, 2023a; Weday et al., 2023). The complexity and high cost involved in managing urban floods have further compounded the issue (Erena & Worku, 2018; Leta & Adugna, 2023a). While the Disaster Prevention and Preparedness Commission is responsible for addressing flood-related concerns, its lack of integration with other stakeholders impeded effective urban flood management practices. The consequences of these floods have been devastating, resulting in loss of lives, destruction of homes and crops, and damage to critical infrastructure such as bridges and roads (Legese et al., 2020). The disruption of the power supply has also hindered rescue efforts and made it challenging for affected individuals to assess the extent of the flood and rescue their belongings (Aryal et al., 2021). The increased frequency and intensity of flooding in the country can be attributed to climate change, which has led to heavy rains and unpredictable weather patterns (Perry et al., 2022). As a result, daily life has been severely disrupted, posing significant challenges for affected communities (Herslund et al., 2015; Leta & Adugna, 2023a).

According to the National Disaster Risk Management Commission (NDRMC, 2020), Ethiopia has twelve major river basins, with Adama City located in the Awash River Basin. This basin has a history of severe flooding, making it a threat to human lives and property compared to other natural disasters. Recent studies have emphasized the growing impact of floods in Adama City, as they affect more people, economic activities, and ecosystems (Erena & Worku, 2019; Grecu et al., 2017; Khan et al., 2021). Historical data shows that floods have caused more damage to Adama City than any other natural disaster (Bulti et al., 2017). Although the severity of flooding may vary over time, it remains the most substantial hazard for Adama City due to its susceptibility to inundation. In addition to direct impacts on property and infrastructure, floods also have indirect consequences that disrupt communities for extended periods. These include water contamination, loss of life, traffic congestion leading to service delays, and destruction of homes, crops, and livestock (Dong et al., 2022; Pregnolato et al., 2017; Rebally et al., 2021).

Therefore, it is crucial to investigate the flood vulnerability of Adama City. This research focuses on identifying and mapping flood-prone areas, characterizing flood vulnerability levels, investigating flood-resilient neighborhoods, and developing strategies and tools for flood management. The findings of this study will apply not only to the study area but also to other urban areas that are frequently affected by flooding. The findings of the research will undoubtedly help to develop effective strategies to mitigate the impact of flooding, protect properties, and the environment, and save lives.

1.2 Concise literature review

Definition of terms

Flood

Floods are one of the most common and destructive natural disasters, causing billions in damages and claiming thousands of lives each year (Amirkhani et al., 2022; Das & Gupta, 2021; Vojinovic et al., 2016). They can occur through various mechanisms, including heavy rainfall overwhelming drainage systems (pluvial flooding), rivers overflowing their banks (fluvial flooding), coastal storm surges, and rapid snowmelt (Balica et al., 2012; Re, 2012). Urban flooding has become an increasingly pressing issue due to a combination of factors, including climate change, urbanization, and aging infrastructure by creating surfaces that prevent water absorption and speed up runoff (Choubin et al., 2019; Miller & Hutchins, 2017; Wang et al., 2022b). Climate change is expected to exacerbate flood risks by increasing extreme precipitation, storm surges, and sea level rise (Bibi & Kara, 2023; Hirabayashi et al., 2013; Manandhar et al., 2023; Yang et al., 2021).

Hazard

Hazards refer to potential sources of harm or adverse effects on people, property, or the environment (Gao et al., 2022; Hirabayashi et al., 2013). Flood hazard refers to the potential for a flood event to occur in a given area, and is influenced by factors such as precipitation patterns, river/coastal dynamics, and land use characteristics (Hirabayashi et al., 2013). Hazard assessment is a critical component of risk management, involving the identification, analysis, and evaluation of hazards that could lead to undesirable events (Bhatkoti et al., 2016; Oubennaceur et al., 2021; Yamazaki et al., 2018).

Vulnerability

Vulnerability refers to the state of being exposed to risks or harm, particularly in the context of urban areas (Chang et al., 2021). It encompasses a combination of factors that make individuals or communities more susceptible to negative impacts, such as flooding, poverty, inadequate infrastructure, and social exclusion (Nasiri et al., 2019). Vulnerable populations, including low-income residents and marginalized groups, are often at greater risk due to their limited resources and lack of access to support systems (Salami et al., 2017b). Addressing vulnerability requires a comprehensive approach that involves understanding and assessing the specific challenges faced by different groups, engaging with the community to develop tailored solutions, and implementing measures to enhance resilience and reduce the impacts of future disasters (Kashyap & Mahanta, 2021; Van et al., 2022).

Risk

Risk refers to the potential for loss, harm, or negative outcomes resulting from exposure to uncertain or hazardous situations (Denchak, 2019; Wing et al., 2022). It encompasses the likelihood of an event occurring and the magnitude of its impact and can be influenced by various factors such as environmental conditions, human activities, and infrastructure vulnerabilities (Wobus et al., 2017). Urban flood risk specifically refers to the probability and potential consequences of flooding in a city or urban area (Bose & Mazumdar, 2023). This includes the likelihood of flooding occurring due to factors such as heavy rainfall, inadequate drainage systems, or rising sea levels, as well as the impact on people, property, and infrastructure within the urban environment (Kadaverugu et al., 2022; Semaw et al., 2022; Srivastava & Roy, 2023; Tariq et al., 2020; Tiepolo et al., 2021).

Resilience

Resilience refers to the ability of a system, community, or individual to withstand and recover from adverse events or challenges, adapting and bouncing back in the face of adversity (Holling, 1973). It involves the capacity to anticipate, prepare for, respond to, and recover from disruptions, maintaining essential functions and structures while also learning and improving from the experience (Breen & Anderies, 2011; McClymont et al., 2020). Urban flood resilience specifically pertains to the capacity of a city or urban area to effectively mitigate, withstand, and recover from flooding events, minimizing the impact on people, property, and infrastructure (Schelfaut et al., 2011; Yin et al., 2022). This encompasses measures such as infrastructure, effective early warning systems, comprehensive risk assessment and management strategies, community engagement, and participation, as well as sustainable urban planning and development practices that enhance resilience to flooding hazards (Bukvic et al., 2021; Rözer et al., 2022).

1.2.1 Mapping flood-prone areas

Flooding is a natural hazard that affects the ecological, economic, and societal implications globally (Manzoor et al., 2022; Tariq et al., 2020). In this context, the development of flood risk maps is crucial for effective mitigation planning. As flood hazard areas cannot be circumvented or mitigated on the ground, flood maps facilitate improved preparation against flooding risks and vulnerability (Farhadi & Najafzadeh, 2021; Minucci et al., 2020). Leveraging GIS and remote sensing-based data enables the creation of diverse maps illustrating the extent of flood-prone areas, risk assessments, and vulnerability by easily manipulating different layers of information (Gao et al.; Sadiq et al., 2023; Srivastava & Roy, 2023).

Flood hazard maps are integral to sustainable flood risk management, delineating susceptible areas and predicting potential severe floods within specific timeframes (Fischer & Stanchev, 2022). This information is crucial for conducting comprehensive flood risk assessments and guiding urban planning to protect lives and properties from flood risks (Argaz et al., 2019; Çetinkaya et al., 2016; Forkuo, 2011; Wang et al., 2011). The reliability of flood hazard maps depends on the methodology used for flood hazard assessment, which relies on data availability and resources. Various methods have been established since 1970 (Tang et al., 2018), ranging from historical statistical models to numerical hydrologic and hydrodynamic models, and the integration of statistical laws and expert-knowledge-based indicators for detailed insights into potential flood risks from all relevant sources (Nott, 2006; Pouya et al., 2017; Wang et al., 2011).

Multi-Criteria Decision Analysis (MCDA) is a sophisticated and extensively employed methodology for mapping flood hazards in urban settings (Rahmati et al., 2016; Rimba et al., 2017; Seejata et al., 2018). This approach involves a nuanced spatial overlay analysis that assigns weights to a range of flood-triggering factors, encompassing natural and anthropogenic elements such as land use patterns, slope characteristics, drainage density, soil composition, and elevation levels (Aydin & Birincioğlu, 2022). The relative importance of these factors is typically determined using the Analytical Hierarchical Process (AHP) before being integrated into a Geographic Information System (GIS) framework (Desalegn & Mulu, 2021; Hagos et al., 2022; Ogato et al., 2020). This integration not only enhances visualization and mapping capabilities but also expedites the production of hazard maps. Consequently, this methodology appreciates widespread adoption across various regions worldwide.

1.2.1.1 The importance of mapping flood-prone areas

Utilizing Geographic Information System (GIS) methods for mapping flood-prone areas offers numerous advantages. To begin with, it improves flood management by precisely identifying vulnerable zones and enhancing disaster preparedness and risk mitigation strategies (Abdelkarim et al., 2020; Fischer & Stanchev, 2022; Mohanty & Simonovic, 2022). This tool empowers decision-makers to implement flood protection measures and prioritize interventions based on critical data, thereby enhancing flood management and response planning (Argaz et al., 2019; Wang et al., 2011; Weday et al., 2023).

In addition, flood hazard mapping aids in better land-use planning by advising restrictions on development in flood-prone regions, reducing the exposure of susceptible areas to potential flood damage (Bodoque et al., 2023). Moreover, it serves as a valued tool for insurance and investment decisions, providing a solid foundation for property, crop, and infrastructure insurance, leading to more informed investment and risk assessment choices (Bose & Mazumdar, 2023). Furthermore, it promotes community awareness by visually representing flood risks, assisting in effective emergency response planning, and identifying evacuation routes and flood shelters (Farhadi & Najafzadeh, 2021; Khosravi et al., 2016; Kim et al., 2019; Leta & Adugna, 2023b).

In summary, utilizing GIS and remote sensing techniques to map flood-prone areas not only assists in pinpointing and addressing flood risks but also facilitates well-informed decision-making, community awareness, and enhanced flood disaster management. By using precise and comprehensive data on flood-vulnerable regions, GIS technology enables decision-makers to formulate proactive measures that mitigate the repercussions of floods on communities. A holistic approach towards flood risk management not only improves preparedness but also promotes sustainable land-use planning and cultivates heightened community resilience in anticipation of potential disasters.

1.2.2 Characterizing the level of flood vulnerability

The expansion of human populations and subsequent development have brought about significant changes in floodplains and flood-storage basins (Wang et al., 2022a; You, 2023; Youssef et al., 2023; Yusmah et al., 2020). Vulnerability to flooding is worsened by the increase in impermeable surfaces, modifications to flood plains and channels, and inadequate stormwater drain systems (Konrad, 2003). Moreover, risky weather events and shifting climatic conditions may play a great role in aggravating flood severity (McDermott, 2022). The inundation of floodwater poses a danger to both communities and natural habitats, especially as urban areas encroach further on the remaining green spaces and cultivated lands within these natural systems (Rentschler et al., 2023). The link between urbanization and flooding in floodplain regions is well-documented (Feng et al., 2021; Freni et al., 2010; Güneralp et al., 2017; Hammond et al., 2015). The growth of urban areas heightens the flood risk by boosting peak discharge and volume, while also shortening the time it takes for water levels to peak (Feng et al., 2021; Gwenzi & Nyamadzawo, 2014; Hemmati et al., 2021; Iliadis et al., 2023). Human activities, such as the presence of structures, lax maintenance regulations, and deforestation, render the floodplain particularly susceptible to flooding (Bulti & Abebe, 2020; Erena et al., 2018; Leta & Adugna, 2023b).

Vulnerability, in this context, refers to the degree to which an area, its residents, physical structures, or assets are exposed to the risk of loss, harm, or damage due to flooding (Chan et al., 2022; Erena & Worku, 2019; Hoque et al., 2019). The extent and impact of flood-related damage depend on the nature of the affected population and the state of local infrastructure (Chan et al., 2022). Consequently, understanding the leading causes of vulnerability, identifying the most affected groups, and recognizing different degrees of vulnerability are essential elements of effective flood risk management (Nasiri et al., 2016; Salami et al., 2017b). Addressing flood vulnerability can be achieved through various approaches, one of which involves conducting vulnerability assessments and mapping vulnerability. In urban settings, vulnerability to flooding is assessed by examining sensitivity, exposure, and adaptive capacity (Chang et al., 2021; Hong et al., 2018; Hussain et al., 2021; Santos et al., 2022).

Floodplain areas in urban settings become vulnerable to flooding due to human activities, such as unconsciously modifying the natural landforms, lack of regulations for building codes, and deforestation (Tate et al., 2021; Zeng, 2022). This highlights the need to address urban flood vulnerability, which is a global issue. With the acceleration of urbanization and consequent changes in physical forms, floods are becoming more frequent and severe worldwide (Wang et al., 2022b; Ziegler et al., 2012). Vulnerability to flooding is influenced by both human and natural factors, such as agricultural activity, urbanization, deforestation, land degradation, heavy rainfall, and storm surges. Climate change, above-average rainfall, and deforestation also contribute to flood hazards. (Baky et al., 2020; Chiara et al., 2015; Samuel et al., 2019; Tanoue et al., 2016). As urban areas continue to grow and human activities intensify, these areas become increasingly vulnerable to extreme hydrologic events such as heavy precipitation and flooding (Chang & Franczyk, 2008; Chen & Leandro, 2019; Waghwala & Agnihotri, 2019).

1.2.2.1 Social Systems and Flood Vulnerability

Social vulnerability plays a critical role in assessing the risk and consequences of flood events. Studies indicate that social vulnerability is influenced by various socioeconomic factors such as poverty, social standing, resource accessibility, and community resilience (Chang et al., 2021; McDermott, 2022). When assessing vulnerability, a prevalent range of elements is susceptible to damage during a flood, encompassing enormous physical infrastructures that were used by communities. Hospitals and roads, for instance, are examples of vulnerable assets due to flood hazards (Isia et al., 2023). It is essential to integrate social vulnerability into flood risk evaluations to pinpoint the most vulnerable groups and tailor disaster preparedness measures accordingly (Srivastava & Roy, 2023). Indicators of social vulnerability encompass demographic factors (e.g., age, language proficiency), neighborhood characteristics (e.g., population density), and socioeconomic factors (Chang et al., 2021; Ermagun et al., 2024; Isia et al., 2023; Srivastava & Roy, 2023). By emphasizing social vulnerability, flood risk analysis can assist policymakers in focusing on risk mitigation strategies for communities in greatest need.

1.2.2.2 Ecological Systems and Flood Vulnerability

The complexity of ecological systems' susceptibility to floods poses a nuanced and intricate challenge (Tariq et al., 2020). Understanding the dynamic interaction between ecological systems and flood vulnerability is crucial for developing effective strategies to mitigate flooding impacts and protect vulnerable communities (Chang et al., 2021). For instance, resilient ecosystems can act as natural defenses against floods by absorbing and holding excess water, thereby lowering the risk of downstream flooding (Birkholz et al., 2014). Additionally, preserving and restoring wetlands, which play a vital role in flood management, can help decrease nearby communities' vulnerability to flooding (Bertilsson et al., 2019; Elum & Lawal, 2022; Pallathadka et al., 2022; Ramiaramanana & Teller, 2021). Indicators of ecological vulnerability include land surface attributes (such as slope and land cover), landscape characteristics (like proximity to hazards and fragmentation), and green spaces (such as wetland presence and productivity) (Birkholz et al., 2014; Chan et al., 2022; Chang et al., 2021; Srivastava & Roy, 2023).

1.2.2.3 Technological Systems and Flood Vulnerability

The complex association between technological systems and flood vulnerability delves into the intricate balance between reliance on technology and the exposure of communities to flooding risks (Chang et al., 2021). This complex dynamic underscores the myriad of potential dangers and obstacles that emerge when technological progress and infrastructure development intersect with flood-prone regions (Chang et al., 2021). While structures like dams, levees, floodwalls, and drainage networks are typically erected to reduce flood hazards and safeguard susceptible populations, they can also introduce fresh vulnerabilities and unforeseen repercussions (Chang et al., 2021; Schotten & Bachmann, 2023). Dependence on structural solutions may foster complacency, leading to inadequate readiness for extreme flooding events (Brody et al., 2010; Fekete & Sandholz, 2021; Wilby & Keenan, 2012). Furthermore, the escalating intricacy of technological systems, encompassing interconnected infrastructure grids and automated control mechanisms, can introduce new points of failure and susceptibilities (Chang et al., 2021). Failures or glitches in these systems during floods can intensify the impacts and impede emergency response endeavors. A holistic understanding of this interplay is essential for formulating sustainable and resilient flood management strategies, necessitating meticulous evaluation of the potential advantages and constraints of technological interventions, alongside the combination of social, economic, and environmental considerations (Leta & Adugna, 2023a; McPhearson et al., 2022; Qiang, 2019; Schotten & Bachmann, 2023). Thus, in summary, by adopting a holistic approach that integrates diverse perspectives and factors, including social dynamics, economic considerations, and environmental impacts, decision-makers can navigate the complexities of technological vulnerabilities in light of flood management, fostering a more resilient and adaptive response to flooding risks.

1.2.3 Investigation of flood-resilient neighborhoods

The concept of urban flood resilience has undergone a substantial transformation over the past two decades (Rözer et al., 2022). Initially centered on the built environment's ability to withstand flooding, it has since expanded to encompass a more fluid and adaptable comprehension of resilience. Urban flood resilience is described as the capacity to endure, absorb, recover from, and adjust to flooding (Chang et al., 2021; Mugume & Butler, 2017; Murdock et al., 2018; Rufat et al., 2015; Rus et al., 2018). This concept is intricately linked with the principles of green infrastructure and holistic spatial planning methodologies. It underscores the importance of interdisciplinary research and the incorporation of varied strategies to enhance urban flood resilience, underscoring its dynamic and progressive essence (Abshirini et al., 2017; Breen & Anderies, 2011; McClymont et al., 2020; Sharifi, 2023). Building upon the pioneering work of Holling (1973), who introduced the concept of "resilience" in ecology, numerous studies have applied this concept across a range of disciplines including disaster management, social science, and psychiatry (McClymont et al., 2020). These studies have integrated resilience as a pivotal element within interdisciplinary frameworks such as complex adaptive systems, engineering, and systems theory (Breen & Anderies, 2011; Gao et al., 2022; Rus et al., 2018).

1.2.3.1 Contribution of proper urban planning to flood resilience

Urban planning plays a pivotal role in enhancing flood resilience by integrating green infrastructure and spatial planning strategies (Khodadad et al., 2023; Takin et al., 2023). Green infrastructure, such as parks, green roofs, and rain gardens, effectively absorbs and manages excess water during floods, reducing potential damage to buildings and infrastructure (Alshaikh et al., 2023; O'Donnell et al., 2020). Simultaneously, spatial planning approaches help identify flood-prone areas and prioritize interventions, such as constructing flood-resistant structures and relocating vulnerable populations (Meng et al., 2022).

The combination of these strategies not only helps pinpoint high-risk flood areas and prioritize interventions but also encourages community engagement in decision-making processes, enhancing the sustainability of flood resilience strategies (Khodadad et al., 2023; O'Donnell et al., 2020; Takin et al., 2023). Additionally, within urban environments, certain neighborhoods are inherently more suspectable to flooding risks, while others demonstrate greater resilience due to their physical layout (Alshaikh et al., 2023; Bajracharya et al., 2015; Barreiro et al., 2020; Bixler et al., 2021; Cea & Costabile, 2022; Hemmati et al., 2020). As a result, neighborhood-specific considerations are essential for developing resilient community plans in urban settings. Exploring flood-resilient neighborhoods is crucial for effective flood mitigation, sustainable spatial planning, and overall improvement of flood resilience within communities (Alshaikh et al., 2023; Meng et al., 2022).

1.2.4 Strategies for flood management

Flood management stands as a critical pillar in safeguarding lives and minimizing the risks associated with flooding (de Bruijn et al., 2022; Wang et al., 2022). While the complete control of floods remains an elusive goal, the implementation of effective management strategies can significantly reduce the adverse impacts on human activities, lives, and property (de Bruijn et al., 2022; Wang et al., 2022). Given the unpredictable nature of climate-induced flooding, proactive and systematic preparations play a pivotal role in mitigating the devastating effects of inundation (Takin et al., 2023; Wang et al., 2022). Particularly in many developing countries, notably in Africa, deficiencies in state infrastructure and inadequate legal and policy frameworks pose significant obstacles to effective flood mitigation efforts (Takin et al., 2023; Wang et al., 2022).

Understanding the spatial intricacies of flood hazards and implementing robust disaster preparedness measures are fundamental steps toward effective flood control and management(Takin et al., 2023; Wang et al., 2022). Recent studies (Wang et al., 2022) underscore the importance of developing flood risk maps to analyze flood dynamics comprehensively, thereby facilitating informed spatial planning and land management strategies. Flood hazards are often described as 'quasi-natural,' stemming from a complex interplay of natural phenomena and human activities(de Bruijn et al., 2022). Factors such as climatic conditions, meteorological events, geomorphological features, hydrological patterns, and improper land use practices collectively contribute to the occurrence of floods (Alshaikh et al., 2023; Amirkhani et al., 2022; Chang & Franczyk, 2008; Der Sarkissian et al., 2022; Rogger et al., 2017). Inappropriate housing developments in high-risk zones and human interventions that disrupt natural processes further escalate the likelihood and impact of flooding, underscoring the critical importance of integrated approaches to flood resilience and disaster risk reduction (Wang et al., 2022).

Mitigating flood hazards requires a multifaceted approach that combines both structural and non-structural methods (Minea & Zaharia, 2011; Takin et al., 2023; Truu et al., 2021; ZurichFloodResilienceAlliance, 2014). Structural measures involve the construction of physical infrastructure to protect human settlements, while non-structural techniques encompass land use planning, flood warning systems, and policies aimed at steering development away from vulnerable areas like floodplains (Minea & Zaharia, 2011; Takin et al., 2023). Many flood-prone urban regions have traditionally relied on 'hard-engineered' flood defenses such as walls and embankments for defense, but the growing populations and economic assets in these areas have rendered existing defenses inadequate (Chan et al., 2018).

However, structural approaches come with limitations, including providing complacency to downstream residents and posing environmental concerns due to their high costs (Ogie et al., 2020; Tasseff et al., 2019). The potential failure of structural defenses like dams during extreme weather events can exacerbate risks of casualties and property damage (Amirkhani et al., 2022; Bajracharya et al., 2015; Bulti et al., 2021b; Ogie et al., 2020). In response to these challenges, a holistic flood management approach that integrates both non-structural and structural measures while prioritizing environmental sustainability is imperative (Minea & Zaharia, 2011; Qin, 2020; Rus et al., 2018).

1.3 Research problem statement

The study area, Adama City, is one of the fastest-growing cities in Ethiopia and faces a significant flood risk attributed to its geographical location and rapid urban development. The city is situated on a floodplain and surrounded by mountains and ridges, making it vulnerable to flooding. The city is located in the Awash River basin, which is known for frequent and destructive flooding.

The watershed of the study area is composed of six catchments that drain into the Awash River basin, except for two closed basins within the city, namely Dembela, and Migira. These closed basins contribute to inundation during the rainy season. According to Wodnimu et al. (2022), poor stormwater drains, a lack of proper hydrologic discharge areas, and unregulated human interventions have left the study area vulnerable to flooding.

In recent years, the issue of flooding in the study area has become increasingly severe due to rapid urbanization including uncontrolled expansion of the city. The built-up area of the city has increased significantly, increasing from 2% in 1973 to 23% in 2010. and expected to reach 60.27% by 2040 (Regassa et al., 2020). The proximity of the study area to Addis Ababa, as well as its location along the road and railway connecting Addis Ababa to Djibouti, has contributed to its growth. Unfortunately, the consequences of this expansion have been devastating. Flooding caused extensive damage in various neighborhoods and surrounding settlements in 2008, 2009, and 2016 (Bulti et al., 2017). These incidents highlight the urgent need for comprehensive research and effective strategies to alleviate the effect of flooding in the study area.

Studies have highlighted the significant impact of flooding in the study area, as it affects a growing number of people, economic activities, and ecosystems. Historical records show that flooding has been the most destructive natural disaster in the study area (Bulti et al., 2017; Wodnimu et al., 2022). Despite efforts by the city administration to address flooding through structural measures, such as diverting water channels away from the city, flood risk and vulnerabilities continue to increase (Bulti & Abebe, 2020). The Adama City Structure Plan Revision (ACSPR, 2018a) primarily focuses on structural measures, which have proven to be ineffective in managing floods. The combined effects of urbanization and potentially increasing extreme precipitation events due to a poorly planned and operated stormwater drainage system will likely lead to frequent and devastating urban flooding, leaving the city even more vulnerable to future floods.

Previous studies conducted on flooding in the study area have been limited in scope and coverage (Bulti et al., 2017). These studies focused on identifying the causes of flooding and assessing the associated risks, but only within the urbanized areas of the city. For example, Bulti and Abebe (2020) examined the urban flood hazard in the study area and its future variations due to rapid urban growth and climate change, while Hailemariam & Ajeme (2014) and Woldetsadik (2017) reported the impact of poor solid waste management on flooding. However, these studies did not cover other important aspects such as characterizing flood vulnerability, the spatial pattern of floods, urban morphology, and the correlation with resilience to manage the frequent impacts urban flooding for sustainable urban development and mitigation strategies.

To address these gaps, it is necessary to study the settlement pattern and morphology of the study area to quantify and implement strategies for mitigating floods, which is essential for informed decision-making. The increasing trend of floods, property damage, and human casualties further emphasizes the need for detailed research to effectively tackle the problem of flooding.

Therefore, this research is undertaken to identify and map both man-made and natural flood-causing factors to assist in its mitigation. Additionally, it characterized the level of vulnerability, investigated flood-resilient neighborhoods, and came up with appropriate flood management strategies and tools.

1.4 Aims and objective of the study

1.4.1 Aim of the study

The overarching aim of this study is to fill various research gaps related to flood-prone area identification and mapping, vulnerability characterization, and the identification of flood-resilient neighborhoods and developing flood management tools and strategies for Adama City and its watershed.

1.4.2 Specific objectives

The specific objectives of the research are:

- To map the flood-prone areas of Adama City and its watershed
- To characterize the level of flood vulnerability of the study area
- To investigate flood-resilient neighborhoods in the study area
- To develop flood management strategic tools for the study area

1.5 Research questions

Based on the stated aims and objectives, the following research questions are formulated as presented below.

- Which part of the study area is vulnerable to flood-prone?
    - Which part of the study area is vulnerable to very high flood-prone?
    - Which part of the study area is vulnerable to high flood-prone?
    - Which part of the study area is vulnerable to medium flood-prone?
    - Which part of the study area is vulnerable to low flood-prone?
    - Which part of the study areas is vulnerable to very low flood-prone?
- How to characterize the flood vulnerability of the study area?
    - What are the spatial patterns in urban flood vulnerability when considering social (S), ecological (E), and technological (T) indicators individually? How do these factors and their interplay contribute to the variation in flood vulnerability across different areas?
    - To what extent do the vulnerable areas identified by each of the S, E, and T indicators spatially correlate with each other?

    - How are the vulnerability indicators grouped to explain the integrated SETS flood vulnerability?
    - What are the benefits of examining flood vulnerability using a SETS framework to the study areas and their watershed?
- Which neighborhoods of the study area are resilient to flooding?
    - Which neighborhood is more resilient to flooding due to settlement pattern and morphology?
    - Why do certain neighborhoods recover quicker than the other even though they are inundated by flood?
- What are flood management strategic tools that could be applied to mitigate flood-prone in the study area?
    - Which tools are applicable at watershed levels?
    - Which tools are applicable at main catchments?
    - Which tools are applicable at sub-catchment levels(neighborhoods-block/site and building level)?

1.6 Significance of the study

The findings of this research have significant implications for policymakers, urban planners, and managers. By providing insights into how to identify, map, and characterize flood vulnerability, as well as how to identify flood-resilient neighborhoods in city planning and management, the study offers valuable guidance for decision-makers. The hierarchical approach to flood management proposed in this research can assist policymakers and urban planners in developing more effective strategies for mitigating the impact of floods on communities. By integrating the research's findings into their decision-making processes, policymakers and urban planners can work towards creating more resilient and sustainable cities.

1.7 Scope of the Study

1.7.1 Thematic scope

Thematically, the study focused on flood management strategies and tools for mitigating flood-prone areas at various scales, including city and neighborhood levels. This involved the identification and mapping of flood-prone areas using man-made and natural flood conditioning factors. Additionally, the research focused on characterizing the level of flood vulnerability through an examination of social-ecological and technological systems. Furthermore, the study investigated flood-resilient neighborhoods through an analysis of spatial morphology and the development of flood management strategies and tools for mitigating flood-prone areas.

1.7.2 Spatial scope

Spatially the present study is limited to Adama City and its watershed.

1.8 Conceptual frameworks

The study began by identifying and mapping flood-prone areas, characterizing flood vulnerability, and identifying flood-resilient neighborhoods. Data was collected for various selected indicators, observations, measures ranking, categorizing, and detecting the study area, with a focus on flood mitigation measures. This research utilizes quantitative methods, collecting data for spatial, social, environmental, and economic aspects of the study area to assess vulnerability. The collected data was analyzed using numerical and statistical inference and evaluated empirically, giving the research empirical characteristics. The general approach of the research is inductive, and the overall conceptual framework is illustrated in Figure 1.1.

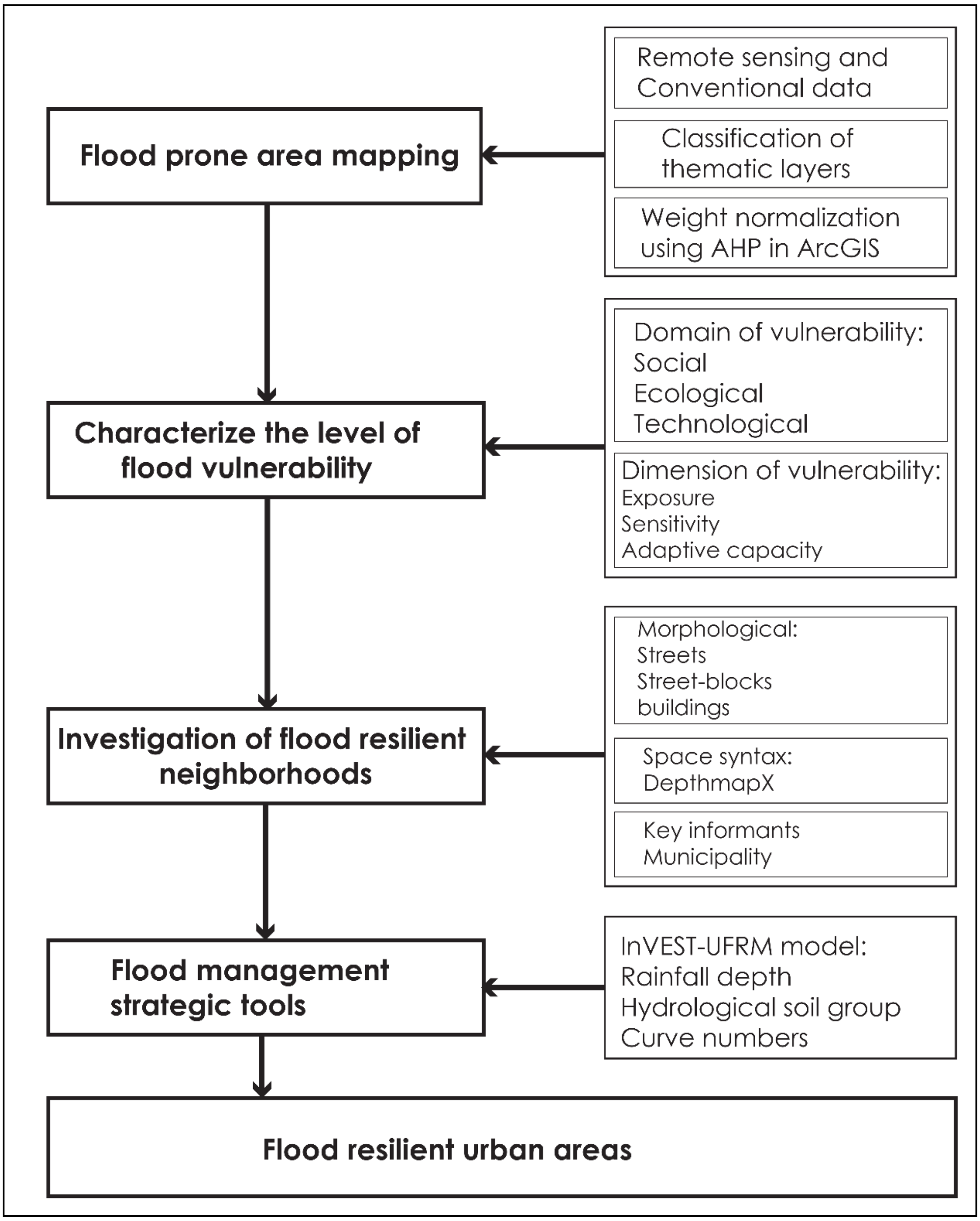

Figure 1.0.1: Conceptual framework of the study

1.9 Limitations of the study

The study is limited by the lack of spatial data in the Adama City Administration, hindering the mapping of flood-prone areas and assessment of flood vulnerability. Furthermore, there is a lack of literature exploring the connection between space syntax and spatial morphology in urban flood contexts. Despite conducting a thorough literature review, it was evident that previous studies on the linkage between space syntax and spatial morphology are scarce, highlighting a significant gap in current research. As a result, this investigation could be the first to examine the relationship between space syntax and spatial morphology, posing a challenge in drawing comparisons with existing research due to the scarcity of relevant studies in this specific field. It is crucial to address these limitations by rigorously collecting and making spatial data accessible, as well as promoting further research in this area to enhance understanding of urban flood dynamics and mitigation strategies.

1.10 Description of the study area

The present study was conducted in Adama City, Ethiopia. The City is one of the rapidly expanding and second-largest urban centers in the country. Established in 1916, the city is settled on a level landscape surrounded by plateaus, mountain ranges, and challenging terrain, situated within the Awash River Watershed and the East African Rift Valley. The study area is located between $8^0$26’15”– 8^0 37’00” N, and 39^0 12’15”-$39^0$19’45” E.

The Adama City Structure Plan Report (ACSPR, 2018a) highlights the susceptibility of the study area and its environs to recurrent flood incidents. Encompassing 31,100.95 hectares delineated by the Adama City Administration's approved boundary, based on watershed demarcations, the study zone comprises six catchments: Dabe, Dakaadi, Dembela, Jogo, Migira, and Wonji.

According to the National Disaster Risk Management Commission (NDRMC, 2020), the study area encounters an average annual precipitation of 866.25 mm, predominantly during the rainy season from June to September. The study area's climate is categorized as hot semi-arid, with mean minimum and maximum annual temperature varying from 12.47-32.8 °C.

The study area has an elevation range from 1489 to 1976 meters above sea level in terms of elevation. The eastern periphery contains the lowest point, where a flat low-lying terrain gathers floodwaters from the 'Borticha' ridge (Daabe Solloqqe) and the eastern edge of 'Migira' ridges, creating temporary ponds during specific seasons. In contrast, the northernmost point of the Wind Farm II substation claims the highest elevation, reaching heights of 487 meters. This significant difference in altitude plays a key role in creating a range of tropical and subtropical microclimates.

In the study area, five distinct soil types were identified: Fibric Cambisols, Vitric Andosols, Mollic Andosols, Calcaric Fluvisols, Eutric Leptosols, and Pellic Vertisols. About 34.42% of the study area was found to be at a moderate to very high risk of flooding due to specific soil characteristics like shallow depth, gravel content, shrink-swell cycles, and poor drainage, leading to increased erosion hazards (Leta & Adugna, 2023b).

The 2007 census conducted by the Central Statistics Agency of Ethiopia (CSA) found that Adama City's population stood at 222,035 people, showing a growth rate of 5.4%, which surpassed Ethiopia's average urban growth rate of 2.5%. ACSPR (2018a), reported that the population within the city's administrative boundary of 31,100.95 hectares stood at 431,202, with a doubling rate of 13 years, surpassing the national doubling time of 23 years. This rapid population growth is primarily due to Adama's advantageous position along the Addis Ababa - Djibouti railway and its proximity to Addis Ababa. ACSPR (2018a), also stated that the rapid increase in Adama's population has resulted in overcrowding near floodplains, raising the risk of recurring floods due to the city's topography. Additionally, a study analyzing growth rates from 2004 to 2016 found that Adama has seen an annual growth rate of nearly 9%, establishing it as one of Ethiopia's fastest-growing cities (Bulti & Assefa, 2019). The city's rapid expansion and population surge are straining infrastructure and public services while heightening the threat of environmental degradation in the local area (Adugna, 2019b). Figure 1. 2 shows the location map of the study area.

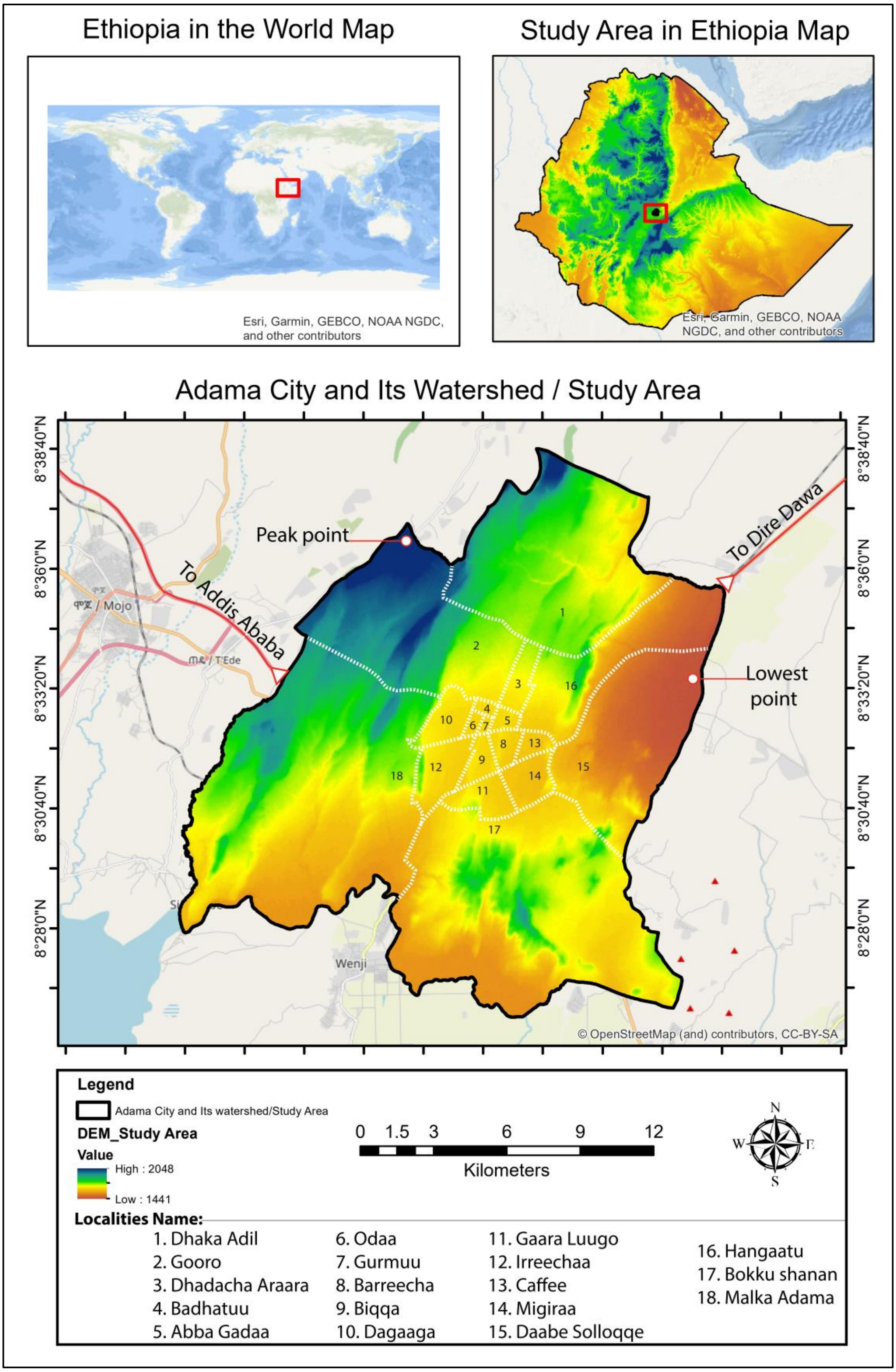

Figure 1..2: Location map of the study area

1.11 Dissertation Structure

This dissertation is organized into seven chapters as follows:

- The first chapter includes the study's background, problem statement, objectives, research questions, and the significance of the study.
- Chapter 2 presents the identification and mapping of flood-vulnerable zones across Adama City's Watershed through the integration of a Geographic Information System (GIS) alongside Multi-Criteria Decision-Making (MCDM) and Analytical Hierarchy Process (AHP). This methodology involved the integration of diverse datasets, including proximity to stormwater drains, elevation, slope, rainfall patterns, land cover, Normalized Difference Vegetation Index (NDVI), Topographic Wetness Index (TWI), distance from rivers and roads, drainage density, and soil types. By combining these data sets, a comprehensive assessment of flood-prone areas was conducted.
- Chapter 3 characterized the degree of urban flood vulnerability, and a Social-Ecological-Technological Systems (SETS) framework was employed. This framework was interconnected with the GIS-based MCDM-AHP and evaluated exposure, sensitivity, and adaptive capacity within each SETS domain. By utilizing this approach, a thorough understanding of flood vulnerability was achieved.
- Chapter 4, identifies flood-resistant neighborhoods, a comprehensive analysis was conducted using morphological analysis, local community responses, and expert insights. By considering existing spatial patterns that are resilient to flooding, these neighborhoods were identified.
- Chapter 5 comprises the strategies for managing floods, the Integrated Valuation of Ecosystem Services, and TradeoffsUrban Flood Risk Mitigation-Urban Flood Risk Mitigation (InVEST-UFRM) model was utilized. This model efficiently investigated urban watersheds and accurately represented flood risk, providing a holistic analysis of the flood scenario in the city. Using this information, adaptation plans were developed to address urban flooding.
- Chapter 6 contains the general discussion, and
- Chapter 7 deals with the general conclusion and recommendations.

CHAPTER TWO:

Identification and Mapping of Flood-Prone Areas Using GIS-Multi-Criteria Decision-Making and Analytical Hierarchy Process: The Case of Adama City's Watershed, Ethiopia

Abstract

Adama is one of the fastest-growing and second-populous cities in Ethiopia. It is highly prone to flooding due to its location and rapid urbanization. The city is densely populated in the floodplain areas. It is a low-lying flat terrain surrounded by mountains and ridge topography. The objective of this study was to identify and map flood-prone areas in Adama City`s Watershed using a Geographic Information System (GIS) based Multi-Criteria Decision-Making (MCDM) and Analytical Hierarchy Process (AHP). Distance from sewers drainage, Topographic Wetness Index (TWI), elevation, slope, rainfall, land cover, Normalized Difference Vegetation Index (NDVI), distance from the river, distance from the road, drainage density, and soil types data sets were combined, processed and interpreted to meet the objective of the study. The result of the present study revealed that about 98.69 % of the study area is moderate to very highly prone to flooding, whereas the other 1.31 % of the area is at low risk. The model-generated flood-prone map matched with the Ground Control Points (GCPs) collected by Handheld GPS, Google Earth Satellite Imagery, experts' opinions, and local community reports. Thus, this model has important implications for decision-making and may also assist professionals in early warning and sustainable flood management systems.

Keywords: Flood-prone area, mapping, GIS, Adama, Ethiopia

2.1 Introduction

Flooding is a natural phenomenon that occurs on a regular, widespread, and destructive basis, causing a disaster to the lives and properties of millions of people as well as infrastructure and the environment all over the world (Amirkhani et al., 2022; Das & Gupta, 2021; EM-DAT, 2015; Vojinovic et al., 2016). Flood incidence has increased globally in recent years as a result of climate change and environmental degradation caused by inadequate land management (Das & Gupta, 2021; Ozkan & Tarhan, 2016; Vojinovic et al., 2016; Yonas et al., 2022).

Flooding can occur in a variety of ways. These are coastal floods, river floods, flash floods, and urban floods (Balica et al., 2012; Re, 2012). Among these, urban flooding is distinctive, primarily caused by the absence of adequate drainage systems in urban areas (Balica et al., 2012). Many flooding cases are attributed to urban flooding, including increased impervious areas, land cover changes, excessive urban sprawl, irrational urban planning, and flood management (Abebe et al., 2018; Miller & Hutchins, 2017). Increased population, rapid urbanization, changes in natural river channel morphology due to anthropogenic interventions, and heavy rainfall also play a great role in urban flooding (Ahmadisharaf et al., 2016; Choubin et al., 2019).

According to a recent report by the Global Facility for Disaster Reduction and Recovery (GFDRR, 2019), floods pose a profound threat to Ethiopia, impacting both livelihoods and the environment. These devastating floods are primarily caused by prolonged heavy and erratic rainfall, compounded by the region's diverse and undulating landforms. Over the period from 1991 to 2019, the country witnessed more than 3,000 deaths attributed to flooding, with 1.3 million people displaced and over 10 million affected (GFDRR, 2019). The consequences have been severe, leading to the destruction of homes, infrastructures, and significant losses in crops and livestock. Furthermore, the Risk-Informed Early Action Partnership (REAP, 2020) reports that during the rainy season (June to September) of 2021, Ethiopia experienced heavy rainstorms, resulting in over 500,000 individuals being affected and around 300,000 people being forced to leave their homes due to flooding incidents.

In Ethiopia, urban flooding has become a major issue in recent years. They are primarily the result of poorly designed urban drainage systems, land use planning, a lack of an early warning system, and poorly coordinated flood disaster mitigation measures at the national and local levels (Legese et al., 2020). Floods are more expensive and difficult to manage in cities (Alemayehu, 2007). In Ethiopia, the Disaster Prevention and Preparedness Commission is responsible for addressing flood issues, as well as other forms of natural hazards, instead of being a separate institution (Erena et al., 2018). This hampered the effectiveness of urban flood management practices in Ethiopia.

According to the National Disaster Risk Management Commission (NDRMC, 2020); Gashaw and Legesse (2011); Legese et al. (2020), among the twelve basins of Ethiopia, the Awash River basin in which Adama City Watershed is located, is one of the most frequently and destructively flooded basins of Ethiopia. In line with this, the present study aimed at mapping the flood-prone area of Adama City`s Watershed. Despite the location being a flood-prone area, there is no previous study undertaken on both urbanized and surrounding areas.

Topographically, the study area is surrounded by plateaus, deforested mountains, and ridges. These surrounding and deforested mountains are external sources of stormwater, which results in flooding. The city is composed of six sub-catchments, namely Dabe, Dakaadi, Dembela, Jogo, Migira, and Wonji (Figure 1). They drain to the Awash River basin, except Dembela and Migira, which are closed basins within the city and create inundation in different areas of the city and its surroundings during rainy seasons. According to Wodnimu et al. (2022), inadequate stormwater drain infrastructure, a lack of viable hydrologic discharge points, and haphazard human interventions have left the city susceptible to flooding.

Historically, flooding has never been an issue for the study area. However, rapid urbanization and uncontrolled city expansion have exacerbated flooding in recent decades. According to, the built-up areas of the study area increased to 1040 hectares (1973–2000), 1876.4 hectares (2000–2010), and were projected to increase to 4604.26 ha (2010–2040). This demonstrates that built-up areas increased rapidly from 2% in 1973 to 10% in 2000 and 23% in 2010, and are projected to be 60.27% by 2040. The stud area's rapid urbanization is associated with increased population and faster economic development because of its proximity to Addis Ababa and along the road and railway, which connect Addis Ababa and Djibouti. Subsequently, flooding in 2008, 2009, and 2016 caused extensive damage in various neighborhoods and surrounding settlements (Bulti et al., 2017).

Nowadays, mapping areas that are prone to flooding is considered a strategic tool to mitigate and manage the impacts of floods by providing viable qualitative and quantitative information on flooding (Abdelkarim et al., 2020; Mohanty & Simonovic, 2022). Furthermore, it helps decision-makers and urban planners identify flood-prone areas and prioritize mitigation measures properly (Argaz et al., 2019; Çetinkaya et al., 2016; Forkuo, 2011; Wang et al., 2011). Numerous flood-prone mapping techniques have been developed since 1970 (Tang et al., 2018). These approaches range from employing bivariate statistical modeling of time series data analysis to relying on numerical hydrologic and hydrodynamic models (Nott, 2006; Wang et al., 2011). Furthermore, multi-criteria analysis has provided details of potential flood risks through the incorporation of statistical laws and expert-knowledge-based indicators (A. Pouya et al., 2017; Tanavud et al., 2004), as well as a practical model that takes into account all relevant hazard sources for precise information.

Multi-criteria analysis (MCA) or multi-criteria evaluation (MCE) methods have mostly been used due to their suitability and integration with remote sensing and GIS techniques. Furthermore, MCA allows for the development and assessment of alternative scenarios as well as decision-making on spatial (e.g., land use, slope, drainage system, etc.) and non-spatial (e.g., expert opinion, standards, surveys, etc.) issues and has provided new insights into flood studies (Rahmati et al., 2016; Rimba et al., 2017; Seejata et al., 2018). The method has been widely employed in flood-prone area mapping due to its efficiency and ease of use in supporting data analysis and interaction with decision-makers (Beltramone et al., 2017; A. Pouya et al., 2017; Rahmati et al., 2016). MCA employs analytical hierarchy process (AHP) techniques because of its ability to evaluate complex issues in flood-prone area mapping using several flood-controlling variables (Abdelkarim et al., 2020; Ali et al., 2020; Das & Gupta, 2021).

In recent years, several researchers have explored the use of GIS-based MCA and AHP for mapping flood-prone areas across the globe. In support of this, Aydin and Birincioğlu (2022) used a GIS-based AHP to map flood-prone areas in Turkey's Bitlis Province. Similarly, Desalegn and Mulu (2021); Negese et al. (2022); Ogato et al. (2020); Yonas et al. (2022) have undertaken MCA analysis utilizing GIS and the AHP to develop maps of areas prone to flooding in various parts of the world. Table 2.1 shows the prevalent factors used for mapping flood-prone areas. Most studies applied elevation, slope, land cover, rainfall, drainage density, soil types, and distance to the river. Few studies have also considered additional factors such as the normalized difference vegetation index, the topographic wetness index, the distance from sewer drainage, and the distance from the road.

Table 2.1:literature review of the flood conditioning factors used to identify and map flood-prone areas

Sources	**DSD**	**TWI**	**El**	**Sl**	**Rf**	**LC**	**NDVI**	**Driver**	**Droad**	**DD**	**ST**
Aydin and Birincioğlu (2022)			✓	✓	✓	✓		✓			
Edamo et al. (2022)		✓	✓		✓	✓		✓		✓	✓
Yonas et al. (2022)			✓	✓	✓	✓		✓		✓	✓
Negese et al. (2022)		✓	✓	✓	✓	✓	✓	✓		✓	✓
Ramesh and Iqbal (2022)	✓	✓	✓	✓		✓					✓
Nsangou et al. (2022)		✓	✓	✓	✓	✓		✓		✓	
Desalegn and Mulu (2021)			✓	✓	✓	✓				✓	✓
Arya and Singh (2021)				✓	✓	✓				✓	✓
Das and Gupta (2021)		✓	✓	✓	✓	✓		✓		✓	✓
Hussain et al. (2021)			✓	✓	✓	✓					
Roy et al. (2021)		✓	✓	✓	✓			✓		✓	✓
Ajibade et al. (2021)		✓	✓	✓							
Allafta and Opp (2021)			✓	✓	✓	✓		✓		✓	
Abdelkarim et al. (2020)				✓	✓	✓				✓	
Arshad et al. (2020)			✓		✓	✓				✓	✓
			✓	✓	✓	✓		✓		✓	
Ullah and Zhang (2020)		✓	✓	✓	✓	✓	✓			✓	
Ogato et al. (2020)			✓	✓	✓	✓					✓
Subbarayan and Sivaranjani (2020)			✓	✓	✓			✓		✓	
Chakraborty and Mukhopadhyay (2019)			✓	✓	✓	✓				✓	
Gambini and Laymito (2019)			✓	✓	✓	✓		✓		✓	✓
Hoque et al. (2019)			✓	✓	✓	✓		✓			
Rahman et al. (2019)			✓	✓	✓	✓			✓		✓
Cabrera and Lee (2018)			✓	✓	✓			✓		✓	✓
Ghosh and Kar (2018)			✓	✓	✓			✓			
Rincón et al. (2018)			✓	✓	✓			✓			
Bulti et al. (2017)			✓	✓		✓				✓	

Note: DSD = Distance from Sewers Drainage; TWI = Topographic Wetness Index ; El=Elevation; Sl=Slope; Rf = Rainfall; LC=Land Cover; NDVI= Normalized Difference Vegetation Index; Driver=Distance from river; Droad=Distance from road; DD=Driange Density; ST=Soil Types

Similar to other developing countries, Ethiopia lacks hydro-meteorological data significantly (Allafta & Opp, 2021; Cabrera & Lee, 2018). This data limitation poses a great challenge in mapping flood-prone areas and implementing proactive measures to safeguard people from these disasters. This leads to exacerbated consequences as the lack of information undermines the capability to make rational decisions and proper planning for emergencies as indicated in Figure 2.1.

Figure 2.1: Flood event observed during heavy rainy months (July and August), 2022. (a). Sewer blockages and overflow around Wonji Mazoriya, (b). Flooding overflow around Migira neighborhood, (c). Waterlogging around Migira pond, (d). Flooding in the RRC store.

Therefore, the main objective of this study is to identify and map flood-prone areas in the study areas through the use of GIS-based MCA and AHP techniques. This study implements an advanced GIS-MCA model incorporating eleven major natural and human-made flood conditioning factors including drainage distance, topographic wetness index, elevation, slope, rainfall, land cover, normalized difference vegetation index, river distance, road distance, soil types, and drainage density. These factors were integrated and carefully selected through a comprehensive literature review, and their weights were assigned based on experts' judgment. The findings have crucial implications for decision-makers in urban planning and management of flood-prone areas in low-lying flat terrains surrounded by plateaus, mountain ranges, and ridged topography located in the Rift Valley, similar to the study area.

2.2 Materials and Methods

2.2.1 Data types and sources

This study acquired and used data from several sources. Data on rainfall in the years from 1990 to 2022 measured at nine metrology stations (Adama, Arerti, Bishoftu, Bofa, Bologiorgis, Ejere, Mojo, Sire, and Welenchiti) was collected from the National Meteorological Agency of Ethiopia (NMA, 2022). Digital soil types for the study area were provided by the Water and Land Resource Center (WLRC) in Ethiopia. Further, a Digital Elevation Model (DEM) with a 12.5 m spatial resolution for studying different flooding factors (such as slope, elevation, Topographic Wetness Index (TWI), drainage density, and stream health index) was downloaded from the USGS website (http://earthexplorer.usgs.gov/) (acquired on March 3, 2022). Furthermore, a Normalized Difference Vegetation Index (NDVI) map with a 10 m spatial resolution was downloaded using a Sentinel 2A satellite imagery with minimal cloud coverage during the location's driest season. Additionally, a Land Cover (LC) map of 2022 with a 10m resolution was obtained from the ESRI website *(http://earthexplorer.usgs.gov/)* *(acquired in December 2022).* A summary of the data type and sources utilized in the study is presented in Table 2.1.

Table 2.1: Data types used and the sources

S. N	Data types	Derivable	Data Sources
1	ASTER- Global DEM with 12.5 m size grids	Slope, elevation, TWI, and drainage density map	Downloaded from USGS (http://earthexplorer.usgs.gov/.). acquired on March 3, 2022, with the least land and scene cloud cover (0.01).
2	Sentinel-2A Satellite Image with 10 m size grids	*NDVI map*	*Downloaded from USGS (http://earthexplorer.usgs.gov/.) acquired on December 20, 2022.*
3	Digital LC map of 2022 with 10 m size grids	*LC map*	*ESRI: (https://livingatlas.arcgis.com/Landover/). acquired on December 06, 2022.*
4	Digital Soil Map, Scale 1:25,000	Soil map	WLRC
5	Monthly Rainfall Data (1990–2022)	Rainfall map	NMA
6	Road shape file	Road density map	ACA and digitization by Google Earth Pro (version 7.3.6)
7	River shape file	River density map	ACA
8	Sewers Drainage shapefile	Sewer drainage map	ACA
9	Shapefile of the Administrative boundary of the study area	Study area extraction	ACA

2.2.2 Methods

The present study applied GIS-based MCA and AHP to effectively analyze and map areas that are susceptible to flooding. The investigation took into consideration the context of the study area, on-site observations, insights from experts and residents, as well as an extensive review of relevant literature. Eleven key factors that contribute to flood conditions were rigorously identified during this process, namely: Distance from Sewers Drainage (DSD), TWI, Elevation (El), Rainfall (RF), LC, NDVI, Slope (Sl), Distance from the river (Driver), Distance from the road (DRoad), Drainage Density (DD), and Soil Type (ST). Subsequently, these factors were appropriately ranked according to their level of influence.

All flood conditioning factors were categorized from very low (1) to very high (5) factors based on their importance in contributing to flooding. Reclassification was performed in a GIS environment using the reclassify tool from spatial analysis tools, rescaled by raster data management tools with 10 x 10-meter grids, and geo-referenced with the same coordinate system of WGS_1984_UTM_Zone_37N. The AHP model was employed to assign comparative importance to each flood-influencing factor. This data was then used in a weighted overlay method in ArcGIS (version 10.8) to create a flood susceptibility map of the study area. Microsoft Excel (version 2016) was utilized extensively for AHP analysis. The general workflow followed by this study is represented in Figure 2.2.

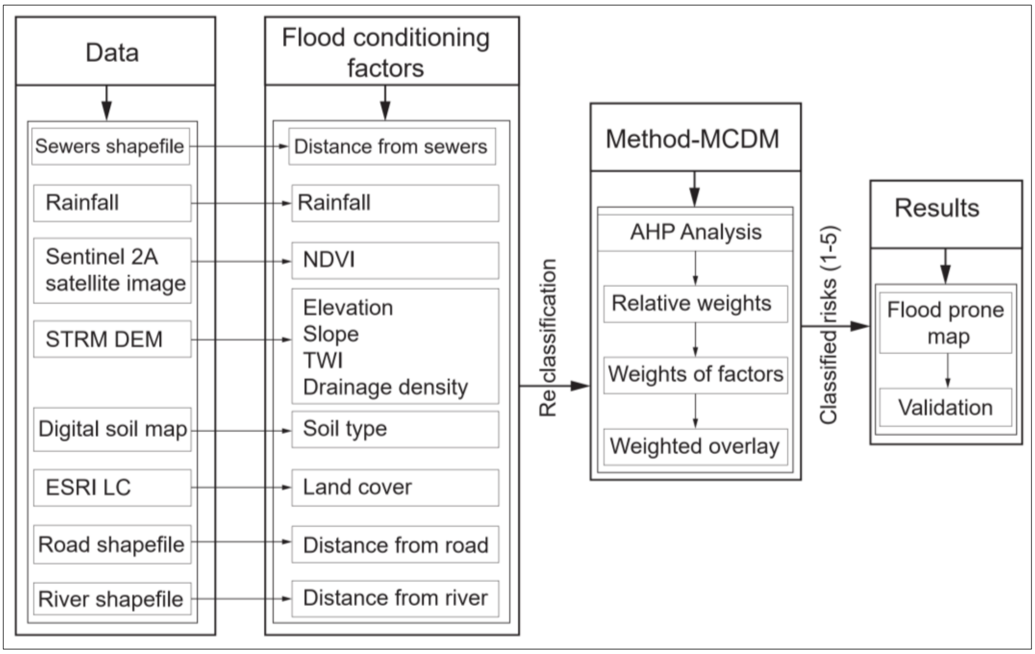

Figure 2.2: Flow chart of the methodology used to map flood-prone areas

2.2.2.1 Methods of Analyzing Flood Conditioning Factors

The process of selecting flood conditioning factors plays a vital role in identifying the most relevant features of areas prone to flooding. Evidence suggests that there is a correlation between floods and multiple natural and man-made contributing elements that influence the occurrence of flooding (Tehrany et al., 2014). It is important to have a better understanding of the various factors that cause flooding before producing a flood-prone map of any area (Kia et al., 2012). Establishing the relationship between selected factors is critical for mapping flood-prone areas (Liu & De Smedt, 2005). Accordingly, the present study considered eleven flood conditioning factors, and the techniques employed are outlined below.

To develop the elevation map, the DEM map of the study area was obtained, reclassified into five categories, and resampled to 10 x 10-meter grids based on previous studies (Das & Gupta, 2021; Mukherjee & Singh, 2020; Negese et al., 2022; Ogato et al., 2020; Yonas et al., 2022). Additionally, a slope map representing rates of elevation change according to steepness (Rahman et al., 2019) was generated from DEM. Then, based on the ACA structural plan`s (ACSPR, 2018b) land suitability class for development, the slope for the study area was reclassified and ranked into five categories. Furthermore, the DEM map was filled to remove sinks, ultimately resulting in flow direction and accumulation maps that served as the basis for preparing the TWI map.

The TWI map was processed using the ArcGIS Raster Calculator and Hydrology modules of Spatial Analyst as well as Equation 2.1 as formulated by Moore et al. (1991). Moreover, the corresponding DEM was employed to generate flow direction, flow accumulation, slope in degrees, the radius of a slope, and a tan slope.

$$TWI = Ln\left(\frac{As}{\tan\beta}\right) \qquad \text{Equation: 2.1}$$

Where, $'As'$ represents the area of catchment (km/km^2) and $'\beta'$ represents the slope in degrees. There is a direct correlation between flood risk and TWI, where the greater the TWI, the greater the flood risk could be. The classification of TWI was done based on previous research by Ali et al. (2020); Das and Gupta (2021); Ogato et al. (2020).

To develop a rainfall map, rainfall data were collected from eight nearby rain gauge stations besides the single most reliable rain gauge station available in the study area (NMA, 2022). Excel-based rainfall data obtained from the NMA of Ethiopia was imported into ArcGIS 10.8. The Inverse Distance Weighted (IDW) with a 10 x 10 m grid cell size was processed as an interpolation tool to create a continuous surface model of total annual precipitation for the study area delimited by a shape file representing its boundaries. It is then, classified into five classes using Equal Intervals.

The study area's LC was extracted from an ESRI website, *https://livingatlas.arcgis.com/Landcover/ (acquired on December 20, 2022)* with a 10 x 10-meter grid resolution. Then, the various land uses were attributed to an ArcGIS environment. According to the research conducted by Allafta and Opp (2021); Das and Gupta (2021); Negese et al. (2022); Ogato et al. (2020). LC was classified into five categories (forest, grassland, cultivated land, built-up cover, and water feature), and each was assigned a level of vulnerability ranging from very low to very high to flooding.

A Sentinel 2A satellite image was acquired from the USGS website (http://earthexplorer.usgs.gov/) (accessed on December 20th, 2022) and was utilized to generate the NDVI map. Equation 2.2 was applied in the ArcGIS environment to calculate the NDVI. The NDVI values were classified into five classes of susceptibility to flooding, including very high, high, moderate, low, and very low based on results from Ali et al. (2020); Negese et al. (2022).

$$NDVI = \frac{NIR - RED}{NIR + RED} = \frac{Band\ 8 - Band\ 4}{Band\ 8 + Band\ 4}$$ Equation: 2.2

The distance from the river map was generated from the shapefile of the river obtained from the ACA. The Euclidean Distance function from the ArcGIS Spatial Analyst Tools was employed to construct the raster map. Then, distance from the river was investigated to determine the flood risk at different distances from rivers based on the classifications done by Rimba et al. (2017); Das and Gupta (2021); Mukherjee and Singh (2020); Negese et al. (2022); Toosi et al. (2019).

The distance from the road was developed by utilizing the road shapefile from ACA, and the missing road information was added by digitizing high-resolution Google Earth Pro-Satellite Imagery (Version 7.3.6). The distance from the road was developed using the Euclidean distance in ArcGIS Spatial Analyst Tools and was employed as a criterion to categorize flood proneness into five, based on the findings of Mukherjee and Singh (2020); Swain et al. (2020); Tehrany; et al. (2017).

The drainage density map was developed by applying the Line Density tool from the ArcGIS Spatial Analyst Tools from a line density network. Based on the categorizations of Ali et al. (2020); Das and Gupta (2021); Lin et al. (2019); Negese et al. (2022), the drainage density of the study area was classified into five classes. Drainage density refers to the proportion of stream length within a watershed relative to its area (Kalédjé et al., 2019; Nsangou et al., 2022). Higher density values are associated with increased flood potential and thus underscore the importance of drainage density in flood occurrence (Nsangou et al., 2022).

The soil map of the study area was obtained from the WLRC and converted into a raster in the ArcGIS environment for further processing. Based on classification from Negese et al. (2022); Ogato et al. (2020), this study analyzed the varying levels of susceptibility to flooding across five distinct soil types; Eutric Cambisols, Eutric Nitisols, Chromic Luvisols, Leptosols, and Chromic Vertisols.

Sewer systems are artificial drains designed to transport excessive runoff or stormwater to facilities for treatment or disposal purposes (Ramesh & Iqbal, 2022). It is important to consider sewer drainage in flood-prone mapping in a city like Adama, as it is a top contributor to waterlogging in many areas due to the inability of sewer structures to contain or effectively drain water. A distance from the sewer drainage map was created using the shapefile data of sewer drainage obtained from the ACA. The Euclidean distance tool from ArcGIS Spatial Analyst Tools was applied to determine the distance from sewer drainage, which was then utilized as a classification criterion to categorize flood proneness into five levels, as outlined in Nsangou et al. (2022); Ramesh and Iqbal (2022).

2.2.2.2 Method of Analytical Hierarchy Processing (AHP)

The AHP techniques developed by Saaty (1987) were used for determining the priorities of multiple criteria decision problems in flood analysis. In urban flood-prone area analysis, AHP was used for multi-criteria decisions by many researchers: Aydin and Birincioğlu (2022); Balica et al. (2012); Lin et al. (2019); Negese et al. (2022); Ramesh and Iqbal (2022); Rimba et al. (2017).

AHP analysis was implemented to quantify the comparative significance of flood-conditioning factors. In this process, a matrix of pairwise comparisons was computed (Table 2.6), followed by its normalization and weighted assignment of the factors (Table 2.7). To check the consistency, a further evaluation was carried out (Table 2.8) following the reclassification of each conditioning factor as presented in Figure 2.8.

As recommended by Saaty (1987) the succeeding procedures were used to determine relative weights to each flood-conditioning factor including:

1. The matrix of pair-wise comparisons is constructed based on Saaty's 1 to 9 scale, where each flood-conditioning factor is represented in Table 2.3.
2. Then, each entry in the given matrix of pair-wise comparisons column was divided by its corresponding sum.
3. Finally, each weight was determined by dividing the total of each line in the normalized matrix by eleven (refer to Table 2.5).

Table 2.2: Saaty's pair-wise comparison scale(adapted from Saaty, 1987)

Intensity of importance	Degree of preference	Explanation
1	Equal importance	Two elements contribute equally to the objective
3	Moderate importance	Experience and judgment slightly favor one parameter over another
5	The strong or essential importance	Experience and judgment strongly favor one activity over another
7	Very strong importance	One parameter is favored very strongly and is considered superior to another; its dominance is demonstrated in practice
9	Extreme importance	The evidence favoring one parameter as superior to another is of the highest possible order of affirmation
2,4,6,8	Intermediate values	When parameters that are very close in importance

After calculating the weights of each factor related to flood proneness, a consistency index (CI) check was computed using Equation 2.3 developed by Saaty (1987), and if the comparison was accurate.

$$CI = \frac{\lambda_{\max - n}}{n - 1}$$ Equation:2. 3

Where,$'n'$stands for the number of factors being examined, and 'λ' max represents the maximum eigenvalue of the comparison pairwise matrix.

The following steps were used to compute the maximum Eigenvalue (λ_{max}) of the comparison pair-wise matrix (Saaty, 1987).

1. Multiplying each column value (in the non-normalized matrix) by the weight criteria
2. The rows' values are added to calculate the weighted sum
3. Weighting each criterion value based on its weighted sum value, and
4. The weighted sum of the mean with regard to the criteria weights.

Then, the calculated consistency ratio (CR) which demonstrates the validity of Saaty (1987) comparison was computed using Equation 2.4.

$$CR = \frac{CI}{RI}$$ Equation: 2.4

According to Saaty (1987), if the consistency ratio is less than 0.10, the matrix of pair-wise comparisons is considered consistent, however, if it is greater or equal to 0.10, insufficient consistency is present and the procedure must be iterated several times until the CR value drops below this threshold. Table 2.3 presents the random consistency index to the matrix size.

Table 2.3: Random consistency index (adopted from Saaty (1987)

Size of matrix	1	2	3	4	5	6	7	8	9	10	11
Random consistency index	0	0	0.58	0.9	1.12	1.24	1.32	1.41	1.45	1.49	1.51

2.2.2.3 Method of flood-prone map preparation

To develop a flood-prone map of the study area, all flood-conditioning factors were reclassified to the scale ranging from very low (1) to very high (5) and weighted via the Analytic Hierarchy Process. Afterward, ArcGIS's Spatial Analyst extension's weighted overlay technique was employed using Equation 2.5. This equation has been employed in several studies for detecting areas that have a high risk of flooding and consequently to map flood-prone areas (Aydin & Birincioğlu, 2022; Negese et al., 2022).

$$FP = \sum_{i=0}^{n} Xi * Wi \quad \text{Equation: 2.5}$$

Where; '*FP*' denotes flood-prone, '*n*' *the* number of decision-making criteria, '*Xi*' *the* specific normalized criterion, and '*WI*' the criterion's weight.

2.2.2.4 Validation of the flood-prone map

Validation is an essential step to demonstrate that the model outputs accurately reflect the real-world situation on the ground. Several previous studies have employed diverse approaches to validate their final output model. Hussain et al. (2021); Mahmoud and Gan (2018); Negese et al. (2022); Ogato et al. (2020) validate their models by comparing the model to the actual flood occurrence on the ground and conducting interviews with nearby residents. Similarly, to provide a better understanding and precision of the outcome, this study applied field-based visits and interviews with local dwellers before and after modeling. Additionally, an interview with experts from ACA and the flood inundation in the past were cross-checked with Google Earth Pro satellite imagery. This study examines the flood inundation in the study area during the rainy season of 2022 (June–September). The flood-prone areas were evaluated by comparing a final flood-prone map with 143 Ground Control Points (GCPs) using a handheld Global Positioning System (GPS) device (Model: BHCNav6). The GCPs were subsequently converted to shape files and superimposed onto the final overlay flood-prone map, as illustrated in Figure 2.4. By analyzing GCPs, Google Earth satellite imagery, and expert interviews, it was confirmed that the model accurately identified the high and very high flood-prone zones. This confirms the accuracy of the model, as shown in Figure 2.3.

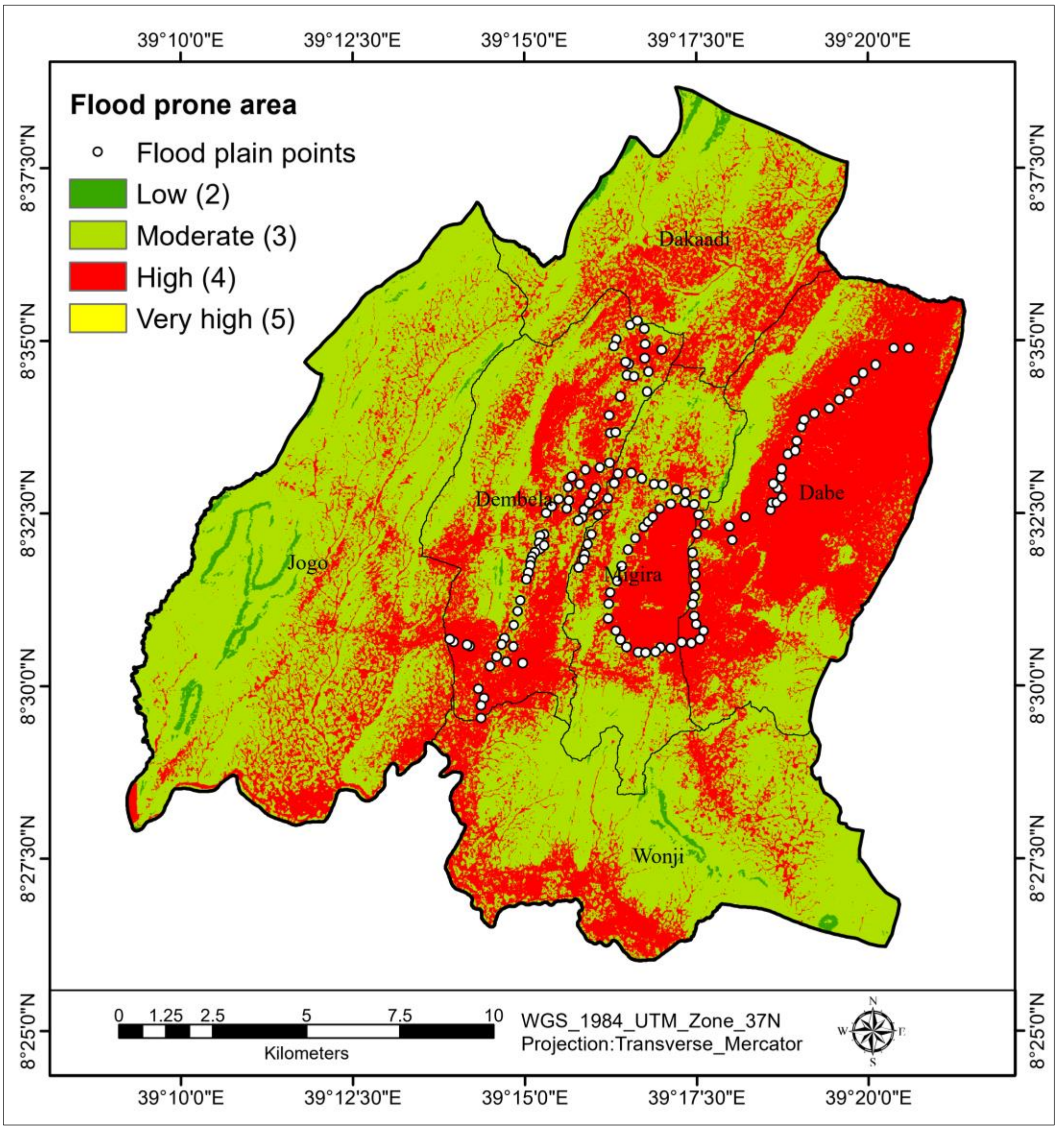

Figure 2.3: Flood-prone map and ground truth points(GCP)

2.3 Results and Discussion

2.3.1 Flood conditioning factors

The eleven flooding conditioning factors: their unit, classes, flood susceptibility, rating values, and weight of the study area as analyzed using ArcGIS (version 10.8) Multi-Criteria Decision-Making and Analytical Hierarchy Process are presented in Table 2.5.

Table 2.4: Flood conditioning factors: their classes, flood susceptibility, rating values, and weight

Number	Flood conditioning factors	Class	Flood susceptibility	Susceptibility rating	Weight (%)
1	Distance from Sewers Drainage(m)	< 50	Very low	1	18.74
		50 -100	Low	2	
		100 – 200	Moderate	3	
		200-500	High	4	
		> 500	Very high	5	
2	Topographic Wetness Index(TWI)	2.61 - 6.11	Very low	1	14.25
		6.11 - 8.11	Low	2	
		8.11 - 10.11	Moderate	3	
		10.11 - 12.11	High	4	
		12.11 - 21.56	Very high	5	
3	Elevation(m)	1441 – 1540	Very high	5	12.46
		1540 – 1640	High	4	
		1640 – 1740	Moderate	3	
		1740 – 1900	Low	2	
		1900 - 2048	Very low	1	
4	Slope (%)	0 – 5	Very high	5	12.79
		5 – 10	High	4	
		10 – 15	Moderate	3	
		15 – 20	Low	2	
		20 - 53.42	Very low	1	
5	Rainfall(mm)	695.10 - 787.23	Very low	1	9.62
		787.23 - 834.44	Low	2	
		834.44 - 877.45	Moderate	3	
		877.45 - 918.36	High	4	
		918.36 - 962.24	Very high	5	
6	Land cover (class)	Forest	Very low	1	9.50
		Grassland	Low	2	
		Cropland	Moderate	3	
		Built-up area	High	4	
		Water Body	Very high	5	
7	Normalized Difference Vegetation Index (NDVI)	-0.15-0.09	Very high	5	6.61
		0.09 - 0.11	High	4	
		0.11- 0.21	Moderate	3	
		0.21-0.33	Low	2	
		0.33- 0.46	Very low	1	
8	Distance from rivers(m)	0-500	Very high	5	4.66

		500-1000	High	4	
		1000-1500	Moderate	3	
		1500-2000	Low	2	
		2000-6598.19	Very low	1	
9	Distance from roads(m)	0-25	Very high	5	5.65
		25-50	High	4	
		50-100	Moderate	3	
		100-300	Low	2	
		300-6,953.42	Very low	1	
10	Drainage density(km/km^2)	0.91 - 1.5	Very low	1	3.10
		1.5 - 2.5	Low	2	
		2.5 - 3	Moderate	3	
		3 - 4	High	4	
		4 - 5	Very high	5	
11	Soil type (class)	Pellic Vertisols	Very high	5	2.63
		Eutric Leptosols	High	4	
		Calcaric Fluvisols	Moderate	3	
		Vitric Andosols and Mollic Andosols	Low	2	
		Fibric Cambisols	Very low	1	

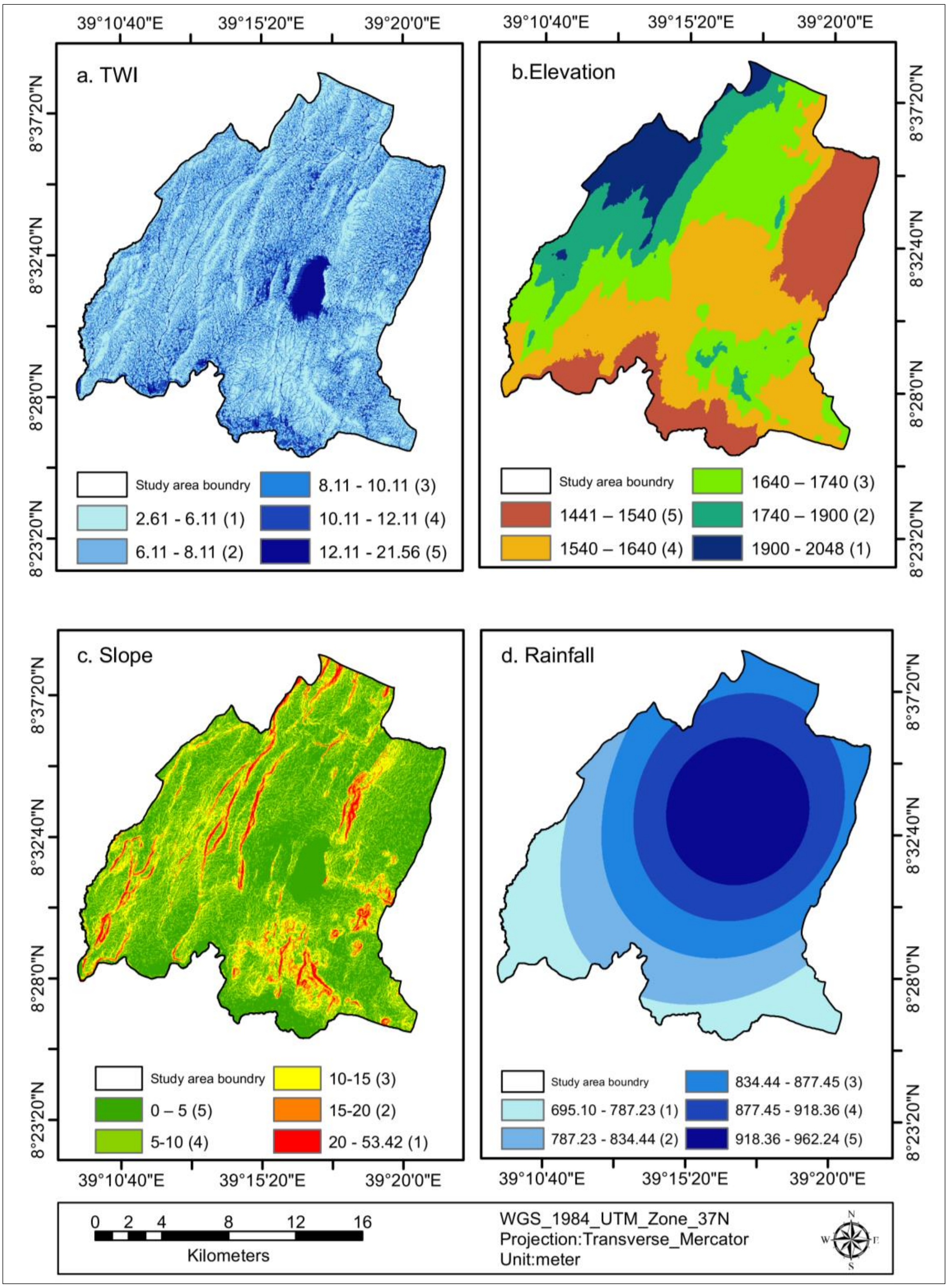

Figure 2.4: TWI(a), Elevation (b), Slope (c), Rainfall (d) flood conditioning maps

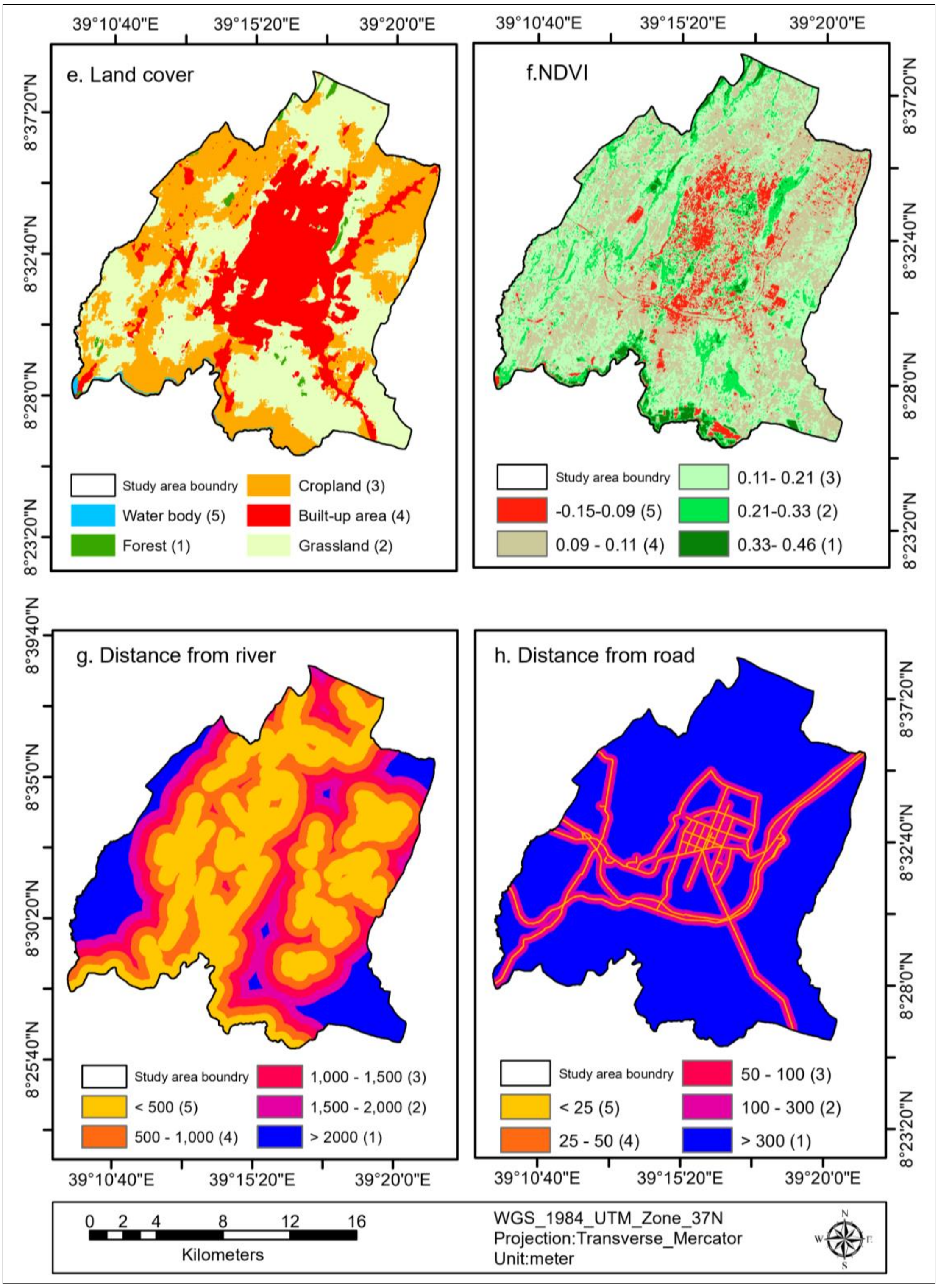

Figure 2.5: LC (e), NDVI (f), Distance from the river (g), and Distance from road (h) flood conditioning maps

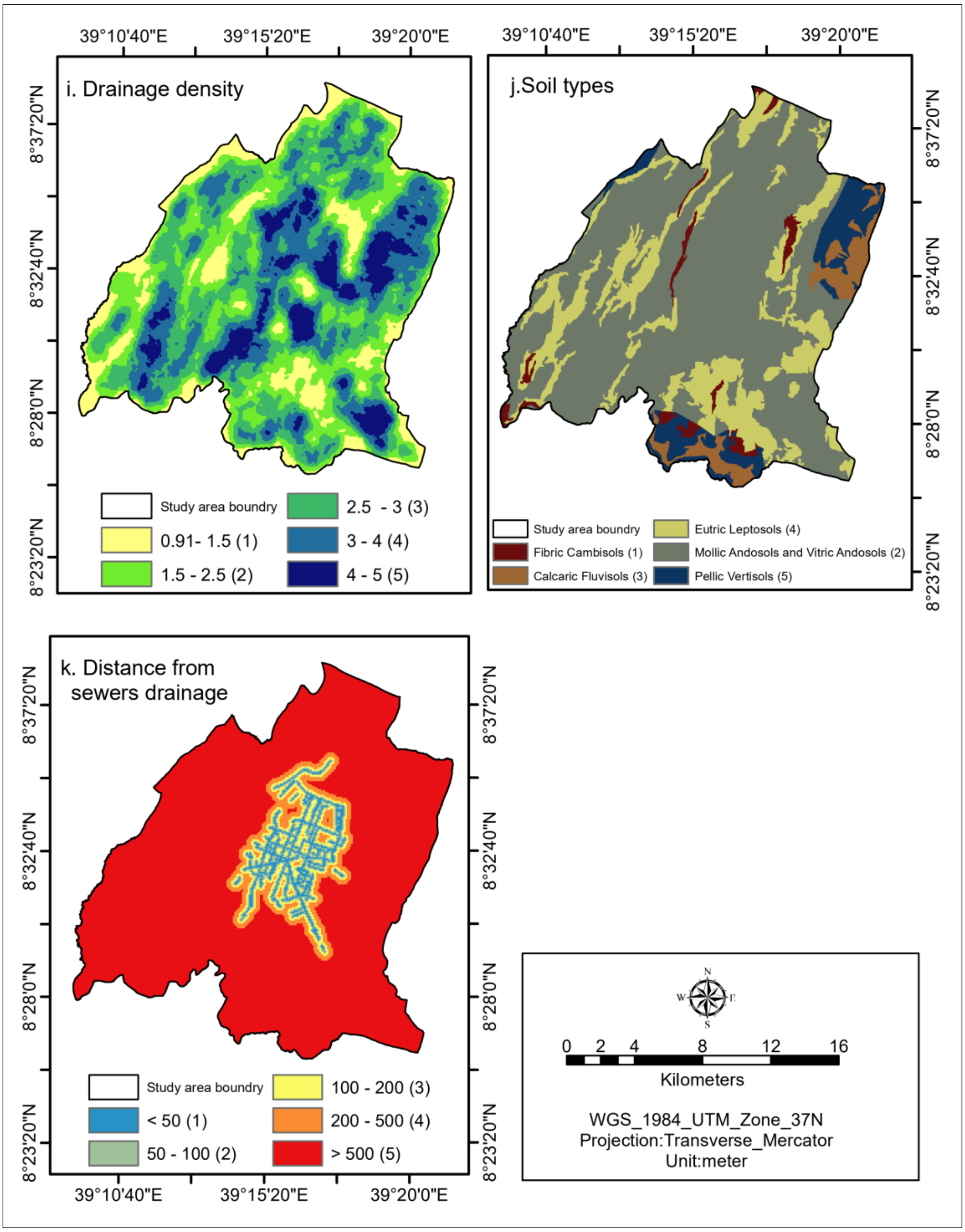

Figure 2.6: Drainage density (i), soil type (j), and distance from sewers drainage(k) flood conditioning maps

2.3.1.1 Topographic wetness index

The TWI of the study area ranged from 2.61 to 21.56 and was reorganized into five classes: 2.61 - 6.11 (very low), 6.11 - 8.11 (low), 8.11 - 10.11 (medium), 10.11 - 12.11 (high), and 12.11 - 21.56 (very high), which covers 38.31%, 36.64 %, 12.28%, 7.05%, and 5.73%, respectively as represented in Figure 2.5a and Table 2.5. About 25% of the area has moderate to very high TWI. The implication of these is that a quarter of the study area has a high probability of accumulating water or flowing downwards, exacerbated by the impervious area and urban settlements. The present study was consistent with previous studies conducted by Das and Gupta (2021); Hong et al. (2018) which employed the TPI to investigate the impact of topography on runoff and accumulation capacity at various locations within a watershed. TWI has been demonstrated to be positively associated with flood severity, suggesting high TWI values can lead to increased flooding risks (Lee & Rezaie, 2022).

2.3.1.2 Elevation

The elevation of the study area ranged from 1441 to 2048 meters above sea level. In line with this, it is classified into five classes, as represented as, 1441 – 1540 (very high), 1540 – 1640 (high), 1640 – 1740 (moderate), 1740 – 1900 (low), and 1900 – 2048 (very low), which covers 13.56%, 34.86%, 30.11%, 16.74%, and 4.73% respectively. This result suggests that approximately 78.53% of the area is at a moderate to very high risk for flooding due to its low-lying and flat terrain (Figure 2.5b). Elevation plays an important role in flooding, with lower and flatter areas displaying higher flood risk compared to higher elevations as they are more vulnerable to higher river discharges which lead to faster flooding (Hong et al., 2018; Lee & Rezaie, 2022; Tehrany; et al., 2017).

2.3.1.3 Slope

The slope of the study area was reclassified and ranked into five categories as shown in Figure 2.5c and Table 5: 0–5 (very high), 5–10 (high), 10-15 (moderate), 15-20 (low), and 20–53.42 (very low), which cover 63.28% (19740.22 ha), 24.43% (7622.16 ha), 6.55% (2042.26 ha), 2.85% (888.88 ha), and 2.89% (900.42 ha), respectively. Results of this slope class show that nearly 94.26% of the study area has moderate to very high susceptibility to flooding. Gentle slopes have been identified as a major contributor to flooding in an urban environment (Meraj et al., 2015). The slope is a principal factor influencing the spread of surface water and its propensity for flooding (Wang et al., 2015). Specifically, flat lands with gentle slopes are more prone to flooding than mountainous areas with steeper gradients, which impede the collection of water.

2.3.1.4 Rainfall

The rainfall map was classified into five classes using Equal Intervals. The rainfall classification results demonstrate that 2.54%, 18.8%, 20%, 29.75%, and 28.91% of the evaluated areas belonged to categories very low, low, moderate, high, and very high, respectively, as presented in Figure 2.5d and Table 2.5. Rainfall is a significant contributor to flood formation due to the massive runoff caused by heavy rain (Allafta & Opp, 2021; Hong et al., 2018). The prevalence of hard-scape surfaces, such as rooftops, roads, and parking lots, in built-up areas reduces the infiltration capacity of the ground and it is directly proportional to flooding (Tehrany; et al., 2017).

2.3.1.5 Land cover (LC)

The LC of the study area was classified as water body (very high), built-up area (high), cropland/bare land (moderate), grassland (low), and forest/dense vegetation (very low) flood susceptibility. The spatial coverage of LC represents 12457.28 ha (39.8%), 10609.28 ha (33.9%), 7871.34 ha (25.15%), 248.32 ha (0.79%), and 113.26 ha (0.36%), as grassland, cropland/bare land, built-up area, forest, dense vegetation, and water body, respectively (Figure 2.6e and Table 2.5). Based on the LC, about 59.41% of the study areas have moderate to very high flood susceptibility due to LC. The findings from Migosi (2014); Nsangou et al. (2022); Ogato et al. (2020) demonstrated that LC changes, such as urban growth, impervious surfaces, and decreased forest coverage, attributed to an increase in flood incidents. The findings of the current study indicate that urbanized areas, cropland/bare land, and waterbodies experienced a greater potential for flooding compared to forests/dense vegetation and grasslands, which can infiltrate water into the ground and reduce flood risk. This finding is consistent with the finding that, in cities, stormwater run-off is common whereas forested areas function as an effective buffer against inundation (Mojaddadi et al., 2017; Tehrany; et al., 2017). Additionally, Nsangou et al. (2022); Rahman et al. (2021); Rogger et al. (2017), have highlighted that the presence of vegetation facilitates infiltration, effectively reducing the potential for flooding.

2.3.1.6 Normalized Difference Vegetation Index (NDVI)

The study area's NDVI value ranged from -0.15 to 0.46 and was classified into five classes: -0.15-0.09 (very high), 0.09-0.11 (high), 0.11-0.2 (moderate), 0.21-0.33 (low), and 0.33-0.46 (very low) to flood-prone. According to Figure 2.6f and Table 2.5, the study areas were classified based on their spatial catchment in terms of NDVI. The results indicate that 1584.87 ha (5.07%) are classified as very high flood-prone areas, while 7061.72 ha (22.58%) fall into the high flood-prone category. Additionally, the study identifies 17651.84 ha (56.45%) as moderate flood-prone areas, with 4061.48 hectares (12.99%) categorized as low flood-prone areas. Finally, 909.01 ha (2.91%) are classified as very low flood-prone areas. The NDVI results of this study revealed that 84.1% of the study area has very low to moderate NDVI, which increases the probability of flooding. This finding agrees with Khosravi et al. (2016), who found a negative relationship between NDVI and flooding; specifically, higher NDVI values indicate a lower probability of flooding, and lower NDVI values significantly increase the risk. In addition, Lin et al. (2019) stated that a higher NDVI is an indicator of the density and condition of vegetation, which can impact rainwater infiltration.

2.3.1.7 Distance from rivers

As represented in Figure 2.6g and Table 2.5, distance from the river of the study area was categorized into five classes: very high, high, moderate, low, and very low flood proneness at distances of 500 m, 1000 m, 1500 m, 2000 m, and > 2000 m, respectively. About 77.75% (91,214.77 ha) of the study area has medium to very high flood susceptibility as it was close to a river. These findings were consistent with previous studies by Elkhrachy (2015); Mahmoud and Gan (2018); Mukherjee and Singh (2020), who suggested that the probability of flooding risk is higher in areas closer to rivers as a result of overflow in heavy rain. In addition, Das and Gupta (2021) stated that hydro-geomorphic response plays a role in the severity of flooding relative to the vicinity of bodies of water.

2.3.1.8 Distance from roads

Distance from the road of the study area was categorized into five classes: very high, high, moderate, low, and very low flood proneness at distances of 25 m, 50 m, 100 m, 300 m, and >300 m, respectively. Based on the distance to river measurements indicate that 76.39% (23908.16 ha) was very low flood proneness, 13.6% (4255.41 ha) was low, 4.49% (1406.64 ha) was moderate, 2.64% (826.91 ha) was high, and 2.87% (898.46 ha) was very high flood proneness as distance from road increased from 25 m up to > 300 m, respectively (Figure 2.6h and Table 2.5). This indicates that about 3,132.01 ha located near roads are at a higher risk of flooding due to their reduced environmental ability to percolate water through the soil surface into the subsurface layers. This result is consistent with previous research conducted by Mukherjee and Singh (2020); Shuster et al. (2005); Tehrany; et al. (2017), which found that impervious surfaces such as roads decrease terrain infiltration capacity, increase surface water runoff due to decreased capability of rainwater percolation through soils and consequently have considerable influence over flooding in urban areas.

2.3.1.9 Drainage density

The drainage density of the study area ranged from 0.91 to 5 and was classified into five classes: 0.91–1.5 (very low), 1.5–2.5 (low), 2.5–3 (moderate), 3–4 (high), and 4-5 (very high), respectively, as shown in Figure 7i and Table 5. The study revealed that 13.92%, 25.01%, 29.77%, 22.03%, and 9.26% of the study area are very low, low, medium, high, and very high prone to flooding, respectively. This implies that 61% of the study area is at risk of flooding due to a high drainage density and low infiltration, which can lead to accelerated water flows that contribute to flooding. This result is consistent with a previous study conducted by Alemayehu (2007); Gashaw and Legesse (2011), who explained that factors such as slope, bedrock form, and long-range and local fissure patterns have an impact on the region's drainage density and consequently result in higher surface runoff areas that are at risk for flooding. Rimba et al. (2017); Dragičević et al. (2019); Kumar; et al. (2007) also agreed with the correlation between high drainage density and an increase in areas prone to flooding due to fast water entering channels without infiltration or percolation.

2.3.1.10 Soil type

In the study area, five soil classes were identified: Fibric Cambisols (very low flood susceptibility), Vitric Andosols and Mollic Andosoks (low), Calcaric Fluvisols (moderate), Eutric Leptosols (high) and Pellic Vertisox (very high). As illustrated in Figure 2.7j and Table 2.5, the spatial catchment of soil cover was 2803.63 ha (8.97%) of very high, 6578.38 ha (21.04%) of high, 1379 ha (4.41%) of moderate, 20429.21 ha (65.33%) of low, and 80.38 ha (0.26%) of very low susceptibility to flooding. This implies that about 34.42% of the study area was found to be moderate to very highly prone to flooding due to soil types. The soil types in Adama City were characterized as shallow depth, presence of gravel, shrink-swell cycles, and inadequate drainage leading to increased erosion (Legas, 2020; Woldechirkos, 2016). The findings of this research aligned with previous studies conducted by Mojaddadi et al. (2017); Rimba et al. (2017), which underline the influence of soil type on local water storage, permeability, drainage, and rainfall patterns. The findings of Ouma and Tateishi (2014), also supported that the infiltration rates of different soil types affect flooding probabilities when the bottoming capacity is reduced. As the absorption potential of soil decreases, surface runoff increases, thereby increasing flooding.

2.3.1.11 Distance from sewer drainage

The distance from sewer drainage to the study area was categorized into five classes, including very low, low, moderate, high, and very high flood proneness at distances of 50 m, 100 m, 200 m, 500 m, and > 500 m, respectively. The findings indicated that within the study area, 929.93 ha (2.97%) exhibited a very low flood proneness, 1188.87 ha (3.8%) had a low proneness, and 1117.86 ha (3.57%) fell into the moderate category, while 1578.68 ha (5.04%) and 26499.26 ha (84.62%) had a high and very high flood proneness, respectively (Figure 2.7k and Table 2.5). This implies that about 93.23% of the study area is susceptible to flooding due to inadequate sewer drainage. This finding aligns with previous research conducted by Jensen and Khalis (2020), which asserts that as the distance from sewer systems increases, the susceptibility to flooding also increases. In areas with inadequate sewer infrastructure, heavy rainfall can lead to blockages in the sewer system, exacerbating flooding issues. In addition, Louw et al. (2019) identified that inadequate sewage management in urban areas can result in infrastructure blockages, further exacerbating flood vulnerability in surrounding regions. Conversely, locations in proximity to open drains or sewers have a lower vulnerability to flooding, as these structures help mitigate surface runoff and facilitate rainwater drainage into the sewer system. On the other hand, the further an area is from the sewer system, the greater its vulnerability to flooding becomes.

2.3.2 Analytical Hierarchy Processing (AHP)

The weight for all flood-conditioning factors was taken into consideration as shown in Table 2.5, reflecting the relative influence each one as follows: distance from sewer drainage (18.74%), TPI (14.25%), elevation (12.46%), slope (12.79%), rainfall (9.62%), LC (9.50%), NDVI (6.61%), distance from road (5.65%), distance from the river (4.66%), drainage density (3.10%), and soil type (2.62%). To compute the consistency index and the consistency ratio, Equations (2.3) and (2.4), respectively, were employed using the highest eigenvalue of 11.81 and several flood conditioning factors n = 11, as well as the random index 1.51, to calculate the CR as 0.05 (5%). According to previous research by Aydin and Birincioğlu (2022); Saaty (1987); Xiaoxin et al. (2018), random index variations depend on several factors tested which is equal to 1.51 when n = 11 is considered and a consistent ratio of less than 0.1(10%) was accepted in this study, and then reclassified into 1 to 5 classes (Figure 2.7) to develop the final flood prone map.

Table 2.5:Pair-wise comparison matrix for selected flood-conditioning factors for the study area

Factors	**DSD**	**TWI**	**El**	**Sl**	**Rf**	**LC**	**NDVI**	**Driver**	**Droad**	**DD**	**ST**
DSD	1	3	3	2	2	2	3	3	2	3	4
TWI	1/3	1	2	2	2	2	3	3	2	3	4
El	1/3	1	1	1	3	2	3	3	1	4	5
Sl	1/2	1/2	1	1	2	2	3	3	3	4	4
Rf	1/2	1/2	1/3	1/2	1	2	2	3	2	3	4
LC	1/2	1/2	1/2	1/2	1/2	1	2	3	3	4	4
NDVI	1/3	1/3	1/3	1/3	1/2	1/2	1	2	2	3	4
Driver	1/3	0	1/3	1/3	1/3	1/3	1	1	1	2	3
Droad	1/2	1/2	1	1/3	1/2	1/3	1/2	1	1	2	2
DD	1/3	1/3	1/4	1/4	1/3	1/4	1/3	1/2	1/2	1	1
ST	1/4	1/4	1/5	1/4	1/4	1/4	1/4	1/3	1/2	1	1
Sum	4.92	7.75	9.95	8.50	12.42	12.67	18.58	22.83	18.00	30.00	36.00

Table 2.6: Normalized Pair-wise Comparison Matrix

Factors	**DSD**	**TWI**	**El**	**Sl**	**Rf**	**LC**	**NDVI**	**Driver**	**Droad**	**DD**	**ST**	**Sum**	**CW**	**CW (%)**
DSD	0.2034	0.3871	0.3015	0.2353	0.1611	0.1579	0.1614	0.1314	0.1111	0.1000	0.1111	**2.0613**	**0.1874**	**18.7**
TWI	0.0678	0.1290	0.2010	0.2353	0.1611	0.1579	0.1614	0.1314	0.1111	0.1000	0.1111	**1.5671**	**0.1425**	**14.2**
El	0.0678	0.0645	0.1005	0.1176	0.2416	0.1579	0.1614	0.1314	0.0556	0.1333	0.1389	**1.3706**	**0.1246**	**12.5**
Sl	0.1017	0.0645	0.1005	0.1176	0.1611	0.1579	0.1614	0.1314	0.1667	0.1333	0.1111	**1.4073**	**0.1279**	**12.8**
Rf	0.1017	0.0645	0.0335	0.0588	0.0805	0.1579	0.1076	0.1314	0.1111	0.1000	0.1111	**1.0582**	**0.0962**	**9.6**
LC	0.1017	0.0645	0.0503	0.0588	0.0403	0.0789	0.1076	0.1314	0.1667	0.1333	0.1111	**1.0446**	**0.0950**	**9.5**
NDVI	0.0678	0.0430	0.0335	0.0392	0.0403	0.0395	0.0538	0.0876	0.1111	0.1000	0.1111	**0.7269**	**0.0661**	**6.6**
Driver	0.0678	0.0430	0.0335	0.0392	0.0268	0.0263	0.0269	0.0438	0.0556	0.0667	0.0833	**0.5129**	**0.0466**	**4.7**
Droad	0.1017	0.0645	0.1005	0.0392	0.0403	0.0263	0.0269	0.0438	0.0556	0.0667	0.0556	**0.6210**	**0.0565**	**5.6**
DD	0.0678	0.0430	0.0251	0.0294	0.0268	0.0197	0.0179	0.0219	0.0278	0.0333	0.0278	**0.3407**	**0.0310**	**3.1**
ST	0.0508	0.0323	0.0201	0.0294	0.0201	0.0197	0.0135	0.0146	0.0278	0.0333	0.0278	**0.2894**	**0.0263**	**2.6**
												11	**1**	**100**

Where; *CW* criteria weigh

Table 2.7: Calculating the consistency of pairwise comparison (CR = 0.05)

Factors	DSD	TWI	El	Sl	Rf	LC	NDVI	Driver	Droad	DD	ST	**WSV**	**CW**	WSV/CW
DSD	0.1874	0.4274	0.3738	0.2559	0.1924	0.1899	0.1982	0.1399	0.1129	0.0929	0.1052	**2.2760**	0.1874	**12.15**
TWI	0.0625	0.1425	0.2492	0.2559	0.1924	0.1899	0.1982	0.1399	0.1129	0.0929	0.1052	**1.7415**	0.1425	**12.22**
El	0.0625	0.0712	0.1246	0.1279	0.2886	0.1899	0.1982	0.1399	0.0565	0.1239	0.1316	**1.5148**	0.1246	**12.16**
Sl	0.0937	0.0712	0.1246	0.1279	0.1924	0.1899	0.1982	0.1399	0.1694	0.1239	0.1052	**1.5364**	0.1279	**12.01**
Rf	0.0937	0.0712	0.0415	0.0640	0.0962	0.1899	0.1322	0.1399	0.1129	0.0929	0.1052	**1.1397**	0.0962	**11.85**
LC	0.0937	0.0712	0.0623	0.0640	0.0481	0.0950	0.1322	0.1399	0.1694	0.1239	0.1052	**1.1048**	0.0950	**11.63**
NDVI	0.0625	0.0475	0.0415	0.0426	0.0481	0.0475	0.0661	0.0933	0.1129	0.0929	0.1052	**0.7601**	0.0661	**11.50**
Driver	0.0625	0.0475	0.0415	0.0426	0.0321	0.0317	0.0330	0.0466	0.0565	0.0619	0.0789	**0.5348**	0.0466	**11.47**
Droad	0.0937	0.0712	0.1246	0.0426	0.0481	0.0317	0.0330	0.0466	0.0565	0.0619	0.0526	**0.6626**	0.0565	**11.74**
DD	0.0625	0.0475	0.0311	0.0320	0.0321	0.0237	0.0220	0.0233	0.0282	0.0310	0.0263	**0.3597**	0.0310	**11.62**
ST	0.0468	0.0356	0.0249	0.0320	0.0240	0.0237	0.0165	0.0155	0.0282	0.0310	0.0263	**0.3047**	0.0263	**11.58**
													L.max=	**11.81**

Where: *WSV* weighted sum value, *CW* criteria weight

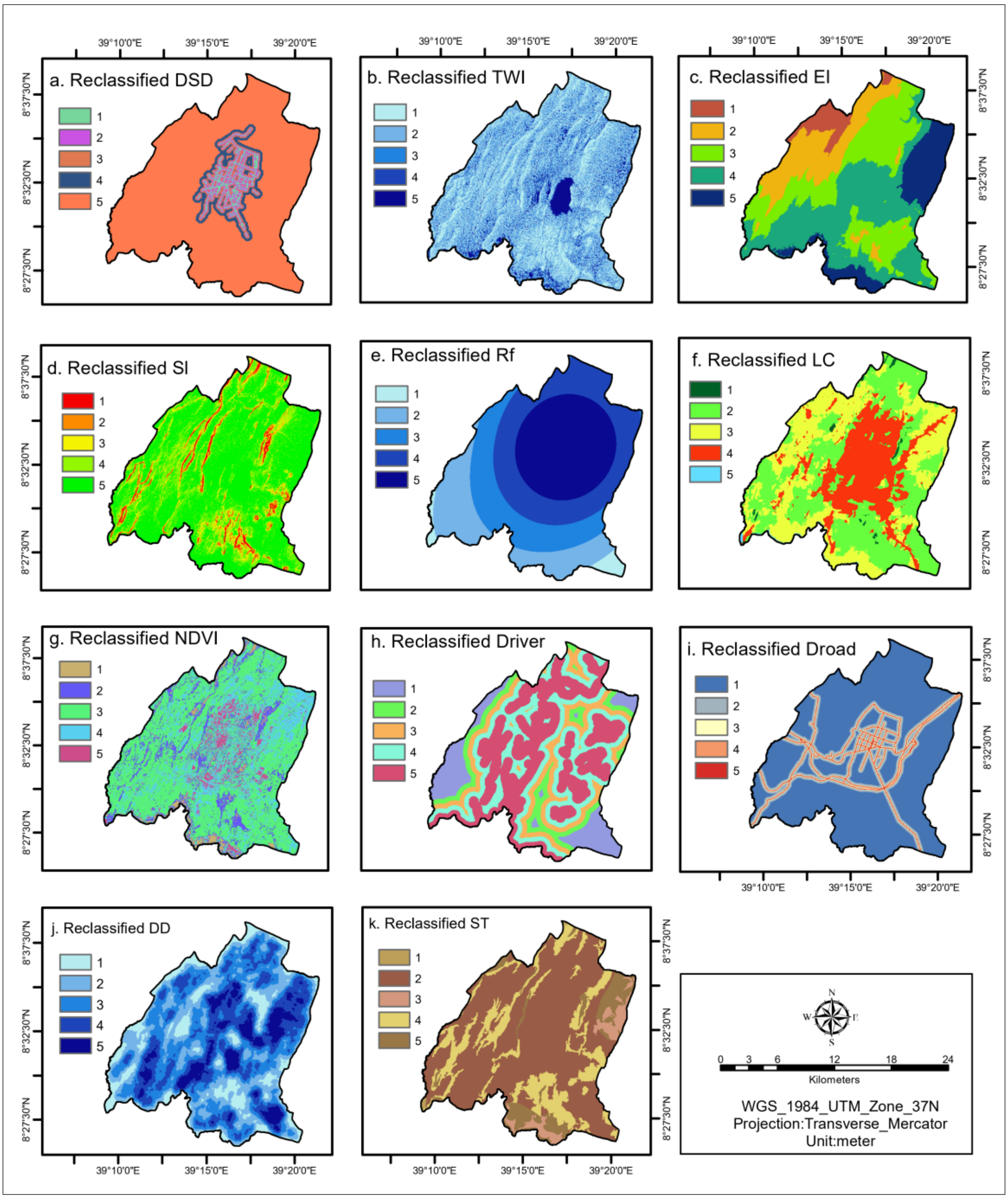

Figure 2.7: Reclassification of flood conditioning factors (a-k)

2.3.3 Flood-prone area map of the study area

The final flood-prone areas map indicates the degree of the study area's susceptibility to flooding which is developed through the combination of eleven flood-controlling factors as illustrated in Figure 2.9. Through employing weighted overlay analysis, the result has categorized the study area into four classes based on flood-prone levels: low (2), moderate (3), high (4), and very highly prone (5) to flooding. Table 2.9 displays the spatial distribution of each flood-prone class in the catchments. In terms of flood susceptibility, the study area was grouped into four levels: low (1.31%, 406.83 ha), moderate (61.27%, 19056.31 ha), high (37.37%, 11623.09 ha), and very high (0.05%, 14.72 ha). It was found that approximately 98.69% of the study area exhibits a moderate to very high susceptibility to flooding.

The flood-prone map shows that a significant portion of the urban catchment, including the expansion site located to the east of the city along the highway and rail line to Dire Dawa-Djibouti corridor, as well as the northern and southeastern areas along Arsi Road, are prone to flooding. Specifically, areas with flat surfaces, low-lying flat terrain, proximity to rivers, built-up areas, and those adjacent to highway roads are characterized as high and very highly prone to flooding.

On the other hand, the remaining 1.31% of the study area shows low susceptibility to flooding. These low flood-prone zones are primarily situated in the upper section of the mountains surrounding the city. They are distinguished by their steep slopes, higher elevations, distance from rivers and road networks, and low drainage density areas, as depicted in Figure 2.9. This finding is consistent with the findings of a flood-prone area identification study conducted by Tehrany; et al. (2017) ; Argaz et al. (2019); Desalegn and Mulu (2021); Edamo et al. (2022); Negese et al. (2022).

Table 2.10 presents the spatial coverage of different catchments in the study area, including their respective areas and percentages. The finding indicates that the Dabe catchment possesses 0.25% low, 71.77% high, and 27.95% moderate. The factors contributing to flooding in the Dabe catchment are diverse and include insufficient sewer drainage, flat terrain encircled by plateaus and mountain ranges, high drainage density, and Pellic vertisols that contribute to flooding. In addition, the Dakaadi catchment claims higher levels of susceptibility, with 30.79% high, 67.50% moderate, and 1.71% low prone to flooding. These flood-prone zones have inadequate sewer drainage, low-lying areas, proximity to highway roads, and proximity to rivers.

Similarly, the Dembela catchment shows 0.02% very high coverage, 50.86% high, 48.91% moderate, and 0.2% low-prone to flooding. This area is characterized by deforestation and rapid urbanization, resulting in land cover changes in built-up areas and highly impervious surfaces. The Jogo catchment records 17.91% high coverage, 79.57% moderate coverage, and only 2.53% low-prone flooding. The closeness to river networks, highway roads, and deforestation were the triggering factors of recurring inundation.

The study also revealed that the Migira catchment has 0.001% as very high, 42.63% as high, 56.88% as moderate, and 0.49% as low prone to flooding. These results were attributed to various factors such as extensive low-lying flat terrain, minimal slope variation, a highly built area, proximity to rivers and roads, and a higher drainage density. Furthermore, in the Wonji catchment area, flood susceptibility levels were labeled as 25.67% high, 72.93% moderate, and 1.39% low. This area exhibits vulnerability due to inadequate sewerage drainage systems, deforestation, and rugged topographic features, which are the leading factors for flooding.

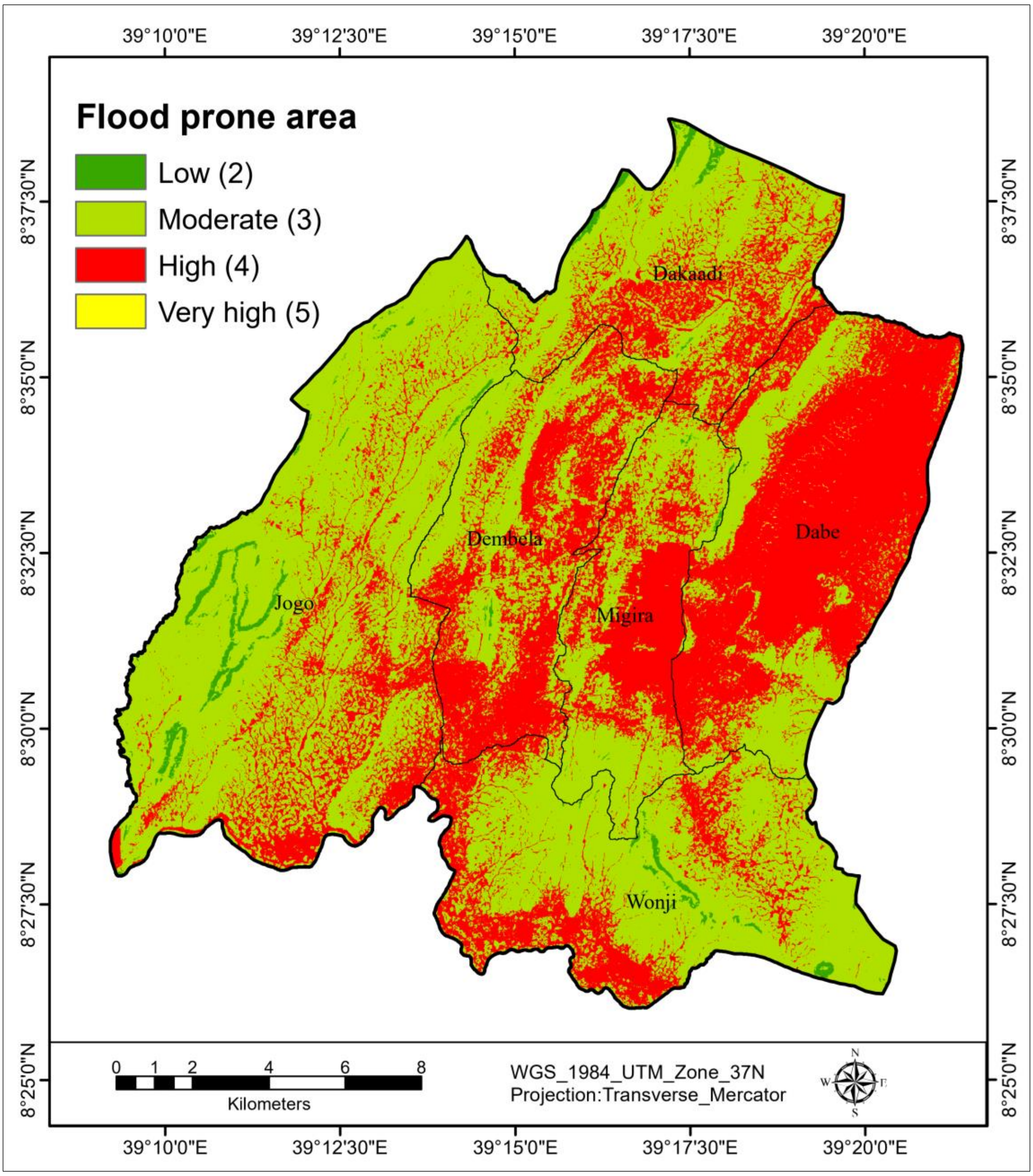

Figure 2.8: Flood-prone map of the study area

Table 2.8: Flood-prone level class pixels, area, and percentage of the study area

Flood prone level	Class pixels	Area (ha)	Percent (%)
Very high (5)	1472	14.72	0.05
High (4)	1162309	11623.09	37.37
Moderate (3)	1905631	19056.31	61.27
Low (2)	40683	406.83	1.31
Total	3110095	31100.95	100.00

Table 2.9: Flood-prone area of the study area by Catchment

Flood prone level	Catchment name											
	Dabe		Dakaadi		Dembela		Jogo		Migira		Wonji	
	ha	%	ha	%	ha	%	ha	%	ha	%	ha	%
Very high (5)	13.9	0.25	-	-	0.78	0.02	-	-	0.04	0.001	-	-
High (4)	4068.83	71.77	1175.06	30.79	2093.86	50.86	1598.43	17.91	1272.91	42.63	1390.5	25.67
Moderate (3)	1584.38	27.95	2575.85	67.50	2013.55	48.91	7102.08	79.57	1698.5	56.88	3950.85	72.93
Low (2)	2.27	0.04	65.29	1.71	8.37	0.2	225.56	2.53	14.75	0.49	75.46	1.39

2.4 Discussions

Mapping urban-prone areas offers numerous benefits for urban planning and disaster management. It provides a clear understanding of at-risk areas, allowing authorities to prioritize resources and develop targeted mitigation strategies. Accurate mapping helps identify vulnerable populations, tailor interventions, and assess infrastructure effectiveness for resilience enhancement. By integrating geospatial data, potential flood-prone areas for proactive decision-making. Sharing these maps with the public raises awareness and empowers communities to take proactive steps to reduce vulnerability.

Konrad (2003) stated that rapid urbanization increases the size and frequency of floods, putting communities at greater risk. Activities such as deforestation, land grading, and the unplanned construction of drainage networks amplify runoff, causing nearby streams to experience higher peak discharge and flood frequency. The rapid growth of urban populations seeking housing has resulted in unregulated and poorly organized development in flood-prone areas. As a result, urban areas have experienced extensive damage due to flooding. Various factors contribute to this problem, including the haphazard expansion of cities and the spontaneous creation of informal settlements on floodplains, without proper consideration for land use planning (Asiedu, 2020; Eldho et al., 2018; Salami et al., 2017b). Additionally, the changes in precipitation patterns due to climate change contributed to the severity of floods within cities (Serre et al., 2018). Thus, inadequate planning and insufficient drainage systems significantly contribute to urban flooding, which has devastating consequences for affected areas.

Deforestation and land grading lead to amplified water flow in streams as a result of rainfall, subsequently leading to heightened occurrences of severe flooding in adjacent streams. Urban development practices such as modifying stream channels and constructing infrastructure in flood-prone zones increase the risks of inundation and erosion, persisting even as development progresses (Konrad, 2003; Truu et al., 2021).

Ongoing urbanization and climate change are driving significant transformations in cities, leading to an elevated risk of flooding and heightened severity (Serre et al., 2018). The conversion of flood-prone areas into urban spaces has nearly doubled since 1985, resulting in increased exposure to flooding due to population growth and urban expansion (Andreadis et al., 2022; Serre et al., 2018). Recent studies have explained that urban flooding is increasing as a result of climate change (Manandhar et al., 2023). Consequently, a combination of changing climate, precipitation patterns, and rapid urbanization may necessitate adjustments in flood management strategies and decision-making processes (Daksiya et al., 2021).

The growing demand for housing in urban areas has led to unregulated and poorly organized development in flood-prone regions. As a consequence, urban areas have suffered extensive damage from flooding. Several factors, including the haphazard expansion of cities and the spontaneous creation of informal settlements on floodplains without adequate land use planning, contribute to this problem (Asiedu, 2020; Eldho et al., 2018; Salami et al., 2017b). Moreover, shifts in precipitation patterns due to climate change have also played a role in exacerbating the severity of floods within cities (Serre et al., 2018).

Insufficient planning and inadequate drainage systems significantly contribute to the occurrence and impact of urban flooding, which has devastating consequences for affected areas. The expansion of urbanization has resulted in the growth of flash flood-prone areas and floodplains. This expansion is influenced not only by the extent of impermeable surfaces but also by the spatial distribution of impervious surface coverage (Feng et al., 2021).

2.5 Conclusions

Identification and mapping of flood-prone areas in and around the Adama City. The study area is one of the fastest-urbanizing areas and the second-most populous city in Ethiopia. This, coupled with its topography and its foundation on low-lying flat terrain surrounded by plateaus and mountain ranges, makes the city highly vulnerable to flooding. To address this problem, eleven flood-conditioning factors were carried out using a geographic information system and analytical hierarchy processes. These include the distance from sewer drainage, topographic wetness index, elevation, land cover, slope, rainfall, normalized difference vegetation index, distance from rivers, distance from roads, drainage density, and soil type, yielding a comprehensive final flood-prone map.

The findings from the flood-prone map indicated that different levels of flooding risk were observed across the study area. Specifically, 0.05% (14.72 ha), 37.37% (11623.09 ha), 61.27% (19056.31 ha), and 1.31% (406.83 ha) of the total area exhibited very high, high, moderate, and low levels of flooding risk, respectively. This implies that 98.69% of the investigated area was exposed to moderate to very high flooding risks, primarily due to geographical attributes such as being situated on low-lying flat terrain surrounded by plateaus and ridged topography, as well as man-made factors like rapid urbanization and deforestation. On the other hand, 1.31% of the study area posed a significantly lower risk of flooding due to its distance from rivers and roads, as well as its higher elevation with steeper slopes.

The accuracy of the model was assessed by cross-checking the collected GCPs using a handheld GPS device (Model: BHCNav6), satellite images from Google Earth, and input from professionals and community members against the final flood hazard map. This validation confirmed that the model accurately represented the actual conditions on the ground.

The combination of remote sensing, geographic information system tools, and the analytical hierarchy process have great significance in identifying flood-prone areas as well as constructing layered flood conditioning factors to assist decision-makers and professionals in implementing appropriate flood management strategies and tools in urban areas and corresponding watersheds.

CHAPTER THREE:

Characterizing the level of urban flooding vulnerability using the social-ecological-technological systems framework: the case of Adama City, Ethiopia

Abstract

This study characterizes the flood vulnerability of Adama City, Ethiopia. The study applied an interlinked Social-Ecological-Technological-Systems (SETS) vulnerability framework using a GIS-based Multi-Criteria Decision-Making and Analytical Hierarchy Process (MCDM-AHP). The framework analyzed exposure, sensitivity, and adaptive capacity to flooding for each of the three SETS domains. The study analyzed 18 variables at the city level within each SETS domain. The result revealed that clusters of flood-vulnerable areas were identified by each SETS domain showing the concentration of flood vulnerability in the study area and the need to consider prompt adaptive measures to mitigate severe and recurring flooding. The finding has significant implications for holistic approaches to sustainable cities. Moreover, the reduction of complex urban flood vulnerabilities according to their priority as individual or combined solutions for decision-makers and professionals in early warning and flood management systems is the other contribution of the study.

Keywords: Vulnerability to flooding, Social-Ecological-Technological Systems, GIS, MCDM-AHP, Adama City.

3.1 Introduction

Flooding has become a significant global hazard that has affected the lives of millions of people. Recent studies have revealed that approximately 1.81 billion people, accounting for 23% of the global population, are exposed to considerable flood risk (McDermott, 2022; Rentschler et al., 2022). Floods have become one of the most frequent natural disasters and are expected to occur more frequently in the future driven by climate changes (Quan et al., 2021; Wang et al., 2022b; Yue et al., 2021). The consequences of floods extend beyond physical damage, posing a substantial threat to human health, well-being, and the economy, as well as causing harm to ecosystems (Ansah et al., 2020; Rentschler et al., 2022; Talbot et al., 2018). In terms of economic losses alone, floods cause over $40 billion in damages annually across the globe (OECD, 2016). Furthermore, it is projected that by 2050, an additional two billion people will be at risk of flood disasters (UNESCO, 2012). Urban areas situated in floodplains are particularly vulnerable to floods and face heightened risks due to the amplification of flood magnitudes (Dumedah et al., 2021; Rentschler et al., 2022).

Flooding in cities has been widely attributed to urbanization in floodplain areas (Al-Zahrani, 2018; Nkwunonwo et al., 2020; Rafiq et al., 2016). Urbanization increases population and building densities, which directly increases surface sealing leading to rapid amplification in the volume and velocity of surface runoff (Chang et al., 2021; Hemmati et al., 2021). Urbanization in floodplain areas increases the risk of flooding due to increased peak discharge and volume and decreased time to peak (Feng et al., 2021; Gori et al., 2019; Xu & Zhao, 2016). Urban watersheds, on average, lose 90% of the storm rainfall to runoff, whereas non-urban forested watersheds retain 25% of the rainfall (Sheng & Wilson, 2009). Floodplain areas are highly vulnerable to flooding due to human activities such as the presence of structures, lack of regulations for their maintenance, and deforestation (Tate et al., 2021; Zeng, 2022).

Vulnerability to flooding in urban areas is determined by analyzing the components of exposure, sensitivity, and adaptive capacity. According to Chang et al. (2021), the SETS framework was developed for assessing urban flood vulnerability through 18 indicators representing social, environmental, and technological dimensions. Similarly, Van et al. (2022) established a flood vulnerability index based on social, economic, environmental, and physical elements. Furthermore, Kashyap and Mahanta (2021) proposed an approach combining characteristics associated with exposure, sensitivity, and adaptive capacity (Wang et al., 2022b).

Urban floods are one of the most frequent natural disasters, resulting in severe economic damage and loss of lives (Kashyap & Mahanta, 2021). Therefore, tools used to assess urban flood vulnerability are essential. The SET framework is one such tool that incorporates selected exposure, sensitivity, and adaptive capacity indicators in three domains – Social, Ecological, and Technological Systems (Chang et al., 2021; Wang et al., 2022b). The social domain includes indicators such as population density, age distribution, and income level; the ecological domain includes indicators such as land use and vegetation cover; and the technological domain includes indicators such as infrastructure quality and availability of emergency services (Chang et al., 2021). The SETS framework has been widely utilized in various research studies, encompassing areas such as urban ecosystem services (McPhearson et al., 2022), urban flood vulnerability (Chang et al., 2021), metropolitan changes (Bixler et al., 2019), climate change adaptation (Kim et al., 2021), and urban sustainability transformations (Krueger et al., 2022). This framework offers a holistic approach to vulnerability assessment by effectively integrating social, ecological, and technological factors (Chang et al., 2021). Additionally, the application of geographic information systems (GIS) enhances the accuracy and precision of the assessment process (Kashyap & Mahanta, 2021; Van et al., 2022; Wang et al., 2022b).

Assessment of flood vulnerability is recognized as a pre-emptive undertaking for hazard management and planning (Nasiri et al., 2016). Researchers widely acknowledged that vulnerability consists of three main components: degree of exposure, sensitivity, and adaptive capacity (Salami et al., 2017). Studies have also shown that both physical factors, such as access to infrastructure and services, and socio-economic characteristics, such as population density and income levels, are important indicators for assessing flood risk (Wang et al., 2022b). Case studies from Santiago de Chile (Müller et al., 2011) and Côte d'Ivoire (Wang et al., 2022b), utilizing an indicator-based approach proved to be successful in accurately assessing urban flood vulnerability. Furthermore, considering social aspects in addition to technological elements is becoming increasingly important for understanding more complex issues regarding the vulnerability of communities that may not have access to technology or information about floods (Chang et al., 2021; Morishita et al., 2017). To build cities that are resilient to extreme weather events and climate change impacts, policymakers and urban planners must understand the drivers of flood vulnerability in their municipalities (Chang et al., 2021; Gao et al., 2022; Wang et al., 2022b).

Urban flooding has become a major issue in developing countries, particularly in Africa, due to rapid urbanization and population growth (Güneralp et al., 2017; Ramiaramanana & Teller, 2021; Saghir & Santoro, 2018; Satterthwaite, 2017; TheGlobalRisksReport, 2018). Insufficient management of land use practices, combined with the impacts of climate change, lead to occurrences of natural disasters like floods (Briones et al., 2020; Manandhar et al., 2023; Niekerk, 2015). Additionally, increased rooftops, parking lots, and asphalt surfaces contribute to faster floodwater run-off than vegetated lands and bare soils (Ferreira et al., 2021). The impact is worse in these areas due to inadequate housing facilities, infrastructure, water availability, and heightened exposure to pathogens (Dewan, 2015; Okaka & Odhiambo, 2018).

Urban flooding has emerged as a significant concern in Ethiopia due to various factors including inadequate urban drainage infrastructure, insufficient land use planning measures, the absence of early warning systems, and a lack of coordination in flood management activities at both federal and local levels (Legese et al., 2020). According to the National Disaster Risk Management Commission (NDRMC, 2020), Ethiopia is home to twelve major river basins, with the study area situated in the Awash River Basin. The Awash River Basin has a history of recurrent severe flooding incidents, posing a greater risk to human well-being and property damage compared to other natural disasters in the basin.

Recent research highlighted the increasingly significant influence of flood issues in the study area, given the increasing number of people, economic activities, and ecosystems affected by their unfavorable consequences (Erena & Worku, 2019; Grecu et al., 2017; Khan et al., 2021). Historical records indicate that floods have had a more detrimental effect on the study area than any other natural disaster (Bulti et al., 2017). Though varying in severity with time, urban flooding still represents one of the greatest hazards to the study area due to its vulnerability to inundation. In addition to having a tangible impact on property, transport, and other critical infrastructure, flooding has far-reaching indirect effects that disrupt communities for extended periods. These include water contamination, fatalities, increased traffic congestion leading to delays in the provision of services, and loss of housing, crops, and livestock (Dong et al., 2022; Pregnolato et al., 2017; Rebally et al., 2021).

Multi-criteria decision-making techniques offer a robust and precise evaluation of urban flood vulnerability, allowing for a comprehensive and accurate assessment. This approach effectively identifies the key factors that significantly contribute to flood risk and determines their relative importance in the decision-making process (Abdelkarim et al., 2020; Ali et al., 2020; Allafta & Opp, 2021; Das & Gupta, 2021). The efficiency of multi-criteria decision-making in analyzing data and making informed decisions has led to its widespread adoption as a tool for assessing flood vulnerability (Beltramone et al., 2017; Pouya et al., 2017; Rahmati et al., 2016). Previous studies on urban flood vulnerability assessment have primarily relied on indicator methods, which often fail to explicitly consider the different domains and dimensions of vulnerability. These methods have limitations such as a limited set of criteria, factors, and giving equal weights for each variable (Chang et al., 2021; Nasiri et al., 2016), lack of stakeholder engagement (De Brito et al., 2018), and simplistic weighting and aggregation techniques (Li et al., 2019). Consequently, the assessments provided by these studies are challenging to implement in practical urban flood management.

In line with this, the objective of this study is to characterize the level of urban flood vulnerability in the study are using SET frameworks. The study builds upon previous work done by Chang et al. (2021), which utilizes the same SET vulnerability framework to evaluate six cities in the US for fluvial/riverine flooding using equal weighting for eighteen indicators. However, this study incorporates stakeholder perspectives to prioritize the indicators within the local context through the utilization of multi-criteria decision-making techniques in pluvial flood vulnerability analysis. This assessment examines various dimensions of vulnerability, including exposure, sensitivity, and adaptive capacity to gain a deeper understanding of the intricate nature of urban flood vulnerability. It is important to note that this study stands out due to its application of the SET framework to assess both separate and combined domains of vulnerability. Moreover, it is assumed that this study is the first to use the SET framework with an Analytical and Hierarchical Process as a whole, and the first to use the SET framework for developing countries in particular. The results will assist city managers and practitioners in improving contextual solutions and promoting sustainable approaches to mitigate the risks associated with flooding in the study area.

3.2 Methodology

3.2.1 Data sources

The information and data related to socio-demographic, ecological, and technological frameworks in the study area were collected both from primary and secondary sources. The secondary data was collected from different bureaus and websites. The spatial data obtained from the study area city administration was updated by field visits and Google Earth digitalization. For analysis, the collected data was transferred into Arc GIS (version 10.7.1), as presented in Table 3.1.

Table 3.1: The selected SETS flood vulnerability indicators together with their source

No	Category	Variables	Abbrevation	Data sources
1	Social exposure	Total population	PT	www.worldpop.org (assessed in March 2023)
2		Population density	PD	www.worldpop.org (assessed in March 2023)
3	Social sensitivity	Percentage of children < 5 years	PC	www.worldpop.org (assessed in March 2023)
4		Percentage of population > 65 years	PO	www.worldpop.org (assessed in March 2023)
5	Social adaptive capacity	Percentage of women	PW	www.worldpop.org (assessed in March 2023)
6		Percentage of people who are unemployed	PU	ACA 2020
7	Ecological exposure	Slope variation	S	ASTER- Global DEM with 12.5m size grids.USGS: (http://earthexplorer.usgs.gov/)(accessed in February 2023.
8		The proximity of ecosystem to toxic release sites	PE	Adama City Environmental Protection Bureau , field visit, and google earth digitization
9	Ecological sensitivity	Combination of shape index and average patch size	SP	Developed from ACA vegetation layers, field visit, and google earth digitization
10		Percentage of bare soil within the area	BS	World Land Resource Center, Ethiopia
11	Ecological adaptive capacity	Percentage of wetland within the area	W	Adama City Environmental Protection Bureau, field visit, and google earth digitization
12		Productivity based on Normalized Difference in Vegetation Index (NDVI)	PNDVI	Sentinel-2A Satellite Image with 10 m size grids. Downloaded from USGS (http://earthexplorer.usgs.gov/) acquired in February 2023
13	Technological exposure	Building area (percentage of building area within the area)	BA	ESRI: https://livingatlas.arcgis.com/Landover/.acquired in February 2023
14		Critical infrastructure (CI) (wastewater, polluted industries, gas terminal) in the area	CI	Adama City Environmental Protection Bureau, field visit, google earth digitization
15	Technological sensitivity	Road density	RD	ACA, field visit, google earth digitization
16		Fractional Impervious surface	FIS	Developed from NDVI (Sentinel-2A Satellite Image with 10 m size grids. Downloaded from USGS (http://earthexplorer.usgs.gov/) assessed in February 2023)
17	Technological adaptive capacity	Green Infrastructure (GI) density	GI	ACA, Field visit, Google Earth digitization
18		Emergency centers (distance of emergency centers (e.g., hospitals, schools, community centers))	EC	ACA, Field visit, Google Earth digitization

The SETS variables listed in Table 2.1 above were developed based on ; Babanawo et al. (2022); Chang et al. (2021); and Salami et al. (2017).

3.2.2 Methods

This study utilized the SET frameworks and employed GIS-based AHP to assess the flood vulnerability of the study area. The analysis encompassed 18 variables, which were categorized into three domains: social, ecological, and technological aspects. These variables were processed and rasterized on a scale of 1 to 5 in a GIS environment, to represent very low to very high vulnerability levels. The reclassification of the variables was conducted in a GIS environment using the reclassify tool from spatial analysis tools. The resulting data was rescaled and geo-referenced with the same coordinate system of WGS_1984_UTM_Zone_37N.

To determine the importance of each flood-influencing factor, an AHP model was employed. This involved interviewing 20 experts and 20 local elders to gather their insights on the most significant factors contributing to flooding in the study area. The pair-wise comparison matrix was used to calculate the prioritization of these factors, with each factor's weight expressed as a percentage value between 0 and 100%. The sum of all weights equaled 100% to ensure consistency.

The ranking of each reclassified factor was based on a combination of a literature review, expert interviews, and residents' input. Factors were ranked on a scale of 1 to 5, with rank 5 indicating the highest level of influence and rank 1 indicating the lowest. The assigned weight for each factor reflected its contribution to flooding relative to other factors.

Using ArcGIS (version 10.7.1), a multi-criteria analysis was conducted to produce the flooding vulnerability map. This approach allowed for a comprehensive characterization of the various factors contributing to flooding vulnerability in the study area. The resulting map provides valuable insights into the level of flood vulnerability in the study area. The general workflow followed by this study is represented in Figure 3.1.

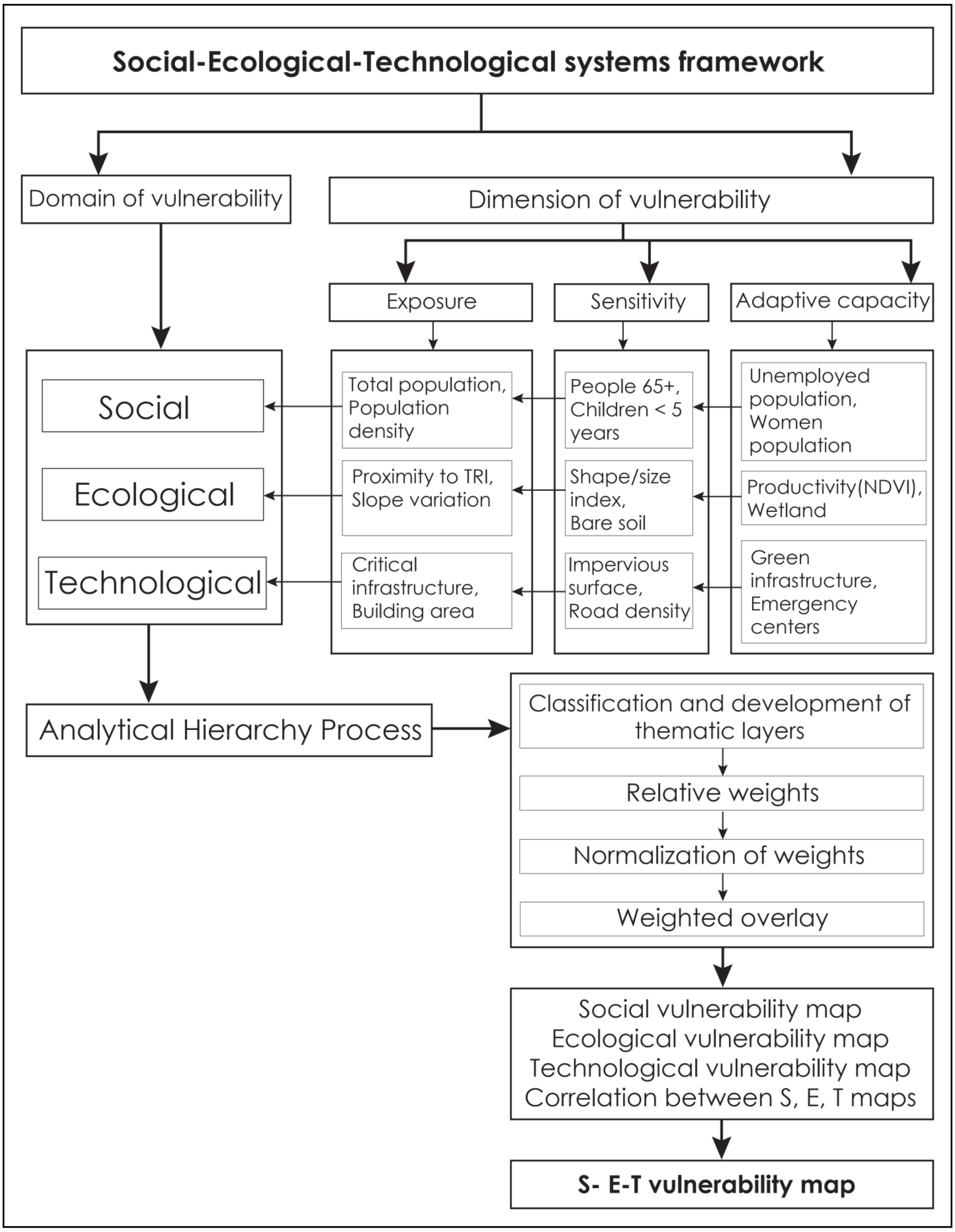

Figure 3.1: Flowchart showing the domains and dimensions of flood vulnerability of the study area

3.2.2.1 Methods of Mapping SET Variables

The spatial population distribution of the 2020 population count of the Ethiopia raster dataset was obtained from www.worldpop.org. The dataset was adjusted to match the corresponding UNPD estimate at the country level and had a spatial resolution of 100 x 100-meter cell size grids. The study area's map was extracted from the dataset, resampled to 10 x 10-meter cell size grids, and reclassified into five classes using the Natural Breaks standard classification scheme in ArcGIS 10.7.1. The categorization assigned values 1 through 5 to different hazard ratings based on increasing population count. Lower population count categories were assigned lower values due to their low susceptibility to flooding, while higher population count categories were assigned higher values due to their high susceptibility as more people living in an area increased exposure to floods (Santos et al., 2022; Tate et al., 2021).

The population density of Ethiopia for the year 2020 was obtained from www.worldpop.org. The acquired raster dataset was calibrated to conform to the corresponding United Nations Population Division's estimates at the country level, and it possessed a spatial resolution of 1000 x 1000 meter cell size grids. Subsequently, the study area was extracted from the dataset and subjected to resampling, whereby the initial grid-cell size was altered to 10 x 10-meter cell size grids ArcGIS 10.7.1. Finally, a five-class Natural Breaks standard classification scheme was employed to reclassify the data set, and the outputs were evaluated from 1 (very low) to 5 (very high) population density. Lower population densities indicate a lower susceptibility to flooding, while higher population densities signify increased vulnerability (Smith et al., 2019; Tate et al., 2021).

The spatial distribution of the population in 2020, disaggregated by gender (specifically women) and age groups (less than 5 years and greater than 65 years), was obtained from https://www.worldpop.org. The data was collected at a spatial resolution of 100 x 100-meter cell size grids. These grids were then resampled to a finer resolution of 10 x 10-meter cell size grids. To assess flood vulnerability, the population data was reclassified into five categories using Natural Breaks ranging from 1 (very low vulnerability) to 5 (very high vulnerability) using ArcGIS 10.7.1. It is important to note that older individuals above the age of 65, young children below the age of 5, and women, who tend to have limited mobility, are more susceptible to flooding hazards and require additional assistance due to their heightened vulnerability (Antwi et al., 2015; Babanawo et al., 2022; Foster et al., 2019; Tanoue et al., 2016; Tate et al., 2021).

The study area's unemployed population, categorized by age and gender, was obtained from ACA. By applying the "Calculate Density" tool within ArcGIS 10.7.1 and a newly added field in the attribute table, a population density map of the study area was generated from input point features. The resulting map was then resampled to 10 x 10-meter cell-size grids and classified into five discrete classes based on Natural Breaks at increasing levels of unemployment. unemployment levels indicate less coping with flood risk and heightened flood vulnerability (Khajehei et al., 2020; Salami et al., 2017; Tate et al., 2021).

The study area's slope map was generated using DEM with 12.5 m size grids, downloaded from ASTER- Global (http://earthexplorer.usgs.gov/) acquired in February 2023 and resampled to 10 x 10-meter cell size grids. The spatial analysis tool slope in percentage ranges was developed using ArcGIS, 10.7.1, and a standard classification scheme called Natural Breaks was applied to classify the slope into five classes. The classification considered the susceptibility of the slope to flooding and assigned each value to a specific hazard rating. The susceptibility decreases from the lowest slope category, which was assigned a value of 5, to the highest slope category with a value of 1. The flatter topography, associated with lower slope values, was particularly vulnerable to flooding, whereas steeper topography, represented by higher slope values, was less vulnerable to flooding (Desalegn & Mulu, 2021; Singh et al., 2020).

The productivity of the study area was mapped from the Normalized Difference in Vegetation Index (NDVI). A Sentinel 2A satellite image, acquired from the USGS website (http://earthexplorer.usgs.gov/.accessed in February 2023) was utilized to generate the NDVI map. Equation 2 was applied in the ArcGIS (version 10.7.1) environment to calculate the NDVI. The NDVI values were resampled to 10 x 10-meter cell size grids and classified into five Natural Breaks of susceptibility to flooding from very low to very high. Higher NDVI values indicate healthier vegetation cover, which reduces flood vulnerability by absorbing water and reducing runoff (Cian et al., 2018; Martinez & Labib, 2023; Zhang et al., 2018).In line with this, the NDVI map was produced based on equation 3.1.

$$NDVI = \frac{NIR - RED}{NIR + RED} = \frac{Band\ 8 - Band\ 4}{Band\ 8 + Band\ 4} \qquad \text{Equation: 3.1}$$

The fractional impervious surface (FIS) of the study area was derived from the NDVI of the study area. Based on Kaspersen et al. (2015), equations 3.2, 3.3, and 3.4 were applied in ArcGIS 10.7.1 spatial analyst tools, map algebra, and raster calculator. Then resampled to 10 x 10-meter cell size grids and classified into five classes based on Natural Breaks. High impervious surface fractions increase the risk of flooding by reducing the area available for water to infiltrate and increasing the speed of runoff (Kaspersen et al., 2015).

$$NDVI(S) = \frac{NDVI - NDVI(Low)}{NDVI(High) - NDVI(Low)}$$ Equation: 3.2

$$FVC(Fractional\ Vegetation\ Cover) = (NDVI(S))^2$$ Equation: 3.3

$$FIS(Fractional\ Impervious\ Surface) = 1 - FVC$$ Equation: 3.4

To map the proximity of ecosystems to potential toxic industries, shapefiles of potential toxic industries were obtained from ACA and analysis tools from ArcGIS 10.7.1 were utilized to create multiple ring buffers within a given distance for the study area. The resulting index was then subjected to a union process to identify all ecosystems that intersect with potentially toxic industries such as toxic industries, landfill sites, and abattoirs. The obtained map of ecosystems and potential toxic industry locations were then resampled to 10 x 10-meter cell size grids and classified into five categories based on Natural Breaks to identify areas at risk of exposure to toxic substances during floods. Ecosystems near toxic industries are more vulnerable to flooding than further areas due to the potential exposure to toxic substances during floods as it exposes nearby communities to toxic chemicals and hazardous waste (Chang et al., 2021; Jongman et al., 2015; Talbot et al., 2018).

To map the index and average patch size of the study area's vegetation layer from ACA were derived and digitized to update the layer digitizing based on field visits and high-resolution Google Earth Pro-Satellite imagery (Google Earth Pro_Version 7.3.6). Then, patch sizes of vegetation layers were classified based on their area. Then resampled to 10 x 10-meter cell size grids and classified into five classes based on Natural Breaks in ArcGIS 10.7.1. The size of the patches determines areas that are vulnerable to flooding. Smaller patches indicate areas that are more fragmented and less able to provide ecosystem services that help mitigate flood impacts (Bousquin & Hychka, 2019; Rehman et al., 2021).

The bare soil raster dataset was obtained from the Water and Land Resource Center (WLRC), Ethiopia, and the wetland data of the study area was obtained from ACA. Then, resampled to 10 x 10-meter cell size grids and computed into percentages in ArcGIS 10.7.1. Bare-soil areas are more vulnerable to flooding due to their low infiltration capacity and high erodibility (Chang et al., 2021) whereas wetlands absorb flood water and reduce flooding (Chan et al., 2018).

The built-up area of the study area was extracted from an ESRI website: *https://livingatlas.arcgis.com/Land cover/* (acquired in February 2023) with 10 x 10-meter cell size grids. Then, computed into percentages in an ArcGIS 10.7.1 environment. Built-up areas are more vulnerable to flooding due to their inability to percolate water into the subsurface, which makes the area more vulnerable (Deepak et al., 2020).

A road density map was created using a road shapefile acquired from ACA, with any missing data supplemented by digitizing based on field visits and high-resolution Google Earth Pro-Satellite imagery (Google Earth ProVersion 7.3.6). Kernel line density tools were utilized to derive linear feature density, which was then resampled to 10 x 10-meter cell size grids and classified into five classes based on Natural Breaks. High road density increases the risk of flooding by reducing the area available for water to infiltrate and increasing the speed of runoff (Baky et al., 2020; Hagos et al., 2022). A green infrastructure density map was similarly generated using a corresponding GI shapefile, with its polygon features converted to point form before kernel point density was computed in ArcGIS 10.7.1. This resulting GI density map was also resampled and classified in the same manner as that of the road density map. Green infrastructure reduces the vulnerability of an area to flooding by increasing infiltration and reducing runoff (Khodadad et al., 2023; Pallathadka et al., 2022).

Critical infrastructure (water/wastewater, power plants, and gas terminals) that affect public health and safety shapefiles were obtained from ACA was obtained from ACA and analysis tools from ArcGIS 10.7.1 were utilized to create multiple ring buffers within a given distance for the study area. The resulting map was then resampled to 10 x 10-meter cell-size grids and classified into five classes based on Natural Breaks. Critical infrastructure such as toxic industries, landfill sites, abattoirs, and gas terminals are exposed to floods and important to identify the areas from the point sources (Len et al., 2018; Murdock et al., 2018; Qiang, 2019).

Emergency centers (hospitals, schools, universities, and community centers) shapefiles were obtained from ACA and the missing emergency centers through digitizing based on field visits and high-resolution Google Earth Pro-Satellite imagery (Google Earth Pro version 7.3.6). Then, analysis tools from ArcGIS 10.7.1 were utilized to create multiple ring buffers within a given distance for the study area. The resulting map was then resampled to 10 x 10-meter cell-size grids and classified into five classes based on Natural Breaks. Emergency centers such as hospitals, schools, and universities play a critical role in assisting the community during floods and serve as emergency response sites (Atanga & Tankpa, 2022; Cutter et al., 2003).

3.2.2.2 Method of Analytical Hierarchy Processing (AHP)

The AHP techniques developed by Saaty (1987) were used for determining the priorities of multiple criteria decision problems in characterizing flood vulnerability. In urban flood vulnerability analysis, AHP was used for multi-criteria decisions by many researchers (Aydin & Birincioğlu, 2022; Lin et al., 2019; Ramesh & Iqbal, 2022; Rimba et al., 2017).

AHP analysis was implemented to quantify the comparative significance of flood-controlling variables. In this process, a matrix of pairwise comparisons was computed (Table 3.5), followed by its normalization and weighted assignment of the factors (Table 3.6). To check the consistency, a further evaluation was carried out (Table 3.7) following the reclassification of each variable.

As suggested by Saaty (1987) the succeeding procedures were used to determine relative weights to each flood-conditioning factor including:

1. The matrix of pair-wise comparisons is constructed based on Saaty's 1 to 9 scale, where each variable is represented in Table 3.2.
2. Then, each entry in the given matrix of pair-wise comparisons column was divided by its corresponding sum.

3. Finally, each weight was determined by dividing the total of each line in the normalized matrix by eighteen (Table 3.5).

Table 3.2: Saaty's pair-wise comparison scale (adapted from Saaty (1977)

Intensity of importance	Degree of preference	Explanation
1	Equal importance	Two elements contribute equally to the objective
3	Moderate importance	Experience and judgment slightly favor one parameter over another
5	The strong or essential importance	Experience and judgment strongly favor one activity over another
7	Very strong importance	One parameter is favored very strongly and is considered superior to another; its dominance is demonstrated in practice
9	Extreme importance	The evidence favoring one parameter as superior to another is of the highest possible order of affirmation
2,4,6,8	Intermediate values	When parameters that are very close in importance

After calculating the weights of each variable related to flood vulnerability characterization, a consistency index (CI) check was computed using equation 3.5 (Saaty, 1987), if the comparison is accurate.

$$CI = \frac{\lambda_{\max - n}}{n - 1} \qquad \text{Equation: 3.5}$$

Where,$'n'$stands for the number of factors being examined, and 'λ' max represents the maximum eigenvalue of the comparison pairwise matrix.

The following steps were used to compute the maximum Eigenvalue (λ_{max}) of the comparison pair-wise matrix (Saaty, 1987).

1. Multiplying each column value (in the non-normalized matrix) by the weight criteria
2. The rows' values are added to calculate the weighted sum
3. Weighting each criterion value based on its weighted sum value, and
4. A weighted sum of the mean concerning the criteria weights.

Then, the calculated consistency ratio (CR) which demonstrates the validity of Saaty (1987) comparison was computed using Equation 3.6.

$$CR = \frac{CI}{RI} \qquad \text{Equation: 3.6}$$

According to Saaty (1987), if the consistency ratio is less than 0.10, the matrix of pair-wise comparisons is considered consistent, however, if it is greater or equal to 0.10, insufficient consistency is present and the procedure must be iterated several times until the CR value drops below this threshold. Table 3.3 presents the random consistency index to the matrix size.

Table 3.3: Table 3.3: Random consistency index(RCI)(Adapted from Saaty (1987)

Size of matrix	**1**	**2**	**3**	**4**	**5**	**6**	**7**	**8**	**9**	**10**	**11**	**12**	**13**	**14**	**15**	**16**	**17**	**18**
RCI	0	0	0.58	0.9	1.12	1.24	1.32	1.41	1.45	1.49	1.51	1.48	1.56	1.57	1.59	1.605	1.61	1.615

3.2.2.3 Method of Preparing the SET Vulnerability Map

To develop the flood vulnerability map of the study area, all the selected SET variables were geo-referenced with the same coordinate system of WGS_1984_UTM_Zone_37N, resampled to 10 x 10-meter cell size grids, reclassified, and weighted via Analytic Hierarchy. Afterward, ArcGIS's Spatial Analyst extension's weighted overlay technique was employed, with Equation 3.7. This equation has been employed in numerous prior studies for assessing areas posed with a heightened risk of flooding (Aydin & Birincioğlu, 2022; Hagos et al., 2022; Ramesh & Iqbal, 2022). Accordingly, the vulnerability maps for the seven classes (i.e., S, E, T, S-E, S-T, E-T, S-E-T) were mapped.

$$FP = \sum_{i=0}^{n} Xi * Wi \qquad \text{Equation: 3.7}$$

Where; '*FP*' denotes flood vulnerability, '*n*' *is the* number of decision-making criteria, '*Xi*' *is the* specific normalized criterion, and '*WI*' *is* the criterion's weight.

3.2.2.4 Methods of analyzing the spatial distribution of vulnerability maps

To assess the spatial patterns of flood vulnerability, Global Moran's I in ArcGIS 10.7.1. was utilized. This statistical measure allowed us to determine whether the distribution of vulnerability was clustered, dispersed, or random. A Moran's I value close to zero suggests a random spatial distribution, while positive and negative values indicate clustering or dispersed patterns, respectively. By employing this analysis, we were able to gain insights into the spatial dynamics of flood vulnerability and better understand how susceptible areas were geographically related to one another (Chang et al., 2021; Moran, 1950).

3.2.2.5 Method of validation of the SETS map

Validation is a crucial step in ensuring that model outputs accurately portray real-world conditions on the ground. For this study, field-based visits and interviews with local dwellers were conducted both before and after modeling to enhance understanding and precision. In addition, ACA experts were interviewed, and historical flood inundation data were cross-checked with satellite imagery from Google Earth Pro Version 7.3.6. Furthermore, the final SETS map was compared with 120 Ground Control Points (GCPs) collected using a handheld Global Positioning System (GPS) device (Model: BHCNav6). The GCPs were then converted to shapefiles, overlaid onto the final SETS map on ArcGIS version 10.7.1 for verification.

3.3 Result

3.3.1 SET Variables

The eighteen SETS variables with their unit, classes, flood susceptibility, rating values, and weight of the study area as analyzed using ArcGIS 10.7.1 Multi-Criteria Decision-Making and Analytical Hierarchy Process. Table 3.4 shows the SETS variables, unit, classes, susceptibility, rating values, and weight. The AHP model utilized the pair-wise comparison matrix (shown in Table 3.5) to determine the prioritization of these factors, with each factor's weight represented as a percentage value ranging from 0 to 100%. The weight and ranking of each factor were calculated by employing both the pair-wise comparison matrix and the factor map. The weight value assigned to each factor indicated its prioritization and was expressed as a percentage value between 0 and 100%. The sum of all weights equaled 100% due to the use of a linear weighted combination.

Table 3.4: SETS variables their abbreviation (Abb.), unit, classes, flood susceptibility, rating values, and weight

No	Variables	Abbreviation	Unit	Class	Flood susceptibility	Susceptibility rating	Weight (%)
1	Total population count	PT	total number of people per grid-cell	0.45 - 8.73	Very low	1	6.08
				8.73 - 35.36	Low	2	
				35.36 - 74.40	Medium	3	
				74.40- 109.31	High	4	
				109.31 - 151.39	Very high	5	
2	Population density	PD	# of people/area	57 - 1,323	Very low	1	6.77
				1,323 - 4,208	Low	2	
				4,208 - 8,289	Medium	3	
				8,289 - 12,792	High	4	
				12,792 - 17,999	Very high	5	
3	Percentage of children < 5 years	PC	%	0.04 - 0.25	Very low	1	6.64
				0.25 - 0.58	Low	2	
				0.58 - 1.00	Medium	3	
				1.00 - 1.43	High	4	
				1.43- 2.25	Very high	5	
4	Percentage of the population over 65 years	PO	%	0.02 - 0.12	Very low	1	6.13
				0.12 - 0.30	Low	2	
				0.30 - 0.52	Medium	3	
				0.52 - 0.75	High	4	
				0.75 - 1.17	Very high	5	
5	Percentage of women	PW	%	0.0094 - 0.062	Very low	1	6.70
				0.063 - 0.15	Low	2	
				0.16 - 0.26	Medium	3	
				0.27 - 0.38	High	4	
				0.39 - 0.59	Very high	5	
6	Percentage of unemployed people	PU	%	0.03 - 0.15	Very low	1	6.25
				0.15 - 4.22	Low	2	
				4.22 - 11.49	Medium	3	
				11.49 - 18.26	High	4	
				18.26 - 31.45	Very high	5	
7	Slope variation	S	%	0 - 3.14	Very high	5	8.49
				3.14 - 7.12	High	4	

				7.12 - 13.21	Medium	3	
				13.21 - 22.21	Low	2	
				22.22 - 53.42	Very low	1	
8	The proximity of the ecosystem to toxic release sites	PE	Level	1 - 3	Very low	1	7.04
				3 - 4	Low	2	
				4 - 5	Medium	3	
				5 - 6	High	4	
				6 - 7	Very high	5	
9	Combination of shape index and average patch size	SIPS	Area(m^2)	0.0034 - 22.77	Very high	5	6.78
				22.77 - 50.90	High	4	
				50.91 - 99.13	Medium	3	
				99.13 - 136.64	Low	2	
				136.65 - 341.61	Very low	1	
10	Percentage of bare soil within the area	BS	%	2.32	Very high	5	5.49
11	Percentage of wetlands within the area	W	%	0.83	Very low	1	5.32
12	Productivity based on Normalized Difference in Vegetation Index (NDVI)	PNDVI	Level	-0.16 - 0.098	Very high	5	4.35
				0.099 - 0.13	High	4	
				0.14 - 0.16	Medium	3	
				0.17 - 0.23	Low	2	
				0.24 - 0.46	Very low	1	
13	Building area (percentage of building area within the area)	BA	%	25.50	High	4	4.36
14	Critical infrastructure (CI) in the area	CI	Meter(m)	< 100	Very high	5	4.38
				100 - 500	High	4	
				500 - 1,000	Medium	3	
				1,000 - 3,000	Low	2	
				> 3,000	Very low	1	
15	Road density	RD	Length of road/area	0 - 2.07	Very low	1	4.21
				2.07 - 6.31	Low	2	
				6.31 - 12.86	Medium	3	
				12.87 - 19.41	High	4	
				19.41 - 29.28	Very high	5	
16	Fractional Impervious surface	FIS	%	-0.0000012 - 0.61	Very low	1	3.49
				0.62 - 0.77	Low	2	
				0.78 - 0.87	Medium	3	
				0.88 - 0.92	High	4	
				0.93 - 1	Very high	5	
17	Green Infrastructure (GI) density	GI	Number of GI/area	0 - 26.57	Very high	5	3.46
				26.57 - 75.64	High	4	
				75.64 - 145.15	Medium	3	
				145.16 - 265.77	Low	2	
				265.78 - 521.31	Very low	1	
18	Emergency centers	EC	Meter (m)	< 500	Very low	1	4.05
				500 -1500	Low	2	
				1500 - 2500	Medium	3	
				2500 - 5000	High	4	
				> 5000	Very high	5	
						Total	100.00

The spatial distribution of the population count in the study area is represented as rasterized data, which varies between 0.45 and 151.39. The data is divided into five categories based on these values: 0.45 - 8.73 (very low), 8.73 - 35.36 (low), 35.36 - 74.40 (medium), 74.40- 109.31 (high), and 109.31 - 151.39 (very high). These categories cover 78.96%, 11.75%, 2.64%, 3.33%, and 3.32% of the population respectively, as shown in Figure 3.3 (a) and Table 3.4. Based on these findings, around 9.29% of the population residing in the study region has moderate to high vulnerability to flooding. This implies that the individuals belonging to this particular percentage of the overall population of the study area were prone to the risk of flooding due to their settlements.

The population density of the study area ranges from 56.81 to 17,998.16 and is categorized into five classes 56.81 - 1,323.26 (very low), 1,323.26 - 4,207.94 (low), 4,207.94 - 8,288.72 (medium), 8,288.72 - 12,791.64 (high) and 12,791.64 - 17,998.16 (very high) which covers 79.53%, 9.38%, 4.16%, 3.18%, and 3.75%, as shown in Figure 3.3 (b) and Table 4. This indicates that about 11.09% of the population of the study area is moderate to very highly vulnerable to flooding as a result of being densely populated.

The population of children less than five years was ranges from 0.04 to 2.25 and categorized into five classes 0.04 - 0.25 (very low), 0.25 - 0.58 (low), 0.58 - 1.00 (medium), 1.00 - 1.43 (high), and 1.43- 2.25 (very high) which covers 54.37%, 18.37%, 9.18%, 10.67%, 7.41%, as indicated in Figure 3.3 (c) and Table 4. This implies that about 27.26% children population is vulnerable to flooding during flooding in the study area.

The population of people greater than 65 years was ranges from 0.02 to 1.17 and categorized into five classes 0.02 - 0.12 (very low), 0.12 - 0.30 (low), 0.30 - 0.52 (medium), 0.52 - 0.75 (high), 0.75 - 1.17 (very high) which covers 54.95%, 17.99%, 9.06%, 10.73%, and 7.26% respectively, as indicated in Figure 3.3 (d) and Table 4. This implies that about 27.05 of the elderly population is vulnerable to flooding during flooding.

The women population of the study area ranges from 0.0094 to 0.59 and is categorized into five classes 0.0094 - 0.062 (very low), 0.063 - 0.15(low), 0.16 - 0.26 (medium), 0.27 - 0.38 (high), and 0.39 - 0.59 (very high) which covers 55.17%, 17.75%, 8.84%, 10.69%, and 7.55%, as indicated in Figure 3.3 (e) and Table 4. This implies that about 27.08% of the women population is vulnerable to flooding.

The unemployment population density of the study area ranges from 0.03 to 31.45 and is categorized into five classes 0.03 - 0.15 (very low), 0.15 - 4.22 (low), 4.22 - 11.49 (medium), 11.49 - 18.26 (high), and 18.26 - 31.45 (very high) which covers 63.9, 28.05, 5.98, 1.65, and 0.43, as indicated in Figure 3.3 (f) and Table 4. About 8.06% of the population is moderately to very highly vulnerable to flooding due to unemployment.

The slope of the study area was classified into five classes 0 - 3.14°(very high), 3.14 - 7.12°(high), 7.12 - 13.21°(medium), 13.21 - 22.21°(low), and 22.22 - 53.42°(very low) which covers 2.08%, 5.32%, 14.38%, 38.21%, and 40% of the total area, as indicated in Figure 3.4 (a) and Table 3.4. This implies that about 92.59% of the area covers moderate to very high flood vulnerability. The implication of this is that the study area's gentle slopes (flat surfaces) triggered flooding.

The Proximity of the ecosystem to toxic release areas was classified into five classes 1 – 3 (very low), 3 – 4 (low), 4 – 5 (medium), 5 – 6 (high), and 6 - 7(very high) which covers 21.4%, 23.51%, 19.43%, 24.84%, 10.82% respectively, as indicated in Figure 3.4 (b) and Table 3.4. This implies that about 55.09% of the ecosystem has a medium to very high susceptibility to flooding. Therefore, over half of the ecosystems are near sites where harmful substances may be released and are at a greater risk of flooding during inundation.

The combination of shape index and average patch sizes are categorized into five classes 0.0034 - 22.77 (very high), 22.77 - 50.90 (high), 50.91 - 99.13(medium), 99.13 - 136.64 (low), and 136.65 - 341.61 (very low) which covers 42.76%, 18.95%, 14.26%, 10.87%, and 13.16%, as shown in Figure 3.4 (c) and Table 4. This implies that about 38.73 % of shape index and patch sizes are medium to very highly vulnerable to flooding. The implication of this is that the small size shape index and scattered patches are vulnerable to flooding.

The percentage of the bare soil in the study area accounted for 2.3% (718.74 ha) as indicated in Figure 3.4 (d) and Table 4. This was reclassified as having a very high flood vulnerability due to limited water infiltration, which facilitates the flow of floodwater across the surface. The built area covered 25.23% (7871.49 ha) of the study area, as depicted in Figure 3.5 (a) and Table 3.4, and was reclassified as having a high flood vulnerability. This is because structures and paved surfaces hinder water infiltration, leading to increased flooding. Furthermore, about 0.7% (217.93 ha) of the study area consisted of wetlands, as shown in Figure 3.4 (e) and Table 3.4. These wetlands were reclassified as having a very low flood vulnerability due to their capacity to retain significant amounts of water, thereby reducing the risk of flooding.

The productivity-based NDVI of the study area was classified into five classes -0.16 - 0.098 (very high), 0.099 - 0.13 (high), 0.14 - 0.16 (medium), 0.17 - 0.23 (low), and 0.24 - 0.46 (very low), which covers 7.54%, 39.66%, 38.68%, 11.74%, and 2.38% of the study area respectively, as shown in Figure 3.4 (f) and Table 3.4. This implies that about 85.88% area was medium to very highly vulnerable to flooding. As a result of less healthy vegetation cover, increased runoff, and flood vulnerability prevail.

Critical Infrastructures((potential toxic industries, landfill site, abattoir, gas terminals) of the study area were buffered and categorized into five classes < 100 m (very high), 100 – 500 m (high), 500 - 1,000 m (medium), 1,000 - 3,000 (low), and >3,000 (very low) which covers 3.41%, 10.34%, 13.54%, 44.28%, and 28.44% respectively, as indicated in Figure 3.5 (b) and Table 3.4. This implies that 27.29% of the Critical infrastructure are found within moderate to very high flood vulnerability area. This implies that a quarter of the area is exposed to flooding due to the availability of nearby CI.

Road density of the study area was classified into five classes 0 - 2.07 (very low), 2.07 - 6.31(low), 6.31 - 12.86 (medium), 12.87 - 19.41(high), and 19.41 - 29.28 (very high) which covers 50.86 %, 26.97%, 7.13%, 6.86%, and 8.18% of the study area respectively, as shown in Figure 3.5 (c) and Table 3.4. This implies that 22.17% of the area is moderate to very high flood vulnerability. This implies that more than a quarter of the road density increases the risk of flooding by reducing the area available for water to infiltrate and increasing the speed of runoff.

The fractional impervious surface of the study area is classified into five classes - 0.0000012 - 0.61(very low), 0.62 - 0.77(low), 0.78 - 0.87(medium), 0.88 - 0.92 (high), and 0.93 – 1 (very high) which covers 0.67%, 2.21%, 8.86%, 34.29%, and 53.97% respectively, as shown in Figure 3.5 (d) and Table 3.4. This implies that about 97.12 of the area was moderate to very highly vulnerable to flooding by reducing the area available for water to infiltrate and increasing the speed of runoff.

The green infrastructure density of the area was classified into five classes 0 - 26.57(very high), 26.57 - 75.64(high), 75.64 - 145.15 (medium), 145.16 - 265.77(low), and 265.78 - 521.31(very low) which covers 60.42, 22.74, 11.28, 4.36, and 1.2 respectively, as shown in Figure 3.5 (e) and Table 3.4. This implies that about 94.4 of the study are moderate to very highly vulnerable to flooding. This implies that the green infrastructure density of the area was very low to reduce flood vulnerability by increasing infiltration and reducing runoff.

Emergency centers (hospitals, schools, universities, and community centers) of the study area buffer were classified into five classes < 500 m (very low), 500 -1500 m (low), 1500 – 2500 m (medium), 2500 – 5000 m (high), and > 5000 m((very high) which covers 15.86%, 21.89%, 22.73%, 32.41%, and 7.11% respectively, as shown in Figure 3.5 (f) and Table 3.4. This implies that about 62.25% of the study area has moderate to very high vulnerability to flooding. This signifies that the availability of emergency centers such as hospitals, schools, and universities is less to assist the community during floods and serve as emergency response sites.

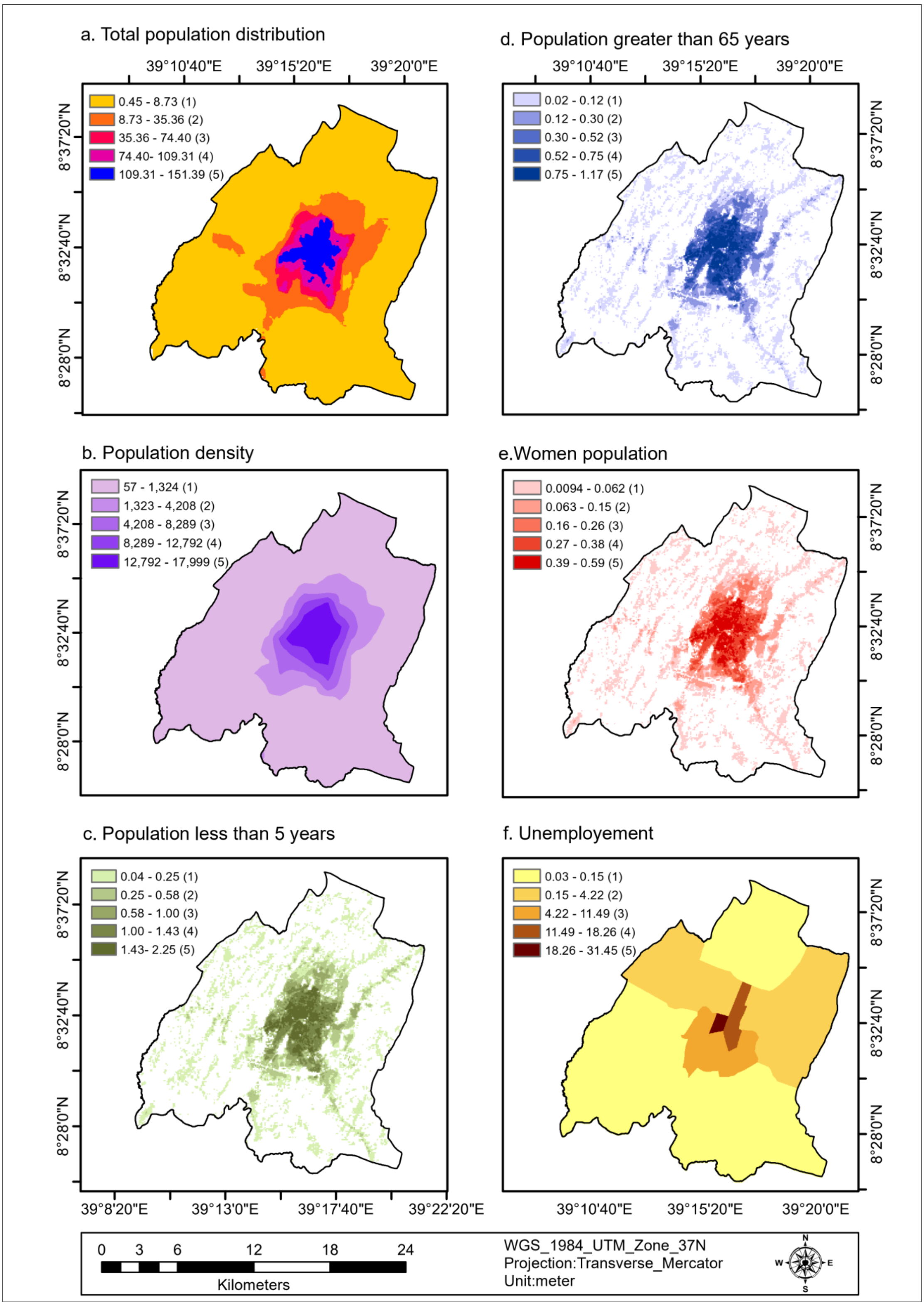

Figure 3.2: Total population distribution (a), population density (b), population < 5 years(c), population >65 years (d), women population (e), unemployment (f).

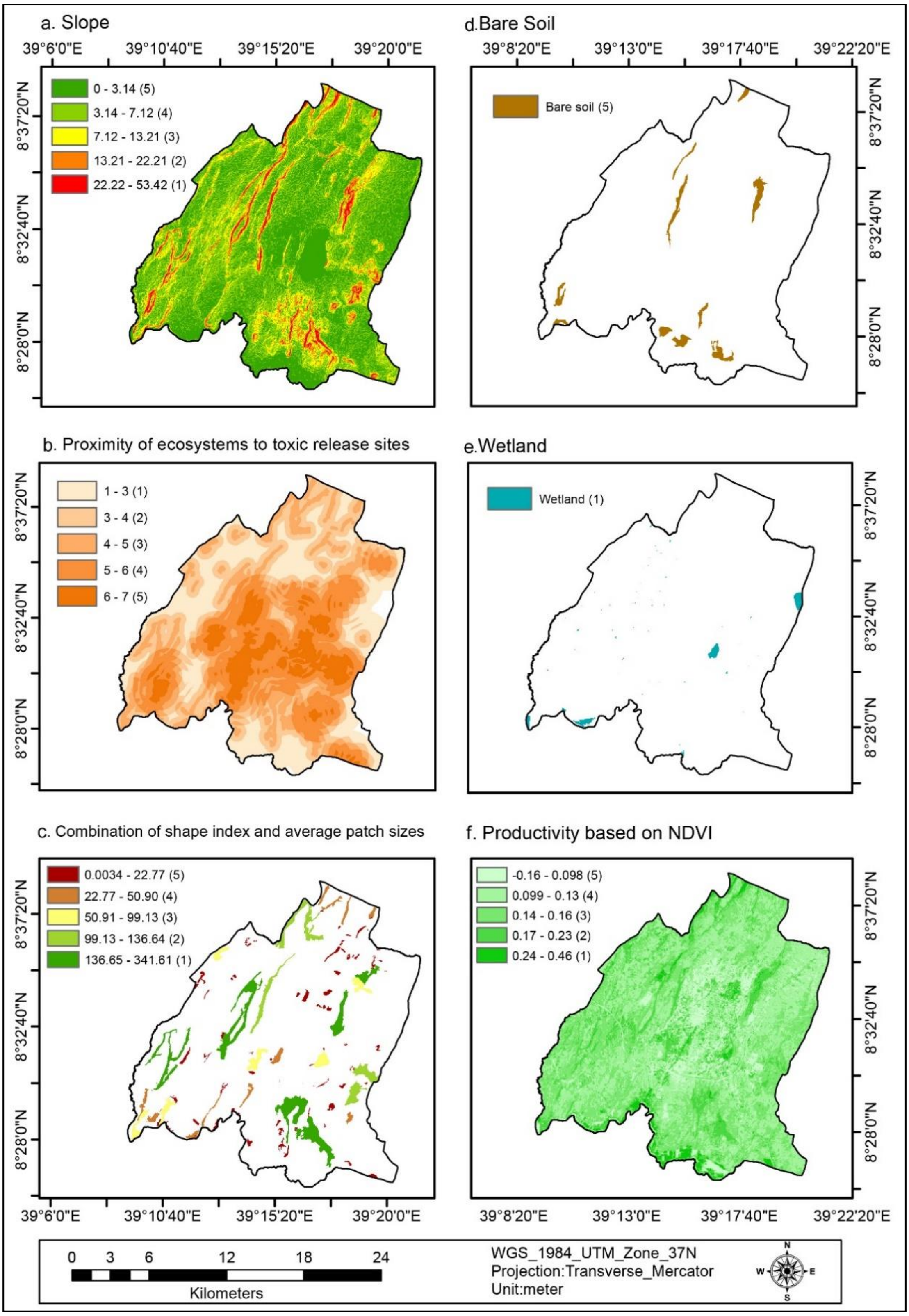

Figure 3.3: Slope(a), the proximity of ecosystems to toxic release sites (b), the combination of shape index and average patch sizes(c), bare soil (d), wetland(e), productivity based on NDVI (f).

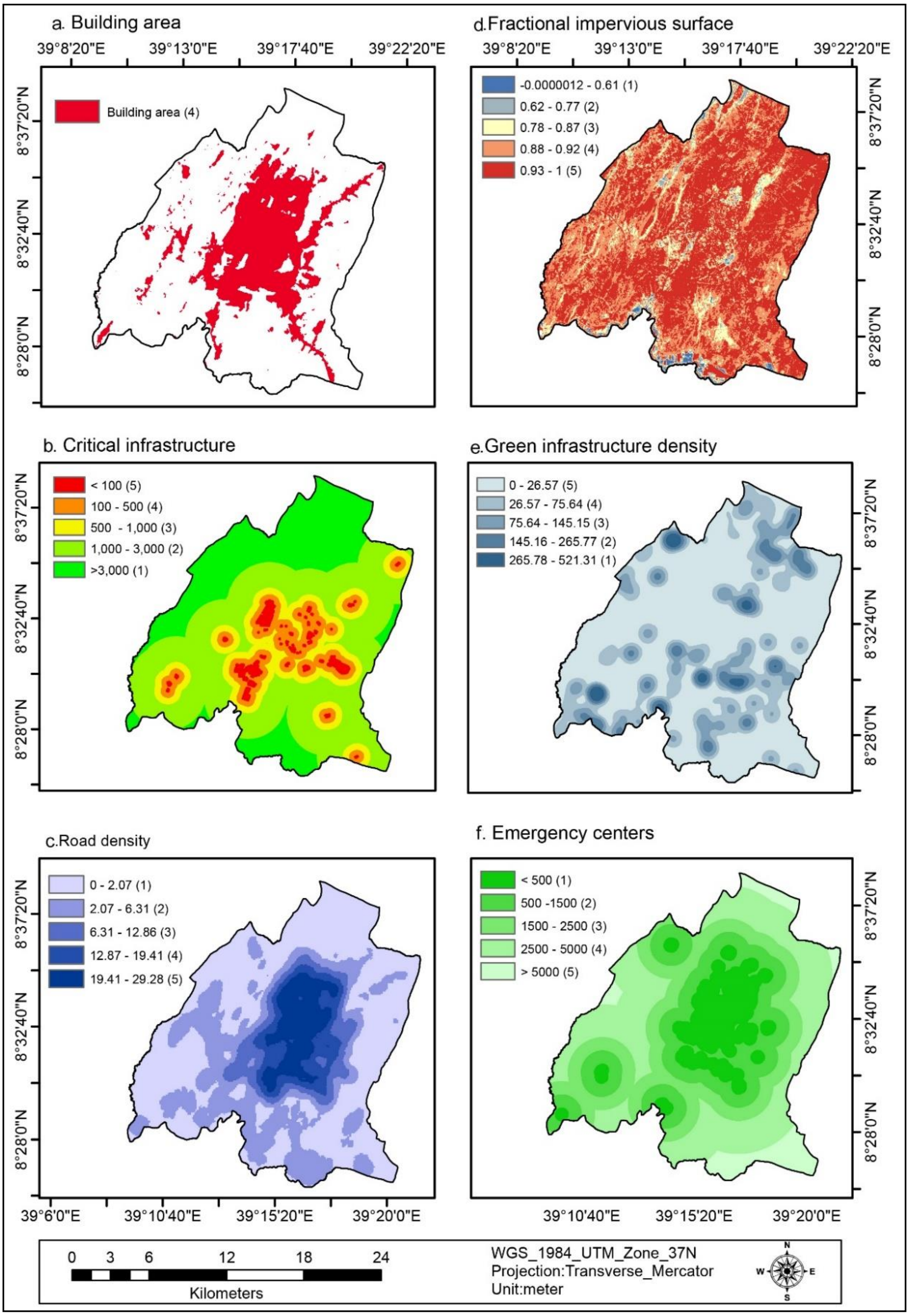

Figure 3.4: Building area (a), critical infrastructure (b), road density (c), FIS (d), GI density (e), and emergency centers(f).

3.2.3 Analytical Hierarchy Processing (AHP)

The weight for all SET variables was taken into consideration as demonstrated in Table 3.4, reflecting the relative influence of each variable. Total population (6.08%), population density (6.77%), percentage of children < 5 years (6.64%), percentage of the population over 65 years (6.13%), percentage of women (6.70%), percentage of unemployed people (6.25%). Additionally, slope variation (8.49%), the proximity of the ecosystem to toxic release sites (7.04), a combination of shape index and average patch size (6.78%), percentage of bare soil within the area (5.49%), percentage of wetland within the area (5.32%), productivity based on Normalized Difference in Vegetation Index (NDVI) (4.35%). Furthermore, the percentage of the built area within the area (4.36%), critical infrastructure in the area (4.38%), road density (4.21%), fractional impervious surface (3.49%), green infrastructure density (3.46%), and emergency centers (4.05%).

Table 3.5: Pair-wise Comparison Matrix

Variables	PT	PD	PC	PO	PW	PU	S	PE	SIPS	BS	W	PNDVI	BA	CI	RD	FIS	GI	EC
PT	1	1	1	1	1	1	1	2	1	1	1	1	2	1	1	2	1	2
PD	1	1	1	2	1	2	1	1	1	2	2	2	2	1	1	1	1	1
PC	0	1	1	1	1	2	2	2	1	1	1	2	2	2	1	2	1	1
PO	1	0	1	1	1	2	2	2	2	1	1	1	1	1	1	1	1	1
PW	1	1	0	1	1	1	2	2	2	2	2	2	2	1	1	1	1	1
PU	1	1/2	1/2	0	1	1	1	2	2	1	1	2	3	2	2	1	2	1
S	1	1	1/2	1/2	0	1	1	2	3	3	2	3	3	2	3	3	3	2
PE	1/2	1	1/2	1/2	1/2	0	1/2	1	1	2	3	2	3	3	3	3	3	2
SIPS	1	1	1	1/2	1/2	1/2	0	1	1	2	3	3	2	1	1	3	3	3
BS	1	1/2	1	1	1/2	1	1/3	0	1/2	1	2	2	2	2	2	2	2	1
W	1	1/2	1	1	1/2	1	1/2	1/3	0	1/2	1	3	2	2	2	2	2	1
PNDVI	1	1/2	1/2	1	1/2	1/2	1/3	1/2	1/3	0	1/3	1	1	2	2	2	2	2
BA	1/2	1/2	1/2	1	1/2	1/3	1/3	1/3	1/2	1/2	0	1	1	2	3	2	2	2
CI	1	1	1/2	1	1	1/2	1/2	1/3	1	1/2	1/2	0	1/2	1	2	2	2	1
RD	1	1	1	1	1	1/2	1/3	1/3	1	1/2	1/2	1/2	0	1/2	1	2	2	1
FIS	1/2	1	1/2	1	1	1	1/3	1/3	1/3	1/2	1/2	1/2	1/2	0	1/2	1	2	1
GI	1	1	1	1	1	1/2	1/3	1/3	1/3	1/2	1/2	1/2	1/2	1/2	0	1/2	1	1
EC	1/2	1	1	1	1	1	1/2	1/2	1/3	1	1	1/2	1/2	1	1	0	1	1
Sum	15.00	14.50	13.50	16.50	14.00	16.83	14.00	18.00	18.33	20.00	22.33	27.00	28.00	25.00	27.50	30.50	32.00	25.00

Table 3.6: Normalized Pair-wise Comparison Matrix

Variables	PT	PD	PC	PO	PW	PU	S	PE	SIPS	BS	W	PNDVI	BA	CI	RD	FIS	GI	EC	Sum	WSV	CW (%)
PT	0.0667	0.0690	0.0741	0.0606	0.0714	0.0594	0.0714	0.1111	0.0545	0.0500	0.0448	0.0370	0.0714	0.0400	0.0364	0.0656	0.0313	0.0800	**1.0947**	**0.0608**	**6.08**
PD	0.0667	0.0690	0.0741	0.1212	0.0714	0.1188	0.0714	0.0556	0.0545	0.1000	0.0896	0.0741	0.0714	0.0400	0.0364	0.0328	0.0313	0.0400	**1.2181**	**0.0677**	**6.77**
PC	0.0000	0.0690	0.0741	0.0606	0.0714	0.1188	0.1429	0.1111	0.0545	0.0500	0.0448	0.0741	0.0714	0.0800	0.0364	0.0656	0.0313	0.0400	**1.1959**	**0.0664**	**6.64**
PO	0.0667	0.0000	0.0741	0.0606	0.0714	0.1188	0.1429	0.1111	0.1091	0.0500	0.0448	0.0370	0.0357	0.0400	0.0364	0.0328	0.0313	0.0400	**1.1026**	**0.0613**	**6.13**
PW	0.0667	0.0690	0.0000	0.0606	0.0714	0.0594	0.1429	0.1111	0.1091	0.1000	0.0896	0.0741	0.0714	0.0400	0.0364	0.0328	0.0313	0.0400	**1.2056**	**0.0670**	**6.70**
PU	0.0667	0.0345	0.0370	0.0000	0.0714	0.0594	0.0714	0.1111	0.1091	0.0500	0.0448	0.0741	0.1071	0.0800	0.0727	0.0328	0.0625	0.0400	**1.1247**	**0.0625**	**6.25**
S	0.0667	0.0690	0.0370	0.0303	0.0000	0.0594	0.0714	0.1111	0.1636	0.1500	0.0896	0.1111	0.1071	0.0800	0.1091	0.0984	0.0938	0.0800	**1.5276**	**0.0849**	**8.49**
PE	0.0333	0.0690	0.0370	0.0303	0.0357	0.0000	0.0357	0.0556	0.0545	0.1000	0.1343	0.0741	0.1071	0.1200	0.1091	0.0984	0.0938	0.0800	**1.2679**	**0.0704**	**7.04**
SIPS	0.0667	0.0690	0.0741	0.0303	0.0357	0.0297	0.0000	0.0556	0.0545	0.1000	0.1343	0.1111	0.0714	0.0400	0.0364	0.0984	0.0938	0.1200	**1.2209**	**0.0678**	**6.78**
BS	0.0667	0.0345	0.0741	0.0606	0.0357	0.0594	0.0238	0.0000	0.0273	0.0500	0.0896	0.0741	0.0714	0.0800	0.0727	0.0656	0.0625	0.0400	**0.9879**	**0.0549**	**5.49**
W	0.0667	0.0345	0.0741	0.0606	0.0357	0.0594	0.0357	0.0185	0.0000	0.0250	0.0448	0.1111	0.0714	0.0800	0.0727	0.0656	0.0625	0.0400	**0.9583**	**0.0532**	**5.32**
PNDVI	0.0667	0.0345	0.0370	0.0606	0.0357	0.0297	0.0238	0.0278	0.0182	0.0000	0.0149	0.0370	0.0357	0.0800	0.0727	0.0656	0.0625	0.0800	**0.7825**	**0.0435**	**4.35**
BA	0.0333	0.0345	0.0370	0.0606	0.0357	0.0198	0.0238	0.0185	0.0273	0.0250	0.0000	0.0370	0.0357	0.0800	0.1091	0.0656	0.0625	0.0800	**0.7855**	**0.0436**	**4.36**
CI	0.0667	0.0690	0.0370	0.0606	0.0714	0.0297	0.0357	0.0185	0.0545	0.0250	0.0224	0.0000	0.0179	0.0400	0.0727	0.0656	0.0625	0.0400	**0.7892**	**0.0438**	**4.38**
RD	0.0667	0.0690	0.0741	0.0606	0.0714	0.0297	0.0238	0.0185	0.0545	0.0250	0.0224	0.0185	0.0000	0.0200	0.0364	0.0656	0.0625	0.0400	**0.7587**	**0.0421**	**4.21**
FIS	0.0333	0.0690	0.0370	0.0606	0.0714	0.0594	0.0238	0.0185	0.0182	0.0250	0.0224	0.0185	0.0179	0.0000	0.0182	0.0328	0.0625	0.0400	**0.6285**	**0.0349**	**3.49**
GI	0.0667	0.0690	0.0741	0.0606	0.0714	0.0297	0.0238	0.0185	0.0182	0.0250	0.0224	0.0185	0.0179	0.0200	0.0000	0.0164	0.0313	0.0400	**0.6234**	**0.0346**	**3.46**
EC	0.0333	0.0690	0.0741	0.0606	0.0714	0.0594	0.0357	0.0278	0.0182	0.0500	0.0448	0.0185	0.0179	0.0400	0.0364	0.0000	0.0313	0.0400	**0.7283**	**0.0405**	**4.05**
																				Total	**100**

Where: *WSV* weighted sum value, *CW* criteria weight

*Table 3.7: Calculating the consistency of pairwise comparison (**CR = 0.05**)*

variables	PT	PD	PC	PO	PW	PU	S	PE	SIPS	BS	W	PNDVI	BA	CI	RD	FIS	GI	EC
PT	0.060814506	0.0677	0.0664	0.0613	0.0670	0.0625	0.0849	0.1409	0.0678	0.0549	0.0532	0.0435	0.0873	0.0438	0.0421	0.0698	0.0346	0.0809
PD	0.060814506	0.0677	0.0664	0.1225	0.0670	0.1250	0.0849	0.0704	0.0678	0.1098	0.1065	0.0869	0.0873	0.0438	0.0421	0.0349	0.0346	0.0405
PC	0	0.0677	0.0664	0.0613	0.0670	0.1250	0.1697	0.1409	0.0678	0.0549	0.0532	0.0869	0.0873	0.0877	0.0421	0.0698	0.0346	0.0405
PO	0.060814506	0.0000	0.0664	0.0613	0.0670	0.1250	0.1697	0.1409	0.1357	0.0549	0.0532	0.0435	0.0436	0.0438	0.0421	0.0349	0.0346	0.0405
PW	0.060814506	0.0677	0.0000	0.0613	0.0670	0.0625	0.1697	0.1409	0.1357	0.1098	0.1065	0.0869	0.0873	0.0438	0.0421	0.0349	0.0346	0.0405
PU	0.060814506	0.0338	0.0332	0.0000	0.0670	0.0625	0.0849	0.1409	0.1357	0.0549	0.0532	0.0869	0.1309	0.0877	0.0843	0.0349	0.0693	0.0405
S	0.060814506	0.0677	0.0332	0.0306	0.0000	0.0625	0.0849	0.1409	0.2035	0.1646	0.1065	0.1304	0.1309	0.0877	0.1264	0.1048	0.1039	0.0809
PE	0.030407253	0.0677	0.0332	0.0306	0.0335	0.0000	0.0424	0.0704	0.0678	0.1098	0.1597	0.0869	0.1309	0.1315	0.1264	0.1048	0.1039	0.0809
SIPS	0.060814506	0.0677	0.0664	0.0306	0.0335	0.0312	0.0000	0.0704	0.0678	0.1098	0.1597	0.1304	0.0873	0.0438	0.0421	0.1048	0.1039	0.1214
BS	0.060814506	0.0338	0.0664	0.0613	0.0335	0.0625	0.0283	0.0000	0.0339	0.0549	0.1065	0.0869	0.0873	0.0877	0.0843	0.0698	0.0693	0.0405
W	0.060814506	0.0338	0.0664	0.0613	0.0335	0.0625	0.0424	0.0235	0.0000	0.0274	0.0532	0.1304	0.0873	0.0877	0.0843	0.0698	0.0693	0.0405
PNDVI	0.060814506	0.0338	0.0332	0.0613	0.0335	0.0312	0.0283	0.0352	0.0226	0.0000	0.0177	0.0435	0.0436	0.0877	0.0843	0.0698	0.0693	0.0809
BA	0.030407253	0.0338	0.0332	0.0613	0.0335	0.0208	0.0283	0.0235	0.0339	0.0274	0.0000	0.0435	0.0436	0.0877	0.1264	0.0698	0.0693	0.0809
CI	0.060814506	0.0677	0.0332	0.0613	0.0670	0.0312	0.0424	0.0235	0.0678	0.0274	0.0266	0.0000	0.0218	0.0438	0.0843	0.0698	0.0693	0.0405
RD	0.060814506	0.0677	0.0664	0.0613	0.0670	0.0312	0.0283	0.0235	0.0678	0.0274	0.0266	0.0217	0.0000	0.0219	0.0421	0.0698	0.0693	0.0405
FIS	0	0.0677	0.0332	0.0613	0.0670	0.0625	0.0283	0.0235	0.0226	0.0274	0.0266	0.0217	0.0218	0.0000	0.0211	0.0349	0.0693	0.0405
GI	0	0.0677	0.0664	0.0613	0.0670	0.0312	0.0283	0.0235	0.0226	0.0274	0.0266	0.0217	0.0218	0.0219	0.0000	0.0175	0.0346	0.0405
EC	0.030407253	0.0677	0.0664	0.0613	0.0670	0.0625	0.0424	0.0352	0.0226	0.0549	0.0532	0.0217	0.0218	0.0438	0.0421	0.0000	0.0346	0.0405

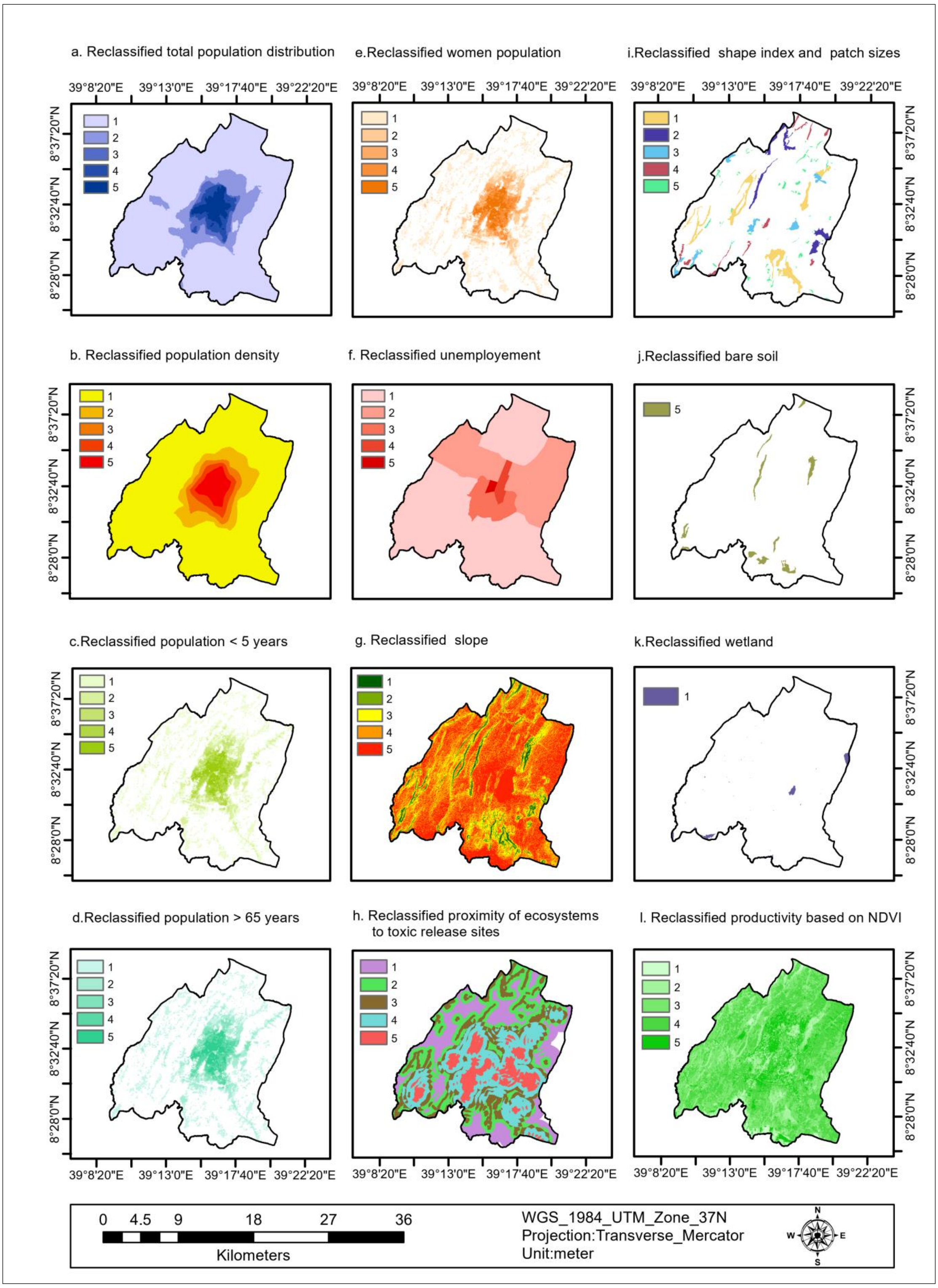

Figure 3.5: Reclassified SETS variables (a-l)

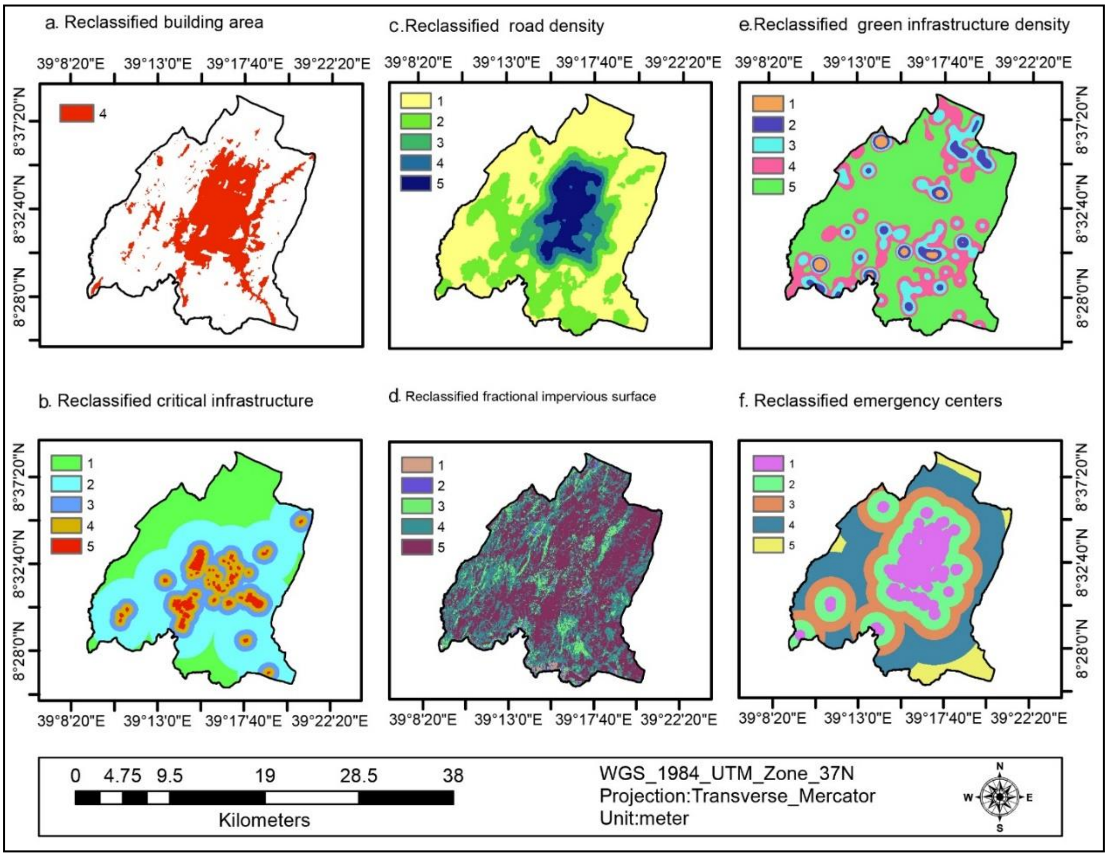

Figure 3.6: Reclassified SETS variables (a-f)

According to the social vulnerability map of the study area, approximately 28.32% of the total area is moderate to very highly vulnerable to flooding, with 5.16% (478.55 ha) as very high, 12.26% (1136.35 ha) as high, 10.9% (1010.55 ha) as moderate, 18.58% (1722.36 ha) as low, and 53.11% (4923.62 ha) as very low. The vulnerable area is located in the central part of the city, including Badhatuu, Odaa, Gurmuu, Dhadacha Araara, Abba Gadaa, Barreecha, Biqqa, Caffee, and Dagaaga, which are densely populated areas where a majority of the residents are women, children under five years, elderly over 65 years, and unemployed individuals. These findings are illustrated in Figure 3.3 (a-f) and Figure 3.8 (a).

The ecological vulnerability map of the study area revealed that a significant percentage of the land is vulnerable to flooding. Specifically, 4.18% is very highly vulnerable, 38.95% is highly vulnerable, 50.9% is moderately vulnerable, 5.85% is lowly vulnerable, and 0.11% is very lowly vulnerable. This indicates that an overwhelming majority of the total area (about 94.03%) is susceptible to flooding, particularly in the densely urbanized regions characterized by flat terrain, proximity to toxic sites, smaller fragmented patches, bare soil areas, and less productive areas. These regions, which include Migiraa, Dagaaga, Dhadacha Araara, Gaara Luugo, and Irreechaa areas, are represented in Figure 3.4 (a-f) and Figure 3.8 (b).

The technological vulnerability map of the study area revealed that 14.94 % (4655.28 ha) is high, 77.17% (24046.26 ha) is moderate and 7.88 %(2456.69 ha) is low vulnerable to flooding. This implies that about 92.11% of the area is technologically vulnerable to flooding. This area is characterized by most built-up areas, less availability of critical infrastructures, high road density, less impervious areas, and less green infrastructure density areas. These areas are all part of Dagaaga, Odaa, Badhatuu, Gurmuu, Abba Gadaa, Barreecha, Biqqa, and parts of Gaara Luugo, Migiraa, Irreechaa, and Gooro as shown in Figure 3.5 (a-f) and Figure 3.8 (c).

According to the study's SET vulnerability map of the study area, flooding vulnerability levels varied across different neighborhoods. Specifically, 67.3 ha or 0.73% of the area was identified as very highly vulnerable, while 2307.7 ha or 24.94%, 3924.55 ha or 42.41%, 2954.81 ha or 31.93%, and 0.38 ha or 0.004% were identified as high, moderate, low, and very low vulnerable, respectively. These findings indicate that approximately 68.08% of the study area is at moderate to very high risk of flooding. In particular, local neighborhoods such as Dagaaga, Badhatuu, Odaa, Gurmuu, Abba Gadaa, Barreecha, Biqqa, and Dhadacha Araara were found to be among the most vulnerable (very high-to-high), while surrounding areas were deemed highly vulnerable to flooding. Factors contributing to this vulnerability include densely built environments, limited vegetation cover, high population density, proximity to toxic waste sites, unemployment, and impervious surface areas, as illustrated in Figure 3.8 (g).

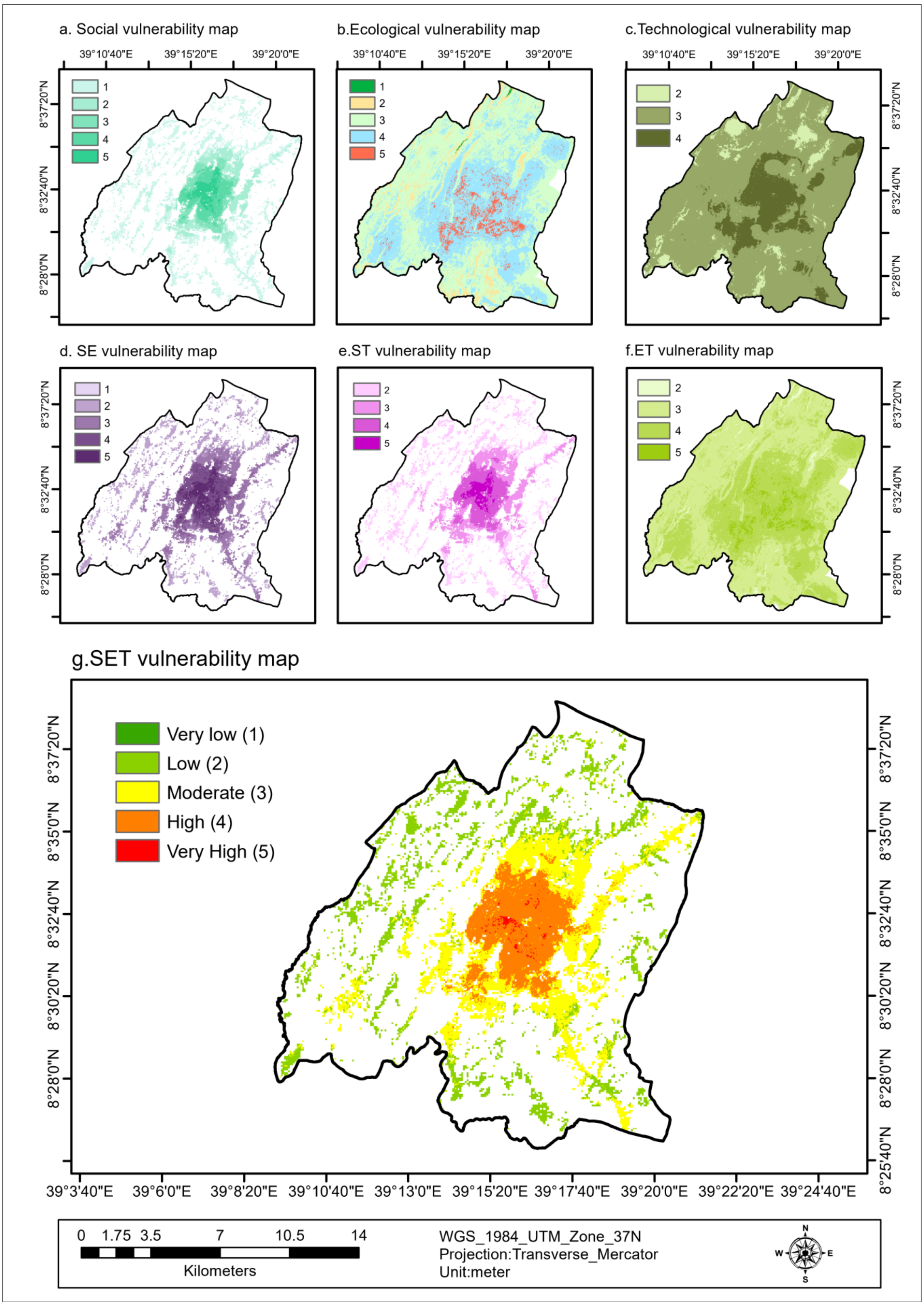

Figure 3.7: S, E, T, SE, ST, ET, SET flood vulnerability maps of the study area

Spatial autocorrelation of SETS flood vulnerability maps

According to the Global Moran's I summary, all SETS vulnerability maps exhibit clustering and positive autocorrelation (Table 3.8), as evidenced by the positive Moran's I index values. In particular, for the SET vulnerability map displayed in Figure 3.8, Moran's I Index was 0.237236, indicating a positive spatial autocorrelation in the map. This implies that similar values tended to be clustered together in space rather than being randomly distributed. The Expected Index was close to zero (-0.000181), suggesting the absence of any spatial pattern if the data were randomly distributed. The data variance (0.000187) describes the degree of variation present, whereas the Z score (17.344497) indicates a significant difference between the observed and expected indices. The p-value (0.000000) being less than the significance level of 0.05 provides strong evidence to reject the null hypothesis that the spatial pattern is random. Consequently, the Global Moran's I Summary result suggests a clustered spatial pattern for SET vulnerability maps.

A clustered spatial pattern in Global Moran I for flood vulnerability indicates that areas with high flood vulnerability tend to be clustered together, and this has important implications for the allocation of resources and mitigation strategies. Understanding the clustering of different areas can aid in prioritizing interventions and allocating resources effectively to mitigate flood vulnerability. This information is depicted in Figure 3.8 (a-g), which presents separate, combined, and overall SET flood vulnerability maps, allowing for targeted actions with maximum impact. It can also help identify areas where measures such as building codes or land use regulations can be implemented to reduce vulnerability cost-effectively. Overall, understanding the clustered spatial pattern of flood vulnerability can provide valuable insight for decision-makers and planners seeking to reduce the impact of floods on communities and infrastructure.

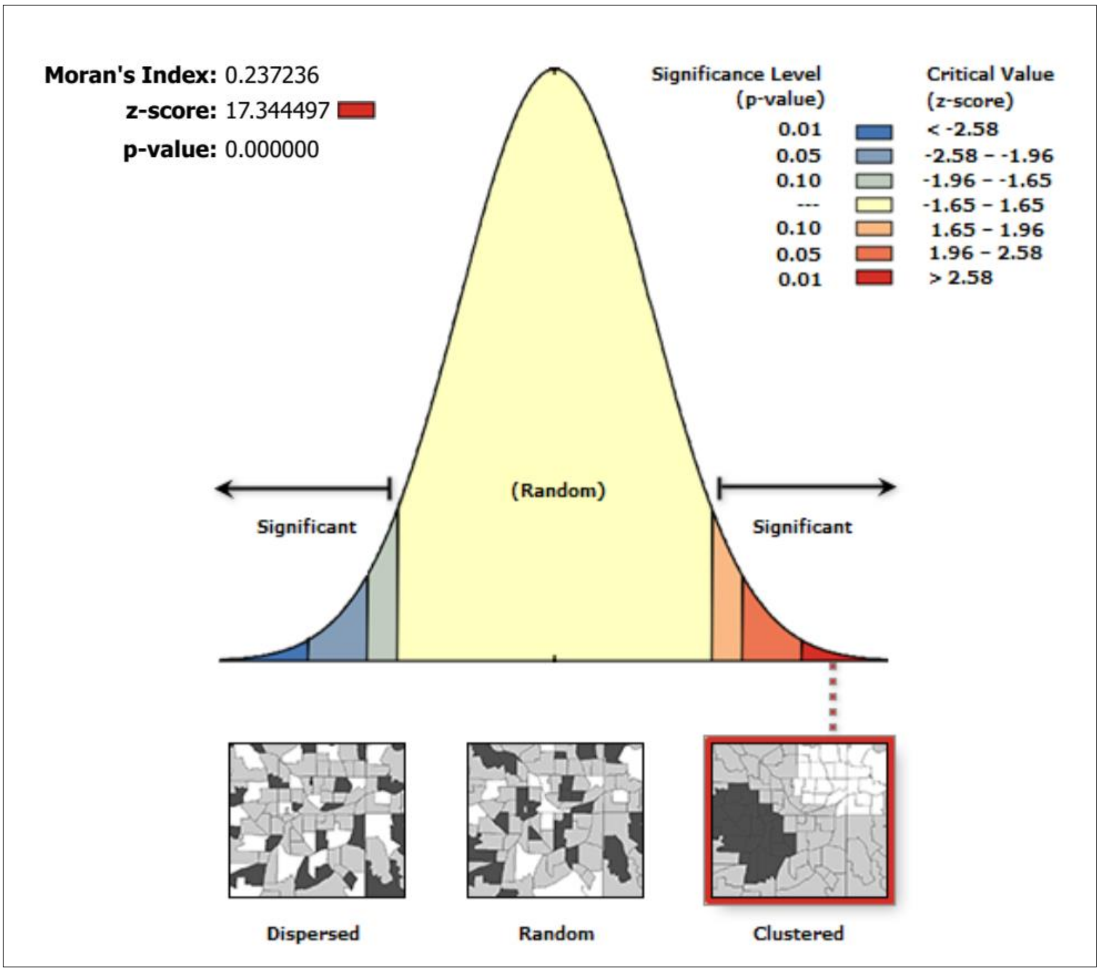

Figure 3.8: Spatial autocorrelation of SET flood vulnerability map

Table 3.8: Global Moran`s I Summary for S, E, T, SE, ST, ET, and SET flood vulnerability maps

Global Moran's I Summary	S	E	T	SE	ST	ET	SET
Moran's Index	1.136199	0.283748	0.205036	0.445320	0.671565	0.147702	0.237236
Expected Index:	-0.000818	-0.000051	-0.000356	-0.000151	-0.000586	-0.000071	-0.000181
Variance:	0.001418	0.000036	0.000229	0.000151	0.000829	0.000051	0.000187
z-score	30.196861	47.099950	13.580173	36.266498	23.347086	20.648194	17.344497
p-value	0.000000	0.000000	0.000000	0.000000	0.000000	0.000000	0.000000
Spatial pattern	Clustered	Clustered	Clustered	Clustered	Clustered	Clustered	Clustered

3.4 Discussions

Analyzing urban flooding complexities through the SETS approach is essential as it examines interdependencies between social, ecological, and technological systems that escalate flood vulnerability of residents in flood-prone areas due to changes in land use, hydrology, population, economic growth, and climate (Chang et al., 2021; Tanoue et al., 2016; Tate et al., 2021). Due to this, it is imperative to give due consideration to the SETS framework as it facilitates an analysis of floods on both an individual and interconnected basis. This is especially the case in developing countries, where limited infrastructure and resources exacerbate the severity of flooding impacts (Deria et al., 2020; Salami et al., 2017). The findings of the study revealed that locally known neighborhoods such as Badhatuu, Odaa, Gurmuu, Dhadacha Araara, Abba Gadaa, Barreecha, Biqqa, Caffee, and Dagaaga face the risk of negative impacts from flooding events. These areas have high rates of unemployment, significant elderly and child populations under five years of age, and predominantly women residents. The findings of the current study are consistent with studies conducted by (Rufat et al., 2015; Tanoue et al., 2016; Tate et al., 2021) as flood exposure and social vulnerability are interconnected, and socially vulnerable populations, including children, the elderly, the disabled, the poor, and minorities, are more likely to experience injury and death from flooding relative to the others.

The vulnerability of floods increases in depression and flat areas, proximity to toxic release sites from industries, smaller and fragmented patches, and bare soil areas. Those areas were found within the study area locally known as Migiraa, Dagaaga, Dhadacha Araara, Gaara Luugo, and Irreechaa areas. This study supports the findings of prior research indicating that flatter topographies are prone to flooding and have lower slope values (Singh et al., 2020). Vegetation cover is seen as an effective means of mitigating flood vulnerability by reducing surface runoff and absorbing water, which is in agreement with studies conducted by Cian et al. (2018), and Zhang et al. (2018). Moreover, proximity to toxic industries, where the potential for exposure to hazardous waste poses risks to surrounding communities as conducted by Chang et al. (2021), Jongman et al. (2015), and Talbot et al. (2018). Similarly, fragmented and smaller patches of ecosystems are less effective at providing flood mitigation services, as demonstrated in studies by ; and Rehman et al. (2021). In addition, bare soil areas pose a greater risk in terms of their low infiltration capacity and high erodibility in the event of floods, as posited by (Chang et al., 2021).

The vulnerability to flooding in certain areas can be attributed to a high concentration of built-up areas, a dense road network, limited impervious areas, and a low density of green infrastructure. Specifically, the neighborhoods of Dagaaga, Odaa, Badhatuu, Gurmuu, Abba Gadaa, Barreecha, Biqqa, and parts of Gaara Luugo, Migiraa, Irreechaa, and Gooro are particularly susceptible to flooding. These findings align with previous studies conducted in various urban areas, highlighting the consistent spatial patterns of flood vulnerability (Briones et al., 2020). The inability of the built-up areas to allow water to percolate through the subsurface makes them more vulnerable in the study area, which is consistent with the study conducted by Deepak et al. (2020).

The presence of high fractions of impervious surfaces and dense road networks also exacerbate the risk of floods by impeding water infiltration and accelerating surface runoff (Baky et al., 2020; Kaspersen et al., 2015). Consequently, these factors contribute significantly to flood vulnerability within the study area. The aforementioned studies have established this connection between the lack of subsurface permeability and the increased susceptibility of built-up areas to flooding, as well as the role played by impervious surfaces and road density in exacerbating flood risks.

The study reveals that the area characterized by a lower density of green infrastructure also faces increased susceptibility to flooding. This poses a hindrance to infiltration processes and exacerbates runoff. These findings further support a previous study, conducted by Khodadad et al. (2023) and Pallathadka et al. (2022), which highlights the crucial role of green infrastructure in mitigating an area's vulnerability to flooding through its ability to enhance infiltration and reduce runoff. The consistency between these studies reinforces the significance of incorporating green infrastructure as a means to alleviate flood-related risks in urban environments. This correlation underscores the importance of pursuing strategies that prioritize the integration of green infrastructure to enhance the resilience of areas prone to flooding.

According to the findings of the present study, certain areas close to critical infrastructure such as toxic industries, landfill sites, abattoirs, and gas terminals face a significant vulnerability to flooding, thus posing a threat to the local community. This finding aligns with previous studies conducted by Lin et al. (2019); Murdock et al. (2018); Qiang (2019), who highlighted the potential flood vulnerability associated with proximity to such infrastructure. Conversely, this study found that areas near emergency centers, including hospitals, schools, and universities, play a crucial role during floods by acting as essential assets for support and serving as emergency response sites. This finding is consistent with the previous research carried out by Atanga and Tankpa (2022); Cutter et al. (2003), further emphasizing the importance of these locations in flood response and underscoring their significance in safeguarding affected communities.

3.5 Conclusion

The SETS framework has been successfully applied in this research to characterize the flood vulnerability of urban areas, the city of Adama, and its environs. The findings indicated that vulnerability to flooding across the Social-Ecological-Technological domains follows a clustered distribution pattern. Moreover, the study identified spatial correlations between Social-Ecological, Social-Technological, and Ecological-Technological vulnerabilities, indicating opportunities to enhance flood mitigation measures in multiple domains simultaneously. This research can provide insights into developing more effective flood vulnerability reduction strategies in the study area and can be applied to other urban areas facing similar challenges.

The study explored the implications of sustainable urban development, with specific emphasis on exposure, sensitivity, and adaptability to flood vulnerability. The findings of the research have significant implications for cities undertaking sustainable urban development. Based on the SET vulnerability map developed for the study area, it was observed that the levels of vulnerability to flooding differed among various neighborhoods. The results highlighted that approximately 68.08% of the study area was exposed to moderate to very high flood vulnerability, necessitating immediate attention and mitigation efforts. By utilizing the SETS framework, a better understanding of the interconnectivity between social, environmental, and infrastructure was gained, which is critical in achieving sustainable urban development. The relevance of this study for other developing cities lies in the potential application of the SETS framework, which was initially tested in the study area. By adopting this framework, municipalities can draw insights from these findings and assess their susceptibility to flooding. As flooding is spatially confined to specific areas, municipal administrators and practitioners can effectively target vulnerable neighborhoods to adapt to flooding. Ultimately, this study provides insights into an improved understanding of the complex nature of sustainable urban development, particularly regarding natural hazard management.

CHAPTER FOUR:

Investigation of flood-resilient Neighborhoods: The Case of Adama City, Central Ethiopia

Abstract

Adama is the second most populous city in Ethiopia, and experiences frequent flash floods that have a detrimental impact on the community's livelihood. To this effect, a comprehensive investigation to identify flood-resilient neighborhoods in the study area has been undertaken. By considering the existing spatial pattern and morphology that are resilient to urban flooding, the city can enhance its flood management strategies in the future. Detailed examination of two neighborhoods identified through space syntax analysis with high and low spatial connectivity revealed important insights into flood resilience. neighborhoods with high spatial connectivity exhibited well-interconnected street systems with manageable street spacing, facilitating efficient runoff flow and effective flood management during flooding events. These neighborhoods also had shorter block sizes with frequent intersections, promoting better water drainage and reducing the risk of flooding during heavy rainfall events. The grid spatial pattern observed in these areas allowed for efficient water runoff through multiple drainage paths, including the street surfaces. On the contrary, neighborhoods with low spatial connectivity exacerbated urban flooding. The lack of connectivity and abundance of dead-end streets posed challenges for flood evacuation during emergencies. Irregular block arrangements disrupted the natural drainage system, aggravating the potential for urban flooding. These findings have implications for other flood-prone areas of neighborhoods in the study area and other similar urban areas in the global south on how human settlements are arranged spatially to mitigate urban flood vulnerability.

Key words: Urban flood; Spatial morphology; Space syntax; Resilience; Adama; Ethiopia

4.1 Introduction

Urban flood vulnerability is a global issue that requires attention and action. It’s a major natural global hazard that is becoming increasingly frequent and serious worldwide due to the acceleration of urbanization processes and dramatic urban physical forms changes (Wang et al., 2022a; Ziegler et al., 2012). Human and natural factors affect vulnerability to flooding, such as agricultural activity, urbanization, deforestation, and land degradation. Devastating flood risk increases due to climate change, heavier rainfall, and deforestation (Baky et al., 2020; Chiara et al., 2015; Samuel et al., 2019; Tanoue et al., 2016). Urban areas are vulnerable to extreme hydrologic events such as heavy precipitation and floods. This is due to the concentration of population, rising runoff volume, increase in built-up infrastructure, and other human activities (Chang & Franczyk, 2008; Chen & Leandro, 2019; Waghwala & Agnihotri, 2019).

Urban flood vulnerability varies across regions of the world, with some areas being more vulnerable than others. Rapid urbanization in developing countries, particularly in Africa and Asia, is a challenge for flood risk management (Duc, 2013; Kovacs et al., 2017; Wang et al., 2022a). Due to the interconnection between flood exposure and poverty, low and middle-income countries are particularly vulnerable to flood risks given the challenges associated with social safety nets and infrastructure quality, with 89% of the world's flood-exposed population residing in these countries (McDermott, 2022; Rentschler & Salhab, 2020; Rentschler et al., 2022). In addition, informal settlements in various global southern nations face enormous challenges that contribute to their vulnerability to flooding (Anwana & Owojori, 2023; Tietjen et al., 2023). These settlements often lack proper infrastructure, including adequate drainage systems, which increases their susceptibility to flood hazards (Gomez et al., 2023; Peters et al., 2022; Ramiaramanana & Teller, 2021). In contrast, formal and well-planned settlements with appropriate drainage systems demonstrate a reduced vulnerability to flooding (Adegun, 2023; Williams et al., 2019).

Achieving urban flood resilience is considered the best technique for dealing with urban flood vulnerability (Schelfaut et al., 2011; Yin et al., 2022). Urban flood resilience refers to a city's ability to withstand and recover from flooding, effectively managing the physical damage and socioeconomic disruptions that arise, to prevent casualties and injuries, and preserve the existing social, economic, and environmental fabric (Rözer et al., 2022). Within a city, certain neighborhoods may be more vulnerable to flooding than others, while some areas may be more resilient to flooding due to the physical urban form. Neighborhood-level considerations play a crucial role in community resilience planning in urban locations (Bukvic et al., 2021).

Investigating flood-resilient neighborhoods is important for flood mitigation and sustainable spatial planning and contribute to increasing flood resilience in neighborhoods (Bukvic et al., 2021; Fitriyati et al., 2022; Serre et al., 2018; Truu et al., 2021). It is important to consider the specific context and scale of the community when identifying and implementing strategies to increase resilience to flooding. Implementing flood-resilient neighborhoods is challenging due to different factors such as rapid urbanization and climate change (Serre et al., 2018); flood-prone areas are often subject to climate change and socioeconomic development, which can contribute to increasing flooding (Hemmati et al., 2020); and the need for coordination between different stakeholders and the potential for conflicts between different interests (Serre et al., 2018).

Following pioneering research conducted by Holling who coined the term "resilience" in the study of ecology in 1973 (Holling, 1973), many studies were used in various fields such as disaster management, psychiatry, and social science (McClymont et al., 2020). They are used as a part and combination of interdisciplinary frameworks (*engineering*, *systems*, and *complex adaptive systems resilience*)(Breen & Anderies, 2011). Recently, the concept of Social-Ecological-Technological Systems(SETS) resilience provides frameworks for optimizing human-environment interactions and addressing risks posed by natural and climate-induced hazards (Kim et al., 2022; Sharifi, 2023). By analyzing the intricate interplay between environment, infrastructure, and equity considerations, SETS allows us to explore how hazards impact society and their distribution across different domains (Chang et al., 2021). In the urban planning concept, urban resilience pertains to the capacities of the urban system that are essential to the proper functioning of urban services (Rus et al., 2018) and promotes 'living with floods'(Batica & Gourbesville, 2016). In this study, flood resilience is defined as the ability of urban areas to withstand and recover from the impacts of flooding. It involves a comprehensive approach that considers various aspects of urban morphological elements such as street networks/ connectivity, buildings, and block arrangements. By considering these various aspects and their interdependencies, cities can develop comprehensive approaches to mitigate the impacts of flooding and enhance their resilience in the face of future flood events.

Extensive research has been conducted by Bottazzi et al. (2018); Jiménez et al. (2018); Mugume and Butler (2017); Newman et al. (2020) to examine the components of urban flood resilience, including physical infrastructure such as drainage systems, transportation, green infrastructure, housing, and community resilience, as well as social and economic factors. However, given the complex and dynamic nature of urban areas, it is essential to delve into different themes and their interconnectedness to develop a comprehensive understanding of urban flood resilience, as highlighted by Barreiro et al. (2020); Rezende et al. (2019). In line with this, Prashar et al. (2023) stress the importance of uncovering these various themes and connections to enhance our knowledge in this area. Therefore, it is crucial to expand our research scope and explore the multifaceted aspects of urban flood resilience to effectively address the challenges faced by urban communities in the face of flooding events.

Abshirini et al. (2017) examined the resilience of cities based on similarity and sameness measures and focused on the accessibility of street networks to different amenities before and after flooding. He et al. (2022) investigated the resilience of urban road networks, considering their exposure to flood hazards and the indirect effects caused by travel disruptions and cascading failures throughout the city. Martin et al. (2021) conducted a study that measured the resilience of road networks in terms of territorial accessibility, evaluating different orders of network damage using deterministic and random approaches.

Recent research has emphasized the crucial role of spatial morphology in urban flood resilience, highlighting its significance in enhancing cities' ability to withstand and recover from flooding (Marcus & Colding, 2014; Maulana & Nordin, 2019). This concept of integrating resilience with urban morphology has garnered increasing interest among researchers, recognizing the importance of considering the physical layout and structure of urban areas in developing strategies to enhance flood resilience (Stangl, 2018). This includes understanding the spatial arrangement of infrastructure, such as street networks, building composition, and block arrangements, for effectively managing flood risks. By exploring the interconnectedness between spatial morphology and resilience, cities can develop comprehensive approaches that address the complex and dynamic nature of urban flood resilience (Shukla et al., 2023). For example, Serre et al. (2018) evaluated the capacity of urban drainage systems and strategies to reduce building exposure to flood hazards. Feng et al. (2021) also highlighted the importance of the spatial distribution of impervious surface coverage, which is closely related to flood risk. Additionally, utilized urban density-based runoff simulation to project and enhance the flood resilience of cities. However, these studies did not explicitly examine other essential urban elements such as road connectivity and spatial morphologies.

Road connectivity plays a critical role in ensuring that public infrastructure facilities including community flood relief centers, primary health care centers, emergency response managers, and disaster response forces are adequate during floods (Tachaudomdach et al., 2021; Watson & Ahn, 2022; Xu et al., 2022). Connectivity refers to the direct connections that a street has with its neighboring streets within a specific area. A high connectivity value indicates that a street has numerous connections with its side streets, while a low value suggests fewer connections. This static measurement is essential in determining the level of connectivity and its impact on flood resilience in a particular urban area. Unfortunately, during the inundation, the mobility of cities and flood-affected neighborhoods deteriorates, worsening the situation (Asiedu, 2020). Disruption of road network connectivity brings cities to a standstill, leading to substantial emotional trauma and economic losses for those affected (He et al., 2022). The impact of floods on roads is categorized into direct effects such as physical damage to infrastructure and transport facilities, and indirect impacts like disruption to traffic movement, and loss of business, and life (Brown & Dawson, 2016; Hammond et al., 2015; Kadaverugu et al., 2021). During urban flooding inundated roads become inaccessible and risky for movement, negatively impacting essential services and emergency operations. This disruption increases resilience time, further exacerbating the impact on the city's overall resilience (MS et al., 2022).

Spatial morphology has developed frameworks for studying urban form that can be used to organize data on resilience, on smaller and larger-scale units of analysis using GIS applications to examine the impact of forces and responses at multiple scales (Stangl, 2018). Gauthier and Gilliland (2006) provided an exhaustive survey of various scientific studies focusing on spatial morphology, from the empirical analysis of the city as a spatial entity, to normative propositions in multiple fields including urban planning, urban design, architecture, economics, archaeology, and urban history. The methodologies range from general concepts suited for wider application, such as Kevin Lynch's studies, to very specific topics with notation systems, as exemplified by Satoh (1997) to examine various dimensions of threats to urban life and property, such as earthquakes, fires, and flooding (Stangl, 2018). Nowadays, four prominent schools of thought in urban morphology exist, each offering distinct theories, concepts, and methodologies to comprehend the physical structure of cities. These schools of thought are:

1. Morphological analysis, which explores the arrangement of streets, plots, and buildings within a city;
2. Philosophical process, which examines the social dimension of urban space;
3. Typo-morphological analysis, which scrutinizes the overall organization of towns, buildings, and systems; and
4. Space syntax, which investigates the intricate relationship between society and spatial configurations.

These theories have profound implications for the societal, economic, and environmental aspects of urban life (Kropf, 2009; Sima & Zhang, 2009). This study adopts a historico-geographical and space syntax framework to investigate flood-resilient neighborhoods in relation to urban form. Through this approach, it reveals a better understanding of how city layouts impact resilience in the face of flooding events

Therefore, the present study focuses on operationalizing road connectivity, flood event observations, key informants and Municipality interviews, and spatial morphology to investigate urban flood-resilient neighborhood areas that could help reduce impacts, enable evacuation or provide safe havens, or facilitate recovery at the neighborhood level to achieve sustainable urban development to build resilience to urban flooding. Investigating the flood resilience of the study area, a flood-prone city in Ethiopia, at the neighborhood level is crucial for understanding and mitigating flood hazards, highlighting the significance of integrating accessibility and spatial morphology concerns at the urban scale.

4.2 Data and Methodology

4.2.1 Data sources

Data on the existing street network, administration boundary, block arrangements, and land use in the study area was acquired from the Adama City Administration (ACA). To fill in any gaps in the existing road network, digital mapping techniques were employed using Google Earth Pro-Satellite imagery (Version 7.3.6) within the ArcGIS software (Version 10.8). This method ensured an accurate and comprehensive representation of the road infrastructure in the study area. The combination of data obtained from ACA and the digitization process facilitated the creation of a reliable and up-to-date road network dataset.

Similarly, buildings were digitized from high-resolution Google Earth Pro-Satellite imagery (Version 7.3.6) in ArcGIS software (Version 10.8). The acquisition of the existing blocks from the esteemed Adama City Administration (ACA) was undertaken to bridge the gaps in the current inventory, necessitating the utilization of digital mapping methods. Specifically, Google Earth Pro-Satellite imagery (Version 7.3.6) supported by the ArcGIS software (Version 10.8) was employed. This approach not only ensured high precision but also provided a comprehensive depiction of the blocks within the study area. By combining the data procured from ACA with the digitization process, a dependable and contemporary dataset of blocks was successfully generated.

Furthermore, the land use data was used to interpret the function concerning street connectivity. Finally, flood event observations, key informants, and professionals from the municipality actively participated in the research process, providing valuable insights and perspectives.

4.2.2 Methods

The research methodology involved flood events observations, utilization of the depth-map model, insights from experts and key informants, and an extensive review of relevant literature. This comprehensive framework allowed for the investigation of the complex relationship between urban morphology and flood resilience, ultimately informing urban planning and design strategies to create more resilient settlements and communities.

The first step in the research methodology was to use the DepthmapX model output to identify areas in the study area with varying levels of connectivity. Then, flood event observations were conducted during heavy rainfall in the rainy seasons of June, July, and August 2023. Two sites were selected for further morphological analysis: one with low connectivity and one with high connectivity. These sites were chosen due to their proximity to each other, regular inundation with floods, similar landforms, and soil types, and their status as long-standing settlements. Both sites have a history of being heavily impacted by floods during the rainy season, causing significant damage to the local community and affecting their daily livelihoods. The morphological analysis involved the examination of the street system (street hierarchy and material), buildings, land use, and block arrangements.

To gather comprehensive insights, key informant elders who have lived in the area for over 35 years were consulted about flood events situations in their neighborhoods. These elders represented organized local community leaders from religious, women's, security facilitators, and business sectors, with 10 elders from site "a" and 10 from site "b". Additionally, professionals from the municipality were also consulted regarding flood events in the study area. The general workflow followed by this study is represented in Figure 4.1.

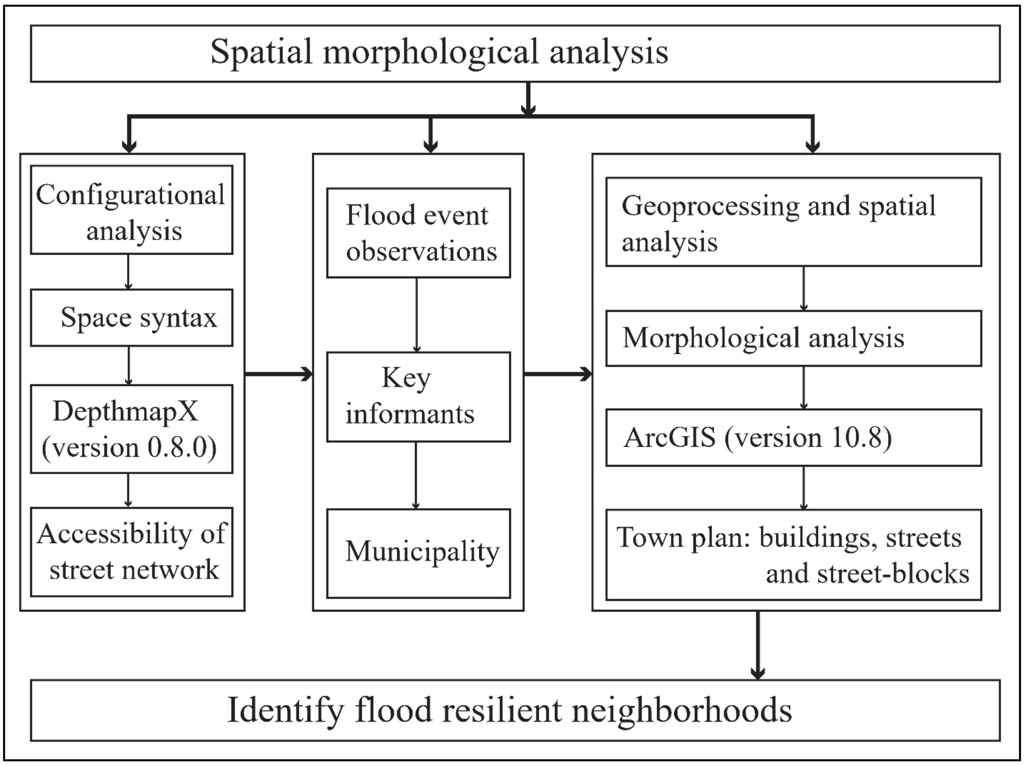

Figure 4.1:Flow chart to identify flood-resilient neighborhoods of the study area

4.2.2.1 Methods of analyzing configurational analysis

Space syntax is a set of analytical techniques used to examine the spatial arrangement of various environments, particularly those in which spatial configuration plays a crucial role in human affairs, such as buildings and cities (Hillier, 1984). This approach scrutinizes diverse phenomena including patterns of movement, spatial layout, awareness, interaction, density, land value, urban growth, societal differentiation, safety, and crime distribution. To conduct the analysis, the research employed DepthmapX software (version 0.8.0), which facilitated the assessment of axial accessibility (Behmanesh & Brown, 2019; Turner, 2007; Varoudis, 2012). By utilizing this software, areas with high and low accessibility were identified and subsequently selected for further morphological analysis.

4.2.2.2 Geoprocessing and Spatial Analysis

The analysis of the town plan for two specific areas, namely high and least-accessible areas, was conducted using ArcGIS 10.8. This software tool enabled the examination of morphological aspects, which encompassed the study of street layout, buildings, and block distribution within the urban setting. The primary focus of this investigation was to identify flood-resilient areas within the city.

4.3 Results

4.3.1 Configurational Analysis of Adama City

The analysis of Adama City's configuration using DepthmapX (version 0.8.0) revealed varying levels of connectivity across different areas in the city as shown in Figure 4. 3. DepthmapX (version 0.8.0) calculates DepthmapX (version 0.8.0) as a tool that calculates the spatial integration of a street axis, or axial line, concerning all other streets in the system. Essentially, it measures how many changes of direction, or syntactic steps, are needed to reach all locations in the system from a particular street. Streets with fewer changes of direction have higher integration values, while those with many changes of direction tend to have lower values and are considered spatially segregated.

These integration values can be represented on a map using a color range. For example, in Figure 4.3, we can see the degree of connectivity for each street in the study area. The streets marked in red and yellow have the highest number of connections to adjacent streets, while those with dark blue colors only have one or two connections nearby. The city center has high connectivity values, and one of the main shopping areas, "site a", also has a high connectivity value. On the other hand, "site b", which is an informal residential area, has low street connectivity.

It is worth noting that the localities of Oda, Badhaatu, Abba Gadaa, and Gurmu exhibit high accessibility, indicating a well-connected and easily navigable street network in the study area. This suggests that these areas may have a better chance of receiving aid and emergency assistance due to their accessibility. In contrast, Dagaaga, Dhadacha Araara, Hangaatu, and Caffee demonstrate moderate accessibility, suggesting a relatively less developed road infrastructure compared to the aforementioned areas. This can make it more challenging for people to move around within these areas. Moreover, the remaining parts of the city have lower levels of accessibility, which could make them more vulnerable to urban flooding. Inaccessibility in these areas can hinder the movement of people and resources during flood events, making it more difficult to provide assistance and mitigate the impacts of flooding.

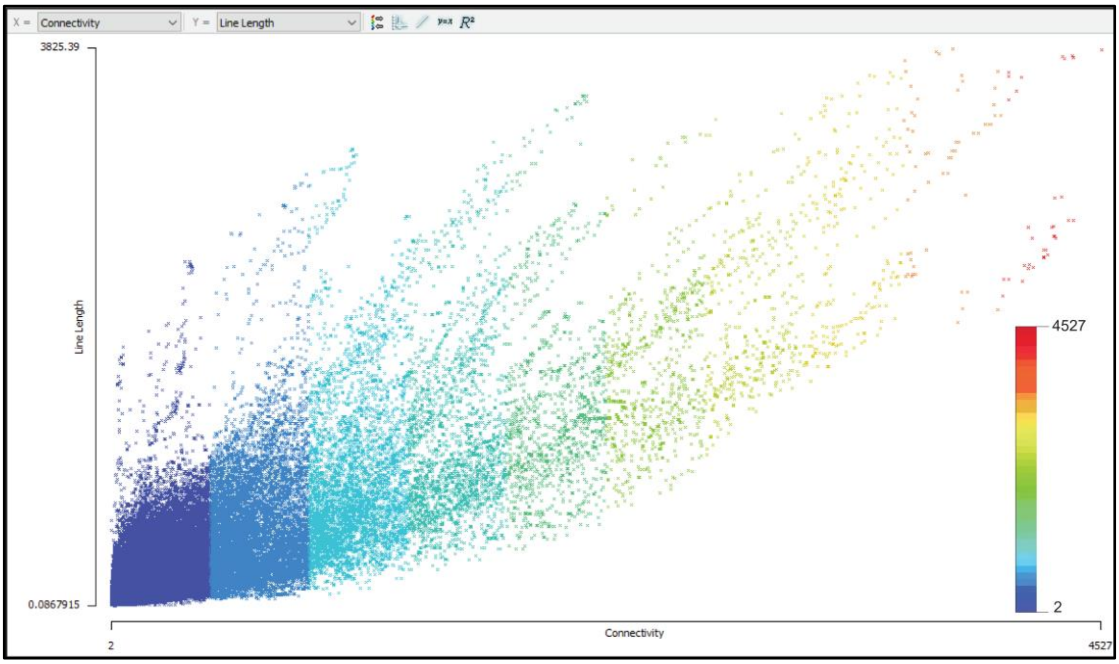

Figure 4.2: Scatter plot of street line length to connectivity for the study area

The DephmapX dataset showed an average connectivity attribute value of 291.96, ranging from a minimum of 2 to a maximum of 4527. The standard deviation was calculated to be 466.48. Furthermore, the total count of line length in the dataset was 116,464, representing the overall extent of the street network of the study area. Based on the information presented in Table 4.1, Figure 4.2, and Figure 4.3, neighborhoods that exhibited connectivity values below 454.5 and above 4074.5 were selected for further morphological analysis. These specific thresholds were chosen to identify areas with significantly low and high connectivity respectively, which may indicate distinct characteristics or patterns within the street network. By focusing on these neighborhoods, further morphology and structure of the network, potentially uncovering valuable insights and understanding how connectivity attributes contribute to the overall functionality and efficiency of flood resilience during heavy rainfall.

Table 4.1: Connectivity Attributes of the study area using DepthmapX (version 0.8.0) Model Output

Value	**Average**	**Min.**	**Max.**	**Std Dev.**	**Count**	**< 454.5**	**454.5-907**	**907-1359.5**	**1359.5 -2264**	**2264.5-3169.5**	**3169.5 - 3622**	**3622 - 4074.5**	**> 4074.5**
Attribute	291.96	2	4527	466.48	116464	95316	11448	4910	3,370	1,121	208	57	34
Remarks on the level of spatial connectivity						Low			Medium				High

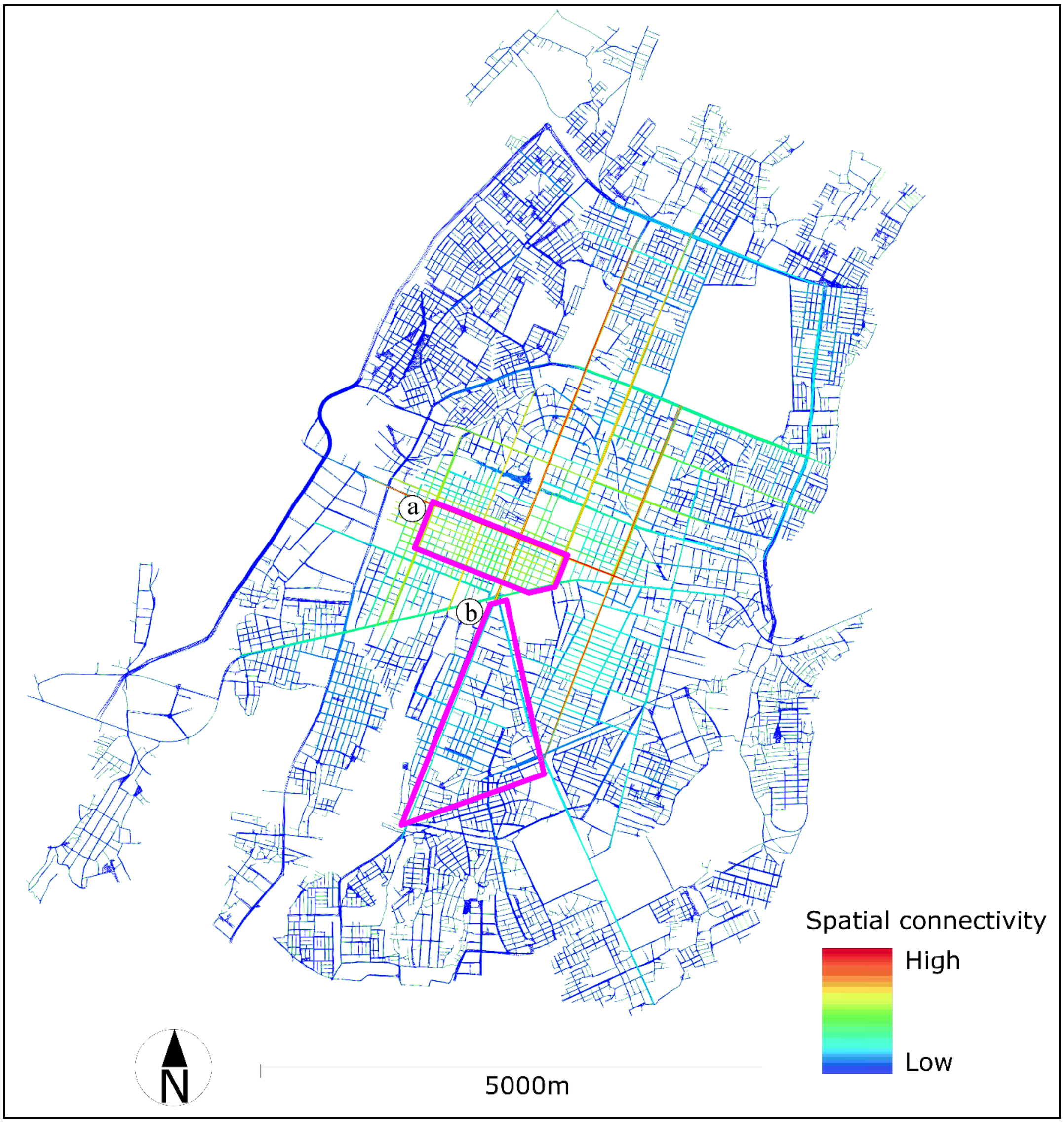

Figure 4.3: Spatial Connectivity Map of the study area

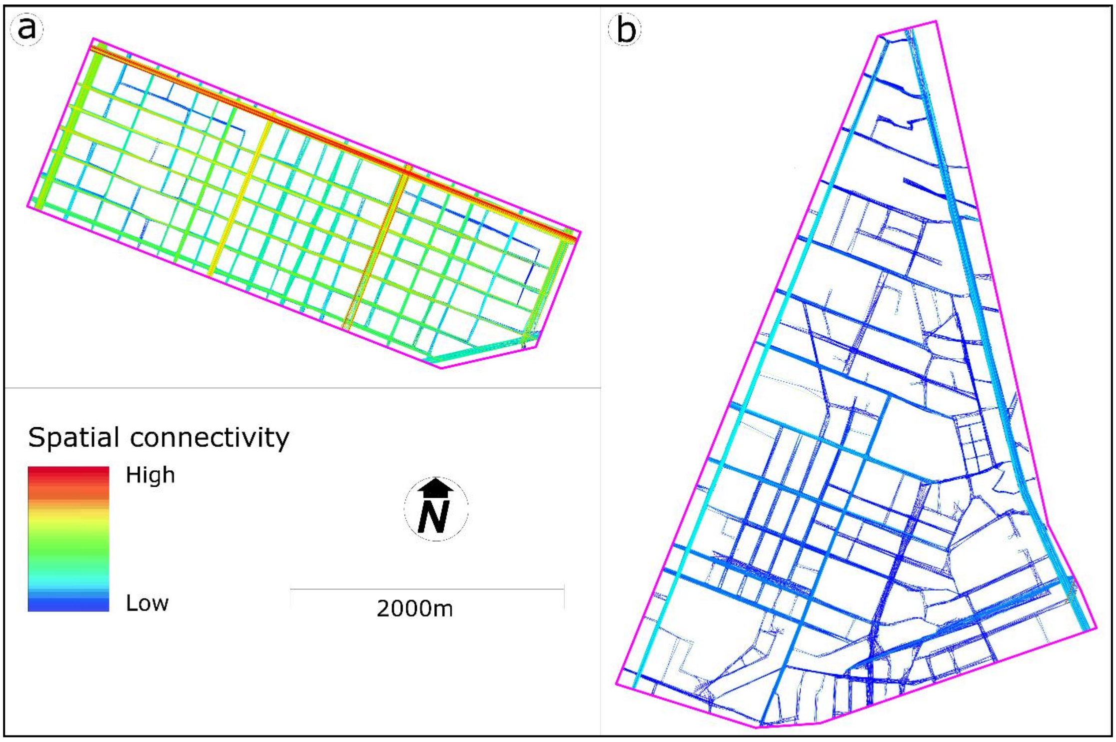

Figure 4.4: Selected sites with high connectivity (a) and low connectivity (b) parts of the study area.

Figure 4.5 shows the two sites chosen for the study, referred to as site “a” and site “b”, which displayed varying degrees of connectivity. Site “a” was identified as having a high level of connectivity, while site “b” was characterized by a low level of connectivity. Site “a” was found to have a vibrant and well-developed central area of the city, with 41.52% of its land use designated for commercial and mixed purposes. On the other hand, site “b” was considered an informal settlement, with only 8% of its land use allocated for commercial and mixed purposes, and primarily consisting of residential quarters, as illustrated in Table 4.2 and Figure 4.6.

Table 4.2: Comparative analysis of land use of the two sites

Land use types	**Area (ha)**		**Percent (%)**	
	Site a	Site b	Site a	Site b
Residential	22.83	60.67	47.31	63
Commercial	10.43	2.78	21.6	3
Service	1.89	8.72	3.92	9
Open and green space	0.46	5.43	0.95	6
Administration	0.66	0.97	1.38	1
Industry and Manufacturing	1.66	11.54	3.43	12
Under construction	0.72	0.73	1.5	1
Mixed-use	9.61	4.69	19.92	5
Vacant land	-	1.38	-	1

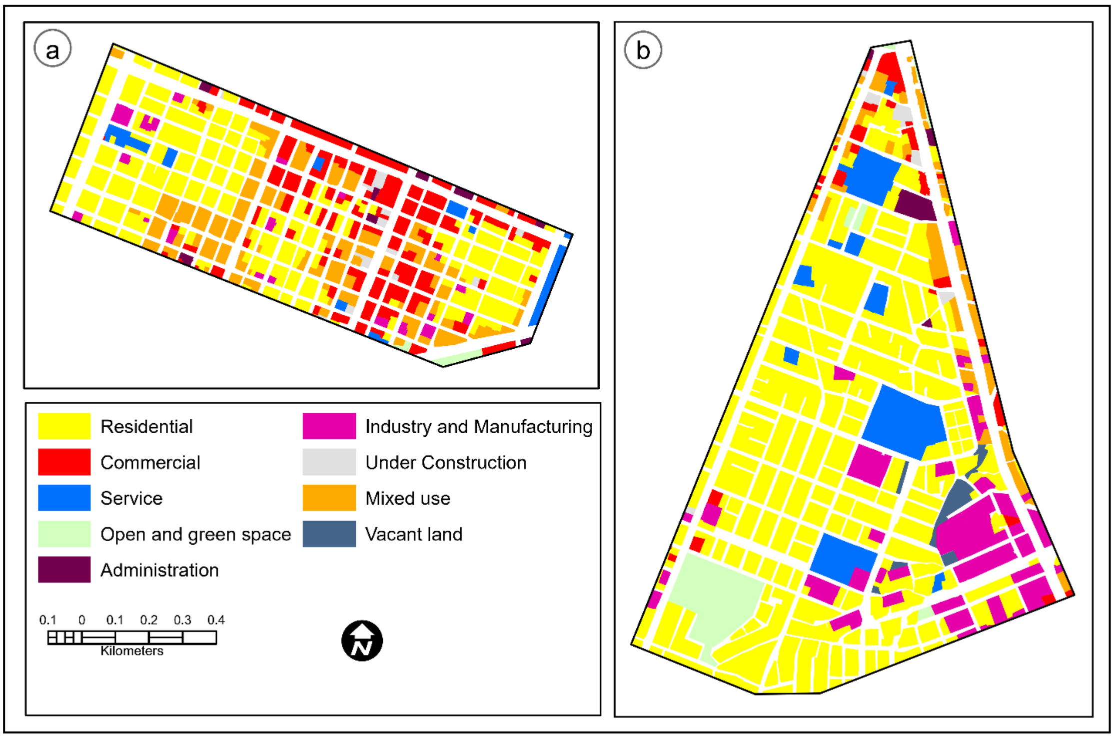

Figure 4.5: Land use map of the two sites

4.3.2 Flood event observations

Observations of flood events in the study area that occurred during the rainy season were conducted, with a particular emphasis on the months of June, July, and August 2023. These floods had substantial consequences for the economic, social, environmental, and health aspects of the community. Many neighborhoods within the city experienced inundation, resulting in road closures and widespread flooding. To gain a better understanding of these events, historical rainfall patterns in the study area over a span of 33 years were analyzed and on-site observations were conducted during the rainy seasons. The flooding of roads and neighborhoods during these periods had detrimental effects on the well-being of the communities, affecting them socially, economically, environmentally, and psychologically. The occurrence of these flood events was corroborated by cross-referencing the data with information from the National Meteorological Agency, as demonstrated in Figure 4.7. Additionally, visual evidence of the inundation was captured through recorded videos and photographs. In site "a," the floodwaters receded swiftly, allowing for a prompt recovery, as depicted in Figure 4.8. However, in site "b," the floodwaters remained stagnant for a prolonged period, significantly impacting the daily lives of the community, as illustrated in Figure 4.9. In site "a," floods were observed as overtopping through drainage manholes, resulting in neighborhood inundation. However, due to efficient water removal measures, the floodwaters receded quickly. In contrast, site "b" experienced issues such as clogging and siltation, causing the floodwaters to linger for an extended duration.

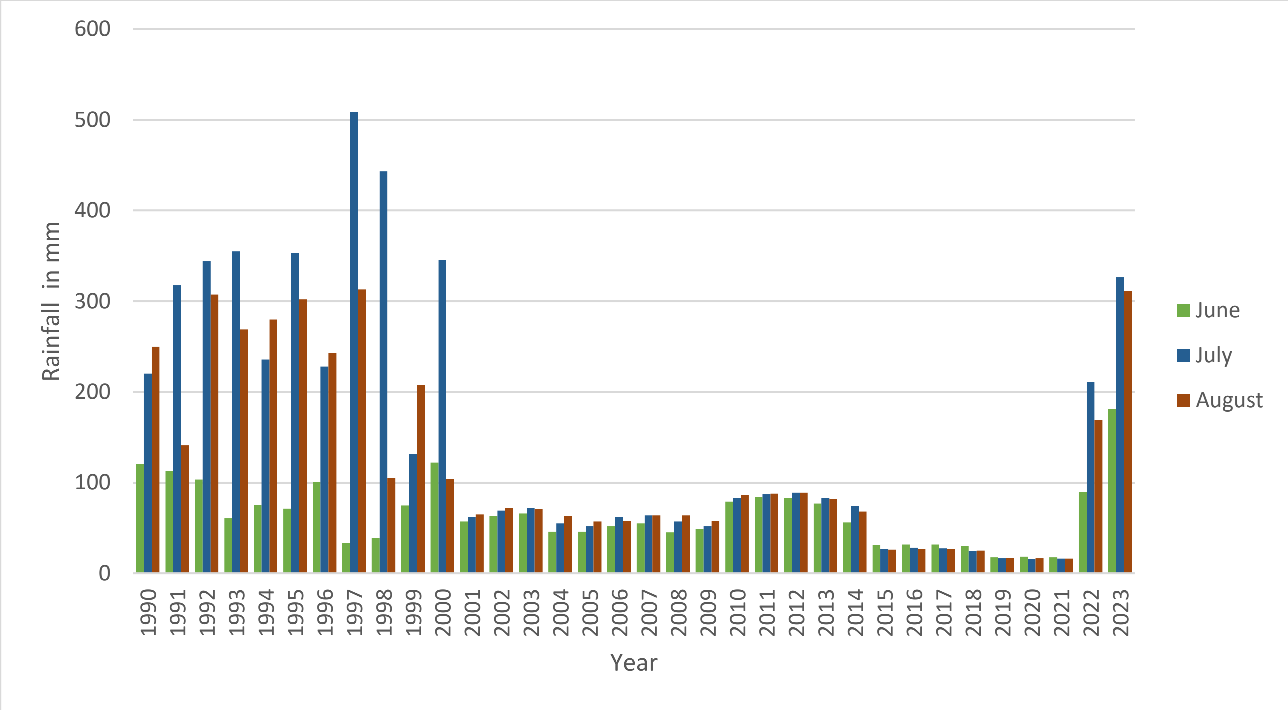

Figure 4.6:Long-term rainfall of the study area (Source: National Meteorological Agency, 2023)

Figure 4.7:Flood event observations in site "a", July 2023

Figure 4.8:Flood event observations in site “b”, July 2023

4.3.3 Key informants and Municipality

To gather information on the historical flood situation in the study area, insights were obtained from 20 key informant elders who have resided there for over 35 years. These informants were evenly distributed, with 10 from site "a" and 10 from site "b". In addition, professionals from the municipality were consulted regarding flood incidents in the study area, specifically focusing on sites "a" and "b" as shown in Figure 4.3.

According to the key informants, the study area experiences flooding during each rainy season (June to August). However, the extent of damage varies over time and depends on the intensity of rainfall. They attributed the cause of these floods to a lack of drainage infrastructure and inadequate maintenance of existing systems. As a result, waste accumulates and blocks the drainage lines, leading to waterlogging, overflow onto roads and settlements, and detrimental impacts on the community's economy, social fabric, psychological well-being, environment, and health.

The municipality acknowledges the concerns raised by the key informants and expands further on their insights. The study area is considered a flood-prone area due to its geographical location on a flat terrain surrounded by plateaus, mountain ranges, and ridged topography. It is situated within the Awash River Watershed and the East African Rift Valley, which are known as the most flood-affected watersheds in Ethiopia. Furthermore, rapid urbanization, informal settlement aggregation, and deforestation exacerbate the flooding situation in the study area. This highlights the need for prompt action to address these issues and mitigate the impact of floods on the community's daily activities.

4.3.4 Morphological analysis of the selected areas

4.3.4.1 Building configurations

Building configurations in planned and unplanned neighborhoods within a block can have both positive and negative effects on flooding. In site “a”, building configurations are meticulously designed to mitigate flood risks. This includes the incorporation of proper drainage systems, open spaces, and permeable surfaces that facilitate better water absorption. Despite being exposed to floods, these neighborhoods can quickly redirect water to other areas, allowing for a faster return to normal conditions. Consequently, planned neighborhoods are less susceptible to flooding due to the strategic placement of buildings and street systems, which minimize runoff and promote effective water management.

In contrast to planned neighborhoods, unplanned neighborhoods, often characterized as informal settlements, lack proper consideration for flood mitigation in their building configurations. Buildings are placed randomly without functional open spaces, resulting in the area being inundated by floods during each rainy season. The informal buildings obstruct the movement of floodwaters, causing water to remain stagnant for longer periods and negatively impacting the socio-economic and health conditions of the community. The haphazard placement of buildings in unplanned neighborhoods exacerbates flooding by increasing runoff on sealed surfaces and reducing the available area for water absorption. Furthermore, the absence of proper drainage systems further contributes to flooding issues in these areas, as shown in Figure 4.10.

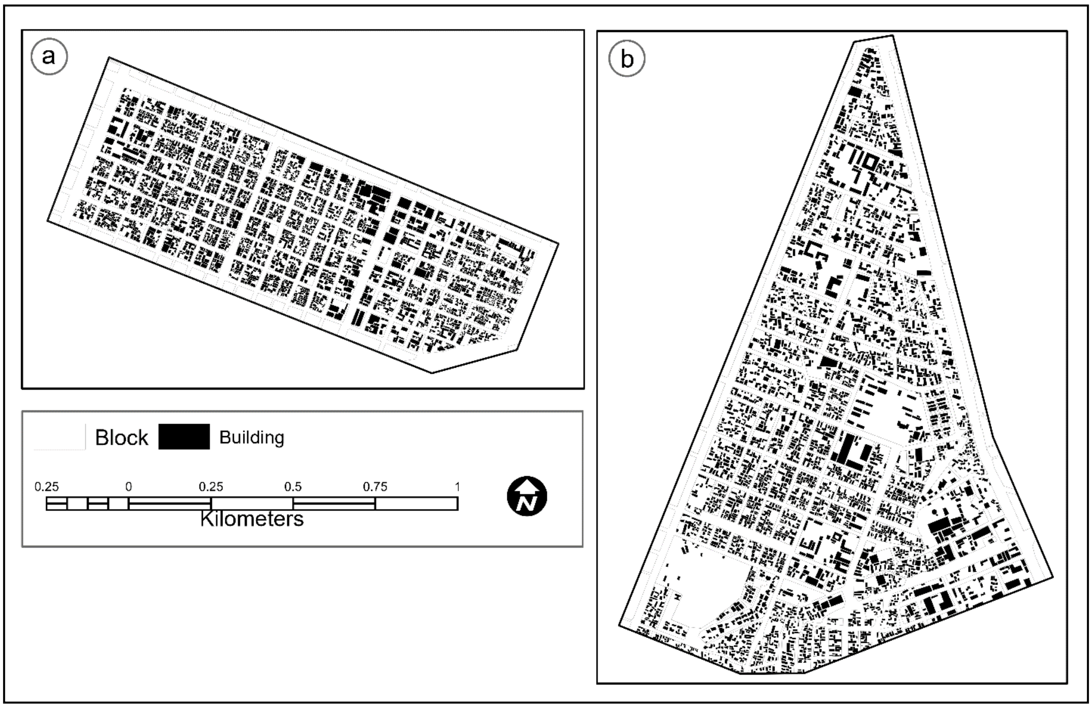

Figure 4.9:Building configurations

4.3.4.2 Street hierarchy

The street hierarchy analysis revealed distinct differences between site a and site b in terms of their street network characteristics. Site “a” has a well-designed and interconnected street system, featuring seven principal arterial streets ranging from 25 to 40 meters in width, as well as local streets measuring 6 to 10 meters, and access roads less than 4 meters wide. Such well-designed street spacing and coverage significantly enhance traffic efficiency and facilitate seamless navigation within the vicinity. Moreover, during extreme rainfall occurrences, these characteristics aid in the smooth flow of water, ensuring effective flood mitigation measures are in place.

In contrast, the street network in site “b” is characterized by a lack of connectivity and a disjointed layout. The area primarily consists of two main arterial streets, one with a width of 25 meters and the other 30 meters, while the rest is covered by access roads. This configuration presents challenges for flood evacuation, as well as impedes the smooth flow of water, and hampers the timely delivery of aid to affected communities during emergencies. The limited connectivity and abundance of dead-end streets in site “b” create obstacles that need to be addressed for effective disaster response and mitigation efforts. Furthermore, due to the absence of adequate cross-drainage infrastructure, coupled with insufficient solid waste disposal practices and infrequent maintenance of drainage lines, stormwater accumulates and causes blockages during flash floods. Consequently, urban roads in the surrounding area become overwhelmed and overflowing, exacerbating the impact of flooding events, as depicted in Figure 4.11.

Figure 4.10:Street hierarchy

4.3.4.3 Street surface material

The analysis of street surface materials revealed significant disparities between site “a” and site “b” in terms of their road infrastructure. Site a boasts a well-maintained and interconnected street system, with seven asphalted roads ranging from 25 to 40 meters in width, complemented by cobblestones and gravel on the remaining streets. This careful selection of surface materials contributes to the efficient flow of stormwater during extreme rain events, traffic flow, and ease of navigation within the area.

In contrast, site “b” exhibits a less developed road network, with only two asphalted roads, some cobblestones, and a predominance of earthen roads. The lack of asphalted surfaces and the dominance of earthen roads in site “b” pose serious challenges during urban flooding events. Earthen roads are more susceptible to damage and erosion caused by heavy rainfall, leading to increased surface runoff and potential blockages, as shown in Figure 4.12. This not only hinders the evacuation of flood-affected communities but also impedes the delivery of essential aid and emergency services.

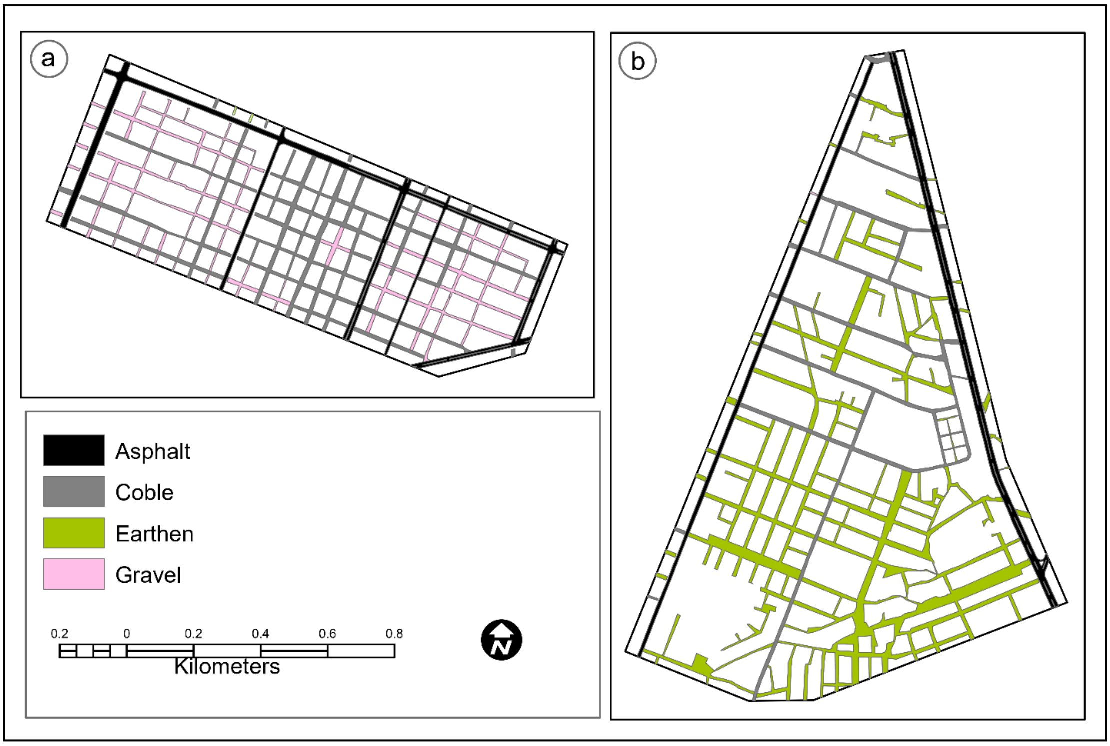

Figure 4.11:Street surface material

4.3.4.4 Blocks

Site "a" has short block sizes, with smaller dimensions and more frequent intersections, which tend to promote better water drainage and reduce the risk of flooding. On the other hand, site "b" has long block sizes that hinder the natural flow of water, increasing the likelihood of water accumulation during heavy rainfall events. Similarly, site "a" has a grid pattern that allows for efficient water runoff, as it provides multiple drainage paths. In contrast, site b has irregular block arrangements that disrupt the natural drainage system, impeding water flow and exacerbating the potential for urban flooding, as shown in Figure 4.13.

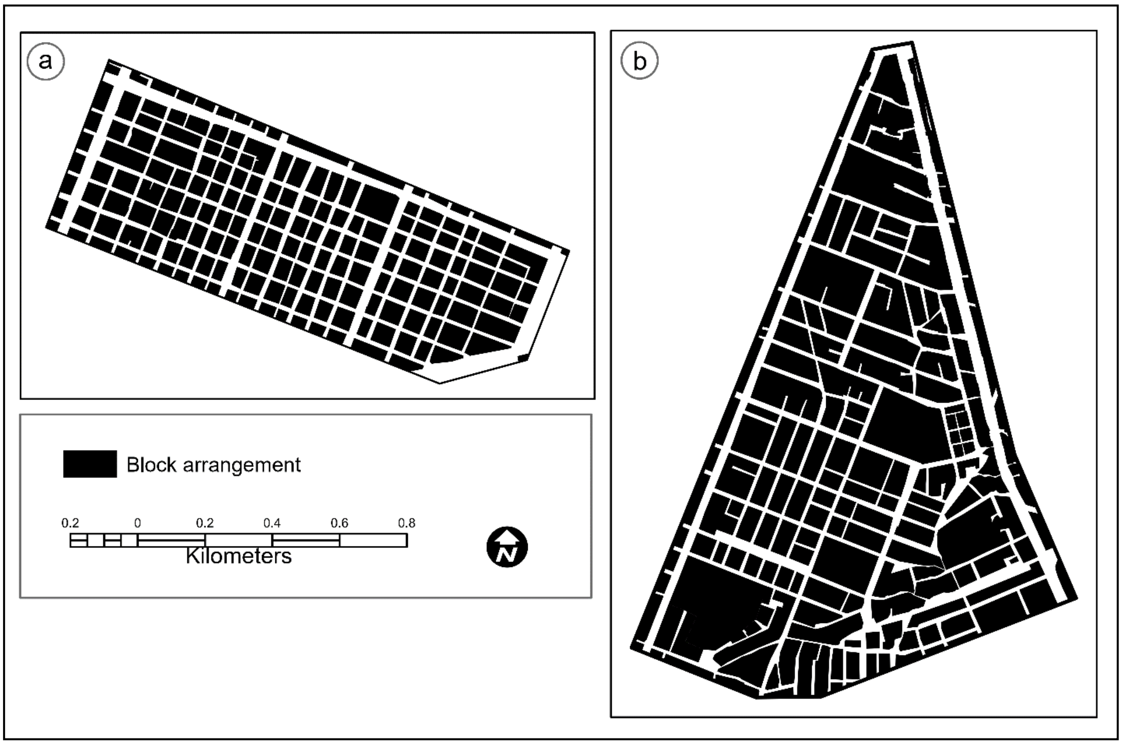

Figure 4.12:Block arrangements

4.4 Discussions

It is crucial to identify flood-resilient neighborhoods in the study area through a comprehensive analysis that includes configurational analysis, flood event observations, insights from key informants and the municipality, and morphological analysis (Wang et al., 2022a; Yusmah et al., 2020; Zhou; et al., 2022). This approach allows for a cascaded analysis that considers the overall spatial connectivity of the city, as well as specific aspects such as street and block arrangements. By integrating flood event observations and input from key informants and the municipality, a more holistic understanding of the city's flood-resilient neighborhoods can be identified (Eric et al., 2021; Mohammadtaghi et al., 2023; Tanoue et al., 2016). This type of analysis is particularly important in developing countries like Ethiopia, where limited information and resources exacerbate the severity of flooding impacts in rapidly urbanizing contexts (Deria et al., 2020; Rentschler et al., 2022; Salami et al., 2017a). Therefore, a combination of spatial and morphological analysis, coupled with flood event observations, and key informants is essential for effectively addressing the challenges posed by flooding in the study area.

The depth map of analysis of the study area revealed varying levels of accessibility across different areas. Specifically, the localities of Oda, Badhaatu, Abba Gadaa, and Gurmu demonstrate high accessibility, indicating a well-connected and easily navigable street network in these regions. This suggests that these areas are more likely convenient for flood event action, emergency aid, and evacuation due to their accessibility. In contrast, Dagaaga, Dhadacha Araara, Hangaatu, and Caffee exhibit moderate accessibility, suggesting a relatively less developed road infrastructure compared to the aforementioned areas. This implies that these areas may face challenges in terms of road connectivity and ease of movement within them. Additionally, the remaining parts of the city display lower levels of accessibility, indicating potential vulnerability to urban flooding. The inaccessibility in these areas can hinder the movement of people and resources during flood events, making it more difficult to provide assistance and mitigate the impacts of flooding. The results of this study align with previous research conducted by Gangwal et al. (2023); He et al. (2021); Lee et al. (2023); Zhou; et al. (2022), which suggests that areas with high accessibility and well-connected street networks are more capable of effectively managing flood vulnerability compared to less accessible areas in facilitating flood event actions, aid distribution, and evacuation efforts.

According to the findings of the present study, neighborhoods that had well-designed and interconnected street systems with manageable street spacing demonstrated a higher level of resilience to urban flooding. These features facilitated efficient runoff flow and effective flood management during flooding events. Conversely, neighborhoods with poor spatial connectivity, such as dead-end streets and irregular block arrangements, exacerbated urban flooding by impeding water flow and disrupting the natural drainage system. These findings emphasize the importance of considering flood mitigation measures in building configurations to mitigate flooding risks. Neglecting proper flood mitigation in building configurations can contribute to the worsening of urban flooding. This finding aligns with previous studies conducted by Sarkissian et al. (2022); Talbot et al. (2018), who highlighted that urban areas that have an appropriate building configuration can effectively reduce flood risk due to the presence of a variety of land cover that allows for greater water absorption and reducing surface runoff.

The present study findings indicated that the design and connectivity of the street system play a crucial role in both efficient traffic flow and flood management. Specifically, areas with a well-planned and interconnected street network, featuring manageable street spacing coverage, were found to contribute to smooth traffic movement and easy navigation. Additionally, such areas were able to effectively manage flood inundation damage during urban flooding events. On the other hand, neighborhoods characterized by a lack of street connectivity and an abundance of dead-end streets, as observed in site b, presented significant challenges for flood evacuation and hindered the delivery of aid to affected communities during emergencies. The absence of adequate road space hampers the smooth, unobstructed flow of runoff into downstream areas, coupled with insufficient solid waste disposal practices and infrequent maintenance of drainage lines, resulting in the accumulation of stormwater and subsequent blockages during flash floods. Consequently, the surrounding urban roads became overwhelmed and overflowed, exacerbating the impact of flooding events. These findings are consistent with a previous study conducted by Farahmand et al. (2021); Karley (2009); Li et al. (2020); Rosa and Pappalardo (2020), which emphasizes the importance of street connectivity and proper drainage systems in mitigating flood risks.

The selection of street surface materials plays a crucial role in ensuring efficient traffic flow and easy navigation in urban areas. However, the prevalence of earthen roads and the absence of asphalted surfaces pose significant challenges during urban flooding events. Earthen roads are more susceptible to damage and erosion caused by heavy rainfall, leading to increased surface runoff and potential blockages. This not only hampers the evacuation of flood-affected communities but also delays the delivery of essential aid and emergency services. Previous studies have shown that permeable pavements, such as porous asphalt, pervious concrete, permeable interlocking concrete pavers, and grid pavers, can enhance traffic flow and facilitate easy navigation (Sansalone et al., 2012; Xie et al., 2017). Nevertheless, the absence of asphalted surfaces and the dominance of earthen roads remain major obstacles during urban flooding events (Ahlmer et al., 2018; Konrad & Booth, 2005). Earthen roads are particularly vulnerable to damage and erosion caused by heavy rainfall, resulting in increased surface runoff and potential blockages (Eisenberg et al., 2015; NationalAssociationofCityTransportationOfficials, 2017).

Research has shown that neighborhoods with shorter block sizes, smaller dimensions, and more frequent intersections are beneficial for water drainage and reducing the risk of flooding. Conversely, neighborhoods with longer block sizes impede the natural flow of water, increasing the chances of water accumulation during heavy rainfall. Furthermore, a grid pattern in neighborhood design allows for efficient water runoff by providing multiple drainage paths. On the other hand, irregular block arrangements disrupt the natural drainage system, hinder water flow, and worsen the potential for urban flooding. These findings align with a previous study that emphasized the positive impact of smaller urban blocks on water drainage and flood risk reduction (Feng et al., 2021). Additionally, the presence of more frequent intersections in these neighborhoods can improve traffic flow and ease navigation (Morales et al., 2021). In contrast, larger urban blocks hinder the natural flow of water and are more likely to lead to water accumulation during heavy rainfall events (Zhang et al., 2022). Regular grids are more effective in reducing the risk of flooding as they provide multiple drainage paths, while irregular grids are less effective and contribute to the exacerbation of urban flooding (Feng et al., 2021; Sharifi et al., 2021).

The analysis of floods relies heavily on the observations of flood events, as they offer valuable insights that can aid in mitigating flood risks. Recent studies have emphasized the pivotal role played by flood event observations in reducing flood risk. These observations have proven to be instrumental in identifying areas that are susceptible to economic losses and ecosystem vulnerability. Flood event observations are an essential component of flood analysis, providing valuable information that can be utilized to reduce flood risk. Studies conducted by Kang et al. (2023); Zhang et al. (2021) have highlighted the crucial role of flood event observations in flood risk reduction. These observations have been instrumental in identifying areas at high risk of economic failure and ecosystem vulnerability. By integrating flood event observations with input from key informants and the municipality, a more holistic understanding of the city's flood resilience can be achieved, which is essential for effectively addressing the challenges posed by flooding (Coeur & Lang, 2008; Haltas et al., 2021; Zhang et al., 2021).

4.5 Conclusions

This study emphasizes the importance of conducting a comprehensive analysis of various factors, such as configurational analysis, flood event observations, key informants, municipality information, and morphological analysis, to identify flood-resilient neighborhoods in the study area. By considering the existing spatial pattern and morphology that are resilient to urban flooding, the city can improve its flood management strategies and enhance its overall resilience to flooding in the future.

The findings of this study indicate that the study area exhibits varying levels of spatial connectivity. Two neighborhoods with high and low spatial connectivity were selected for further analysis. The high-connective neighborhoods were characterized by well-designed and interconnected street systems with manageable street spacing coverage. These features contributed to efficient traffic flow, smooth flow of stormwater, and effective management of flood inundation damage during rain events. The use of different street surface materials also played a role in facilitating traffic flow and reducing flood damage and erosion caused by heavy rainfall. Additionally, the presence of short block sizes with smaller dimensions and more frequent intersections helped promote better water drainage and reduce the risk of flooding. The grid pattern observed in these neighborhoods allowed for efficient water runoff by providing multiple drainage paths that aided in the mitigation of flooding risks during inundation.

On the other hand, neighborhoods with low spatial connectivity were found to exacerbate urban flooding. The lack of connectivity and abundance of dead-end streets posed challenges for flood evacuation and hindered the delivery of aid to affected communities during emergencies. Long block sizes impeded the natural flow of water, increasing the likelihood of water accumulation during heavy rainfall events. Irregular block arrangements disrupted the natural drainage system, impeding water flow and exacerbating the potential for urban flooding.

This study provides valuable insights into the spatial pattern and morphology of the study area, focusing on the factors that contribute to resilience against flooding events. The research highlights the importance of well-connected street networks, careful selection of street surface materials, strategic building placement, shorter block sizes, and a grid pattern with frequent intersections in mitigating the impact of flooding. These findings can be applied to other flood-prone areas within the city and inform the enhancement of informal settlements in flood-prone areas across the city and similar urban areas in the global south on how human settlements are arranged spatially to mitigate flood vulnerabilities. In addition to analyzing the spatial pattern and morphology, the study also incorporates flood event observations, key informant interviews, and municipality information to provide a comprehensive understanding of the flood management challenges faced by the study area. The research outcomes have significant implications for urban planning and design, not only in the study area but also in other urban areas in the global south confronting similar flooding issues. Policymakers and urban practitioners can utilize these findings to develop effective flood management strategies that take into account the spatial morphology of the city. This can include incorporating space syntax analysis into existing urban planning and design processes to identify areas that are more vulnerable to floods and develop targeted interventions to mitigate their impact. Additionally, this study highlights the need to consider flood risk in building design and construction, settlement development, and neighborhood design. By incorporating space syntax analysis into these processes, cities can enhance their resilience to flooding and promote sustainable urban development

CHAPTER FIVE:

Quantifying flood risk using the INVEST-UFRM model and mitigation strategies for flood management in Adama City, Ethiopia

Abstract

Adama, the second largest city in Ethiopia, faces regular flash floods. These floods severely impact the city dwellers' livelihoods due to unplanned urbanization in flood-prone low-lying areas surrounding deforested mountains and ridges. To address this issue, the current study employed the Integrated Valuation of Ecosystem Services and Tradeoffs-Urban Flood Risk Mitigation (InVEST-UFRM) model as a tool to quantify adaptation-planning strategies for the study area. The InVEST-UFRM model effectively analyzed urban watersheds and spatially represented flooding, providing a comprehensive understanding of the flood risk scenario in the city. The model was run four times with different rainfall scenarios based on an intensity–duration–frequency curve specific to the study area to assess the impact of varying rainfall depths. These scenarios produced significant findings in terms of increased runoff retention and highlighting the varying capacities of micro-catchments in the study area for retaining runoff and generating floods. The study also emphasized the suitability of the InVEST-UFRM model in quantifying trade-offs associated with structural and non-structural flood mitigation measures. It underscored the importance of integrating multidisciplinary fields such as hydrology, remote sensing, geographic information systems, and natural capital assessment tools in urban planning strategies to achieve flood resilience and sustainable urban development. Overall, the InVEST-UFRM model proved to be a valuable tool for urban planners and policymakers for adaptive strategies to cope with urban flood events.

Keywords: Flood mitigation, Intensity-Duration-Frequency, InVEST-UFRM model, Flood volume, Runoff retention

5.1 Introduction

Urban floods have emerged as a pressing global issue, with rising vulnerability attributed to rapid urbanization and climate change (Bibi & Kara, 2023; Manandhar et al., 2023; Yang et al., 2021). The increasing urban population and expanding urbanization exert substantial stress on existing drainage systems, heightening the risk of inundation. Moreover, urban areas experience amplified impacts from flooding due to their dense population, infrastructure, and valuable properties (Rodríguez et al., 2017). Urbanization trends further exacerbate the scale and frequency of floods, posing escalating hazards to communities (Kadaverugu et al., 2021; Konrad, 2003). An alarming consequence is the nearly doubled urbanized area in floodplains with a 1/100-year flood probability since 1985 (Andreadis et al., 2022). It is widely acknowledged that climate change and human activities, such as land use and drainage, are exacerbating the frequency and intensity of extreme flood events (Brief, 2021; Kreibich et al., 2015). Furthermore, as global warming continues to contribute to rising sea levels and more extreme weather conditions, the risks associated with floodplains are projected to increase by approximately 45 percent by the end of the century (Denchak, 2019).

Between 2000 and 2018, there were 3798 flash flood events worldwide, resulting in an estimated loss of 592 billion USD and a death toll of approximately 0.1 million people (NatCatSERVICE, 2020). In 2020, global floods claimed over six thousand lives (Hamidifar & Nones, 2021). According to Smith et al. (2023), the United States has suffered significant economic losses due to weather-related disasters, such as flash floods, with particular emphasis on the events of May 2023 when a series of tornadoes and severe hail storms caused extensive damage to residential properties, businesses, and vehicles. Similarly, in 2022, Africa and parts of the Middle East reported nearly 2,000 fatalities from flash floods (Yin et al., 2023).

Ethiopia is highly susceptible to natural disasters such as flooding and drought due to its diverse topography (Mamo et al., 2019; WorldBankGroup, 2021; WorldRiskReport, 2022). The country has a history of experiencing flash floods and river floods, with major occurrences in 1988, 1996, 1998, 2006, 2010, 2012, and 2016, often associated with La Niña events. Typically, La Niña events result in above-average rainfall from

June to September in central and highland Ethiopia, causing flooding (Graf, 2020). Recent events have demonstrated the devastating consequences of flooding in Ethiopia. In 2016, early seasonal rains resulted in deadly floods that claimed the lives of at least 200 people, displaced over 200,000 individuals, and over 559 hectares of crops were destroyed (Hagos; et al., 2022; Mamo et al., 2019; Semaw et al., 2022). Similarly, in 2022, parts of Ethiopia faced the most severe drought in forty years, while other areas were affected by flooding, placing millions of people at risk (Dessie et al., 2022; Matanó et al., 2022; Tesfaw, 2022).

Urban flooding in Ethiopia has resulted in the loss of lives and resources, including houses and crops, and damaged bridges and roads (Weday et al., 2023). The flooding has led to interruptions in the power supply, making it difficult for people to assess the volume and intensity of the flood and rescue their property (Erena & Worku, 2018). Additionally, the heavy rains and unpredictable weather patterns are believed to be influenced by climate change, leading to more frequent and intense flooding in Ethiopia (Simane et al., 2017; WorldBankGroup, 2020). This has caused widespread damage to homes, roads, and other infrastructure in affected regions, disrupting daily life and posing challenges to the affected communities (Mekuria, 2022).

Erratic and heavy rainfall patterns, influenced by climate change, have resulted in more frequent and intense flooding events in Ethiopia's urban centers (Bibi & Kara, 2023). The lack of stormwater infrastructure in these areas exacerbates the risk of flooding (Erena & Worku, 2018). Insufficient infrastructure that is unable to handle the increased runoff, results in rapid inundation and damage to infrastructure (Erena & Worku, 2018). Additionally, the rapid expansion of urban built-up areas in Ethiopia has led to increased runoff and inundation (Bibi & Kara, 2023; Jemberie & Melesse, 2021). This expansion can be attributed to the conversion of green spaces into sealed surfaces, reducing the land's ability to absorb water (Jemberie & Melesse, 2021). Urban floods have both immediate and direct effects, such as fatalities, transportation inconvenience, traffic congestion, evacuation, electricity and telecommunications interruption, property damage, and discomfort (Gomariz et al., 2019; Konrad, 2003; Merz et al., 2010; ZurichFloodResilienceAlliance, 2014). Furthermore, post-flood consequences include water contamination, deposition of solid waste in waterlogged areas, and the spread of water-related diseases (Weday et al., 2023). Moreover, the inundation of houses leads to significant psychological distress among affected residents (Azuma et al., 2014).

Measuring flood retention and economic damage is crucial for developing economically viable flood mitigation strategies, informed decision-making and prioritizing investments in infrastructure, and disaster management to reduce the impacts of urban floods and enhance resilience (Huidobro et al., 2017; Martina et al., 2017). Estimating economic damage from urban floods involves flood inundation/hazard mapping and vulnerability mapping (Alabbad et al., 2023; Chang et al., 2021; Wu et al., 2021). To determine direct economic losses, previous studies often rely on the overlap between flood hazards and built-up or agricultural areas (Botzen et al., 2019; Craig et al., 2021; Rahman et al., 2021; Zhang et al., 2021). Evaluating the damage to built-up areas usually involves insurance data, unit cost approaches, and stage-depth damage curves (Aishwarya et al., 2023; Freni et al., 2010; Kim et al., 2019). While some studies have used damage curves, social survey-based monetary damage estimation is more commonly employed. However, these methods can introduce uncertainty, especially with a limited number of samples (Albano et al., 2015).

Measuring flood inundation is achieved through the use of hydrological modeling tools like HEC-RAS, MIKE Urban, ANUGA, Tuflow, iTree, MUSIC, SWMM, SWAT, HEC-HMS, MIKE-SHE, and FLO-2D (Alaminie et al., 2023; Brunner et al., 2021; Chen et al., 2022; Erena et al., 2018; Kumar et al., 2023). These tools play a crucial role in simulating urban flood modeling, but they are computationally expensive and require accurate input datasets (Brunner et al., 2021; D'Ambrosio et al., 2019; Kumar et al., 2023). This poses a challenge for policymakers in developing countries like Ethiopia, where limited data and resources are available (Alaminie et al., 2023; Fenglin et al., 2023; Tola & Shetty, 2023).

To address this issue, alternative approaches such as simple empirical models based on statistical correlations or machine learning algorithms, remote sensing and Geographic Information System (GIS) applications, and hybrid approaches prove to be useful when hydrological data is limited (Domeneghetti et al., 2019; Kumar et al., 2023; Li & Jun, 2022; Seydi et al., 2023). These approaches offer a handy tool for large study areas and are well-aligned with the unit cost method of damage estimation (Olesen et al., 2017). Furthermore, the successful conversion of modeling results from high to low spatial resolution is essential for the wider applicability of the models without compromising their hydrological essence (Hou et al., 2019). In this regard, the Integrated Valuation of Ecosystem Services and Tradeoffs (InVEST) platform emerges as a new and open-source modeling platform that can provide valuable insights into the rainfall-runoff relationship and runoff retention potentiality in flood-prone urban areas like Adama City.

InVEST, which was developed by the Natural Capital Foundation, is a tool used to assess natural capital in policy planning (Sharp et al., 2020). It is commonly employed in ecologically balanced urban planning and to measure ecosystem services such as carbon storage, water yield, habitat quality, and soil conservation (Terrado et al., 2016; Xu et al., 2019; Yang et al., 2019; Zhao et al., 2019). However, there is limited research on using InVEST for urban flood mitigation (Kadaverugu; et al., 2021). The model integrates factors like land use, land cover, watersheds, and the US soil conservation service-curve number (SCS-CN) method to estimate run-off based on rainfall (Bose & Mazumdar, 2023; Kadaverugu et al., 2022). By integrating these elements into the water balance equation, InVEST offers a comprehensive approach to evaluating the potential contributions to urban planning and flood management strategies. Previous studies on urban flood measurement have commonly utilized the InVEST-UFRM model, employing a design storm of 1-hour (Kadaverugu et al., 2021) and 2-hour (Bose & Mazumdar, 2023) rainfall duration for both 2 and 5-year retention periods. However, it is important to note that in urban areas, intense rainfall events that lead to flood inundation often occur within shorter timeframes, typically up to 30 minutes (Iliadis et al., 2023; Xiuquan et al., 2019). Additionally, intermediate rainfall events can extend up to 1 hour (Tu et al., 2023). Moreover, it is recommended to consider storm structure drainage prediction return periods of 5 and 10 years (Brasil et al., 2022; Iliadis et al., 2023; Joo et al., 2013; Tuyls et al., 2018).

In line with this, the objective of this study is to utilize the InVEST-UFRM model to evaluate and quantify the economic consequences of flooding caused by varying levels of rainfall intensity within a specific timeframe in the study area using 30-minute and 1-hour rainfall duration for both 5-and 10-year return period respectively. Additionally, the study seeks to examine the spatial differences in the relationship between rainfall and runoff throughout the city, identifying areas where runoff retention could be implemented to assist urban policymakers in their efforts to mitigate flooding. Moreover, the study intends to prioritize and propose practical measures to reduce the risk of urban flooding in the study area. By achieving these objectives, this research will provide valuable insights and recommendations for urban planners and policymakers to effectively manage and minimize the impact of flooding in the city. It is worth noting that this study represents the first utilization of the InVEST model for urban flood mitigation in developing countries, specifically in Ethiopia.

5.2 Materials and methods

5.2.1 Data types and sources

In this study, data were collected from various sources for analysis. Specifically, rainfall data from 1990 to 2023 at the Adama meteorological station were obtained from the National Meteorological Agency of Ethiopia (NMA, 2023). Digital soil types for the study area were provided by the Water and Land Resource Center (WLRC) in Ethiopia. Additionally, a high-resolution ASTER-Global Digital Elevation Model (DEM) with a spatial resolution of 12.5m was downloaded from the USGS website (http://earthexplorer.usgs.gov/) on March 3, 2022, with minimal land and scene cloud cover (0.01). Furthermore, the Land Use Land Cover (LULC) map of 2022 with a resolution of 10m was acquired from the ESRI website (http://earthexplorer.usgs.gov/) in December 2022. The Administrative boundary shapefile of the study area for Study area extraction was obtained from the Adam City Administration. A comprehensive summary of the data types and their respective sources is provided in Table 1.

Table 5.1: Data types and data sources

S.N	Data types	Derivable	Data Sources
1	ASTER- Global DEM with 12.5 m size grids	Micro watersheds delineation	Downloaded from USGS (http://earthexplorer.usgs.gov/.). acquired on March 3, 2022, with the least land and scene cloud cover (0.01).
2	Land Use Land Cover (LULC) map of 2022 with 10 m size grids	*LULC map*	*ESRI: (https://livingatlas.arcgis.com/Landover/). acquired on December 06, 2022.*
3	Soil Map, Scale 1:25,000	HSG map	Water and Land Resource Center (WLRC), Ethiopia
4	Daily Rainfall Data (1990–2023)	Rainfall depth and IDF Curve	National Meteorology Agency (NMA), Ethiopia
5	Shapefile of the Administrative boundary of the study area	Study area extraction	Adam City Administration (ACA)

5.2.2 Methods

To obtain the desired outcomes from the InVEST-UFRM model, a series of key steps were undertaken. Initially, remote sensing technology was employed to classify the land use and land cover of the city, with a specific focus on identifying impervious and permeable surfaces. This process resulted in the creation of a land cover raster file format. Subsequently, data on the hydrological soil group (HSG) was collected in raster file format to define the study area. This information played a crucial role in comprehending the hydrological characteristics of the soil. The third step involved the identification of watersheds and water channels within the study area using a Digital Elevation Model (DEM) file, leading to the production of a vector file format encompassing the entire study area's watersheds. Once these initial steps were completed, an analysis of daily rainfall data was conducted.

Rainfall analysis was essential for understanding rainfall patterns and calculating rainfall intensity, which is vital for estimating rainfall depth over various timeframes. Advanced statistical techniques were utilized, employing available secondary data. Moreover, a biophysical table was created, incorporating data on different land covers and their corresponding curve number data. This table provided insights into the hydrological soil condition of the study area and was indispensable for accurate modeling. Furthermore, comprehensive data on built infrastructure was collected and integrated into the study. This was achieved by utilizing a built infrastructure vector file containing detailed information about the built-up structures within the study area. Lastly, another table was generated to capture data on built infrastructure damage loss. This table encompassed information on building types and their potential damage loss. It is crucial to consider local or global currency valuation to ensure accurate assessment. By following these systematic steps, the InVEST-UFRM model can generate the necessary results for studying and comprehending urban flood risk management effectively.

The InVEST-UFRM model was utilized to effectively address the empirical representation of hydrological processes and estimate runoff production and retention in the study area. The model was run four times, with all parameters remaining consistent except for the rainfall depth. Four different rainfall depths were utilized to create four distinct rainfall events. To obtain these depths, an Intensity–Duration–

Frequency (IDF) curve specific to the study area was employed. In the first scenario, the model ran with a rainfall depth of 45.47 mm over 30 minutes, corresponding to a five-year return period. In the second scenario, the rainfall depth was increased to 50.90 mm over the same 30-minute period, representing a ten-year return period. For the third scenario, a rainfall depth of 54.72 mm was used over one hour, with a five-year return period. Lastly, in the fourth scenario, a rainfall depth of 58.62 mm was applied over one hour, corresponding to a ten-year return period. These four significant rainfall events were then selected and compared through spatial mapping in ArcGIS 10.8. The general workflow followed by this study is represented in Figure 5.2.

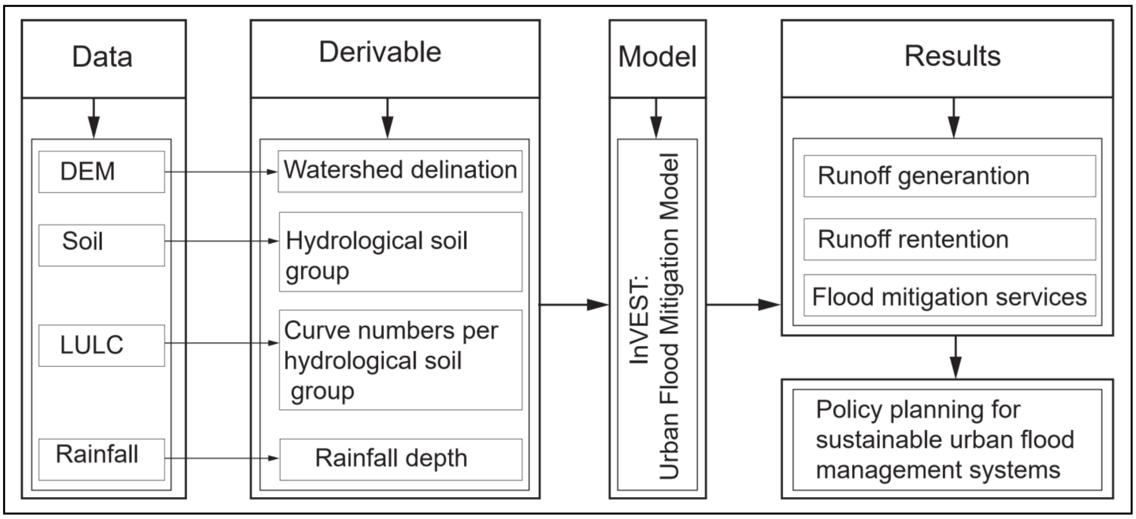

Figure 5.1: The general workflow of the study

5.2.2.1 InVEST-UFRM model description

The Urban Flood Risk Mitigation (UFRM) Model was added to the Natural Capital Project's tools in 2019 as a recent addition to the Integrated Valuation of Ecosystem Services and Tradeoffs (InVEST) software(Quagliolo et al., 2021). It specifically focuses on the impact of built-up areas on ecosystem services provided by natural capital in urban settings. Its primary objective is to assess cities' capacity to reduce runoff and mitigate potential flooding caused by extreme rainfall events. By considering precipitation within a watershed, this hydrological model accurately estimates the resulting runoff discharge. Moreover, the model recognizes the importance of natural infrastructures in flood reduction and incorporates the potential of permeable green spaces to decrease runoff, slow surface flows, and create space for water in floodplains or basins(Hamel et al., 2021).

The InVEST-urban flood risk mitigation model is a valuable tool that calculates the reduction in runoff and potential economic damage for each watershed by overlaying information on flood extent potential and built infrastructure. Its main function is to reduce runoff production, slow surface flows, and create space for water in floodplains or basins. This model has been widely applied in various studies, including those related to urban ecosystem services(Kadaverugu et al., 2021; Kramer et al., 2019), urban flood vulnerability(Bose & Mazumdar, 2023; Kadaverugu et al., 2022), and urban sustainability transformations (Quagliolo et al., 2021), nature-based climate change adaptation (Cortinovis et al., 2022; Ronchi et al., 2020). Additionally, it has been successfully utilized in NASA DEVELOP projects to address issues related to disaster mitigation, urban planning, and environmental justice (Do & Besnier, 2023).

The InVEST-UFRM model utilizes specific algorithms for its calculations, with the Python programming language running in the backend (Sharp et al., 2020). These algorithms include dedicated equations that are crucial for determining the model's outcomes. These equations, which are outlined below, contribute to the accuracy and reliability of the model's results.

The runoff production (*Qp,i*) resulting from precipitation (*P*) was calculated using the SCS-CN method, which takes into account the potential maximum retention (*S*max,*i*) and CN*i* values associated with each pixel using equation 5.1.

$$Q_{p,i} = \begin{cases} \dfrac{(P - \lambda S_{max_i})^2}{P + (1-\lambda) S_{max,i}} & if \quad P > \lambda \cdot S_{max,i} \\ 0 & otherwise \end{cases} \qquad \text{Equation:5. 1}$$

Where P is the design storm depth in mm, $S_{max,i}$ is the potential retention in mm, and $\lambda \cdot S_{max}$ is the rainfall depth needed to initiate runoff, also called the initial abstraction ($\lambda = 0.2$=for simplification).

The empirical relation between$S_{max,i}$, and CN*i* was calculated using equation 5.2;

$$S_{max,i} = \frac{25400}{CN_i} - 254 \qquad \text{Equation:5. 2}$$

The runoff retention per pixel$R_i$was calculated using equation 3;

$$R_i = 1 - \frac{Q_{p,i}}{P}$$ Equation: 5.3

The runoff retention volume per pixel$R_m3_i$was calculated using equation 5.4;

$$R\_m3_i = R_i \cdot P \cdot pixel.area \cdot 10^{-3}$$ Equation: 5.4

Runoff volume (flood volume) per pixel $Q_m3_i$was also calculated using equation 5.5;

$$Q\_m3_i = Q_{p,i} \cdot pixel.area \cdot 10^{-3}$$ Equation:5.5

The InVEST-UFRM model utilizes the aforementioned equations to produce raster data containing runoff values. Additionally, it generates a runoff retention raster file that presents relative values to rainfall, as well as a raster file displaying runoff retention values. Furthermore, the model generates an attribute table in vector file format, which includes flood risk calculations. The raster data with calculated values assists in identifying spatial variations within the designated area.

5.2.2.2 Method of processing Input data for the InVEST-UFRM model

Land use land cover

The land use land cover (LULC) data for the study area was obtained from the freely available ESRI website (https://livingatlas.arcgis.com/Landcover/) on December 20, 2022. The extraction process was conducted using a grid resolution of 10 x 10 meters. The LULC data was classified into five categories: forest, grassland, cultivated land, built-up cover, and water features (Allafta & Opp, 2021; Ogato et al., 2020). Forests include dense vegetation, which mainly consists of stunted trees and bushes. On the other hand, grasslands are open ecosystems characterized by low-growing vegetation, including grasses and wildflowers. Croplands, on the contrary, consist of agricultural areas such as livestock grazing, as well as the cultivation of grains, fruits, and vegetables. The built-up areas encompass various types of human settlements, such as residential, industrial, and commercial buildings, along with the accompanying road infrastructure. Lastly, the water bodies include ponds and rivers within the study area. The prioritization of land use types was based on urban area classification, commonly used for SCS-CN (Soil Conservation Service-Curve Numbers), to suit the InVEST-UFRM model (Bose & Mazumdar, 2023). To verify the accuracy of the land use and land cover (LULC) map, a thorough validation process was conducted involving field visits to 143 randomly selected locations within the study area using handheld GPS devices. This verification process included ground truthing, where the selected spatial points were assessed using high-resolution images from Google Earth Satellite Imagery Pro Version 7.3.6, as well as on-site field visits.

Micro-watersheds delineation

To create micro-watersheds in ArcGIS (version 10.8) using a DEM, the following steps were followed respectively :

Step 1: Identification of pour points: Typically, these points are found at the mouths of streams or other hydrologic features. Using the hydrologic analysis tools, pour points were selected. In this case, the stream network was used as the pour points, resulting in the creation of watersheds for each segment between stream junctions.

Step 2: Creation of a flow direction raster: A raster indicating the direction of water flow was generated using the Flow Direction tool.

Step 3: Creation of a flow accumulation raster: The Flow Accumulation tool was utilized to calculate the accumulated flow to each cell in the input raster based on the flow direction.

Step 4: Delineation of watersheds: The Watershed tool was employed to delineate watersheds from the DEM. This involved computing the flow direction and using it as input for the Watershed tool. By utilizing the flow direction, the tool determined the upslope contributing area for each cell, resulting in the delineation of watersheds.

Step 5: Conversion of raster to polygon: To obtain a polygon representation of the micro-watersheds, the raster was converted into a polygon shapefile using the Raster to Polygon tool. This conversion allowed for further analysis and visualization of the micro-watersheds.

Hydrological soil group

The soil type information for the study area was obtained from the WLRC at a scale of 1:25,000 and then converted into a raster format in the ArcGIS environment for further processing and hydrological soil group classification. The study area consists of five distinct soil types: Eutric Cambisols, Eutric Nitisols, Chromic Luvisols, Leptosols, and

Chromic Vertisols. These soil types were converted into hydrological soil groups based on their runoff potentiality.

The United States Department of Agriculture (USDA) has classified soils into four major textures, denoted as A, B, C, and D. Texture A represents sandy soil, texture B defines sandy loam and loamy sand, texture C denotes clayey loam and silty clayey loam, and texture D mainly represents clayey soil. This classification is based on the proportions of sand, loam, and clay present in the soil. These four classes represent the potentiality of runoff from lowest to highest.

The converted hydrological soil groups (HSG) were resampled with a resolution of 10 meters for further processing in the InVEST-UFRM model. Each soil group is represented by a category of A, B, C, or D with varying degrees of responsiveness towards the generation of runoff as stipulated in the InVEST-UFRM model manual.

Rainfall and rainfall depth

The rainfall data of the study area spanning the last 30 years (1990-2020) was acquired from the National Meteorology Agency of Ethiopia. Additionally, sub-hourly data from 2011-2020 was collected (NMA, 2023). This dataset was crucial for examining the trends in rainfall amounts and seasonal variations, providing a better understanding of how rainfall patterns change throughout the year. Moreover, by identifying the highest amount of rainfall in a single day for each year, valuable information was obtained regarding the magnitude of rainfall events and their potential flood risks associated with various rainfall patterns.

As rainfall depth plays a crucial role in the InVEST-UFRM model, the dataset obtained from NMA (2023) was utilized. The intensity of rainfall, which directly influences flood risk, is determined by both the depth and duration of rainfall. To assess the potential rainfall intensity in the study area, the intensity-duration-frequency (IDF) curve was computed based on previous studies (Ethiopian Roads Authority, 2013; Hamaamin, 2017; Mahdi & Mohamedmeki, 2020).

The validation of the IDF curve developed using sub-hourly data and daily rainfall data was crucial to ensure its accuracy and reliability. By comparing the predicted intensities with the actual measured intensities for various rainfall events, the level of agreement between the two was determined. This validation process guarantees the reliability of the IDF curve for accurately predicting rainfall intensity for different durations and frequencies in the study area (Ethiopian Roads Authority, 2013; Mahdi & Mohamedmeki, 2020).

$$R_{Rt} = \frac{t}{24}\frac{(b+24)^n}{(b+t)^n} \qquad \text{Equation: 5.6}$$

Where:

R_{Rt}=Rainfall depth RatioR_t:R_{24}

R_t=Rainfall depth in a given duration ’t’

R_{24}=24hrrainfalldepth

bandn=coefficientsb=0.3andn=(0.78-1.09).

Equation 5.6, which represents the equation for disaggregating daily rainfall to finer time steps, exhibited a diverse range of values for the coefficient 'n' (0.78-1.09). Nevertheless, the Ethiopian Road Authority manual (2013) categorized the study area as one with rainfall of moderate to high intensity. To align with the specific conditions of the locality, the 'n' coefficient was modified and varied between 0.93 and 0.99. It is important to note that as the value of 'n' approaches one, the model becomes more accurate. Therefore, for this study, we have set the range of 'n' between 0.93 and 0.99, while keeping the b value constant at 0.3. The 'n' coefficient in the IDF curve formula is a significant factor in determining the accuracy of the model. It represents the shape of the curve and is influenced by various factors such as rainfall patterns and catchment characteristics. The value of 'n' varies depending on the specific location and local conditions. A value close to one indicates a slow decrease in rainfall intensity, while a value close to zero indicates a rapid decrease. Therefore, understanding and considering the 'n' coefficient is crucial for accurately predicting rainfall intensity using the IDF curve model (Courty et al., 2019; Sun et al., 2019).

The InVEST model used rainfall data with 5-year and 10-year return periods, as suggested for urban drainage systems (Agilan & Umamahesh, 2017). Recognizing the increased frequency of flooding in cities, even from short rainfall events, the study also incorporated more realistic durations of 30-minute, 45-minute, and 1-hour duration (Bose & Mazumdar, 2023; Kadaverugu et al., 2022).

Designing stormwater systems for 5-year and 10-year return period rainfalls is advisable to create a resilient urban environment that minimizes the impacts of recurrent flooding due to the following reasons:

1. Frequency of events: these return periods correspond to more frequent storm events that are likely to occur during the lifespan of the infrastructure. Designing for these events ensures that the stormwater system can handle regular rainfall and mitigate flooding in urban areas (Ayda et al., 2024).
2. Balance of cost and protection: systems designed for 5-year and 10-year events offer a good balance between cost and protection. They are less expensive than systems designed for less frequent, higher-intensity storms while still providing significant flood mitigation benefits (Guo, 2006).
3. Adaptability: by addressing more frequent storms, the infrastructure can be more easily adapted or upgraded in the future to handle larger events if climate patterns change or urban development increases runoff (Kibria & Biswas, 2019).
4. Reduction of inundation risk: designing for these return periods can significantly reduce the risk of inundation from frequent, moderate rainfall events, which can cause substantial damage in urban settings (Chen et al., 2023).

Estimating missing precipitation

Several methods have been proposed for estimating missing precipitation. The station average method is the simplest one. The normal ratio and quadrant method provides a weighted mean, with the former biasing the weights on the mean annual precipitation at the gauge and the latter having weights that depend on the distance between gauges where recorded data are available and the point where the value is required. The normal ratio method is used in this study. The method is used when the normal annual precipitation of the index station differs by more than 10% of the missing station. This method assigns weights to each surrounding station. (Sing, 1994). This is the case for the station in the study area. The general formula for computing missing precipitation by equation 5.7.

$$\phi_n = \frac{{\phi_n}^a}{r} \sum_{i=1}^{r} \left[\frac{\phi_i}{{\phi_{ni}}^a} \right] \qquad \text{Equation:5.7}$$

Where ϕ-n is an estimate of missing data for gauged station n,ϕ-ni is the measured rainfall values of station i, ϕ-$n.$-$a.$ is the normal annual rainfall of station n, ϕ-$ni.$- $a.$ is the normal annual rainfall of station i, ϕ-i is the observed value at station i, and r is the number of the station.

Areal Precipitation

A rain gauge records the rainfall at a single point. This point rainfall record has to be converted to aerial rainfall. The average depth of precipitation over the area under the area under consideration is one of the most important parameters in hydrological analysis. There are many methods available to determine the areal rainfall over the catchments from the rain gauge measurement: Arithmetic Mean, Thiessen Polygon, Isohyetal, GridPoint, Percent Normal, Hypsometric, etc. are available for estimating average precipitation (Shaw, 1988). Choice of methods requires judgment in consideration of the quality and nature of the data, and the importance, use, and required precision of the result.

To determine the average depth of rainfall an analysis using a Thiessen polygon method which is the most widely used method compared to others was used in this study. In this method, weights are given to the measuring gauge based on the area coverage of the watershed, thus eliminating the discrepancies in their spacing over the basin. According to Thiessen, the average rainfall, Rareal over the area was computed based on the 5.8 equation.

$$R_{areal} = \sum_{i=1}^{n} \frac{R_i A_i}{A_t}. \qquad \text{Equation:5.8}$$

Where, Ri is the rainfall at station i, Ai is the polygon area of station i, At is the total catchment area, and n is the number of stations. The area functions Ai/At are known as the Thiessen coefficients and once they are determined for a given stable station network, the areal rainfall was computed for the set of rainfall measurements.

Intensity-Duration-Frequency (IDF) curve

An Intensity-Duration-Frequency (IDF) curve is a graphical representation used in hydrology to relate the intensity of rainfall with its duration and frequency of occurrence. IDF curves are crucial for designing stormwater management systems, assessing flood risks, and understanding rainfall patterns.

Rainfall data analysis

Analyzing the data to determine the maximum rainfall amounts for different durations (e.g., 30 minutes, 45 minutes, 1 hour.) for each year. Ranking these maximum values and fitting them to a probability distribution, commonly the ***Gumbel distribution***. To verify whether the given data follows the assumed Gumbel's distribution, the following procedure was adopted. The value of xT for some return periods T<N was calculated by using Gumbel's formula and plotted as xT Vs T on a convenient paper such as a semi-log, log-log, or Gumbel probability using equation 5.9.

$$x_T = \bar{x} + K\sigma_{n-1}$$

Where σ_{n-1} = standard deviation of the sample $= \sqrt{\frac{\sum(x-\bar{x})^2}{N-1}}$

K = frequency factor expressed as $K = \frac{y_T - \bar{y}_n}{S_n}$ Equation:5.9

or

$$y_T = -\left[0.834 + 2.303\ \log\left(\log\left(\frac{T}{T-1}\right)\right)\right]$$

For the given data, values of return periods (plotting positions) for various recorded values, x of the variate are obtained by the relation T = (N+1)/m and plotted on the graph described above.

A good fit of observed data with the theoretical variation line indicates the applicability of Gumbel's distribution to the given data series. By extrapolation of the straight-line x_T Vs T, values of X_T> N were determined.

Intensity Calculation

Calculate the rainfall intensity (I) using the formula: I=P/D; where P is the total rainfall depth and D is the duration. The general formula for the IDF relationship is often expressed by equation 5.10.

$$I = \frac{a}{(D+b)^c}$$ Equation:5.10

where:

- I = rainfall intensity (mm/hr)
- D = duration (minutes or hours)
- a, b, and c are empirical coefficients that depend on the frequency of the rainfall event (5-year, and 10-year events).

Maximum discharges for different return periods

The Generalized Extreme Value I (GEV-I) distribution was used to determine maximum discharge for different return periods due to several key factors:

1. Flexibility**:** GEV-I combines three types of extreme value distributions, allowing it to model various types of extreme events, which makes it versatile for hydrological applications (Namitha & Ravikumar, 2018).
2. Accuracy: tt accurately fits the distribution of annual maximum series data, which is crucial for reliable return level estimation of extreme rainfall and discharge events (Gründemann et al., 2023).
3. Comprehensive Nature**:** GEV-I captures the characteristics of extreme hydrological events effectively, accounting for both the frequency and magnitude of such events over different durations (Ragulina & Reitan, 2017).
4. Shape Parameter**:** the shape parameter in GEV-I allows it to adapt to various types of data distributions, providing better fit and more accurate predictions for different return periods (Ragulina & Reitan, 2017).

Equation 5. 11 was used to calculate the Generalized Extreme Value I (GEV-I) distribution of maximum discharge for different return periods.

$$F(x) = \exp\left(-\left(1+\xi\frac{x-\mu}{\sigma}\right)^{-1/\xi}\right)$$ Equation:5.11

where:

- μ is the location parameter,
- $\sigma > 0$ is the scale parameter,
- ξ is the shape parameter,
- x is the variable of interest.

For return period estimation, the return level x_T can be calculated as:

$$x_T = \mu + \frac{\sigma}{\xi}\left((T \cdot (1-p))^{-\xi} - 1\right)$$

where:

- T is the return period,
- p is the exceedance probability (typically $1/T$).

Generalized Extreme Value I (GEV-I) equation helps in estimating the maximum expected value for a given return period (Namitha & Ravikumar, 2018).

Curve number value for biophysical table

The run-off curve numbers (CN) are empirical estimations used to quantify the depth of run-off resulting from rainfall events. These values are dependent on various factors including the hydrologic soil group (HSG), land use and land cover, and the antecedent moisture condition (AMC) of the soil in a specific geographical location. CN values typically range from 0 to 100, representing the extremes of low and high run-off generation. In this study, we have utilized the CN values developed for urban environments by Chow et al. (2019). These values were considered representative of medium soil moisture conditions (AMC-II). The widely used SCS model, developed by the U.S. Soil Conservation Service, was employed to generate these CN values. This model has numerous applications in water resource management, stormwater modeling (Soomro et al., 2019), and urban flood risk assessment (Bose & Mazumdar, 2023; Kadaverugu et al., 2021). To compute the CN, a Microsoft Excel sheet table based on land use and the land cover type, as well as hydrological soil group classification, was utilized for the InVEST-UFRM model input.

5.3 Results

Land use land cover

The land use land cover analysis revealed that a significant portion of the area was covered by grassland (39.8%) and croplands (33.81%). Built-up areas account for 25.14% of the land, while forested areas make up only 0.79%. Water bodies and bare land constitute 0.36% and 0.09% respectively as shown in Table 5.2. The distribution of land use suggests that the city is expanding predominantly towards the northern region. This can be attributed to favorable topographic features that make it suitable for settlement. Moreover, the city is also expanding towards the northeast, as it serves as a corridor to other major cities such as Dire Dawa and neighboring countries such as Djibouti. The eastern and southeastern parts of the city are also experiencing growth due to their flat surfaces and convenient road connections to resourceful areas in Ethiopia, known for agriculture, coffee production, and gold mining, such as Arsella, Bekoji, Dodola, and Bale.

However, the western part of the city faces challenges in terms of topography, with mountain ranges and hilly areas blocking further expansion in that direction. Similarly, the southwestern part of the city has shown limited development due to similar topographic constraints. These mountainous and hilly terrains hinder urban growth and pose challenges to infrastructure development and accessibility. As a result, the city's expansion is primarily concentrated in the northern, northeastern, eastern, and southeastern directions, where the topography is more favorable for urbanization as shown in Table 2 and Figure 3a.

Table 5.2: Land use land cover

Land use land cover	Area (ha)	Area(Sq.km)	Percentage
Built area	7871.49	78.71	25.14
Forest	248.6	2.48	0.79
Crops	10585.54	105.85	33.81
Water bodies	113.43	1.13	0.36
Bare land	27.98	0.27	0.09
Grassland	12459.62	124.59	39.8

Micro watershed

There are six micro watersheds, each with its unique characteristics, spatial coverage, and local name. The largest micro watershed, named Jogo, covers 28.92% of the total study area. Following Jogo, the Dabe catchment comprises 18.32% of the area, while Wonji covers 17.82%. The Dembela catchment accounts for 13.15% of the total area, followed by Dakaadi at 12.25%. The smallest micro watershed, Migira, covers 9.54% of the study area as shown in Table 5.3 and Figure 5.3b.

Table 5.3: Micro watersheds name and area catchment

Micro watershed name	Area (ha)	Area (Sq.km)	Percentage
Dabe	5733.40	57.33	18.32
Dakaadi	3833.99	38.33	12.25
Dembela	4116.56	41.16	13.15
Jogo	9052.91	90.52	28.92
Migira	2986.19	29.86	9.54
Wonji	5577.42	55.77	17.82

Hydrological soil group

The study area underwent a reclassification of soil types into Hydrological soil groups. Within the study area, three hydrological soil groups were identified: Group A, Group B, and Group D. Group A has a low runoff potential due to high infiltration rates. These soils primarily consist of deep, well-drained sands and gravels; Group B has a moderately low runoff potential due to moderate infiltration rates; Group D has a high runoff potential due to very slow infiltration rates. In line with the study area, Group A consisted of Eutric Leptosols and covered 21.24% of the study area. Group B included Calcaric Fluvisols, Mollic Andosols, and Vitric Andosols, and accounted for 69.74% of the study area. Group D comprised Fibric Cambisols, Lava/Rocky, and Pellic Vertisols, making up 9.05% of the study area, as depicted in Table 5.4 and Figure 5.3c.

Table 5.4:Hydrological soil group and catchment area

Soil types(HSG)	Area (ha)	Percentage
Eutric Leptosols (A)	6649.53	21.24
Calcaric Fluvisols(B)	1383.75	4.42
Mollic Andosols (B)	18,120.29	57.88
Vitric Andosols (B)	2329.21	7.44
Fibric Cambisols(D)	21.91	0.07
Lava/Rocky(D)	720.05	2.3
Pellic Vertisols (D)	232.29/2091.28	6.68

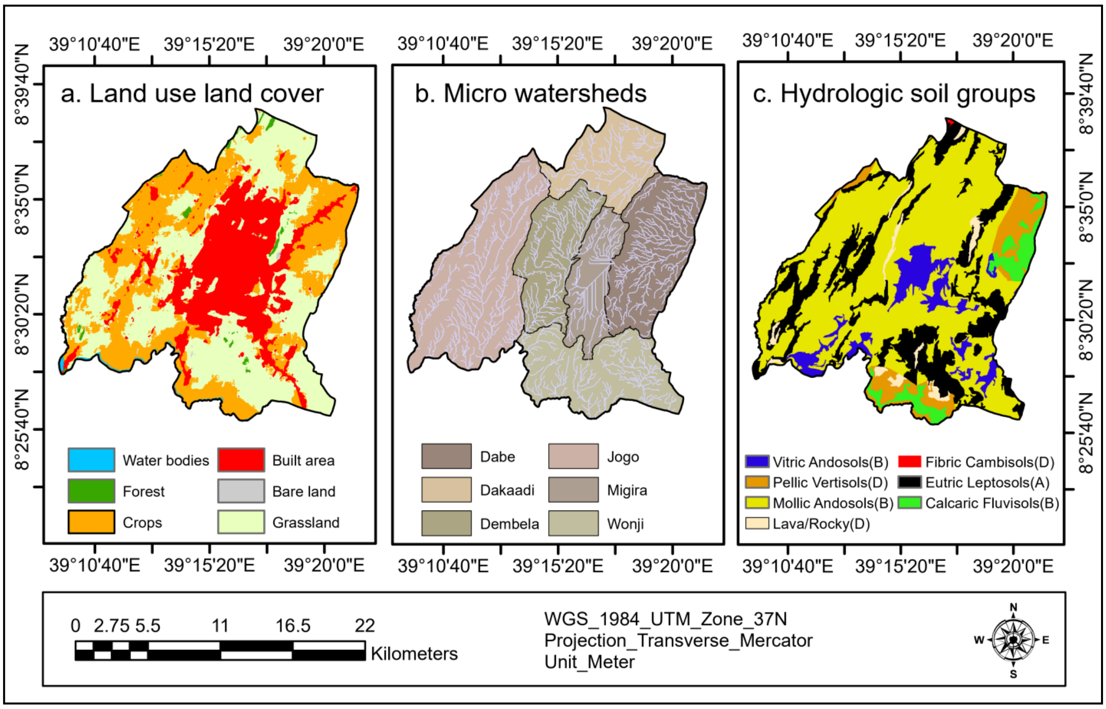

Figure 5.2: Land use land cover, micro watersheds, and hydrological soil groups

IDF Curve

The Intensity-Duration-Frequency (IDF) analysis involves graphical representations that depict the amount of precipitation within a specific period. These graphs are developed using both sub-hourly and daily rainfall data and serve as the foundation for estimating extreme discharge events. Additionally, the IDF analysis was employed to determine the average time interval between occurrences of extreme discharges. Figure

5.3 show the relationship between the intensity, duration, and frequency of extreme discharge events.

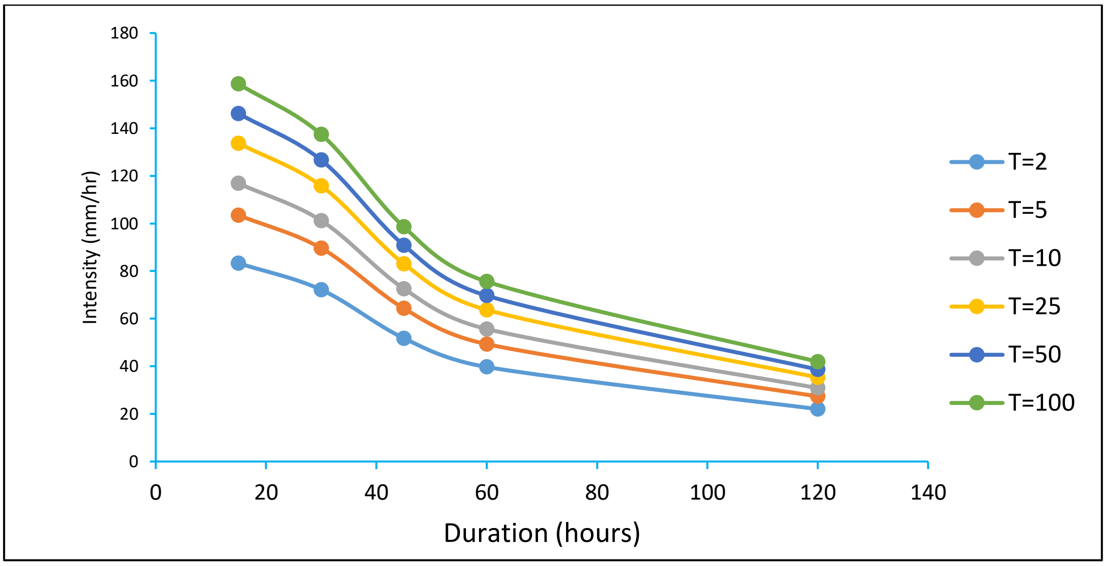

Figure 5.3: IDF curve developed and using daily rainfall data

Curve number

In the study area, curve numbers were assigned to estimate the runoff and infiltration after precipitation. These curve numbers are determined based on two factors: land use and land cover type, and hydrological soil group classification. Table 5.5 presents the specific curve numbers for the InVEST-UFRM model input.

Table 5.5: Land use land cover with respective curve number

Land use land cover	CN_A	CN_B	CN_C	CN_D
Built area	89	92	94	95
Cropland	63	75	83	87
Grassland	49	69	79	84
Forest	36	60	73	79
Bare land	77	86	91	94
Water	0	0	0	0

Micro watershed analysis

The flood potential and runoff retention capacities of the six micro-catchments within the study area were examined through a micro-watershed analysis as follows:

Scenario 1: Rainfall depth of 45.47 mm for 30 minutes and a 5-year return period

The flood potential and runoff retention capacities of the six micro-catchments within the study area vary, as shown in Figure 5.5 and Table 5.6. In Scenario 1, Dabe has an average retention value of 0.74, retaining 1.93 million m3 of rainfall while generating a flood volume of approximately 0.64 million. Dakaadi, on the other hand, exhibits an average retention value of 0.85, with 1.48 million m3 of rainfall resulting in a flood volume of nearly 0.25 million. Dembela showcases an average retention value of 0.58, generating a flood volume of approximately 0.77 million from 1.09 million m3 of rainfall. Jogo demonstrates an average retention value of 0.86, with a significant rainfall of 3.50 million m3 leading to a flood volume of nearly 0.56 million. Migira, with an average retention value of 0.54, experiences a flood volume of about 0.62 million from 0.73 million m3 of rainfall. Lastly, Wonji displays an average retention value of 0.81, generating a flood volume of approximately 0.47 million from 2.00 million m3 of rainfall. Overall, in Scenario 1, the micro-catchments in the study area retain a total of 10.76 million m3 of runoff while generating a flood volume of 3.34 million m3.

Scenario 2: Rainfall depth of 50.90 mm for 30 minutes and a 10-year return period

In Scenario 2, the flood potential and runoff retention capacities of the six micro-catchments within the study area vary, as illustrated in Figure 5.5 and Table 5.6. Dabe demonstrates an average retention value of 0.72, retaining 2.09 million m3 of rainfall while generating a flood volume of approximately 0.80 million. Conversely, Dakaadi exhibits an average retention value of 0.82, with 1.60 million m3 of rainfall resulting in a flood volume of nearly 0.33 million. Dembela showcases an average retention value of 0.55, generating a flood volume of approximately 0.93 million from 1.16 million m3 of rainfall. Jogo demonstrates an average retention value of 0.83, with a significant rainfall of 3.80 million m3 leading to a flood volume of nearly 0.75 million. Migira, with an average retention value of 0.51, experiences a flood volume of about 0.73 million from 0.78 million m3 of rainfall. Lastly, Wonji displays an average retention value of 0.78, generating a flood volume of approximately 0.59 million from 2.18 million m3 of rainfall. Overall, in Scenario 2, the micro-catchments in the study area retain a total of 11.63 million m3 of runoff while generating a flood volume of 4.15 million m3.

Scenario 3: Rainfall depth of 54.72 mm for 1 hour and a 5-year return period.

In Scenario 3, the flood potential and runoff retention capacities of the six micro-catchments within the study area vary, as depicted in Figure 5.5 and Table 5.7. Dabe demonstrates an average retention value of 0.70, retaining 2.19 million m3 of rainfall while generating a flood volume of approximately 0.91 million. Conversely, Dakaadi displays an average retention value of 0.80, with 1.69 million m3 of rainfall resulting in a flood volume of nearly 0.39 million. Dembela showcases an average retention value of 0.53, generating a flood volume of approximately 1.04 million from 1.20 million m3 of rainfall. Jogo demonstrates an average retention value of 0.81, with a significant rainfall of 4.00 million m3 leading to a flood volume of nearly 0.89 million. Migira, with an average retention value of 0.49, experiences a flood volume of about 0.82 million from 0.81 million m3 of rainfall. Lastly, Wonji displays an average retention value of 0.77, generating a flood volume of approximately 0.68 million from 2.29 million m3 of rainfall. Overall, in Scenario 3, the micro-catchments in the study area retain a total of 12.21 million m3 of runoff while generating a flood volume of 4.76 million m3.

Scenario 4: Rainfall depth of 58.62 mm for 1 hour and a 10-year return period

In Scenario 4, the flood potential and runoff retention capacities of the six micro-catchments within the study area vary, as shown in Figure 5.5 and Table 5.7. Dabe has an average retention value of 0.68, retaining 2.29 million m3 of rainfall while generating a flood volume of approximately 1.01 million. Conversely, Dakaadi exhibits an average retention value of 0.79, with 1.77 million m3 of rainfall resulting in a flood volume of nearly 0.46 million. Dembela showcases an average retention value of 0.51, generating a flood volume of approximately 1.16 million from 1.25 million m3 of rainfall. Jogo demonstrates an average retention value of 0.80, with a significant rainfall of 4.20 million m3 leading to a flood volume of nearly 1.04 million. Migira, with an average retention value of 0.48, experiences a flood volume of about 0.90 million from 0.84 million m3 of rainfall. Lastly, Wonji displays an average retention value of 0.75, generating a flood volume of approximately 0.78 million from 2.41 million m3 of rainfall. Overall, in Scenario 4, the micro-catchments in the study area retain a total of 12.78 million m3 of runoff while generating a flood volume of 5.40 million m3.

Table 5.6: Scenario 1 and Scenario 2

Scenario 1: Rainfall depth of 45.47 mm for 30 minutes and a 5-year return period.				**Scenario 2: Rainfall depth of 50.90 mm for 30 minutes and a 10-year return period.**		
Micro watershed	Runoff retention Index	Runoff retention (m3)	Flood volume (m3)	Runoff retention Index	Runoff retention (m3)	Flood volume (m3)
Dabe	0.74	1938490.17	649885.19	0.72	2092706.80	804770.74
Dakaadi	0.85	1481484.85	258602.29	0.82	1609275.12	338611.89
Dembela	0.58	1093173.34	778626.69	0.55	1162407.40	932921.76
Jogo	0.86	3502804.17	569493.81	0.83	3805682.92	752926.37
Migira	0.54	737362.28	620463.04	0.51	783635.00	736340.87
Wonji	0.81	2007600.68	470505.46	0.78	2181038.01	593001.93

Table 5.7: Scenario 3 and Scenario 4

Scenario 3: Rainfall depth of 54.72 mm for 1 hour and a 5-year return period.				**Scenario 4: Rainfall depth of 58.62 mm for 1 hour and a 10-year return period.**		
Micro watershed	Runoff retention Index	Runoff retention (m3)	Flood volume (m3)	Runoff retention Index	Runoff retention (m3)	Flood volume (m3)
Dabe	0.70	2195314.80	919615.97	0.68	2294892.01	1042045.72
Dakaadi	0.80	1694236.09	399838.19	0.79	1776787.43	466535.51
Dembela	0.53	1207740.46	1044841.36	0.51	1251310.39	1161817.18
Jogo	0.81	4007347.57	893381.43	0.80	4203389.58	1046623.55
Migira	0.49	814372.88	819675.95	0.48	844117.25	906393.31
Wonji	0.77	2297504.06	684725.08	0.75	2411105.96	783672.37

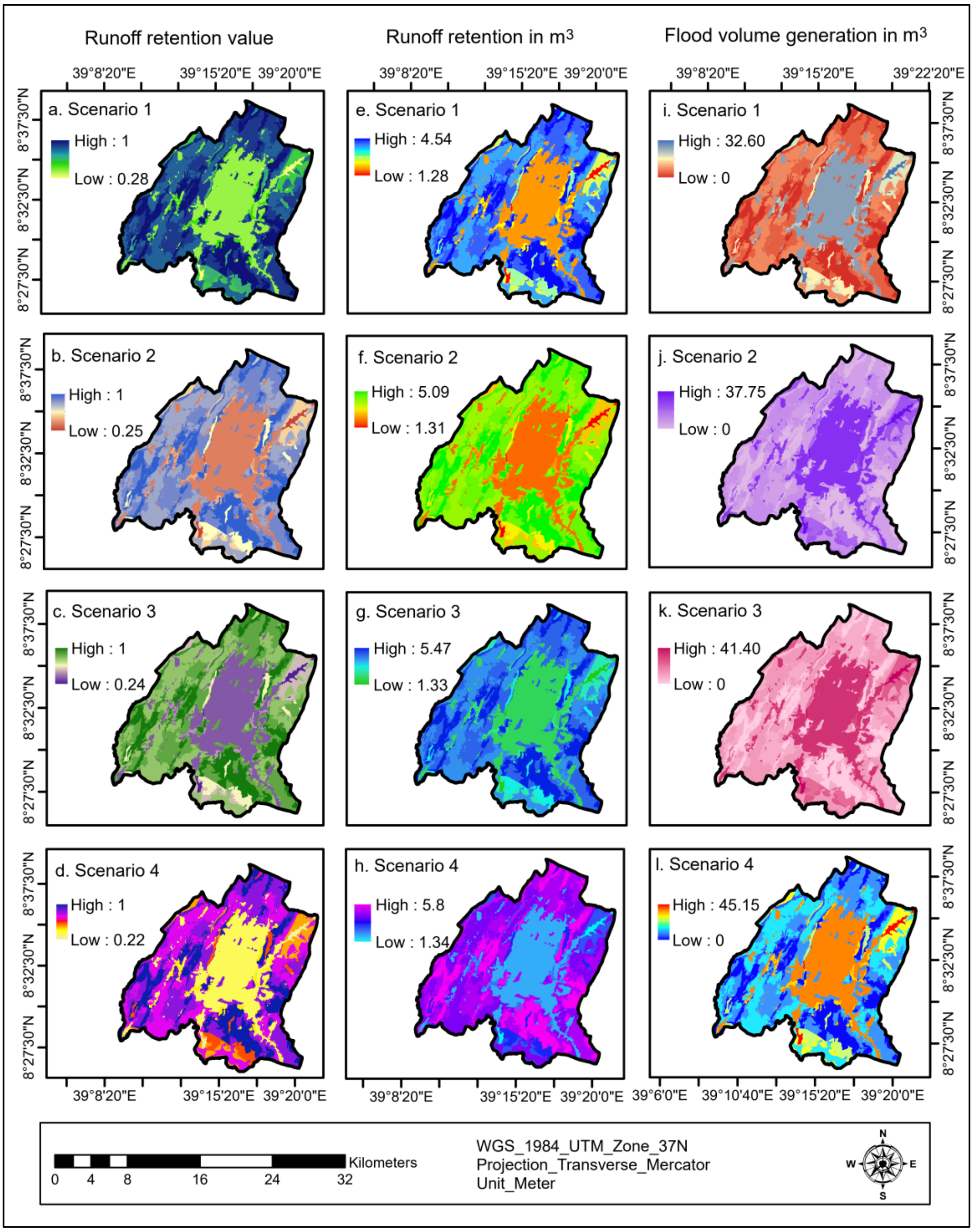

Figure 5.4: Runoff retention value and runoff retention of scenarios 1,2,3, and 4

5.4 Discussions

5.4.1 Quantifying Flood Mitigation Services using the InVEST-UFRM model

The InVEST-UFRM model is highly regarded and valuable for measuring flood mitigation services in urban areas (Bose & Mazumdar, 2023; Kadaverugu et al., 2021; Quagliolo et al., 2021). In this study, a comprehensive analysis of the study area is conducted by dividing it into six micro-watersheds based on catchment and stream network analysis. The sizes of these micro-watersheds ranged from 2986.19 to 5733.40 hectares. Land use-land cover analysis revealed that Rangelands cover 39.8% of the study area, followed by croplands at 33.81%. Built-up areas accounted for 25.14% of the land and forested areas made up of only 0.79%. This lack of forested areas poses a challenge as it limits the space for water to percolate into the ground, making the area more susceptible to flooding (Athick & Shankar, 2019). Water bodies and bare land constituted 0.36% and 0.09% respectively. The distribution of land use patterns indicated that the city is expanding mainly along the major road(s), possibly due to flat landform. Additionally, the city is also expanding towards the northeast, serving as a corridor to other major cities and neighboring countries. The eastern and southeastern parts of the city are also experiencing growth due to their flat surfaces and convenient road connections. However, these expansion areas are at a higher risk of flooding due to their flat surfaces which are known to be affected by recurring flood inundation during most rainy seasons. These findings further support a previous study conducted by (Bulti & Assefa, 2019), which reported a rapid annual change rate of almost 9% in the study area, placing it among Ethiopia's fastest-growing cities. The accelerated expansion and population surge not only put pressure on infrastructure and public services but also expose the local natural environment to a higher risk of degradation (Adugna, 2019a; Jemberie & Melesse, 2021; Masha et al., 2023).

The study area was assessed based on hydrological soil groups, which were categorized into three distinct groups with different levels of runoff potential. Group A, covering 21.24% of the study area, consisted of well-drained sands and gravels with high infiltration rates, resulting in a low potential for runoff. Group B, accounting for 69.74% of the study area, exhibited a moderately low runoff potential due to moderate infiltration rates. Group D, covering 9.05% of the study area, demonstrated a high potential for runoff due to very slow infiltration rates. The majority of the study area was characterized by Group B HSG, including soil types such as Calcaric Fluvisols, Mollic Andosols, and Vitric Andosols, and had a moderately low runoff potential. However, uncontrolled urbanization and deforestation in the area have disrupted the natural hydrological processes and reduced the soil's ability to absorb water, leading to an increase in urban flooding. These findings are consistent with a previous study conducted by (Danáčová et al., 2020; Feng et al., 2021), which emphasized that urbanization contributes to the expansion of impervious surfaces, resulting in a reduction in the time it takes for water to flow and a subsequent increase in flood risk in regional watersheds. The removal of vegetation and soil, land surface grading, and the construction of drainage networks further contribute to increased runoff from rainfall, leading to higher peak discharge rates, larger flood volumes, and more frequent flooding events (Gwenzi & Nyamadzawo, 2014; Janicka & Kanclerz, 2023; Robinson et al., 2022).

The analysis of the study area daily rainfall and sub-hourly data over the past three decades reveals a clear and concerning trend of increasing heavy rainfall. This trend can be attributed to the rapid deforestation and expansion of impervious surfaces in the city (Bajracharya et al., 2015; Bulti & Abebe, 2020). As a result, built-up areas are experiencing a surge in surface runoff, leading to a decline in the soil's ability to retain water. This situation is expected to worsen following storm events, as the maximum amount of rainfall in the study area turns into runoff in built areas (Bulti et al., 2021a). In contrast, vegetated lands and grasslands are better equipped to retain a certain amount of rainfall. However, due to the limited forest spaces in the study area, runoff exceeds the infiltration capacity after continuous rainfall, resulting in increased water runoff. Areas such as the eastern part of Dembela, most of Migira, and Dabe receive a significant amount of rainfall, but their impervious nature makes it difficult for them to retain runoff. Consequently, these areas often experience flood-like situations. On the other hand, the western part of Jogo and most of Dakaadi have more favorable landforms and are less urbanized, allowing excess runoff to flow through water channels and join the nearby drainage system. However, poor management of the drainage system leads to common issues of clogging and siltation. As a result, densely populated areas, particularly in the central part of the city, consistently face waterlogging situations after continuous rainfall. These findings further support a previous study conducted by Bulti et al. (2021b), which highlights the urgent need for effective management strategies to address the escalating heavy rainfall and its implications for rapidly urbanizing areas.

Comparing the results of the four scenarios, it is evident that the flood potential and runoff retention capacities vary depending on the rainfall depth and return period. The flood potential and runoff retention capacities of the micro-catchments in the study area vary across different scenarios. In Scenario 1, the micro-catchments retain a total of 10.76 million m3 of runoff, indicating a moderate ability to retain rainfall, while generating a flood volume of 3.34 million m3. In Scenario 2, the retention capacity improves slightly, with a total retention of 11.63 million m3 of runoff and a higher flood volume of 4.15 million m3. This suggests that the micro-catchments are becoming more effective at retaining rainfall but are still generating significant flood volumes. In Scenario 3, there is further improvement in the retention capacity, with a total retention of 12.21 million m3 of runoff and a flood volume of 4.76 million m3. This indicates that the micro-catchments are becoming more efficient at retaining rainfall, resulting in a decrease in flood volumes. Finally, in Scenario 4, the retention capacity continues to increase, with a total retention of 12.78 million m3 of runoff and a flood volume of 5.40 million m3. This suggests that the micro-catchments are even more effective at retaining rainfall, resulting in a further decrease in flood volumes. These findings highlight the importance of considering different scenarios and rainfall characteristics when evaluating flood potential and runoff retention capabilities to mitigate floods in urban areas like the study area. These findings reinforce the importance of implementing effective management strategies to mitigate the impact of intensifying heavy rainfall and its consequences on rapidly urbanizing regions (Lapointe et al., 2022; Qin, 2020).

The InVEST-UFRM is specifically designed to address flood management and mitigation measures, and it has shown promising outcomes for soil types that are dry and have high infiltration capacity (AMC-I). However, the model's effectiveness diminishes when dealing with soil types that have lower infiltration capacity and are saturated (AMC-II). In these cases, the model fails to produce satisfactory results (Bose & Mazumdar, 2023; Kadaverugu et al., 2021).

5.4.2 Application of Flood Mitigation Measures

To effectively address the issue of flooding in the study area, it is imperative to take action at multiple levels. Firstly, the flood management system should be decentralized, taking into account both the city-level watershed and each micro-watershed within the city (Bertilsson et al., 2019; Jemberie & Melesse, 2021). Each area should be thoroughly assessed to identify specific problems and implement appropriate solutions accordingly. Urban land use planning should also consider the vulnerability of areas to floods at the city level (Bose & Mazumdar, 2023; Kadaverugu et al., 2022). This includes preserving and rehabilitating major natural drainage systems that have been disrupted due to urbanization, deforestation, and other human activities. Additionally, creating space for floodwater in floodplain areas and utilizing them for multipurpose activities, such as recreation centers. Measures like rehabilitating, creating, and preserving water bodies such as check dams, retention ponds, lakes, percolation wells, and interconnectivity through streams or canals can help retain floodwater (Bulti & Abebe, 2020). It is crucial to adopt resilient policy planning and incorporate emerging concepts in urban landscape planning, such as Nature Based solutions (NBS), Water Sensitive Urban Design (WSUD), Low Impact Development (LID), and Sponge Cities (Jemberie & Melesse, 2021; Jiang et al., 2018; Myers & Pezzaniti, 2019).

At the micro-watershed level, it is recommended to implement structural flood retention measures, such as promoting green roofs and walls, rainwater harvesting pits, underground stormwater networks or collection pools, infiltration trenches or wells, micro-reservoirs or cisterns, bioswales, and porous pavements (Delgado et al., 2023; Twohig et al., 2022). The placement of these measures should be carefully considered in terms of their location within or outside of flood plains, as well as the required quantity for effective control (Leite & Antunes, 2023). The use of permeable and impermeable surfaces, along with vegetative cover, can help manage runoff and retain water (Ferreira et al., 2021). Implementing raised and flood-proofed buildings, like green roofs, and gutter eliminations, can reduce and slow down runoff (Twohig et al., 2022; Zhou, 2019). To prevent overflow on urban roads during flash floods, it is important to provide adequate cross-drainage works. This not only prevents stagnation but also avoids the clogging of stormwater drains with municipal solid waste (Iffland et al., 2021; Zhang et al., 2020). Installing sustainable mesh materials at cross-drainage structures can further prevent clogging during floods.

In addition to implementing various structural and non-structural measures, research suggests that socio-demographic factors and adaptive capacity, including access to healthcare infrastructure and flood relief centers, awareness among the citizens should be imposed through rules and regulations play a crucial role in post-flood mitigation efforts (Bixler et al., 2021; Cao et al., 2020; Deria et al., 2020; Peden et al., 2023). By considering these factors, urban areas can better address the challenges posed by floods and enhance their resilience.

5.5 Conclusions

The InVEST-UFRM model has been used as a tool to define adaptation planning strategies to address urban flood events caused by extreme rainfalls in the study area. By quantifying runoff in a spatially explicit manner, a comparative analysis to assess vulnerabilities to flash floods at both watershed and micro-watershed levels was conducted. The InVEST-UFRM model provided a comprehensive understanding of the flood risk scenario in the city and proved effective in analyzing urban watersheds and spatially representing flooding. This innovative model holds great potential for identifying solutions to mitigate urban flood risks.

The model was run four times, keeping all parameters consistent except for the rainfall depth. Four distinct rainfall events were created by utilizing different rainfall depths. These depths were obtained using an IDF curve specific to the study area. In the first scenario, the model was run with a rainfall depth of 45.47 mm over 30 minutes, corresponding to a five-year return period. The second scenario involved an increased rainfall depth of 50.90 mm over the same 30-minute period, representing a ten-year return period. For the third scenario, a rainfall depth of 54.72 mm was used over one hour, with a five-year return period. Lastly, in the fourth scenario, a rainfall depth of 58.62 mm was applied over one hour, corresponding to a ten-year return period. These four significant rainfall events were then compared through spatial mapping in ArcGIS 10.8.

The findings showed that significant values were obtained in terms of runoff retention and flood volume. The flood potential and runoff retention capacities of the micro-catchments in the study area varied across the different scenarios. In Scenario 1, the micro-catchments retained a total of 10.76 million m3 of runoff, indicating a moderate ability to retain rainfall, while generating a flood volume of 3.34 million m3. In Scenario 2, there was a slight improvement in retention capacity, with a total retention of 11.63 million m3 of runoff and a higher flood volume of 4.15 million m3. This suggests that the micro-catchments are becoming more effective at retaining rainfall but are still producing significant flood volumes. In Scenario 3, there was further improvement in retention capacity, with a total retention of 12.21 million m3 of runoff and a flood volume of 4.76 million m3. This indicates that the micro-catchments are becoming more efficient at retaining rainfall, resulting in a decrease in flood volumes. Finally, in Scenario 4, the retention capacity continued to increase, with a total retention of 12.78 million m3 of runoff and a flood volume of 5.40 million m3.

To summarize, InVEST-UFRM has the potential to identify effective solutions for urban flood risk mitigation. In addition, various structural and non-structural flood mitigation measures, highlight the suitability of the InVEST-UFRM model in quantifying the trade-offs associated with these measures. Furthermore, the InVEST-UFRM model appears to be a useful tool for urban planners and policymakers in defining adaptive strategies to cope with urban flood events. Emphasis should be given to the importance of integrating multidisciplinary fields such as hydrology, remote sensing, geographic information systems, natural capital assessment tools, urban planning, and building by-laws and regulations. Such integration is imperative for achieving flood resilience and sustainable urban development.

CHAPTER SIX:

GENERAL DISCUSSIONS

Identifying and mapping flood-prone areas, characterizing the degree of urban flood vulnerabilities, investigating flood-resilient neighborhoods, and developing flood mitigation strategies are essential for managing the impacts of floods, providing qualitative and quantitative information on flooding (Abdelkarim et al., 2020; Mohanty & Simonovic, 2022). This information assists urban planners and decision-makers in effectively prioritizing mitigation measures (Argaz et al., 2019; Çetinkaya et al., 2016; Forkuo, 2011; Wang et al., 2011).

6.1. Identification and mapping of flood Prone-area

To identify and map flood-prone areas, this study incorporated eleven major flood conditioning factors, including both man-made and natural factors, to map the flood-prone zone of the study area. These factors include distance from stormwater drains, elevation, slope, rainfall, land cover, topographic wetness index, normalized difference vegetation index, distance from river, distance from road, soil types, and drainage density. Using weighted overlay integration, the resulting model divided the study area into four classes based on flood-prone levels: low (2), moderate (3), high (4), and very highly prone (5) to flooding. In terms of flood-prone, the study area was categorized into four levels: low (1.31%, 406.83 ha), moderate (61.27%, 19056.31 ha), high (37.37%, 11623.09 ha), and very high (0.05%, 14.72 ha). It was found that approximately 98.69% of the study area showed a moderate to very high susceptibility to flooding. Expansion sites east of the city along the highway and rail line to Dire Dawa-Djibouti, as well as areas to the north and southeast along Arsi Road, are prone to flooding due to their flat surfaces, low-lying terrain, proximity to rivers, built-up areas, and their location adjacent to highways. These areas are classified as highly and very highly susceptible to flooding.

Conversely, the remaining 1.31% of the study area exhibited a low vulnerability to flooding. These areas, which are less prone to floods, are mainly located in the higher elevations of the mountains surrounding the city. They are characterized by their steep slopes and low drainage density areas. These findings were in agreement with the findings of flood-prone area identification studies conducted by Argaz et al. (2019), Desalegn and Mulu (2021), Edamo et al. (2022), Negese et al. (2022).

The primary factors leading to flooding in the study area were human activities, specifically rapid urbanization and deforestation. These activities resulted in changes to the land cover and had a substantial impact on the watershed. Additionally, the nature of the landform, which features a low-lying flat landscape surrounded by plateaus and ridge topography, contributes to the problem as there are no natural or artificial stormwater drainage outlets and limited space for floodwater. It is vital to understand the complex interplay between human-induced actions and natural elements in effectively managing flooding. The findings presented in this study agreed with previous research conducted by Argaz et al. (2019), Desalegn and Mulu (2021), Edamo et al. (2022), Negese et al. (2022), Aydin and Birincioğlu (2022), Hagos et al. (2022), Ramesh and Iqbal (2022), Nsangou et al. (2022).

Asiedu (2020); Feng et al. (2021); Hemmati et al. (2020); Konrad (2003) note that rapid urbanization increases the frequency of floods, putting communities at greater risk. Activities such as deforestation, and inadequate stormwater drains intensify runoff, causing nearby streams to experience higher peak discharge and flood frequency. The rapid growth of urban populations seeking housing has resulted in unregulated and poor neighborhoods in flood-suspectable areas, leading to extensive damage due to flooding. Various factors contribute to this problem, including the haphazard expansion of cities and the spontaneous creation of informal settlements on floodplains, without proper consideration for land use planning (Asiedu, 2020; Eldho et al., 2018; Salami et al., 2017b). Additionally, changes in precipitation patterns due to climate change have contributed to the severity of floods within cities (Serre et al., 2018).

Deforestation and land grading lead to amplified water flow in streams as a result of rainfall, subsequently leading to heightened occurrences of severe flooding in adjacent streams (Danáčová et al., 2020; Feng et al., 2021; Lim et al., 2019; Ramadhan et al., 2023). Rapid urbanization practices such as modifying stream channels and constructing infrastructure in flood-prone zones increase the threats of inundation and erosion, persisting even as development progresses(Cea & Costabile, 2022; Chagas et al., 2022; Truu et al., 2021).

Ongoing rapid urban growth and climate change are driving significant transformations in cities, leading to an elevated risk of flooding and heightened severity (Bibi & Kara, 2023; Hemmati et al., 2020; Serre et al., 2018; Yang et al., 2021). The transformation (or conversion) of flood-prone areas into urban spaces has nearly doubled since 1985, resulting in increased exposure to flooding due to population growth and urban expansion (Andreadis et al., 2022; Serre et al., 2018). Recent studies have explained that urban flooding is increasing as a result of climate change (Manandhar et al., 2023). Consequently, a combination of changing climate, precipitation patterns, and rapid urbanization may necessitate adjustments in flood mitigation strategies and decision-making processes (Cantis et al., 2020; Daksiya et al., 2021; Yang et al., 2021).

Insufficient planning and inadequate drainage systems significantly contribute to the occurrence and impact of urban flooding, which has devastating consequences for affected areas. The expansion of urbanization has resulted in settlements in flood suspectable areas. This expansion is influenced not only by the extent of impermeable surfaces but also by the spatial distribution of impermeable surfaces (Feng et al., 2021).

6.2. Characterizing the level of urban flood vulnerability

Analyzing the urban flooding complexities using the SETS approach is vital, as it delves into the connections between social, technological, and ecological systems impacting residents' vulnerability in flood-prone regions. These connections stem from changes in land use, population, economic growth, hydrology, and climate (Chang et al., 2021; Tanoue et al., 2016; Tate et al., 2021). Thus, incorporating the SETS framework is crucial for assessing floods at both individual and interconnected levels, especially in developing nations where limited infrastructure and resources worsen flooding impacts (Deria et al., 2020; Rentschler et al., 2022; Salami et al., 2017b).

The findings of this study indicated that regions characterized by high unemployment rates, a substantial presence of elderly individuals and children under five years old, and a majority of female residents are vulnerable to flooding. This observation is consistent with research by Rufat et al. (2015); Tate et al. (2021), highlighting the multifaceted interconnection between flood exposure and social vulnerability. Specifically, socially disadvantaged groups such as children, the elderly, individuals with disabilities, those living in poverty, and minority populations face a higher risk of suffering injuries and fatalities during flood events compared compared to others.

The study showed that regions with flat terrains, proximity to industrial hazardous material release points, small and isolated ecological areas, and exposed soil patches exhibited heightened exposure to floods. These findings corroborated previous studies suggesting that flat terrains are more susceptible to flooding and possess lower slope gradients (Singh et al., 2020). Studies by Cian et al. (2018), Martinez and Labib (2023), and Zhang et al. (2018) have emphasized the role of vegetation in reducing flood vulnerability through water absorption and runoff control. The risks posed by toxic industries in nearby areas have been underscored by Chang et al. (2021), Jongman et al. (2015), Talbot et al. (2018). Additionally, fragmented ecosystems, as demonstrated by Bousquin and Hychka (2019), and Rehman et al. (2021) are less effective in mitigating floods. Bare soil areas, with their limited infiltration capacity and high erodibility during floods, are particularly risky Chang et al. (2021).

Areas characterized by high road density, built-up areas, and low green infrastructure density in neighborhoods vulnerable to flooding. This is in agreement with previous research conducted at other urban areas (Briones et al., 2020). The lack of permeability in built-up areas makes them more prone to flooding, consistent with the findings of Deepak et al. (2020). Additionally, impervious surfaces and dense road networks contribute to increased flood risk by hindering water infiltration and aggravating stormwater runoff (Baky et al., 2020; Kaspersen et al., 2015).

The study also found that areas with lower green infrastructure density face increased vulnerability to flooding, hindering infiltration processes and exacerbating runoff. This is consistent with previous research by Khodadad et al. (2023) and Pallathadka et al. (2022), highlighting the vital function of green infrastructure in mitigating flood vulnerability. These findings underscore the importance of integrating green infrastructure to improve flood-related risks in urban areas.

Furthermore, the study revealed that areas near to industries with hazardous emissions, landfill sites, and abattoirs are significantly vulnerable to flooding, posing a threat to the local community. The research conducted by Lin et al. (2019), and Qiang (2019), supports the notion that areas close to critical infrastructure face increased flood vulnerability. Conversely, proximity to emergency centers such as hospitals, schools, and universities was found to be vital in flood situations, serving as crucial support and response hubs. This aligns with the findings of Atanga and Tankpa (2022), and Cutter et al. (2003), underscoring the essential role of these facilities in flood response efforts and their significance in protecting communities at risk.

6.3. Investigation and analysis of flood-resilient neighborhoods

To investigate flood-resilient neighborhoods in the designated study area, a thorough investigation is indispensable, encompassing configurational analysis, flood event observations, insights from key informants and municipal authorities, and morphological analysis (Wang et al., 2022b; Yusmah et al., 2020; Zhou; et al., 2022). This approach facilitates a deep understanding of the city's spatial connectivity and specific features like street and block layouts. By amalgamating flood event observations with feedback from key informants and local authorities, a comprehensive view of the flood-resilient neighborhoods in the city can be established (Eric et al., 2021; Mohammadtaghi et al., 2023; Tanoue et al., 2016). Particularly in developing nations such as Ethiopia, where flooding impacts are exacerbated in rapidly urbanizing areas due to limited information and resources, such an analysis is vital (Deria et al., 2020; Rentschler et al., 2022; Salami et al., 2017b).

The analysis of the study area showed varying degrees of accessibility throughout different regions, with some exhibiting high accessibility, indicating a well-interconnected and easily traversable street layout. This implies that these regions are more conducive for flood response, emergency assistance, and evacuation due to their ease of access. Conversely, areas with lower accessibility levels suggest potential susceptibility to urban flooding, as the lack of accessibility in these areas may impede the movement of individuals during flood events, rendering it more challenging to provide aid and alleviate the repercussions of flooding. The results of this study are consistent with previous research conducted by Gangwal et al. (2023); He et al. (2021); Lee et al. (2023); Zhou; et al. (2022), emphasizing that neighborhoods characterized by high accessibility and interconnected street networks are more adept at mitigating flood vulnerability and enhancing response efforts, aid distribution, and evacuation procedures compared to less accessible areas. This alignment underscores the critical role of spatial connectivity in bolstering flood resilience within urban environments.

The study revealed that neighborhoods characterized by well-planned and interconnected street networks with consistent street spacing demonstrated greater resilience against urban flooding. In contrast, neighborhoods with inadequate spatial connectivity, such as dead-end streets and irregular block layouts, exacerbated the effects of flooding by impeding water flow and disrupting drainage systems. These findings underscore the importance of integrating flood mitigation measures into building configurations to address flooding risks effectively. Sarkissian et al. (2022); Talbot et al. (2018), emphasized that urban areas featuring appropriate building configurations can effectively lower flood risk through diverse footprints that facilitate water absorption and minimize surface runoff.

The study's results highlight the critical role of street system design and connectivity in enhancing traffic flow and managing floods. Street networks that are well-planned and connected with consistent spacing were found to play a crucial role in facilitating smooth traffic flow and effective flood mitigation. On the other hand, areas characterized by inadequate street connectivity and a high number of dead-end streets presented obstacles for flood response efforts and emergency assistance distribution. These results align with previous studies emphasizing the importance of street connectivity and drainage infrastructure in mitigating flood hazards (Farahmand et al., 2021; Karley, 2009; Li et al., 2020; Rosa & Pappalardo, 2020).

The type of materials used for street surfaces plays a critical role in managing traffic flow within urban areas. In times of flooding, roads made of earthen materials are particularly at risk of damage and erosion, impeding evacuation procedures and causing delays in aid distribution. Research has consistently demonstrated the beneficial impact of incorporating permeable pavements, such as porous asphalt, on enhancing traffic flow within urban areas. Despite these advancements, the widespread use of earthen roads and the lack of asphalt coverings pose substantial challenges during urban flooding incidents (Ahlmer et al., 2018; Konrad & Booth, 2005). The susceptibility of earthen roads to degradation and erosion is exacerbated by intense precipitation, leading to elevated surface runoff and potential blockages (Eisenberg et al., 2015; NationalAssociationofCityTransportationOfficials, 2017).

Neighborhoods characterized by shorter blocks and frequent intersections are advantageous as they promote water runoff and mitigate flooding, whereas neighborhoods with longer blocks hinder water flow, increasing flood susceptibility. Grid patterns in neighborhood layouts have been identified as facilitating efficient water drainage, while irregular block configurations disrupt natural drainage systems, exacerbating urban flooding challenges. The results align with previous research that emphasizes the beneficial effects of smaller urban blocks on water drainage and mitigating flood risks (Feng et al., 2021). Additionally, the presence of more intersections in such neighborhoods can enhance traffic flow and navigation for residents (Morales et al., 2021). Conversely, larger urban blocks impede water flow and elevate the risk of water accumulation during heavy rainfall events (Zhang et al., 2022). Regular grid layouts are more effective in decreasing flood risk by providing multiple drainage pathways, whereas irregular grid layouts are less efficient and contribute to worsening urban flooding issues (Feng et al., 2021; Sharifi et al., 2021).

Recent studies have highlighted the significance of flood event observation in mitigating flood hazards, as evidenced by Kang et al. (2023) and Zhang et al. (2021). These observations are pivotal in providing insightful viewpoints for flood assessment and identifying areas prone to economic and environmental risks. By combining flood event data with insights from key stakeholders and local officials, a holistic comprehension of a city's flood resilience can be achieved (Coeur & Lang, 2008; Haltas et al., 2021; Zhang et al., 2021).

6.4 . Development of strategies and tools for flood management

Quantifying flood mitigation services is crucial in urban areas to prevent the recurrent devastating flooding effects (Bose & Mazumdar, 2023; Kadaverugu et al., 2021; Quagliolo et al., 2021). Thus, this study conducted a thorough analysis of the study area by dividing it into six micro-watersheds. The sizes of these micro-watersheds ranged from 2986.19 to 5733.40 hectares. The land cover analysis revealed that a significant portion of the area was covered by Rangelands (Grass-flooded vegetation) at 39.8%, followed by croplands at 33.81%. Built-up areas accounted for 25.14% of the land, while forested areas made up only 0.79%. The lack of forested areas presents a challenge as it limits the space for water to percolate into the ground, making the area more prone to flooding (Athick & Shankar, 2019). Water bodies and bare land constituted 0.36% and 0.09% respectively, making them vulnerable to flooding.

The spatial configuration of land use patterns indicated that the city is expanding mainly towards the northern, northeast, eastern, and southeastern zones of the study area are attributed to their flat terrain and easy access to key areas in Ethiopia. However, these urbanized areas are predominantly vulnerable to flooding, a recurring issue during rainy seasons. These findings are in agreement with a study conducted by (Bulti & Assefa, 2019), which noted a rapid annual growth rate of nearly 9%, ranking the city among the fastest-growing in Ethiopia. The expanding population and infrastructure demands not only strain public services but also pose environmental risks (Adugna, 2019b; Jemberie & Melesse, 2021; Masha et al., 2023).

The study area was categorized into three hydrological soil groups, with Group A (21.24% of the area) considered by well-drained sands and gravels with low runoff potential, Group B (69.74%) displaying moderately low runoff potential, and Group D (9.05%) showing high runoff potential due to slow infiltration rates. The predominant soil type in the study area was Group B, consisting of Calcaric Fluvisols, Mollic Andosols, and Vitric Andosols, with moderately low runoff potential. However, the impacts of rapid urban growth and deforestation have disrupted natural hydrological processes, diminishing soil water absorption capacity and escalating urban flooding risks. This is supported by previous research conducted by Danáčová et al. (2020), and Feng et al. (2021), highlighting how urbanization results in increased impervious surfaces, quicker water flow times, and elevated flood risks. Factors such as vegetation removal, improper land grading, and the construction of drainage networks further exacerbate runoff from precipitation, leading to higher peak discharge rates, amplified flood volumes, and more frequent flooding occurrences (Gwenzi & Nyamadzawo, 2014; Janicka & Kanclerz, 2023; Robinson et al., 2022).

The findings of the study area's daily rainfall and sub-hourly data from the last three decades indicated a noticeable and troubling pattern of increasing heavy rainfall. This trend is related to the rapid deforestation and expansion of impervious surfaces within the city (Bajracharya et al., 2015; Bulti & Assefa, 2019). Consequently, developed areas are experiencing a surge in surface runoff, leading to a decrease in the soil's infiltration capacity. This situation is predicted to worsen following storm events, as the rainfall in the study area turns into a runoff in built-up areas (Bulti & Assefa, 2019).

Vegetated lands and grasslands have a natural capacity to retain rainfall, but the limited forest cover in the study area leads to runoff exceeding infiltration levels, resulting in increased water runoff. Inadequate drainage system management contributes to common problems like siltation, and clogging causing waterlogging in densely populated central city areas following heavy rainfall. These findings are in agreement with Bulti and Assefa (2019) study, emphasizing the urgent need for effective management strategies to address escalating heavy rainfall risks in rapidly urbanizing regions. The ongoing urbanization and expansion of impermeable surfaces in the study area are expected to worsen runoff issues, highlighting the necessity for proactive flood risk mitigation measures (Lapointe et al., 2022; Qin, 2020).

Floods are an unavoidable natural phenomenon, especially in complex urban areas. Therefore, it is vital to implement a range of interconnected solutions to effectively manage and coexist with floods (Bernello et al., 2022; Hamers et al., 2023; Ruirui et al., 2022; Tingsanchali, 2012). One approach is to utilize non-structural and structural measures (Chan et al., 2020; Dehkordi et al., 2021; Manandhar et al., 2023). Structural measures involve the construction of stormwater retention ponds, rainwater harvesting structures, well-designed stormwater networks, and green infrastructure (Lihong et al., 2022; Vuik et al., 2016; WorldBank, 2017). These physical solutions help manage floodwaters and mitigate their impact.

Non-structural measures like flood forecasting, early warning systems, and strict building regulations are key proactive strategies for addressing flood risks (Kuang, 2020). Community awareness programs and regulations promoting best practices can also help minimize flood damage (Kang et al., 2009). Nature-based structural approaches, such as urban forestry and rain gardens contributed to flood mitigation by acting as sponges during floods and filtering pollutants (Thomas et al., 2023). Implementing a combination of these measures, including converting open spaces into green cover and rain gardens, as well as groundwater recharge and rainwater harvesting structures, can enhance run-off retention capacity and reduce flood vulnerability (Minea & Zaharia, 2011).

To effectively address flooding in the study area, a multi-level approach is essential. Decentralizing the flood management system to city-level watersheds and micro-watersheds within the city is crucial for targeted solutions (Bertilsson et al., 2019;

Jemberie & Melesse, 2021). Urban land use planning should prioritize areas vulnerable to floods by preserving natural drainage systems and creating space for floodwater in floodplain areas for multipurpose use (Bose & Mazumdar, 2023; Kadaverugu et al., 2022). Implementing measures like check dams, retention ponds, and interconnectivity of water bodies can help retain floodwater (Bulti & Abebe, 2020). Incorporating resilient policy planning and innovative urban landscape concepts such as Nature Based solutions (NBS), Water Sensitive Urban Design (WSUD), Low Impact Development (LID), and Sponge Cities (Jemberie & Melesse, 2021; Jiang et al., 2018; Myers & Pezzaniti, 2019).

At the micro-watershed level, the implementation of structural flood retention measures is crucial for effective flood mitigation. These measures include green roofs and walls, rainwater harvesting pits, underground stormwater networks, infiltration trenches, micro-reservoirs, bioswales, and porous pavements (Delgado et al., 2023; Twohig et al., 2022). Careful consideration of the placement of these measures within or outside flood plains is necessary, along with determining the required quantity for optimal control (Leite & Antunes, 2023). Utilizing a mix of permeable and impermeable surfaces, coupled with vegetative cover, can aid in managing runoff and water retention (Ferreira et al., 2021). Incorporating raised and flood-proofed buildings, such as green roofs, and eliminating gutters can help reduce and slow down runoff (Twohig et al., 2022; Zhou, 2019). To prevent inundation on urban roads during flash floods, adequate cross-drainage works are essential to prevent stagnation and the clogging of stormwater drains (Iffland et al., 2021; Zhang et al., 2020). Installing sustainable mesh materials at cross-drainage structures can further prevent clogging during floods.

In addition to implementing various non-structural and structural measures, research suggests that socio-demographic factors and adaptive capacity, including access to healthcare infrastructure and flood relief centers, awareness among the citizens should be imposed through rules and regulations play a significant role in post-flood mitigation efforts (Bixler et al., 2021; Cao et al., 2020; Deria et al., 2020; Peden et al., 2023). By considering these factors, urban areas can better address the challenges posed by floods and enhance their resilience.

CHAPTER SEVEN:

GENERAL CONCLUSIONS AND RECOMMENDATIONS

7.1 Conclusions

Adama, the second-largest city in Ethiopia and a rapidly growing urban center is highly prone to flooding due to its geographical setting on low-lying flat land surrounded by plateaus and mountain ranges. To tackle this pressing issue, it is essential to identify and map areas prone to flooding, characterize the level of flood vulnerability, investigate flood-resilient neighborhoods, and develop strategic tools for flood management.

Identification and mapping of flood Prone-area

The study employed a geographic information system and analytical hierarchy processes to identify and map areas at risk of flooding by considering eleven flood-conditioning factors. This analysis aimed to provide a comprehensive understanding of flood risk in the study area. These factors such as proximity to stormwater drains, topographic wetness index, elevation, land cover, slope, drainage density, rainfall patterns, normalized difference vegetation index, distance from rivers and roads, and soil type. The result of this analysis produced a detailed and comprehensive flood-prone map tailored specifically for the unique environmental characteristics of the city.

The study's analysis of flood-prone areas revealed varying degrees of flood risk across the City, with different proportions of very high, high, moderate, and low-risk zones. This indicates that the majority of the area, around 98.69%, faces moderate to very high flood risks, primarily due to its geographical position on flat terrain bounded by plateaus and ridges, along with factors like rapid urbanization and deforestation. Areas with flat surfaces, low elevation, proximity to rivers, urban development, and adjacency to highways are highly susceptible to flooding (Argaz et al., 2019; Edamo et al., 2022; Negese et al., 2022). In contrast, a small portion of the study area, approximately 1.31%, has a lower risk of flooding due to its distance from water bodies and roads, higher elevation, and steeper slopes. Regions characterized by steep terrain, higher elevations, distance from water sources and road networks, and low drainage density are less prone to flooding (Das & Gupta, 2021; Desalegn & Mulu, 2021).

Characterizing the level of flood vulnerability

To characterize flood vulnerability, the SETS framework was utilized, revealing a clustered distribution pattern of vulnerability across its domains. The study also found spatial correlations between S-E, S-T, and E-T vulnerabilities, suggesting the potential for providing flood mitigation measures in multiple domains simultaneously. These findings offer valuable insights for developing more effective flood vulnerability reduction strategies in the study area and other urban areas grappling with similar challenges. By utilizing the SETS framework, a comprehensive understanding of flood vulnerability is achieved, facilitating the development of targeted and impactful flood management intervention (Chang et al., 2021; Tate et al., 2021).

Furthermore, the study investigated the implications of sustainable urban development, focusing on exposure, sensitivity, and adaptability to flood vulnerability. The study developed a SET-based vulnerability map for the study area, which reveals varying levels of vulnerability to flooding across different neighborhoods. The results showed that around 68.08% of the study area is exposed to moderate to very high flood vulnerability, indicating a need for urgent attention and mitigation efforts. These findings provide valuable insights for developing targeted and impactful flood management interventions in urban areas.

Investigation and analysis of flood-resilient neighborhoods

To identify flood-resilient neighborhoods within the study area, an extensive investigation was conducted, incorporating configurational analysis, observations of past flood events, insights from key informants, municipal data, and morphological analysis. By taking into account the current spatial arrangement and morphology that exhibit resilience to urban flooding, the city can enhance its flood management strategies and resilience to floods in the future. This holistic method offers valuable insights for cities seeking to enhance their capacity to withstand and recover from flood events. The study's thorough approach entailed examining several factors like the city's spatial configuration and morphology, and flood event observations to pinpoint neighborhoods that exhibit resilience to flooding.

The main findings of the research emphasized the varying degrees of spatial connectivity within the research area, leading to the selection of two neighborhoods for further examination based on their high and low connectivity. The high-connectivity neighborhoods stood out due to their interconnected street layouts, manageable street spacing, and efficient traffic circulation, which also facilitated effective stormwater flow management and minimized flood damage during rainfall events (Sarkissian et al., 2022). The utilization of diverse street surface materials significantly supported traffic movement and mitigated flood-related erosion from heavy precipitation. Furthermore, the presence of compact block sizes with more frequent intersections promoted water infiltration and decreased flood risk. The grid layout in these areas enabled efficient stormwater drainage by offering multiple pathways for runoff, thereby reducing the likelihood of flooding incidents during inundation events (Zhang et al., 2022).

Development of strategies and tools for flood management

The study employed the InVEST-UFRM tool to measure and devise strategies for dealing with urban flooding triggered by heavy rainfall in the research area. Through quantifying runoff patterns in specific locations, a comparison was made to evaluate the susceptibility to flash floods at both watershed and micro-watershed levels. The results indicated that the InVEST-UFRM model revealed a thorough understanding of the city's flood risk environment, proving its efficacy in analyzing urban watersheds and visually depicting instances of flooding. The study revealed notable disparities in runoff retention and flood volume among various scenarios, highlighting the diverse flood potential and retention capacities of micro-catchments within the study region. The quantification of flood risk yielded valuable information on the role of micro-catchments in managing urban flood events, thereby guiding future adaptation and mitigation strategies (Bose & Mazumdar, 2023; Kadaverugu et al., 2021).

7.2 Recommendations

To address flooding problems, which is one of the bottlenecks of sustainable development, in the study area and other similar urban areas which was suffering from flooding, the following recommendations are forwarded:

- To improve and protect the primary natural drainage system within a watershed, efforts will be made to rehabilitate and enhance its functionality. This will involve implementing measures to prevent disruption to the major natural stormwater drain systems and maintain the overall health of the ecosystem. By focusing on rehabilitation, and restoration of damaged or degraded elements of the drainage system, such as wetlands or streams, and ensure they can effectively manage water flow and filtration. Enhancements may include the introduction of sustainable practices and infrastructure to support the natural drainage processes, such as green infrastructure or erosion control measures.

- Applying nature-based stormwater management solutions for flood reduction as a proactive measure and incorporating the potential of green spaces to decrease stormwater runoff, slow surface flows, and create space for water in floodplains.
- Adaptation strategies such as cleansing stormwater drains and replacing primary drain systems, encouraging infiltration, increasing depression and street detention storage, re-designing structures, dune reinforcement, creating wetlands as buffer zones against flooding, and protecting existing natural barriers are all important aspects to consider.
- Urban policymakers and practitioners need to develop robust flood management strategies that factor in the spatial layout of the city. By incorporating space syntax analysis into existing urban planning and design frameworks, they can pinpoint flood-prone areas. This comprehensive approach can advance towards attaining flood resilience and fostering sustainable urban development
- Utilizing a combination of remote sensing, geographic information system tools, and the analytical hierarchy process is vital for the identification of flood-prone zones and establishing layered flood conditioning factors. These elements are key in supporting decision-makers and experts in executing efficient flood management plans in urban regions and watersheds.
- Emphasizing the importance of integrating disciplines such as geographic information systems, remote sensing, and hydrology tools for assessing natural capital, urban planning, and building regulations is essential for attaining flood resilience. This integration aids in tackling the intricate obstacles posed by flooding through the formulation of holistic flood management strategies that consider a range of factors affecting flood risk. Ultimately, this interdisciplinary method is critical for establishing resilient and sustainable urban spaces amidst escalating flood threats.

7.2.1 Recommendations for future studies

The present study recommends the following key issues to be considered by future researchers:

- Maximize the utilization of high-resolution satellite imagery, LiDAR data, and advanced spatial analysis techniques to enhance the precision of mapping of flood-prone areas.
- Validation of the flood hazard and vulnerability maps using objective criteria
- Inclusion of more context-specific indicators like solid waste management level for flood vulnerability.
- Sensitivity analysis of the indicators for flood mapping and vulnerability
- Extent of flood risks due to increased urbanization and climate change
- Inclusion of scenarios for various mitigation measures
- Flood vulnerability assessment and mitigation strategies should focus on interdisciplinary collaboration, innovative methodologies, and the integration of advanced technologies to enhance the accuracy and effectiveness of flood management efforts.

REFERENCE

Abdelkarim, A., Al-Alola, S. S., Alogayell, H. M., Mohamed, S. A., Alkadi, I. I., & Ismail, I. Y. (2020). Integration of GIS-based multicriteria decision analysis and analytic hierarchy process to assess flood hazard on the Al-shamal train pathway in Al-Qurayyat region, kingdom of Saudi Arabia. *Water, 12*(6), 1702.

Abebe, Y., Kabir, G., & Tesfamariam, S. (2018). Assessing urban areas vulnerability to pluvial flooding using GIS applications and Bayesian Belief Network model. *Journal of Cleaner Production*, *174*, 1629-1641.

Abshirini, E., Koch, D., & Legeby, A. (2017). Flood Resilient Cities: A Syntactic and Metric Novel on Measuring the Resilience of Cities against Flooding, Gothenburg, Sweden. *Journal of Geographic Information System*, *9*, 505-534.

ACSPR. (2018a). *Adama City Structure Plan Report*

ACSPR. (2018b). *Adama City Structure Plan Report*.

Adegun, O. B. (2023). Flood-related challenges and impacts within coastal informal settlements: a case from LAGOS, NIGERIA. *International Journal of Urban Sustainable Development*, *15*(1), 1-13.

Adugna, A. (2019a). Regional economic favoritism and redistributive politics as a public good: The case of Tigray region in northern Ethiopia. *Journal of Geography and Geology, 11*(1), 1-12.

Adugna, A. (2019b). Regional economic favoritism and redistributive politics as a public good: The case of Tigray region in northern Ethiopia. *Journal of Geography and Geology11*(1), 1-12.

Agilan, V., & Umamahesh, N. (2017). Modelling nonlinear trend for developing non-stationary rainfall intensity–duration–frequency curve. *International Journal of Climatology*, *37*(3), 1265-1281.

Ahlmer, A.-K., Cavalli, M., Hansson, K., Koutsouris, A. J., Crema, S., & Kalantari, Z. (2018). Soil moisture remote-sensing applications for identification of flood-prone areas along transport infrastructure. *Environmental Earth Sciences*, *77*, 1-17.

Ahmadisharaf, E., Tajrishy, M., & Alamdari, N. (2016). Integrating flood hazard into site selection of detention basins using spatial multi-criteria decision-making. *Journal of Environmental Planning and Management*, *59*(8), 1397-1417.

Aishwarya, N., Aniruddha, K., Sutapa, D., & Bharath, H. A. (2023). Developing assessment flow for damage estimation of mud housing typology through a case study against coastal floods. *Scientific reports*, *13*(6712).

Ajibade, F. O., Ajibade, T. F., Idowu, T. E., Nwogwu, N. A., Adelodun, B., Lasisi, K. H., Opafola, O. T., Ajala, O. A., Fadugba, O. G., & Adewumi, J. R. (2021). Flood-prone area mapping using GIS-based analytical hierarchy frameworks for Ibadan city, Nigeria. *Journal of Multi-Criteria Decision Analysis*, *28*(5-6), 283-295.

Al-Zahrani, M. A. (2018). Assessing the impacts of rainfall intensity and urbanization on storm runoff in an arid catchment. *Arabian Journal of Geosciences*, *11*, 1-14.

Alabbad, Y., Yildirim, E., & Demir, I. (2023). A web-based analytical urban flood damage and loss estimation framework. *Environmental Modelling & Software*, *163*, 105670.

Alaminie, A. A., Amarnath, G., Padhee, S. K., Ghosh, S., Tilahun, S. A., Mekonnen, M. A., Assefa, G., Seid, A., Zimale, F. A., & Jury, M. R. (2023). Nested hydrological modeling for flood prediction using CMIP6 inputs around Lake Tana, Ethiopia. *Journal of Hydrology: Regional Studies*, *46*, 101343.

Albano, R., Mancusi, L., Sole, A., & Adamowski, J. (2015). Collaborative strategies for sustainable EU flood risk management: FOSS and geospatial tools—challenges and opportunities for operative risk analysis. *ISPRS International Journal of Geo-Information*, *4*(4), 2704-2727.

Alemayehu, D. (2007). Assessment of flood risk in Dire Dawa town, eastern Ethiopia, using GIS. *Addiss Abeba University*.

Ali, S. A., Parvin, F., Pham, Q. B., Vojtek, M., Vojteková, J., Costache, R., Linh, N. T. T., Nguyen, H. Q., Ahmad, A., & Ghorbani, M. A. (2020). GIS-based comparative assessment of flood susceptibility mapping using hybrid multi-criteria decision-making approach, naïve Bayes tree, bivariate statistics and logistic regression: a case of Topľa basin, Slovakia. *Ecological Indicators*, *117*, 106620.

Allafta, H., & Opp, C. (2021). GIS-based multi-criteria analysis for flood prone areas mapping in the trans-boundary Shatt Al-Arab basin, Iraq-Iran. *Geomatics, Natural Hazards and Risk*, *12*(1), 2087-2116.

Alshaikh, R. Z., Abdulmunem, S. A., & Alkinani, A. S. (2023). A Review on Urban Planning and Its Role in Managing Flood Risks. *Urban Planning and Construction*, *1*(1), 1-8.

Amirkhani, M., Ghaemimood, S., von Schreeb, J., El-Khatib, Z., & Yaya, S. (2022). Extreme weather events and death based on temperature and CO2 emission–A global retrospective study in 77 low-, middle-and high-income countries from 1999 to 2018. *Preventive Medicine Reports*, *28*, 101846.

Andreadis, K. M., Wing, O. E., Colven, E., Gleason, C. J., Bates, P. D., & Brown, C. M. (2022). Urbanizing the floodplain: global changes of imperviousness in flood-prone areas. *Environmental research letters*, *17*(10), 104024.

Ansah, S., Ahiataku, M., Yorke, C., Otu-Larbi, F., Yahaya, B., Lamptey, P., & Tanu, M. (2020). Meteorological analysis of floods in Ghana. *Advances in Meteorology*, *2020*, 1-14.

Antwi, E. K., Boakye-Danquah, J., Owusu, A. B., Loh, S. K., Mensah, R., Boafo, Y. A., & Apronti, P. T. (2015). Community vulnerability assessment index for flood prone savannah agro-ecological zone: A case study of Wa West District, Ghana. *Weather and Climate Extremes*, *10*, 56-69.

Anwana, E. O., & Owojori, O. M. (2023). Analysis of Flooding Vulnerability in Informal Settlements Literature: Mapping and Research Agenda. *Social Sciences*, *12*(1), 40. https://www.mdpi.com/2076-0760/12/1/40

Argaz, A., Ouahman, B., Darkaoui, A., Bikhtar, H., Ayouch, E., & Lazaar, R. (2019). Flood hazard mapping using remote sensing and GIS Tools: a case study of souss watershed. *J. Mater. Environ. Sci*, *10*, 170-181.

Arshad, A., Zhang, Z., Zhang, W., & Dilawar, A. (2020). Mapping favorable groundwater potential recharge zones using a GIS-based analytical hierarchical process and probability frequency ratio model: A case study from an agro-urban region of Pakistan. *Geoscience Frontiers*, *11*(5), 1805-1819.

Arya, A. K., & Singh, A. P. (2021). Multi criteria analysis for flood hazard mapping using GIS techniques: a case study of Ghaghara River basin in Uttar Pradesh, India. *Arabian Journal of Geosciences*, *14*, 1-12.

Aryal, J. P., Sapkota, T. B., Rahut, D. B., Marenya, P., & Stirling, C. M. (2021). Climate risks and adaptation strategies of farmers in East Africa and South Asia. *Scientific reports*, *11*(1), 10489.

Asiedu, J. B. (2020). Reviewing the argument on floods in urban areas: a look at the causes. *Theoretical and Empirical Researches in Urban Management*, *15*(1), 24-41.

Atanga, R. A., & Tankpa, V. (2022). Geospatial analysis of flood emergency evacuation sites in Accra. *Jàmbá: Journal of Disaster Risk Studies*, *14*(1), 9.

Athick, A. M. A., & Shankar, K. (2019). Data on land use and land cover changes in Adama Wereda, Ethiopia, on ETM+, TM and OLI-TIRS landsat sensor using PCC and CDM techniques. *Data in brief*, *24*.

Ayda, B. A., Goshime, D. W., Finsa, M. M., & Ayalew, A. T. (2024). Urban stormwater management under various runoff conditions for Arba Minch town of southern Ethiopia. *Natural Hazards Research*.

Aydin, M., & Birincioğlu, E. (2022). Flood risk analysis using gis-based analytical hierarchy process: a case study of Bitlis Province. *Applied Water Science*, *12*(6), 122.

Azuma, K., Ikeda, K., Kagi, N., Yanagi, U., Hasegawa, K., & Osawa, H. (2014). Effects of water-damaged homes after flooding: health status of the residents and the environmental risk factors. *International journal of environmental health research*, *24*(2), 158-175.

Babanawo, D., Mattah, P. A. D., Agblorti, S. K., Brempong, E. K., Mattah, M. M., & Aheto, D. W. (2022). Local Indicator-Based Flood Vulnerability Indices and Predictors of Relocation in the Ketu South Municipal Area of Ghana. *Sustainability*, *14*(9), 5698.

Bajracharya, A. R., Rai, R. R., & Rana, S. (2015). Effects of Urbanization on Storm Water Run-off: A Case Study of Kathmandu Metropolitan City, Nepal. *Journal of the Institute of Engineering*, *11*(1).

Baky, M. A. A., Islam, M., & Paul, S. (2020). Flood hazard, vulnerability and risk assessment for different land use classes using a flow model. *Earth Systems and Environment*, *4*, 225-244.

Balica, S. F., Wright, N. G., & Van der Meulen, F. (2012). A flood vulnerability index for coastal cities and its use in assessing climate change impacts. *Natural Hazards*, *64*, 73-105.

Barreiro, J., Lopes, R., Ferreira, F., Brito, R., Telhado, M. J., Matos, J. S., & Matos, R. S. (2020). Assessing Urban Resilience in Complex and Dynamic Systems: The

RESCCUE Project Approach in Lisbon Research Site. *Sustainability*, *12*(21), 8931.

Batica, J., & Gourbesville, P. (2016). Resilience in flood risk management–A new communication tool. *Procedia Engineering*, *154*, 811-817.

Behmanesh, H., & Brown, A. (2019). Classification and review of software applications in the context of urban design processes.

Beltramone, G., Alaniz, E., Ferral, A., Aleksinko, A., Arijón, D. R., Bernasconi, I., German, A., & Ferral, A. (2017). Risk mapping of urban areas prone to flash floods in mountain basins using the analytic hierarchy process and geographical information systems. 2017 XVII Workshop on information processing and control (RPIC),

Bernello, G., Mondino, E., & Bortolini, L. (2022). People’s Perception of Nature-Based Solutions for Flood Mitigation: The Case of Veneto Region (Italy). *Sustainability*, *14*(8), 4621. https://www.mdpi.com/2071-1050/14/8/4621

Bertilsson, L., Wiklund, K., de Moura Tebaldi, I., Rezende, O. M., Veról, A. P., & Miguez, M. G. (2019). Urban flood resilience–A multi-criteria index to integrate flood resilience into urban planning. *Journal of hydrology*, *573*, 970-982. https://doi.org/https://doi.org/10.1016/j.jhydrol.2018.06.052

Bhatkoti, R., Moglen, G. E., Murray-Tuite, P. M., & Triantis, K. P. (2016). Changes to bridge flood risk under climate change. *Journal of Hydrologic Engineering*, *21*(12), 04016045.

Bibi, T. S., & Kara, K. G. (2023). Evaluation of climate change, urbanization, and low-impact development practices on urban flooding. *Heliyon*, *9*(1).

Birkholz, S., Muro, M., Jeffrey, P., & Smith, H. M. (2014). Rethinking the relationship between flood risk perception and flood management. *Science of the Total Environment*, *478*, 12-20.

Bixler, R. P., Lieberknecht, K., Leite, F., Felkner, J., Oden, M., Richter, S. M., Atshan, S., Zilveti, A., & Thomas, R. (2019). An Observatory Framework for Metropolitan Change: Understanding Urban Social–Ecological–Technical Systems in Texas and Beyond. Sustainability, 11.(2019), 13. 3611. *Online: https://doi. org/10.3390/su11133611*.

Bixler, R. P., Paul, S., Jones, J., Preisser, M., & Passalacqua, P. (2021). Unpacking Adaptive Capacity to Flooding in Urban Environments: Social Capital, Social

Vulnerability, and Risk Perception [Original Research]. *Frontiers in Water*, *3*. https://doi.org/10.3389/frwa.2021.728730

Bodoque, J. M., Esteban-Muñoz, Á., & Ballesteros-Cánovas, J. A. (2023). Overlooking probabilistic mapping renders urban flood risk management inequitable. *Communications Earth & Environment*, *4*(1), 279.

Bose, S., & Mazumdar, A. (2023). Urban flood risk assessment and mitigation with InVEST-UFRM model: a case study on Kolkata city, West Bengal state (India). *Arabian Journal of Geosciences*, *16*(5), 320. https://doi.org/https://doi.org/10.1007/s12517-023-11412-2

Bottazzi, P., Winkler, M. S., Boillat, S., Diagne, A., Maman Chabi Sika, M., Kpangon, A., Faye, S., & Speranza, C. I. (2018). Measuring subjective flood resilience in suburban Dakar: a before–after evaluation of the "live with water" project. *Sustainability*, *10*(7), 2135.

Botzen, W. W., Deschenes, O., & Sanders, M. (2019). The economic impacts of natural disasters: A review of models and empirical studies. *Review of Environmental Economics and Policy*.

Bousquin, J., & Hychka, K. (2019). A geospatial assessment of flood vulnerability reduction by freshwater wetlands–a benefit indicators approach. *Frontiers in environmental science*, *7*, 54.

Brasil, J. B., Guerreiro, M. S., Andrade, E. M. d., de Queiroz Palácio, H. A., Medeiros, P. H. A., & Ribeiro Filho, J. C. (2022). Minimum Rainfall Inter-Event Time to Separate Rainfall Events in a Low Latitude Semi-Arid Environment. *Sustainability*, *14*(3), 1721. https://www.mdpi.com/2071-1050/14/3/1721

Breen, P., & Anderies, J. M. (2011). Resilience: A literature review.

Brief, C. (2021). Mapped: How climate change affects extreme weather around the world. *Carbon Brief, 21*.

Briones, C., Gibert, J., Banda, M., & Moctezuma, A. (2020). An integrated urban flood vulnerability index for sustainable planning in arid zones of developing countries. *Water*, *12*(2), 608.

Brody, S. D., Kang, J. E., & Bernhardt, S. (2010). Identifying factors influencing flood mitigation at the local level in Texas and Florida: The role of organizational capacity. *Natural Hazards*, *52*, 167-184.

Brown, S., & Dawson, R. (2016). Building network-level resilience to resource disruption from flooding: Case studies from the Shetland Islands and Hurricane Sandy. E3S Web of Conferences,

Brunner, M. I., Slater, L., Tallaksen, L. M., & Clark, M. (2021). Challenges in modeling and predicting floods and droughts: A review. *Wiley Interdisciplinary Reviews: Water*, *8*(3), e1520.

Bukvic, A., Borate, A., Hughes, S., Weaver, R., Imburgia, D., & Stiles Jr, W. A. (2021). Exploring neighborhood-level resilience to flooding: Why the context and scale matter. *Journal of Flood Risk Management*, *14*(2), e12698.

Bulti, D. T., & Abebe, B. G. (2020). Analyzing the impacts of urbanization on runoff characteristics in Adama city, Ethiopia. *SN Appl. Sci.*, *2*. https://doi.org/https://doi.org/10.1007/s42452-020-2961-3

Bulti, D. T., Abebe, B. G., & Biru, Z. (2021a). Analysis of the changes in historical and future extreme precipitation under climate change in Adama city, Ethiopia. *Modeling earth systems and environment*, *7*, 2575-2587.

Bulti, D. T., Abebe, B. G., & Biru, Z. (2021b). Climate change–induced variations in future extreme precipitation intensity–duration–frequency in flood-prone city of Adama, central Ethiopia. *Environmental Monitoring and Assessment*, *193*, 1-14.

Bulti, D. T., & Assefa, T. (2019). Analyzing ecological footprint of residential building construction in Adama City, Ethiopia. *Environmental Systems Research*, *8*, 1-15.

Bulti, D. T., Mekonnen, B., & Bekele, M. (2017). Assessment of Adama city flood risk using multicriteria approach. *The Ethiopian Journal of Science and Sustainable Development (EJSSD)*, *4*(1), 6-23.

Cabrera, J. S., & Lee, H. S. (2018). Impacts of climate change on flood-prone areas in Davao Oriental, Philippines. *Water*, *10*(7), 893.

Cantis, P., Olivotto, V., Grabowski, Z., & McPhearson, T. (2020). Shifting landscapes of coastal flood risk: environmental (in) justice of urban change, sea level rise, and differential vulnerability in New York City. *Urban transformations*, *2*(1), 1-28.

Cao, W., Yang, Y., Huang, J., Sun, D., & Liu, G. (2020). Influential Factors Affecting Protective Coping Behaviors of Flood Disaster: A Case Study in Shenzhen, China. *International Journal of Environmental Research and Public Health*, *17*(16), 5945.

Cea, L., & Costabile, P. (2022). Flood Risk in Urban Areas: Modelling, Management and Adaptation to Climate Change. A Review. *Hydrology*, *9*(3), 50. https://www.mdpi.com/2306-5338/9/3/50

Çetinkaya, C., Özceylan, E., Erbaş, M., & Kabak, M. (2016). GIS-based fuzzy MCDA approach for siting refugee camp: A case study for southeastern Turkey. *International Journal of Disaster Risk Reduction*, *18*, 218-231.

Chagas, V. B., Chaffe, P. L., & Blöschl, G. (2022). Climate and land management accelerate the Brazilian water cycle. *Nature communications*, *13*(1), 5136.

Chakraborty, S., & Mukhopadhyay, S. (2019). Assessing flood risk using analytical hierarchy process (AHP) and geographical information system (GIS): application in Coochbehar district of West Bengal, India. *Natural Hazards*, *99*, 247-274.

Chan, F. K. S., Griffiths, J. A., Higgitt, D., Xu, S., Zhu, F., Tang, Y.-T., Xu, Y., & Thorne, C. R. (2018). "Sponge City" in China—a breakthrough of planning and flood risk management in the urban context. *Land use policy*, *76*, 772-778.

Chan, N. W., Ghani, A. A., Samat, N., Hasan, N. N. N., & Tan, M. L. (2020). Integrating structural and non-structural flood management measures for greater effectiveness in flood loss reduction in the Kelantan River basin, Malaysia. Proceedings of AICCE'19: Transforming the Nation for a Sustainable Tomorrow 4,

Chan, S. W., Abid, S. K., Sulaiman, N., Nazir, U., & Azam, K. (2022). A systematic review of the flood vulnerability using geographic information system. *Heliyon*.

Chang, H., & Franczyk, J. (2008). Climate change, land-use change, and floods: Toward an integrated assessment. *Geography Compass*, *2*(5), 1549-1579.

Chang, H., Pallathadka, A., Sauer, J., Grimm, N. B., Zimmerman, R., Cheng, C., Iwaniec, D. M., Kim, Y., Lloyd, R., & McPhearson, T. (2021). Assessment of urban flood vulnerability using the social-ecological-technological systems framework in six US cities. *Sustainable Cities and Society*, *68*, 102786.

Chen, J., Li, Y., & Zhang, S. (2023). Impact of different design rainfall pattern peak factors on urban flooding. *Water*, *15*(13), 2468.

Chen, K.-F., & Leandro, J. (2019). A conceptual time-varying flood resilience index for urban areas: Munich city. *Water*, *11*(4), 830.

Chen, W., Wu, H., Kimball, J. S., Alfieri, L., Nanding, N., Li, X., Jiang, L., Wu, W., Tao, Y., & Zhao, S. (2022). A Coupled River Basin-Urban Hydrological Model (DRIVE-Urban) for Real-Time Urban Flood Modeling. *Water resources research*, *58*(11), e2021WR031709.

Chiara, T., Francesca, S., and , & Marco, P. (2015). Mapping Flood Vulnerability. *GIM International*.

Choubin, B., Moradi, E., Golshan, M., Adamowski, J., Sajedi-Hosseini, F., & Mosavi, A. (2019). An ensemble prediction of flood susceptibility using multivariate discriminant analysis, classification and regression trees, and support vector machines. *Science of the Total Environment*, *651*, 2087-2096.

Chow, V. T., Maidment, D. R., & Larry, W. (2019). Mays. 1988. Applied Hydrology. *International edition, MacGraw-Hill, Inc, USA*, *149*.

Cian, F., Marconcini, M., & Ceccato, P. (2018). Normalized Difference Flood Index for rapid flood mapping: Taking advantage of EO big data. *Remote Sensing of Environment*, *209*, 712-730.

Coeur, D., & Lang, M. (2008). Use of documentary sources on past flood events for flood risk management and land planning. *Comptes Rendus Geoscience*, *340*(9-10), 644-650.

Cortinovis, C., Olsson, P., Boke-Olén, N., & Hedlund, K. (2022). Scaling up nature-based solutions for climate-change adaptation: Potential and benefits in three European cities. *Urban Forestry & Urban Greening*, *67*, 127450.

Courty, L. G., Wilby, R. L., Hillier, J. K., & Slater, L. J. (2019). Intensity-duration-frequency curves at the global scale. *Environmental research letters*, *14*(8), 084045.

Craig, H., Paulik, R., Djanibekov, U., Walsh, P., Wild, A., & Popovich, B. (2021). Quantifying national-scale changes in agricultural land exposure to fluvial flooding. *Sustainability*, *13*(22), 12495.

Cutter, S. L., Boruff, B. J., & Shirley, W. L. (2003). Social vulnerability to environmental hazards. *Social science quarterly*, *84*(2), 242-261.

D'Ambrosio, E., De Girolamo, A. M., Spanò, M., Corbelli, V., Capasso, G., Morea, M., Velardo, R., Abdelwahab, O. M., Lonigro, A., & Milillo, F. (2019). A spatial analysis to define data requirements for hydrological and water quality models in data-limited regions. *Water*, *11*(2), 267.

Daksiya, V., Mandapaka, P. V., & Lo, E. Y. (2021). Effect of climate change and urbanisation on flood protection decision-making. *Journal of Flood Risk Management*, *14*(1), e12681.

Danáčová, M., Földes, G., Labat, M. M., Kohnová, S., & Hlavčová, K. (2020). Estimating the Effect of Deforestation on Runoff in Small Mountainous Basins in Slovakia. *Water*, *12*(11), 3113. https://www.mdpi.com/2073-4441/12/11/3113

Das, S., & Gupta, A. (2021). Multi-criteria decision based geospatial mapping of flood susceptibility and temporal hydro-geomorphic changes in the Subarnarekha basin, India. *Geoscience Frontiers*, *12*(5), 101206.

De Brito, M. M., Evers, M., & Almoradie, A. D. S. (2018). Participatory flood vulnerability assessment: a multi-criteria approach. *Hydrology and Earth System Sciences*, *22*(1), 373-390.

de Bruijn, K. M., Jafino, B. A., Merz, B., Doorn, N., Priest, S. J., Dahm, R. J., Zevenbergen, C., Aerts, J. C., & Comes, T. (2022). Flood risk management through a resilience lens. *Communications Earth & Environment*, *3*(1), 285.

Deepak, S., Rajan, G., & Jairaj, P. (2020). Geospatial approach for assessment of vulnerability to flood in local self governments. *Geoenvironmental Disasters*, *7*, 1-19.

Dehkordi, M., Haddad, O., Salavitabar, A., Azari, S., & Goharian, E. (2021). Development of flood mitigation strategies toward sustainable development. *Natural Hazards*, *108*(3), 2543-2567.

Delgado, D., Palacios, C. R., Vidales, A. A., & Siller, M. (2023). Possible Scenarios for a Micro-Watershed Based on Level of Urbanization: Using Flood Design to Advance Ecohydrological Principles. *Urban Science*, *7*(1), 24. https://www.mdpi.com/2413-8851/7/1/24

Denchak, M. (2019). Flooding and climate change: Everything you need to know. *Natural Resources Defense Council*.

Der Sarkissian, R., Al Sayah, M. J., Abdallah, C., Zaninetti, J. M., & Nedjai, R. (2022). Land Use Planning to Reduce Flood Risk: Opportunities, Challenges and Uncertainties in Developing Countries. *Sensors (Basel)*, *22*(18). https://doi.org/10.3390/s22186957

Deria, A., Ghannad, P., & Lee, Y.-C. (2020). Evaluating implications of flood vulnerability factors with respect to income levels for building long-term disaster resilience of low-income communities. *International Journal of Disaster Risk Reduction*, *48*, 101608.

Desalegn, H., & Mulu, A. (2021). Flood vulnerability assessment using GIS at Fetam watershed, upper Abbay basin, Ethiopia. *Heliyon*, *7*(1), e05865.

Dessie, Z. G., Zewotir, T., & North, D. (2022). The spatial modification effect of predictors on household level food insecurity in Ethiopia. *Scientific reports*, *12*(1), 19353.

Dewan, T. H. (2015). Societal impacts and vulnerability to floods in Bangladesh and Nepal. *Weather and Climate Extremes*, *7*, 36-42.

Do, S., & Besnier, J. (2023). InVEST Urban Development: Incorporating Earth Observation Data into the Integrated Valuation of Ecosystem Services and Tradeoffs (InVEST) Urban Flood Risk Mitigation Model Python API. NASA DEVELOP Closeout,

Domeneghetti, A., Schumann, G. J.-P., & Tarpanelli, A. (2019). Preface: remote sensing for flood mapping and monitoring of flood dynamics. In (Vol. 11, pp. 943): MDPI.

Dong, S., Gao, X., Mostafavi, A., & Gao, J. (2022). Modest flooding can trigger catastrophic road network collapse due to compound failure. *Communications Earth & Environment*, *3*(1), 38.

Dragičević, N., Karleuša, B., & Ožanić, N. (2019). Different approaches to estimation of drainage density and their effect on the erosion potential method. *Water*, *11*(3), 593.

Duc, T. V. (2013). Which coastal cities are at highest risk of damaging floods? New study crunches the numbers. *World Bank (Access 01/15/2020)*.

Dumedah, G., Andam-Akorful, S. A., Ampofo, S. T., & Abugri, I. (2021). Characterizing urban morphology types for surface runoff estimation in the Oforikrom Municipality of Ghana. *Journal of Hydrology: Regional Studies*, *34*, 100796.

Edamo, M. L., Bushira, K., & Ukumo, T. Y. (2022). Flood susceptibility mapping in the Bilate catchment, Ethiopia. *H2Open Journal*, *5*(4), 691-712.

Eisenberg, B., Lindow, K. C., & Smith, D. R. (2015). Permeable pavements.

Eldho, T., Zope, P., & Kulkarni, A. (2018). Urban flood management in coastal regions using numerical simulation and geographic information system. In *Integrating disaster science and management* (pp. 205-219). Elsevier.

Elkhrachy, I. (2015). Flash flood hazard mapping using satellite images and GIS tools: a case study of Najran City, Kingdom of Saudi Arabia (KSA). *The Egyptian Journal of Remote Sensing and Space Science*, *18*(2), 261-278.

Elum, Z. A., & Lawal, O. (2022). Flood risk perception, disaster preparedness and response in flood-prone urban communities of Rivers State. *Jamba*, *14*(1), 1303. https://doi.org/10.4102/jamba.v14i1.1303

EM-DAT. (2015). *The human cost of weather-related disasters, 1995–2015. Centre for Research on the*

Epidemiology of Disasters, UN Office for Disaster Risk Reduction (UNODRR), Brussels.

Erena, S. H., & Worku, H. (2018). Flood risk analysis: causes and landscape based mitigation strategies in Dire Dawa city, Ethiopia. *Geoenviron Disasters*, *5*(16). https://doi.org/https://doi.org/10.1186/s40677-018-0110-8

Erena, S. H., & Worku, H. (2019). Urban flood vulnerability assessments: the case of Dire Dawa city, Ethiopia. *Natural Hazards*, *97*, 495-516.

Erena, S. H., Worku, H., & De Paola, F. (2018). Flood hazard mapping using FLO-2D and local management strategies of Dire Dawa city, Ethiopia. *Journal of Hydrology: Regional Studies*, *19*, 224-239.

Eric, T., Md Asif, R., Christopher T. , E., & Christopher C. , S. (2021). Flood exposure and social vulnerability in the United States. https://doi.org/https://doi.org/10.1007/s11069-020-04470-2

Ermagun, A., Smith, V., & Janatabadi, F. (2024). High urban flood risk and no shelter access disproportionally impacts vulnerable communities in the USA. *Communications Earth & Environment*, *5*(1), 2.

Ethiopian Roads Authority, E. (2013). *Drainage Design Manual*.

Farahmand, H., Dong, S., & Mostafavi, A. (2021). Network analysis and characterization of vulnerability in flood control infrastructure for system-level risk reduction. *Computers, Environment and Urban Systems*, *89*, 101663.

Farhadi, H., & Najafzadeh, M. (2021). Flood Risk Mapping by Remote Sensing Data and Random Forest Technique. *Water*, *13*(21), 3115. https://www.mdpi.com/2073-4441/13/21/3115

Fekete, A., & Sandholz, S. (2021). Here comes the flood, but not failure? Lessons to learn after the heavy rain and pluvial floods in Germany 2021. *Water*, *13*(21), 3016.

Feng, B., Zhang, Y., & Bourke, R. (2021). Urbanization impacts on flood risks based on urban growth data and coupled flood models. *Natural Hazards, 106*, 613-627.

Fenglin, W., Ahmad, I., Zelenakova, M., Fenta, A., Dar, M. A., Teka, A. H., Belew, A. Z., Damtie, M., Berhan, M., & Shafi, S. N. (2023). Exploratory regression modeling for flood susceptibility mapping in the GIS environment. *Scientific reports*, *13*(1), 247.

Ferreira, Kalantari, Aghmiuni, Ghajarnia, Rahmati, & Solomun. (2021). Rainfall-runoff-erosion processes in urban areas. In *Precipitation* (pp. 481-498). Elsevier.

Ferreira , Potočki , Solomun , & Kalantari (2021). Nature-based solutions for flood mitigation and resilience in urban areas. In *Nature-Based Solutions for Flood Mitigation: Environmental and Socio-Economic Aspects* (pp. 59-78). Springer.

Fischer, C., & Stanchev, P. (2022). Flood hazard and risk maps: A key instrument for flood risk management. *The Water Blog. Retrived from: https://blogs. worldbank. org/water/flood*.

Fitriyati, N., Arifin, H., & Kaswanto, R. (2022). Flood resiliency approach for urban planning: critical review and future research agenda. IOP Conference Series: Earth and Environmental Science,

Forkuo, E. K. (2011). Flood hazard mapping using Aster image data with GIS. *International journal of Geomatics and Geosciences*, *1*(4), 932-950.

Foster, S., Leichenko, R., Nguyen, K. H., Blake, R., Kunreuther, H., Madajewicz, M., Petkova, E. P., Zimmerman, R., Corbin-Mark, C., & Yeampierre, E. (2019). New York City panel on climate change 2019 report chapter 6: community-based assessments of adaptation and equity. *Annals of the New York Academy of Sciences*, *1439*(1), 126-173.

Freni, G., La Loggia, G., & Notaro, V. (2010). Uncertainty in urban flood damage assessment due to urban drainage modelling and depth-damage curve estimation. *Water Science and Technology*, *61*(12), 2979-2993.

Gambini, J. M., & Laymito, J. A. (2019). Multiparametric ahp-based flood hazard zonation approach in northwestern Peru at basin scale. E-Proceedings of the 38th IAHR World Congress,

Gangwal, U., Siders, A., Horney, J., Michael, H. A., & Dong, S. (2023). Critical facility accessibility and road criticality assessment considering flood-induced partial failure. *Sustainable and Resilient Infrastructure*, *8*(sup1), 337-355.

Gao, J., Zhang, X., Duan, J., & Tao, C. Risk Assessment for Infrastructure Vulnerable to Flood Hazards in the Great Lake Region. In *ASCE Inspire 2023* (pp. 418-425).

Gao, M., Wang, Z., & Yang, H. (2022). Review of Urban Flood Resilience: Insights from Scientometric and Systematic Analysis. *International Journal of Environmental Research and Public Health*, *19*(14), 8837. https://www.mdpi.com/1660-4601/19/14/8837

Gashaw, W., & Legesse, D. (2011). Flood hazard and risk assessment using GIS and remote sensing in Fogera Woreda, Northwest Ethiopia. *Nile River Basin: Hydrology, Climate and Water Use*, 179-206.

Gauthier, P., & Gilliland, J. (2006). Mapping urban morphology: a classification scheme for interpreting contributions to the study of urban form. *Urban morphology*, *10*(1), 41.

GFDRR, T. G. F. f. D. R. a. R. (2019). *Disaster Profile of Ethiopia*.

Ghosh, A., & Kar, S. K. (2018). Application of analytical hierarchy process (AHP) for flood risk assessment: a case study in Malda district of West Bengal, India. *Natural Hazards*, *94*, 349-368.

Gomariz, E., Locatelli, L., Guerrero, M., Russo, B., & Martínez, M. (2019). Socio-economic potential impacts due to urban pluvial floods in Badalona (Spain) in a context of climate change. *Water*, *11*(12), 2658.

Gomez, J., Nyabigambo, A., Rudd, A., Ssentongo, J., Kiconco, A., & Mayega, R. W. (2023). Water, Sanitation, and Hygiene Challenges in Informal Settlements in Kampala, Uganda: A Qualitative Study. *International Journal of Environmental Research and Public Health*, *20*(12), 6181.

Gori, A., Blessing, R., Juan, A., Brody, S., & Bedient, P. (2019). Characterizing urbanization impacts on floodplain through integrated land use, hydrologic, and hydraulic modeling. *Journal of hydrology*, *568*, 82-95.

Graf, R. (2020). Extreme hydrology and climate variability, monitoring, modelling, adaptation and mitigation, by A. Melesse, W. Abtew & G. Senay (Eds.), 2019. Elsevier Inc., Amsterdam. 580 pages. Paperback: price $170.00, ISBN 9780128159989. *Geologos*, *26*(2), 171-173.

Grecu, F., Zaharia, L., Ioana-Toroimac, G., & Armaș, I. (2017). Floods and flash-floods related to river channel dynamics. *Landform dynamics and evolution in Romania*, 821-844.

Gründemann, G. J., Zorzetto, E., Beck, H. E., Schleiss, M., Van de Giesen, N., Marani, M., & van der Ent, R. J. (2023). Extreme precipitation return levels for multiple durations on a global scale. *Journal of hydrology*, *621*, 129558.

Güneralp, B., Lwasa, S., Masundire, H., Parnell, S., & Seto, K. C. (2017). Urbanization in Africa: challenges and opportunities for conservation. *Environmental research letters*, *13*(1), 015002.

Guo, Y. (2006). Updating rainfall IDF relationships to maintain urban drainage design standards. *Journal of Hydrologic Engineering*, *11*(5), 506-509.

Gwenzi, W., & Nyamadzawo, G. (2014). Hydrological impacts of urbanization and urban roof water harvesting in water-limited catchments: a review. *Environmental Processes*, *1*, 573-593.

Hagos, Y., Andualem, T., Yibeltal, M., & Mengie, M. (2022). Flood hazard assessment and mapping using GIS integrated with multi-criteria decision analysis in upper Awash River basin, Ethiopia. *Applied Water Science*, *12*(7), 148.

Hagos;, Y., Andualem;, T., Yibeltal;, M., & Mengie, M. (2022). Flood hazard assessment and mapping using GIS integrated with multi-criteria decision analysis in upper Awash River basin, Ethiopia. *Applied Water Science*, *12*(7), 148.

Haltas, I., Yildirim, E., Oztas, F., & Demir, I. (2021). A comprehensive flood event specification and inventory: 1930–2020 Turkey case study. *International Journal of Disaster Risk Reduction*, *56*, 102086.

Hamaamin, Y. A. (2017). Developing of rainfall intensity-duration-frequency model for Sulaimani city. *Journal of Zankoy Sulaimani*, *19*(3-4), p10634.

Hamel, P., Guerry, A., Polasky, S., Han, B., Douglass, J., Hamann, M., Janke, B., Kuiper, J., Levrel, H., & Liu, H. (2021). Mapping the benefits of nature in cities with the InVEST software. *Npj Urban Sustainability*, *1*(1), 25.

Hamers, E. M., Maier, H. R., Zecchin, A. C., & van Delden, H. (2023). Effectiveness of Nature-Based Solutions for Mitigating the Impact of Pluvial Flooding in Urban Areas at the Regional Scale. *Water*, *15*(4), 642. https://www.mdpi.com/2073-4441/15/4/642

Hamidifar, H., & Nones, M. (2021). Global to regional overview of floods fatality: the 1951–2020 period. *Natural Hazards and Earth System Sciences Discussions*, *2021*, 1-22.

Hammond, M. J., Chen, A. S., Djordjević, S., Butler, D., & Mark, O. (2015). Urban flood impact assessment: A state-of-the-art review. *Urban Water Journal*, *12*(1), 14-29.

He, Y., Rentschler, J., Avner, P., Gao, J., Yue, X., & Radke, J. (2022). Mobility and Resilience.

He, Y., Thies, S., Avner, P., & Rentschler, J. (2021). Flood impacts on urban transit and accessibility—A case study of Kinshasa. *Transportation Research Part D: Transport and Environment*, *96*, 102889.

Hemmati, M., Ellingwood, B. R., & Mahmoud, H. N. (2020). The role of urban growth in resilience of communities under flood risk. *Earth's Future*, *8*(3), e2019EF001382.

Hemmati, M., Mahmoud, H. N., Ellingwood, B. R., & Crooks, A. T. (2021). Unraveling the complexity of human behavior and urbanization on community vulnerability to floods. *Scientific reports*, *11*(1), 20085.

Herslund, L., Lund, D. H., Jørgensen, G., Mguni, P., Kombe, W. J., & Yeshitela, K. (2015). Towards climate change resilient cities in Africa–Initiating adaptation in Dar es Salaam and Addis Ababa. *Urban vulnerability and climate change in Africa: a multidisciplinary approach*, 319-348.

Hirabayashi, Y., Mahendran, R., Koirala, S., Konoshima, L., Yamazaki, D., Watanabe, S., Kim, H., & Kanae, S. (2013). Global flood risk under climate change. *Nature Climate Change*, *3*(9), 816-821.

Holling, C. S. (1973). Resilience and stability of ecological systems. *Annual review of ecology and systematics*, *4*(1), 1-23.

Hong, H., Panahi, M., Shirzadi, A., Ma, T., Liu, J., Zhu, A.-X., Chen, W., Kougias, I., & Kazakis, N. (2018). Flood susceptibility assessment in Hengfeng area coupling adaptive neuro-fuzzy inference system with genetic algorithm and differential evolution. *Science of the Total Environment*, *621*, 1124-1141.

Hoque, M. A.-A., Tasfia, S., Ahmed, N., & Pradhan, B. (2019). Assessing spatial flood vulnerability at Kalapara Upazila in Bangladesh using an analytic hierarchy process. *Sensors*, *19*(6), 1302.

Hou, X., Chen, L., Liu, X., Li, M., & Shen, Z. (2019). Parameter transferability across spatial resolutions in urban hydrological modelling: a case study in Beijing, China. *Frontiers of Earth Science*, *13*, 18-32.

Huidobro, Maria Dabrowski, Marcin Tai, Yuting Chan, & Faith Stead, D. (2017). Governance challenges of flood-prone delta cities: Integrating flood risk management and climate change in spatial planning. *Progress in planning*, *114*, 1-27.

Hussain, M., Tayyab, M., Zhang, J., Shah, A. A., Ullah, K., Mehmood, U., & Al-Shaibah, B. (2021). GIS-based multi-criteria approach for flood vulnerability assessment and mapping in district Shangla: Khyber Pakhtunkhwa, Pakistan. *Sustainability*, *13*(6), 3126.

Iffland, R., Förster, K., Westerholt, D., Pesci, M. H., & Lösken, G. (2021). Robust vegetation parameterization for green roofs in the EPA stormwater management model (SWMM). *Hydrology*, *8*(1), 12.

Iliadis, C., Galiatsatou, P., Glenis, V., Prinos, P., & Kilsby, C. (2023). Urban Flood Modelling under Extreme Rainfall Conditions for Building-Level Flood Exposure Analysis. *Hydrology*, *10*(8), 172.

Isia, I., Hadibarata, T., Hapsari, R. I., Jusoh, M. N. H., Bhattacharjya, R. K., & Shahedan, N. F. (2023). Assessing social vulnerability to flood hazards: a case study of Sarawak's divisions. *International Journal of Disaster Risk Reduction*, *97*, 104052.

Janicka, E., & Kanclerz, J. (2023). Assessing the Effects of Urbanization on Water Flow and Flood Events Using the HEC-HMS Model in the Wirynka River Catchment, Poland. *Water*, *15*(1), 86. https://www.mdpi.com/2073-4441/15/1/86

Jemberie, M. A., & Melesse, A. M. (2021). Urban Flood Management through Urban Land Use Optimization Using LID Techniques, City of Addis Ababa, Ethiopia. *Water*, *13*(13), 1721. https://www.mdpi.com/2073-4441/13/13/1721

Jensen, O., & Khalis, A. (2020). Urban water systems: Development of micro-level indicators to support integrated policy. *PLoS One*, *15*(2), e0228295.

Jiang, Y., Zevenbergen, C., & Ma, Y. (2018). Urban pluvial flooding and stormwater management: A contemporary review of China's challenges and "sponge cities" strategy. *Environmental Science & Policy*, *80*, 132-143.

Jiménez, E., Bodoque, J. M., García, J. A., & Díez-Herrero, A. (2018). A quantitative methodology for the assessment of the regional economic vulnerability to flash floods. *Journal of hydrology*, *565*, 386-399.

Jongman, B., Winsemius, H. C., Aerts, J. C., Coughlan de Perez, E., Van Aalst, M. K., Kron, W., & Ward, P. J. (2015). Declining vulnerability to river floods and the global benefits of adaptation. *Proceedings of the National Academy of Sciences*, *112*(18), E2271-E2280.

Joo, J., Lee, J., Kim, J. H., Jun, H., & Jo, D. (2013). Inter-event time definition setting procedure for urban drainage systems. *Water*, *6*(1), 45-58.

Kadaverugu, A., Gorthi, K. V., & Chintala, N. R. (2021). Impacts of urban floods on road connectivity-a review and systematic bibliometric analysis. *Current World Environment*, *16*(2), 575.

Kadaverugu, A., Kadaverugu, R., Chintala, N. R., & Gorthi, K. V. (2022). Flood vulnerability assessment of urban micro-watersheds using multi-criteria decision making and InVEST model: a case of Hyderabad City, India. *Modeling earth systems and environment*, *8*(3), 3447-3459.

Kadaverugu , A., Nageshwar Rao , C., & Viswanadh , G. (2021). Quantification of flood mitigation services by urban green spaces using InVEST model: a case study of Hyderabad city, India. *Modeling earth systems and environment*, *7*(1), 589-602.

Kadaverugu;, A., Nageshwar;, R. C., & Viswanadh;, G. (2021). Quantification of flood mitigation services by urban green spaces using InVEST model: a case study of Hyderabad city, India. *Modeling earth systems and environment*, *7*(1), 589-602.

Kalédjé, P. S. K., Ngoupayou, J.-R. N., Takounjou, A. F., Zebsa, M., Rakotondrabe, F., & Ondoa, J. M. (2019). Floods of 18 and 19 November 2016 in Batouri (East Cameroon): interpretation of the hydro-meteorological parameters and historical context of the post-event survey episode. *The Scientific World Journal*, *2019*.

Kang, S.-J., Lee, S.-J., & Lee, K.-H. (2009). A study on the implementation of non-structural measures to reduce urban flood damage-Focused on the survey results of the experts. *Journal of Asian architecture and building engineering*, *8*(2), 385-392.

Kang, S., Yin, J., Gu, L., Yang, Y., Liu, D., & Slater, L. (2023). Observation-Constrained Projection of Flood Risks and Socioeconomic Exposure in China. *Earth's Future*, *11*(7), e2022EF003308.

Karley, N. K. (2009). Flooding and physical planning in urban areas in West Africa: Situational analysis of Accra, Ghana. *Theoretical and Empirical Researches in Urban Management*, *4*(4 (13), 25-41.

Kashyap, S., & Mahanta, R. (2021). Socioeconomic Vulnerability to Urban Floods in Guwahati, Northeast India: An Indicator-Based Approach. In *Economic Effects of Natural Disasters* (pp. 457-475). Elsevier.

Kaspersen, P., Fensholt, R., & Drews, M. (2015). Using Landsat vegetation indices to estimate impervious surface fractions for European cities. *Remote Sensing*, *7*(6), 8224-8249.

Khajehei, S., Ahmadalipour, A., Shao, W., & Moradkhani, H. (2020). A place-based assessment of flash flood hazard and vulnerability in the contiguous United States. *Scientific reports*, *10*(1), 448.

Khan, I., Lei, H., Shah, A. A., Khan, I., & Muhammad, I. (2021). Climate change impact assessment, flood management, and mitigation strategies in Pakistan for sustainable future. *Environmental Science and Pollution Research*, *28*, 29720-29731.

Khodadad, M., Aguilar-Barajas, I., & Khan, A. Z. (2023). Green Infrastructure for Urban Flood Resilience: A Review of Recent Literature on Bibliometrics, Methodologies, and Typologies. *Water*, *15*(3), 523.

Khosravi, K., Nohani, E., Maroufinia, E., & Pourghasemi, H. R. (2016). A GIS-based flood susceptibility assessment and its mapping in Iran: a comparison between frequency ratio and weights-of-evidence bivariate statistical models with multi-criteria decision-making technique. *Natural Hazards*, *83*, 947-987.

Kia, M. B., Pirasteh, S., Pradhan, B., Mahmud, A. R., Sulaiman, W. N. A., & Moradi, A. (2012). An artificial neural network model for flood simulation using GIS: Johor River Basin, Malaysia. *Environmental Earth Sciences*, *67*, 251-264.

Kibria, S., & Biswas, R. (2019). Design Of Stormwater Drainage Network With Limited Rainfall Data Using GeoSWMM: Case Study For Dinajpur City.

Proceedings on International Conference on Disaster Risk Management, Dhaka, Bangladesh,

Kim, Y., Carvalhaes, T., Helmrich, A., Markolf, S., Hoff, R., Chester, M., Li, R., & Ahmad, N. (2022). Leveraging SETS resilience capabilities for safe-to-fail infrastructure under climate change. *Current Opinion in Environmental Sustainability*, *54*, 101153.

Kim, Y., Mannetti, L. M., Iwaniec, D. M., Grimm, N. B., Berbés-Blázquez, M., & Markolf, S. (2021). Social, ecological, and technological strategies for climate adaptation. *Resilient urban futures*, 29-45.

Kim, Y. D., Tak, Y. H., Park, M. H., & Kang, B. (2019). Improvement of urban flood damage estimation using a high-resolution digital terrain. *flood risk Management 13*(S1). https://doi.org/https://doi.org/10.1111/jfr3.12575

Konrad, C. P. (2003). Effects of urban development on floods. In: US Geological Survey Tacoma.

Konrad, C. P., & Booth, D. B. (2005). Hydrologic changes in urban streams and their ecological significance. American Fisheries Society Symposium,

Kovacs, Y., Doussin, N., Gaussens, M., Pacoud, C. L., & Afd, O. (2017). Flood risk and cities in developing countries. *French Development Agency: Paris, France*.

Kramer, R., Sharp, R., Weil, C., Bennett, E., Pascual, U., Arkema, K., Brauman, K., Bryant, B., Guerry, A., & Haddad, N. (2019). Global modeling of nature's contributions to people. *Science*, *366*(6462), 255-258.

Kreibich, H., Bubeck, P., Van Vliet, M., & De Moel, H. (2015). A review of damage-reducing measures to manage fluvial flood risks in a changing climate. *Mitigation and adaptation strategies for global change*, *20*, 967-989.

Kropf, K. (2009). Aspects of urban form. *Urban morphology*, *13*(2), 105-120.

Krueger, E. H., Constantino, S. M., Centeno, M. A., Elmqvist, T., Weber, E. U., & Levin, S. A. (2022). Governing sustainable transformations of urban social-ecological-technological systems. *Npj Urban Sustainability*, *2*(1), 10.

Kuang, D. (2020). *Learning from Floods: Understanding the Relationship between Flood Experience and Flood Resilience*. The Chinese University of Hong Kong (Hong Kong).

Kumar, V., Sharma, K. V., Caloiero, T., Mehta, D. J., & Singh, K. (2023). Comprehensive Overview of Flood Modeling Approaches: A Review of Recent Advances. *Hydrology*, *10*(7), 141. https://www.mdpi.com/2306-5338/10/7/141

Kumar;, D., Gopinath;, P., & Seralathan, G. (2007). Application of remote sensing and GIS for the demarcation of groundwater potential zones of a river basin in Kerala, southwest coast of India. *International Journal of Remote Sensing*, *28*(24), 5583-5601.

Lapointe, M., Rochman, C. M., & Tufenkji, N. (2022). Sustainable strategies to treat urban runoff needed. *Nature Sustainability*, *5*(5), 366-369.

Lee, S., Choi, Y., Ji, J., Lee, E., Yi, S., & Yi, J. (2023). Flood Vulnerability Assessment of an Urban Area: A Case Study in Seoul, South Korea. *Water*, *15*(11), 1979. https://www.mdpi.com/2073-4441/15/11/1979

Lee, S., & Rezaie, F. (2022). Data used for GIS-based flood susceptibility mapping. *Data Geol Ecol Oceanogr Space Sci Polar Sci*, *41*, 1-15.

Legas, S. K. (2020). *Stabilization of Expansive Soil Using Cement Blended Pumice* Addis Ababa Science and Technology University Addis Ababa, Ethiopia].

Legese, B., Gumi, B., & Bule Hora, E. (2020). Flooding in Ethiopia; causes, impact, and coping mechanism a review. *Int J Res Anal Rev (IJRAR)*.

Leite, F. R., & Antunes, M. L. P. (2023). Green roof recent designs to runoff control: A review of building materials and plant species used in studies. *Ecological Engineering*, *189*. https://doi.org/https://doi.org/10.1016/j.ecoleng.2023.106924

Len, N. L. S., Bolong, N., Roslee, R., Tongkul, F., Mirasa, A. K., & Ayog, J. L. (2018). Flood vulnerability of critical infrastructures-review. *Malaysian Journal of Geosciences*, *2*(1), 31-34.

Leta, B. M., & Adugna, D. (2023a). Characterizing the level of urban Flood vulnerability using the social-ecological-technological systems framework, the case of Adama city, Ethiopia. *Heliyon*, *9*(10).

Leta, B. M., & Adugna, D. (2023b). Identification and mapping of flood-prone areas using GIS-based multi-criteria decision-making and analytical hierarchy process: the case of Adama City’s watershed, Ethiopia. *Applied Geomatics*, *15*(4), 933-955.

Li, L., & Jun, K. S. (2022). A Hybrid Approach to Improve Flood Forecasting by Combining a Hydrodynamic Flow Model and Artificial Neural Networks. *Water*, *14*(9), 1393. https://www.mdpi.com/2073-4441/14/9/1393

Li, L., Uyttenhove, P., & Van Eetvelde, V. (2020). Planning green infrastructure to mitigate urban surface water flooding risk–A methodology to identify priority areas applied in the city of Ghent. *Landscape and Urban Planning*, *194*, 103703.

Li, Z., Zhang, X., Ma, Y., Feng, C., & Hajiyev, A. (2019). A multi-criteria decision making method for urban flood resilience evaluation with hybrid uncertainties. *International Journal of Disaster Risk Reduction*, *36*, 101140.

Lihong, W., Shenghui, C., Yuanzheng, L., Hongjie, H., Bikram , M., Vilas, N., Xuejuan , F., & Wei, H. (2022). A review of the flood management: from flood control to flood resilience. *Heliyon*, *11*. https://doi.org/10.1016/j.heliyon.2022.e11763

Lim, J., Kim, K.-M., & Lee, K.-S. (2019). Does Deforestation Trigger Severe Flood Damage at Hoeryeong City in North Korea? *Forests*, *10*(9), 789. https://www.mdpi.com/1999-4907/10/9/789

Lin, L., Wu, Z., & Liang, Q. (2019). Urban flood susceptibility analysis using a GIS-based multi-criteria analysis framework. *Natural Hazards*, *97*, 455-475.

Liu, Y., & De Smedt, F. (2005). Flood modeling for complex terrain using GIS and remote sensed information. *Water resources management*, *19*, 605-624.

Louw, E., Olanrewaju, C. C., Olanrewaju, O. A., & Chitakira, M. (2019). Impacts of flood disasters in Nigeria: A critical evaluation of health implications and management. *Jàmbá: Journal of Disaster Risk Studies*, *11*(1), 1-9.

Mahdi, E. S., & Mohamedmeki, M. Z. (2020). Analysis of rainfall intensity-duration-frequency (IDF) curves of Baghdad city. IOP Conference Series: Materials Science and Engineering,

Mahmoud, S. H., & Gan, T. Y. (2018). Multi-criteria approach to develop flood susceptibility maps in arid regions of Middle East. *Journal of Cleaner Production*, *196*, 216-229.

Mamo, S., Berhanu, B., & Melesse, A. M. (2019). Historical flood events and hydrological extremes in Ethiopia. In *Extreme hydrology and climate variability* (pp. 379-384). Elsevier.

Manandhar, B., Cui, S., Wang, L., & Shrestha, S. (2023). Urban Flood Hazard Assessment and Management Practices in South Asia: A Review. *Land*, *12*(3), 627.

Manzoor, Z., Ehsan, M., Khan, M. B., Manzoor, A., Akhter, M. M., Sohail, M. T., Hussain, A., Shafi, A., Abu-Alam, T., & Abioui, M. (2022). Floods and flood management and its socio-economic impact on Pakistan: A review of the empirical literature. *Frontiers in environmental science*, *10*, 2480.

Marcus, L., & Colding, J. (2014). Toward an integrated theory of spatial morphology and resilient urban systems. *Ecology and Society*, *19*(4).

Martin, B., Ortega, E., Cuevas-Wizner, R., Ledda, A., & De Montis, A. (2021). Assessing road network resilience: An accessibility comparative analysis. *Transportation Research Part D: Transport and Environment*, *95*, 102851.

Martina, Z., Daniel, C. D., & Ketil, H. (2017). Urban Water Retention Measures. *Procedia Engineering*, *190*, 419 – 426. https://doi.org/https://doi.org/10.1016/j.proeng.2017.05.358

Martinez, & Labib. (2023). Demystifying normalized difference vegetation index (NDVI) for greenness exposure assessments and policy interventions in urban greening. *Environmental Research*, *220*, 115155.

Masha, M., Belayneh, M., & Tedila, G. (2023). Assessment of land use land cover dynamics and its contributing factors in Adama district, central Ethiopia. *EQA-International Journal of Environmental Quality*, *55*, 42-54.

Matanó, A., de Ruiter, M. C., Koehler, J., Ward, P. J., & Van Loon, A. F. (2022). Caught Between Extremes: Understanding Human-Water Interactions During Drought-To-Flood Events in the Horn of Africa. *Earth's Future*, *10*(9), e2022EF002747.

Maulana, S., & Nordin, J. (2019). Flood Disaster Risk Assessment In Urban Morphology Framework To Enhance Resilience Factor. *European Proceedings of Multidisciplinary Sciences*.

McClymont, K., Morrison, D., Beevers, L., & Carmen, E. (2020). Flood resilience: a systematic review. *Journal of Environmental Planning and Management*, *63*(7), 1151-1176.

McDermott, T. K. (2022). Global exposure to flood risk and poverty. *Nature communications*, *13*(1), 3529.

McPhearson, T., Cook, E. M., Berbes-Blazquez, M., Cheng, C., Grimm, N. B., Andersson, E., Barbosa, O., Chandler, D. G., Chang, H., & Chester, M. V. (2022). A social-ecological-technological systems framework for urban ecosystem services. *One Earth*, *5*(5), 505-518.

Mekuria, T. (2022). The effects of Flooding and Drought on Clean Water Accesibility in Ethiopia. *Hydraulic Engineering Repository: Karlsruhe, Germany*.

Meng, M., Dąbrowski, M., Xiong, L., & Stead, D. (2022). Spatial planning in the face of flood risk: Between inertia and transition. *Cities*, *126*, 103702.

Meraj, G., Romshoo, S. A., Yousuf, A., Altaf, S., & Altaf, F. (2015). Assessing the influence of watershed characteristics on the flood vulnerability of Jhelum basin in Kashmir Himalaya: reply to comment by Shah 2015. *Natural Hazards*, *78*, 1-5.

Merz, B., H. Kreibich, R. Schwarze, & Thieken, A. (2010). Assessment of economic flood damage. *Natural Hazards and Earth System Sciences*, *10*, 1697–1724. https://doi.org/https://doi.org/10.17226/25381

Migosi, P. (2014). Effects of urban storm water management strategy in reducing flooding; a case of Mombasa. *Int. J. Manag. Stud. Res*, *2*(4), 82-90.

Miller, J. D., & Hutchins, M. (2017). The impacts of urbanisation and climate change on urban flooding and urban water quality: A review of the evidence concerning the United Kingdom. *Journal of Hydrology: Regional Studies*, *12*, 345-362.

Minea, G., & Zaharia, L. (2011). Structural and Non-Structural Measures for Flood Risk Mitigation in the Bâsca River Catchment (Romania. Forum geografic,

Minucci, G., Molinari, D., Gemini, G., & Pezzoli, S. (2020). Enhancing flood risk maps by a participatory and collaborative design process. *International Journal of Disaster Risk Reduction*, *50*, 101747.

Mohammadtaghi, A., Majid, K., & Bagher, G. (2023). Comprehensive assessment of resilience of flood hazard villages using a modeling and field survey approach. *International Journal of Disaster Risk Reduction 96*. https://doi.org/https://doi.org/10.1016/j.ijdrr.2023.103910

Mohanty, M. P., & Simonovic, S. P. (2022). A Comprehensive Approach for Floodplain Mapping through Identification of Hazard Using Publicly Available Data Sets over Canada. *Water*, *14*(14), 2280.

Mojaddadi, H., Pradhan, B., Nampak, H., Ahmad, N., & Ghazali, A. H. b. (2017). Ensemble machine-learning-based geospatial approach for flood risk assessment using multi-sensor remote-sensing data and GIS. *Geomatics, Natural Hazards and Risk*, *8*(2), 1080-1102.

Moore, I. D., Grayson, R., & Ladson, A. (1991). Digital terrain modelling: a review of hydrological, geomorphological, and biological applications. *Hydrological processes*, *5*(1), 3-30.

Morales, M., Mignot, E., Paquier, A., Sigaud, D., & Proust, S. (2021). Impact of the porosity of an urban block on the flood risk assessment: A laboratory experiment. *Journal of hydrology*, *602*, 126715.

Moran, P. A. (1950). Notes on continuous stochastic phenomena. *Biometrika*, *37*(1/2), 17-23.

Morishita, F., Garfin, A. M. C. G., Lew, W., Oh, K. H., Yadav, R.-P., Reston, J. C., Infante, L. L., Acala, M. R. C., Palanca, D. L., & Kim, H. J. (2017). Bringing state-of-the-art diagnostics to vulnerable populations: The use of a mobile screening unit in active case finding for tuberculosis in Palawan, the Philippines. *PLoS One*, *12*(2), e0171310.

MS, M., Katpatal, Y. B., & Londhe, D. S. (2022). Measurement of city road network resilience in hazardous flood events. *International Journal of Disaster Resilience in the Built Environment*.

Mugume, S. N., & Butler, D. (2017). Evaluation of functional resilience in urban drainage and flood management systems using a global analysis approach. *Urban Water Journal*, *14*(7), 727-736.

Mukherjee, F., & Singh, D. (2020). Detecting flood prone areas in Harris County: a GIS based analysis. *GeoJournal*, *85*(3), 647-663.

Müller, A., Reiter, J., & Weiland, U. (2011). Assessment of urban vulnerability towards floods using an indicator-based approach–a case study for Santiago de Chile. *Natural Hazards and Earth System Sciences*, *11*(8), 2107-2123.

Murdock, H. J., De Bruijn, K. M., & Gersonius, B. (2018). Assessment of critical infrastructure resilience to flooding using a response curve approach. *Sustainability*, *10*(10), 3470.

Myers, B. R., & Pezzaniti, D. (2019). Flood and peak flow management using WSUD systems. In *Approaches to water sensitive urban design* (pp. 119-138). Elsevier.

Namitha, M., & Ravikumar, V. (2018). Analysis of extreme rainfall events and calculation of return levels using generalised extreme value distribution. *Int. J. Pure Appl. Biosci*, *6*, 1309-1316.

Nasiri, H., Mohd Yusof, M. J., & Mohammad Ali, T. A. (2016). An overview to flood vulnerability assessment methods. *Sustainable Water Resources Management*, *2*, 331-336.

Nasiri, H., Yusof, M., Ali, T., & Hussein, M. (2019). District flood vulnerability index: urban decision-making tool. *International Journal of Environmental Science and Technology*, *16*, 2249-2258.

NatCatSERVICE. (2020). *NatCatSERVICE analysis tool*. https://natcatservice.munichre.com/.

NationalAssociationofCityTransportationOfficials. (2017). *Urban Street Stormwater Guide*. Island Press.

NDRMC. (2020). *Flood Alert # 2*. Retrieved from https://www.humanitarianresponse.info/sites/www.humanitarianresponse.info/files/documents/files/ethiopia_national_flood_alert_2_-_june_2020_-_copy.pdf

Negese, A., Worku, D., Shitaye, A., & Getnet, H. (2022). Potential flood-prone area identification and mapping using GIS-based multi-criteria decision-making and analytical hierarchy process in Dega Damot district, northwestern Ethiopia. *Applied Water Science*, *12*(12), 255.

Newman, G., Malecha, M., Yu, S., Qiao, Z., Horney, J. A., Lee, J., Kim, Y. J., Lee, R. J., & Berke, P. (2020). Integrating a resilience scorecard and landscape performance tools into a Geodesign process. *Landscape research*, *45*(1), 63-80.

Niekerk, D. (2015). Disaster risk governance in Africa: A retrospective assessment of progress against the Hyogo Framework for Action (2000-2012). *Disaster Prevention and Management*.

Nkwunonwo, U., Whitworth, M., & Baily, B. (2020). A review of the current status of flood modelling for urban flood risk management in the developing countries. *Scientific African*, *7*, e00269.

NMA. (2022). *National Meteorological Agency of Ethiopia*.

Nott, J. (2006). *Extreme events: a physical reconstruction and risk assessment*. Cambridge University Press.

Nsangou, D., Kpoumié, A., Mfonka, Z., Ngouh, A. N., Fossi, D. H., Jourdan, C., Mbele, H. Z., Mouncherou, O. F., Vandervaere, J.-P., & Ngoupayou, J. R. N. (2022). Urban flood susceptibility modelling using AHP and GIS approach: case of the Mfoundi watershed at Yaoundé in the South-Cameroon plateau. *Scientific African*, *15*, e01043.

O'Donnell, E., Thorne, C., Ahilan, S., Arthur, S., Birkinshaw, S., Butler, D., Dawson, D., Everett, G., Fenner, R., & Glenis, V. (2020). The blue-green path to urban flood resilience. *Blue-Green Systems*, *2*(1), 28-45.

OECD. (2016). *Financial Management of Flood Risk*. https://www.oecd.org/finance/financial-management-of-flood-risk.htm.

Ogato, G. S., Bantider, A., Abebe, K., & Geneletti, D. (2020). Geographic information system (GIS)-Based multicriteria analysis of flooding hazard and risk in Ambo

Town and its watershed, West shoa zone, oromia regional State, Ethiopia. *Journal of Hydrology: Regional Studies*, *27*, 100659.

Ogie, R. I., Adam, C., & Perez, P. (2020). A review of structural approach to flood management in coastal megacities of developing nations: Current research and future directions. *Journal of Environmental Planning and Management*, *63*(2), 127-147.

Okaka, F. O., & Odhiambo, B. (2018). Relationship between flooding and out break of infectious diseasesin Kenya: A review of the literature. *Journal of environmental and public health*, *2018*.

Olesen, L., Löwe, R., & Arnbjerg-Nielsen, K. (2017). Flood damage assessment–Literature review and recommended procedure.

Oubennaceur, K., Chokmani, K., Gauthier, Y., Ratte-Fortin, C., Homayouni, S., & Toussaint, J.-P. (2021). Flood risk assessment under climate change: The petite nation river watershed. *Climate, 9*(8), 125.

Ouma, Y. O., & Tateishi, R. (2014). Urban flood vulnerability and risk mapping using integrated multi-parametric AHP and GIS: methodological overview and case study assessment. *Water*, *6*(6), 1515-1545.

Ozkan, S. P., & Tarhan, C. (2016). Detection of flood hazard in urban areas using GIS: Izmir case. *Procedia Technology*, *22*, 373-381.

Pallathadka, A., Sauer, J., Chang, H., & Grimm, N. B. (2022). Urban flood risk and green infrastructure: Who is exposed to risk and who benefits from investment? A case study of three US Cities. *Landscape and Urban Planning*, *223*, 104417.

Peden, A. E., Mayhew, A., Baker, S. D., Mayedwa, M., & Saunders, C. J. (2023). Exploring flood response challenges, training needs, and the impact of online flood training for lifeguards and water safety professionals in South Africa. *International Journal of Environmental Research and Public Health*, *20*(16), 6573.

Perry, G., Gebresenbet, F., DaPra, M., Branco, P., Whibesilassie, W., Jelacic, M., & Eyob, A. E. (2022). Why urban ecology matters in Ethiopia. *Frontiers in Ecology and Evolution, 10*, 843698.

Peters, L. E., Clark-Ginsberg, A., McCaul, B., Cáceres, G., Nuñez, A. L., Balagna, J., López, A., Patel, S. S., Patel, R. B., & Van Den Hoek, J. (2022). Informality, violence, and disaster risks: Coproducing inclusive early warning and response systems in urban informal settlements in Honduras. *Frontiers in Climate*, *4*, 937244.

Pouya, Nouri, Mansouri, & Lashaki. (2017). An indexing approach to assess flood vulnerability in the western coastal cities of Mazandaran, Iran. *International Journal of Disaster Risk Reduction*, *22,* 304-316.

Pouya, A., Nouri, J., Mansouri, N., & Kia-Lashaki, A. (2017). An indexing approach to assess flood vulnerability in the western coastal cities of Mazandaran, Iran. *International Journal of Disaster Risk Reduction*, *22*, 304-316.

Prashar, N., Lakra, H. S., Kaur, H., & shaw, R. (2023). Urban flood resilience: mapping knowledge, trends and structure through bibliometric analysis. *Environment, Development and Sustainability*, 1-31.

Pregnolato, M., Ford, A., Wilkinson, S. M., & Dawson, R. J. (2017). The impact of flooding on road transport: A depth-disruption function. *Transportation Research Part D: Transport and Environment*, *55*, 67-81.

Qiang, Y. (2019). Flood exposure of critical infrastructures in the United States. *International Journal of Disaster Risk Reduction*, *39*, 101240.

Qin, Y. (2020). Urban Flooding Mitigation Techniques: A Systematic Review and Future Studies. *Water*, *12*(12), 3579. https://www.mdpi.com/2073-4441/12/12/3579

Quagliolo, C., Comino, E., & Pezzoli, A. (2021). Experimental flash floods assessment through urban flood risk mitigation (UFRM) model: The case study of Ligurian coastal cities. *Frontiers in Water*, *3*, 663378.

Quan, Q., Gao, S., Shang, Y., & Wang, B. (2021). Assessment of the sustainability of Gymnocypris eckloni habitat under river damming in the source region of the Yellow River. *Science of the Total Environment*, *778*, 146312.

Rafiq, F., Ahmed, S., Ahmad, S., & Khan, A. A. (2016). Urban floods in India. *International Journal of Scientific & Engineering Research*, *7*(1), 721-734.

Ragulina, G., & Reitan, T. (2017). Generalized extreme value shape parameter and its nature for extreme precipitation using long time series and the Bayesian approach. *Hydrological Sciences Journal*, *62*(6), 863-879.

Rahman, M., Ningsheng, C., Islam, M. M., Dewan, A., Iqbal, J., Washakh, R. M. A., & Shufeng, T. (2019). Flood susceptibility assessment in Bangladesh using machine learning and multi-criteria decision analysis. *Earth Systems and Environment*, *3*, 585-601.

Rahman, M., Ningsheng, C., Mahmud, G. I., Islam, M. M., Pourghasemi, H. R., Ahmad, H., Habumugisha, J. M., Washakh, R. M. A., Alam, M., & Liu, E. (2021). Flooding and its relationship with land cover change, population growth, and road density. *Geoscience Frontiers*, *12*(6), 101224.

Rahmati, O., Zeinivand, H., & Besharat, M. (2016). Flood hazard zoning in Yasooj region, Iran, using GIS and multi-criteria decision analysis. *Geomatics, Natural Hazards and Risk*, *7*(3), 1000-1017.

Ramadhan, C., Dina, R., & Nurjani, E. (2023). Spatial and temporal based deforestation proclivity analysis on flood events with applying watershed scale (case study: Lasolo watershed in Southeast Sulawesi, Central Sulawesi, and South Sulawesi, Indonesia). *International Journal of Disaster Risk Reduction*, *93*, 103745.

Ramesh, V., & Iqbal, S. S. (2022). Urban flood susceptibility zonation mapping using evidential belief function, frequency ratio and fuzzy gamma operator models in GIS: a case study of Greater Mumbai, Maharashtra, India. *Geocarto International*, *37*(2), 581-606.

Ramiaramanana, F. N., & Teller, J. (2021). Urbanization and Floods in Sub-Saharan Africa: Spatiotemporal Study and Analysis of Vulnerability Factors—Case of Antananarivo Agglomeration (Madagascar). *Water*, *13*(2), 149. https://www.mdpi.com/2073-4441/13/2/149

Re, M. (2012). Topics Geo: Natural catastrophes 2011. *Analyses, Assessments, positions, Munich, Germany*.

REAP, R.-i. E. A. P. (2020). *Countries Case Study Ethiopia*.

Rebally, A., Valeo, C., He, J., & Saidi, S. (2021). Flood impact assessments on transportation networks: a review of methods and associated temporal and spatial scales. *Frontiers in Sustainable Cities*, *3*, 732181.

Regassa, B., Kassaw, M., & Bagyaraj, M. (2020). Analysis of urban expansion and modeling of LULC changes using geospatial techniques: the case of Adama City. *Remote Sensing of Land*, *4*(1-2), 40-58.

Rehman, S., Hasan, M. S. U., Rai, A. K., Avtar, R., & Sajjad, H. (2021). Assessing flood-induced ecological vulnerability and risk using GIS-based in situ measurements in Bhagirathi sub-basin, India. *Arabian Journal of Geosciences*, *14*, 1-17.

Rentschler, & Salhab. (2020). *People in harm's way: Flood exposure and poverty in 189 countries*. The World Bank.

Rentschler , Salhab , & Arga (2022). Flood exposure and poverty in 188 countries. *Nature communications*, *13*(1), 3527.

Rentschler, Salhab, & Jafino. (2022). Flood exposure and poverty in 188 countries. *Nature communications*, *13*(1), 3527.

Rentschler, J., Avner, P., Marconcini, M., Su, R., Strano, E., Vousdoukas, M., & Hallegatte, S. (2023). Global evidence of rapid urban growth in flood zones since 1985. *Nature*, *622*(7981), 87-92.

Rezende, O. M., Miranda, F. M., Haddad, A. N., & Miguez, M. G. (2019). A framework to evaluate urban flood resilience of design alternatives for flood defence considering future adverse scenarios. *Water*, *11*(7), 1485.

Rimba, A. B., Setiawati, M. D., Sambah, A. B., & Miura, F. (2017). Physical flood vulnerability mapping applying geospatial techniques in Okazaki City, Aichi Prefecture, Japan. *Urban Science*, *1*(1), 7.

Rincón, D., Khan, U. T., & Armenakis, C. (2018). Flood risk mapping using GIS and multi-criteria analysis: A greater Toronto area case study. *Geosciences*, *8*(8), 275.

Robinson, K.-L., Bogena, H. R., Wang, Q., Cammeraat, E., & Bol, R. (2022). Effects of deforestation on dissolved organic carbon and nitrate in catchment stream water revealed by wavelet analysis. *Frontiers in Water*, *4*, 1003693.

Rodríguez, S., Smith, K., Aivazoglou, M., Pina, R., & Mijic, A. (2017). Urban pluvial flooding and climate change: London (UK), Rafina (Greece) and Coimbra (Portugal). *Grantham Institute: Climate Change and the Environment*.

Rogger, M., Agnoletti, M., Alaoui, A., Bathurst, J., Bodner, G., Borga, M., Chaplot, V., Gallart, F., Glatzel, G., & Hall, J. (2017). Land use change impacts on floods at the catchment scale: Challenges and opportunities for future research. *Water resources research*, *53*(7), 5209-5219.

Ronchi, S., Salata, S., & Arcidiacono, A. (2020). Which urban design parameters provide climate-proof cities? An application of the Urban Cooling InVEST Model in the city of Milan comparing historical planning morphologies. *Sustainable Cities and Society*, *63*, 102459.

Rosa, D., & Pappalardo, V. (2020). Planning for spatial equity-A performance based approach for sustainable urban drainage systems. *Sustainable Cities and Society*, *53*, 101885.

Roy, S., Bose, A., & Chowdhury, I. R. (2021). Flood risk assessment using geospatial data and multi-criteria decision approach: a study from historically active flood-prone region of Himalayan foothill, India. *Arabian Journal of Geosciences*, *14*(11), 999.

Rözer, V., Mehryar, S., & Surminski, S. (2022). From managing risk to increasing resilience: a review on the development of urban flood resilience, its assessment and the implications for decision making. *Environmental research letters*.

Rufat, S., Tate, E., Burton, C. G., & Maroof, A. S. (2015). Social vulnerability to floods: Review of case studies and implications for measurement. *International Journal of Disaster Risk Reduction*, *14*, 470-486.

Ruirui, S., Shaohong, S., Yimingjiang, R., & Songmin, L. (2022). Measurement of urban flood resilience using a quantitative model based on the correlation of vulnerability and resilience. *International Journal of Disaster Risk Reduction*, *82*. https://doi.org/https://doi.org/10.1016/j.ijdrr.2022.103344

Rus, K., Kilar, V., & Koren, D. (2018). Resilience assessment of complex urban systems to natural disasters: A new literature review. *International Journal of Disaster Risk Reduction*, *31*, 311-330.

Saaty, R. W. (1987). The analytic hierarchy process—what it is and how it is used. *Mathematical modelling*, *9*(3-5), 161-176.

Sadiq, R., Imran, M., & Ofli, F. (2023). Remote Sensing for Flood Mapping and Monitoring. *International Handbook of Disaster Research*, 1-19.

Saghir, J., & Santoro, J. (2018). *Urbanization in Sub-Saharan Africa*. https://www.csis.org/analysis/urbanization-sub-saharan-africa

Salami, Giggins, & Meding. (2017a). Urban settlements' vulnerability to flood risks in African cities: A conceptual framework. *Jàmbá: Journal of Disaster Risk Studies*, *9*(1), 1-9.

Salami, Giggins, & Meding. (2017b). Vulnerability of human settlements to flood risk in the core area of Ibadan metropolis, Nigeria. *Jàmbá: Journal of Disaster Risk Studies*, *9*(1), 1-14.

Salami , Meding , & Giggins (2017). Urban settlements' vulnerability to flood risks in African cities: A conceptual framework. *Jamba*, *9*(1), 370. https://doi.org/10.4102/jamba.v9i1.370

Samuel, W. D., María, M. C., Catherine, S., Louis, C., & Jürgen, S. (2019). Vulnerability of informal settlements in the context of rapid urbanization and climate change. *Environment and urbanization*, *31*(1), 157-176.

Sansalone, J., Kuang, X., Ying, G., & Ranieri, V. (2012). Filtration and clogging of permeable pavement loaded by urban drainage. *Water research*, *46*(20), 6763-6774.

Santos, P. P., Pereira, S., Rocha, J., Reis, E., Santos, M., Oliveira, S. C., Garcia, R. A., Melo, R., & Zêzere, J. L. (2022). The role of susceptibility, exposure and vulnerability as drivers of flood disaster risk at the parish level. *Environmental Earth Sciences*, *81*(19), 465.

Sarkissian, R., Sayah, M., Abdallah, C., Zaninetti, M., & Nedjai, R. (2022). Land Use Planning to Reduce Flood Risk: Opportunities, Challenges and Uncertainties in Developing Countries. *Sensors*, *22*(18), 6957. https://www.mdpi.com/1424-8220/22/18/6957

Satoh, S. (1997). The morphological transformation of Japanese castle-town cities. *Urban morphology*, *1*(1), 11-18.

Satterthwaite, D. (2017). The impact of urban development on risk in sub-Saharan Africa's cities with a focus on small and intermediate urban centres. *International Journal of Disaster Risk Reduction*, *26*, 16-23.

Schelfaut, K., Pannemans, B., Van der Craats, I., Krywkow, J., Mysiak, J., & Cools, J. (2011). Bringing flood resilience into practice: the FREEMAN project. *Environmental Science & Policy*, *14*(7), 825-833.

Schotten, R., & Bachmann, D. (2023). Integrating Critical Infrastructure Networks into Flood Risk Management. *Sustainability*, *15*(6), 5475.

Seejata, K., Yodying, A., Wongthadam, T., Mahavik, N., & Tantanee, S. (2018). Assessment of flood hazard areas using analytical hierarchy process over the Lower Yom Basin, Sukhothai Province. *Procedia Engineering*, *212*, 340-347.

Semaw, F., Zeleke, G., & Balew, A. (2022). Evaluating flood risk management practices and vulnerability mapping in Alawuha watershed (North Wollo Zone, Ethiopia) using GIS and remote sensing. *Applied Geomatics*, *14*(2), 347-367.

Serre, D., Barroca, B., Balsells, M., & Becue, V. (2018). Contributing to urban resilience to floods with neighbourhood design: The case of Am Sandtorkai/Dalmannkai in Hamburg. *Journal of Flood Risk Management*, *11*, S69-S83.

Seydi, S. T., Kanani-Sadat, Y., Hasanlou, M., Sahraei, R., Chanussot, J., & Amani, M. (2023). Comparison of Machine Learning Algorithms for Flood Susceptibility Mapping. *Remote Sensing*, *15*(1), 192. https://www.mdpi.com/2072-4292/15/1/192

Sharifi, A. (2023). The Resilience of Urban Social-Ecological-Technological Systems (SETS): A Review. *Sustainable Cities and Society*, 104910.

Sharifi, A., Roosta, M., & Javadpoor, M. (2021). Urban Form Resilience: A Comparative Analysis of Traditional, Semi-Planned, and Planned Neighborhoods in Shiraz, Iran. *Urban Science*, *5*(1), 18. https://www.mdpi.com/2413-8851/5/1/18

Sharp, R., Douglass, J., & Wolny, S. (2020). *InVEST User Guide —*

InVEST documentation. In: InVEST 3.10.2.post21+ug.gb784d7e.

d20220301 User's Guide. Nat. Cap. Proj. Stanford Univ. Univ. Minnesota, Nat. Conserv. World Wildl. Fund Retrieved Accessed 3 August 2023 from https://invest-userguide.readthedocs.io/en/latest/index.html

Sheng, J., & Wilson, J. P. (2009). Watershed urbanization and changing flood behavior across the Los Angeles metropolitan region. *Natural Hazards*, *48*, 41-57.

Shukla, N., Das, A., & Mazumder, T. (2023). Assessment of urban form resilience: A review of literature in the context of the Global South.

Shuster, W. D., Bonta, J., Thurston, H., Warnemuende, E., & Smith, D. (2005). Impacts of impervious surface on watershed hydrology: A review. *Urban Water Journal*, *2*(4), 263-275.

Sima, Y., & Zhang, D. (2009). Comparative precedents on the study of urban morphology. Proceedings of the 7th International Space Syntax Symposium, Stockholm: KTH,

Simane, B., Beyene, H., Deressa, W., Kumie, A., Berhane, K., & Samet, J. (2017). Review of Climate Change and Health in Ethiopia: Status and Gap Analysis. *Ethiop J Health Dev.* , *30*(1), 28–41.

Singh, A. P., Arya, A. K., & Singh, D. S. (2020). Morphometric analysis of Ghaghara River Basin, India, using SRTM data and GIS. *Journal of the Geological Society of India*, *95*, 169-178.

Smith, A., Bates, P. D., Wing, O., Sampson, C., Quinn, N., & Neal, J. (2019). New estimates of flood exposure in developing countries using high-resolution population data. *Nature communications*, *10*(1), 1814.

Smith, A., Lott, N., & Ross, T. (2023). *U.S. Billion-Dollar Weather & Climate Disasters 1980-2023*. https://www.ncei.noaa.gov/access/billions/

Soomro, A. G., Babar, M. M., Memon, A. H., Zaidi, A. Z., Ashraf, A., & Lund, J. (2019). Sensitivity of direct runoff to curve number using the SCS-CN method. *Civ. Eng. J*, *5*, 2738-2746.

Srivastava, S., & Roy, T. (2023). Integrated flood risk assessment of properties and associated population at county scale for Nebraska, USA. *Scientific reports*, *13*(1), 19702.

Stangl, P. (2018). Prospects for urban morphology in resilience assessment. *Resilience-oriented urban planning: Theoretical and empirical insights*, 181-193.

Subbarayan, S., & Sivaranjani, S. (2020). Modelling of flood susceptibility based on GIS and analytical hierarchy process—A Case study of Adayar River Basin, Tamilnadu, India. An interdisciplinary approach for disaster resilience and sustainability,

Sun, Y., Wendi, D., Kim, D. E., & Liong, S.-Y. (2019). Deriving intensity–duration–frequency (IDF) curves using downscaled in situ rainfall assimilated with remote sensing data. *Geoscience Letters*, *6*, 1-12.

Swain, K. C., Singha, C., & Nayak, L. (2020). Flood susceptibility mapping through the GIS-AHP technique using the cloud. *ISPRS International Journal of Geo-Information*, *9*(12), 720.

Tachaudomdach, S., Upayokin, A., Kronprasert, N., & Arunotayanun, K. (2021). Quantifying road-network robustness toward flood-resilient transportation systems. *Sustainability*, *13*(6), 3172.

Takin, M., Cilliers, E., & Ghosh, S. (2023). Advancing flood resilience: the nexus between flood risk management, green infrastructure, and resilience. *Frontiers in Sustainable Cities*.

Talbot, C. J., Bennett, E. M., Cassell, K., Hanes, D. M., Minor, E. C., Paerl, H., Raymond, P. A., Vargas, R., Vidon, P. G., & Wollheim, W. (2018). The impact of flooding on aquatic ecosystem services. *Biogeochemistry*, *141*, 439-461.

Tanavud, C., Yongchalermchai, C., Bennui, A., & Densreeserekul, O. (2004). Assessment of flood risk in Hat Yai municipality, Southern Thailand, using GIS. *Journal of Natural Disaster Science*, *26*(1), 1-14.

Tang, X., Shu, Y., Lian, Y., Zhao, Y., & Fu, Y. (2018). A spatial assessment of urban waterlogging risk based on a Weighted Naïve Bayes classifier. *Science of the Total Environment*, *630*, 264-274. https://doi.org/https://doi.org/10.1016/j.scitotenv.2018.02.172

Tanoue, M., Hirabayashi, Y., & Ikeuchi, H. (2016). Global-scale river flood vulnerability in the last 50 years. *Scientific reports*, *6*(1), 36021.

Tariq, M. A. U. R., Farooq, R., & van de Giesen, N. (2020). A Critical Review of Flood Risk Management and the Selection of Suitable Measures. *Applied Sciences*, *10*(23), 8752. https://www.mdpi.com/2076-3417/10/23/8752

Tasseff, B., Bent, R., & Van Hentenryck, P. (2019). Optimization of structural flood mitigation strategies. *Water resources research*, *55*(2), 1490-1509.

Tate, E., Rahman, M. A., Emrich, C. T., & Sampson, C. C. (2021). Flood exposure and social vulnerability in the United States. *Natural Hazards*, *106*(1), 435-457.

Tehrany, M. S., Pradhan, B., & Jebur, M. N. (2014). Flood susceptibility mapping using a novel ensemble weights-of-evidence and support vector machine models in GIS. *Journal of hydrology*, *512*, 332-343.

Tehrany;, S., Shabani;, M., Jebur;, F. N., Hong;, M., Chen;, H., Xie;, W., & Xiaoshen. (2017). GIS-based spatial prediction of flood prone areas using standalone frequency ratio, logistic regression, weight of evidence and their ensemble techniques. *Geomatics, Natural Hazards and Risk*, *8*(2), 1538-1561.

Terrado, M., Sabater, S., Chaplin-Kramer, B., Mandle, L., Ziv, G., & Acuña, V. (2016). Model development for the assessment of terrestrial and aquatic habitat quality in conservation planning. *Science of the Total Environment*, *540*, 63-70.

Tesfaw, T. A. (2022). Internal displacement in ethiopia: a scoping review of its causes, trends and consequences. *Journal of Internal Displacement*, *12*(1), 2-31.

TheGlobalRisksReport. (2018). *The risks of rapid urbanization in developing countries*. https://www.zurich.com/en/knowledge/topics/global-risks/the-risks-of-rapid-urbanization-in-developing-countries

Thomas , T., Christophe , V., & Colin , G. (2023). Natural flood management: Opportunities to implement nature-based solutions on privately owned land. *Wiley Interdisciplinary Reviews: Water*. https://doi.org/10.1002/wat2.1637

Tiepolo, M., Braccio, S., Fiorillo, E., Galligari, A., Katiellou, G. L., Massazza, G., Sitta, A. A., Tankari, A. M., & Tarchiani, V. (2021). Method for pluvial flood risk assessment in rural settlements characterised by scant information availability. *MethodsX*, *8*, 101532. https://doi.org/10.1016/j.mex.2021.101532

Tietjen, B., Jacobsen, K., & Hollander, J. (2023). Climate Change and Urban Migration in Sub-Saharan African Cities: Impacts and Governance Challenges. *Journal of Climate Resilience and Justice*, *1*, 20-32.

Tingsanchali, T. (2012). Urban flood disaster management. *Procedia Engineering*, *32*, 25-37.

Tola, S. Y., & Shetty, A. (2023). Flood hazard map of the Becho floodplain, Ethiopia, using nonstationary frequency model. *Acta Geophysica*, 1-17.

Toosi, A. S., Calbimonte, G. H., Nouri, H., & Alaghmand, S. (2019). River basin-scale flood hazard assessment using a modified multi-criteria decision analysis approach: A case study. *Journal of hydrology*, *574*, 660-671.

Truu, M., Annus, I., Roosimägi, J., Kändler, N., Vassiljev, A., & Kaur, K. (2021). Integrated decision support system for pluvial flood-resilient spatial planning in urban areas. *Water*, *13*(23), 3340.

Tu, A., Zeng, J., Liu, Z., Zheng, H., & Xie, S. (2023). Effect of minimum inter-event time for rainfall event separation on rainfall properties and rainfall erosivity in a humid area of southern China. *Geoderma*, *431*, 116332.

Turner, A. (2007). UCL Depthmap 7: From isovist analysis to generic spatial network analysis. *New Developments in Space Syntax Software, Istanbul*.

Tuyls, D. M., Thorndahl, S., & Rasmussen, M. R. (2018). Return period assessment of urban pluvial floods through modelling of rainfall–flood response. *Journal of Hydroinformatics*, *20*(4), 829-845.

Twohig, C., Casali, Y., & Aydin, N. Y. (2022). Can green roofs help with stormwater floods? A geospatial planning approach. *Urban Forestry & Urban Greening*, *76*, 127724.

Ullah, K., & Zhang, J. (2020). GIS-based flood hazard mapping using relative frequency ratio method: A case study of Panjkora River Basin, eastern Hindu Kush, Pakistan. e0229153. . *PLoS One*, *15(3)*. https://doi.org/https://doi.org/10.1371/journal.pone.0229153

UNESCO. (2012). *United Nations world water development report 4: Managing water under uncertainty and risk.* https://unesdoc.unesco.org/ark:/48223/pf0000215644.page=812.

Van, C. T., Tuan, N. C., Son, N. T., Tri, D. Q., & Tran, D. D. (2022). Flood vulnerability assessment and mapping: A case of Ben Hai-Thach Han River basin in Vietnam. *International Journal of Disaster Risk Reduction*, *75*, 102969.

Varoudis, T. (2012). DepthmapX multi-platform spatial network analysis software. *Version 0.30 OpenSource, http://varoudis. github. io/depthmapX*.

Vojinovic, Z., Hammond, M., Golub, D., Hirunsalee, S., Weesakul, S., Meesuk, V., Medina, N., Sanchez, A., Kumara, S., & Abbott, M. (2016). Holistic approach to flood risk assessment in areas with cultural heritage: a practical application in Ayutthaya, Thailand. *Natural Hazards*, *81*, 589-616.

Vuik, V., Jonkman, S. N., Borsje, B. W., & Suzuki, T. (2016). Nature-based flood protection: The efficiency of vegetated foreshores for reducing wave loads on coastal dikes. *Coastal engineering*, *116*, 42-56.

Waghwala, R. K., & Agnihotri, P. (2019). Flood risk assessment and resilience strategies for flood risk management: A case study of Surat City. *International Journal of Disaster Risk Reduction*, *40*, 101155.

Wang , Cui , Li , Huang , Manandhar , Nitivattananon , Fang , & Huang (2022). A review of the flood management: from flood control to flood resilience. *Heliyon*, *8*(11).

Wang, Zhu, & Yu. (2022a). Assessment of Urban Flood Vulnerability Using the Integrated Framework and Process Analysis: A Case from Nanjing, China. *International Journal of Environmental Research and Public Health*, *19*(24), 16595.

Wang, Zhu, & Yu. (2022b). Assessment of Urban Flood Vulnerability Using the Integrated Framework and Process Analysis: A Case from Nanjing, China. *Int J Environ Res Public Health*, *19*(24). https://doi.org/10.3390/ijerph192416595

Wang, Y., Li, Z., Tang, Z., & Zeng, G. (2011). A GIS-based spatial multi-criteria approach for flood risk assessment in the Dongting Lake Region, Hunan, Central China. *Water resources management*, *25*, 3465-3484.

Wang, Z., Lai, C., Chen, X., Yang, B., Zhao, S., & Bai, X. (2015). Flood hazard risk assessment model based on random forest. *Journal of hydrology*, *527*, 1130-1141.

Watson, G., & Ahn, J. E. (2022). A systematic review: to increase transportation infrastructure resilience to flooding events. *Applied Sciences*, *12*(23), 12331.

Weday, M. A., Tabor, K. W., & Gemeda, D. O. (2023). Flood hazards and risk mapping using geospatial technologies in Jimma City, southwestern Ethiopia. *Heliyon*, *9*(4).

Wilby, R. L., & Keenan, R. (2012). Adapting to flood risk under climate change. *Progress in physical geography*, *36*(3), 348-378.

Williams, D. S., Manez Costa, M., Sutherland, C., Celliers, L., & Scheffran, J. (2019). Vulnerability of informal settlements in the context of rapid urbanization and climate change. *Environment and urbanization*, *31*(1), 157-176.

Wing, O. E., Lehman, W., Bates, P. D., Sampson, C. C., Quinn, N., Smith, A. M., Neal, J. C., Porter, J. R., & Kousky, C. (2022). Inequitable patterns of US flood risk in the Anthropocene. *Nature Climate Change*, *12*(2), 156-162.

Wobus, C., Gutmann, E., Jones, R., Rissing, M., Mizukami, N., Lorie, M., Mahoney, H., Wood, A. W., Mills, D., & Martinich, J. (2017). Climate change impacts on flood risk and asset damages within mapped 100-year floodplains of the contiguous United States. *Nat. Hazards Earth Syst. Sci.*, *17*(12), 2199-2211. https://doi.org/10.5194/nhess-17-2199-2017

Woldechirkos, Y. (2016). *Application of Dispersive Soils as a Sub Grade and Embankment Materials (Case Study on Adama–Awash Railway Section)* ADDIS ABABA UNIVERSITY ADDIS ABABA].

WorldBank. (2017). *Implementing Nature Based Flood Protection: Principles and Implementation Guidance* Washington, DC Retrieved from http://hdl.handle.net/10986/28837

WorldBankGroup. (2020). *CLIMATE RISK COUNTRY PROFILE: ETHIOPIA*.

WorldBankGroup. (2021). *CLIMATE CHANGE KNOWLEDGE PORTAL (CCKP)*.

WorldRiskReport. (2022). *WorldRiskReport 2022 Focus: Digitalization*.

Wu, X., Guo, J., Wu, X., & Guo, J. (2021). A new economic loss assessment system for urban severe rainfall and flooding disasters based on big data fusion. *Economic impacts and emergency management of disasters in China*, 259-287.

Xiaoxin, Z., Jin, H., Ling, L., Yueping, W., & Xinheng, Z. (2018). Research of AHP/DEA evaluation model for operation performance of municipal wastewater treatment plants. E3S web of conferences, Xie, J., Wu, C., Li, H., & Chen, G. (2017). Study on storm-water management of grassed swales and permeable pavement based on SWMM. *Water*, *9*(11), 840.

Xiuquan , W., Gary, K., Durga , P., & Adam , F. (2019). Urban Flood Prediction Under Heavy Precipitation. *Elsevier*.

Xu, Q., Zheng, X., & Zheng, M. (2019). Do urban planning policies meet sustainable urbanization goals? A scenario-based study in Beijing, China. *Science of the Total Environment*, *670*, 498-507.

Xu, W., Zhang, Y., Proverbs, D., & Zhong, Z. (2022). Enhancing the resilience of road networks to flooding. *International Journal of Building Pathology and Adaptation*.

Xu, Z., & Zhao, G. (2016). Impact of urbanization on rainfall-runoff processes: case study in the Liangshui River Basin in Beijing, China. *Proceedings of the International Association of Hydrological Sciences*, *373*, 7-12.

Yamazaki, D., Watanabe, S., & Hirabayashi, Y. (2018). Global flood risk modeling and projections of climate change impacts. *Global flood hazard: applications in modeling, mapping, and forecasting*, 185-203.

Yang, D., Liu, W., Tang, L., Chen, L., Li, X., & Xu, X. (2019). Estimation of water provision service for monsoon catchments of South China: Applicability of the InVEST model. *Landscape and Urban Planning*, *182*, 133-143.

Yang, Q., Zheng, X., Jin, L., Lei, X., Shao, B., & Chen, Y. (2021). Research progress of urban floods under climate change and urbanization: a scientometric analysis. *Buildings*, *11*(12), 628.

Yin, J., Gao, Y., Chen, R., Yu, D., Wilby, R., Wright, N., Ge, Y., Bricker, J., Gong, H., & Guan, M. (2023). Flash floods: why are more of them devastating the world's driest regions? *Nature*, *615*(7951), 212-215.

Yin, Y., Val, D. V., Zou, Q., & Yurchenko, D. (2022). Resilience of Critical Infrastructure Systems to Floods: A Coupled Probabilistic Network Flow and LISFLOOD-FP Model. *Water, 14*(5), 683.

Yonas, H., Tesfa, A., Mesenbet, Y., & Mequanent, M. (2022). Potential food- prone area identifcation and mapping using GIS MCD, DEGA DAMOT, ETHIOPIA. *Applied Water Science 12*. https://doi.org/https://doi.org/10.1007/s13201-022-01674-8

You, X. (2023). Flood-prone areas are hotspots for urban development. *Nature*.

Youssef, A. M., Pourghasemi, H. R., Mahdi, A. M., & Matar, S. S. (2023). Flood vulnerability mapping and urban sprawl suitability using FR, LR, and SVM models. *Environ Sci Pollut Res Int*, *30*(6), 16081-16105. https://doi.org/10.1007/s11356-022-23140-3

Yue, Z., Zhou, W., & Li, T. (2021). Impact of the Indian Ocean dipole on evolution of the subsequent ENSO: Relative roles of dynamic and thermodynamic processes. *Journal of Climate*, *34*(9), 3591-3607.

Yusmah, M., Bracken, J., Sahdan, Z., Norhaslina, H., Melasutra, M., Ghaffarianhoseini, A., Sumiliana, S., & Farisha, A. (2020). Understanding urban flood vulnerability and resilience: a case study of Kuantan, Pahang, Malaysia. *Natural Hazards*, *101*, 551-571.

Zeng, Y. (2022). Deforestation and Flooding in the Lower Roanoke River Basin.

Zhang, Fang, Zhang, & Yu. (2021). Assessment of direct economic losses of flood disasters based on spatial valuation of land use and quantification of vulnerabilities: a case study on the 2014 flood in Lishui city of China. *Natural Hazards and Earth System Sciences*, *21*(10), 3161-3174.

Zhang , Zhang , She , Wang , Wang , & Zeng (2021). Automatic procedure for selecting flood events and identifying flood characteristics from daily streamflow data. *Environmental Modelling & Software*, *145*, 105180.

Zhang, H., Chang, J., Zhang, L., Wang, Y., Li, Y., & Wang, X. (2018). NDVI dynamic changes and their relationship with meteorological factors and soil moisture. *Environmental Earth Sciences*, *77*, 1-11.

Zhang, H., Zhang, J., Fang, H., & Yang, F. (2022). Urban flooding response to rainstorm scenarios under different return period types. *Sustainable Cities and Society*, *87*, 104184.

Zhang, Y., Zhao, W., Chen, X., Jun, C., Hao, J., Tang, X., & Zhai, J. (2020). Assessment on the effectiveness of urban stormwater management. *Water*, *13*(1), 4.

Zhao, M., He, Z., Du, J., Chen, L., Lin, P., & Fang, S. (2019). Assessing the effects of ecological engineering on carbon storage by linking the CA-Markov and InVEST models. *Ecological Indicators*, *98*, 29-38.

Zhou, L. (2019). Correlations of Stormwater Runoff and Quality: Urban Pavement and Property Value by Land Use at the Parcel Level in a Small Sized American City. *Water*, *11*(11), 2369. https://www.mdpi.com/2073-4441/11/11/2369

Zhou;, R., Zheng;, H., Liu;, Y., Xie;, G., & Wan, W. (2022). Flood impacts on urban road connectivity in southern China. *Sci Rep*, *12*. https://doi.org/https://doi.org/10.1038/s41598-022-20882-5

Ziegler, A. D., Lim, H. S., Jachowski, N. R., & Wasson, R. J. (2012). Reduce urban flood vulnerability. *Nature*, *481*, 145-145.

ZurichFloodResilienceAlliance. (2014). *Making Communities More Flood Resilient: The Role of Cost Benefit Analysis and other Decision-Support Tools in Disaster Risk Reduction*.

ANNEX

A. Adama Surface Water Map

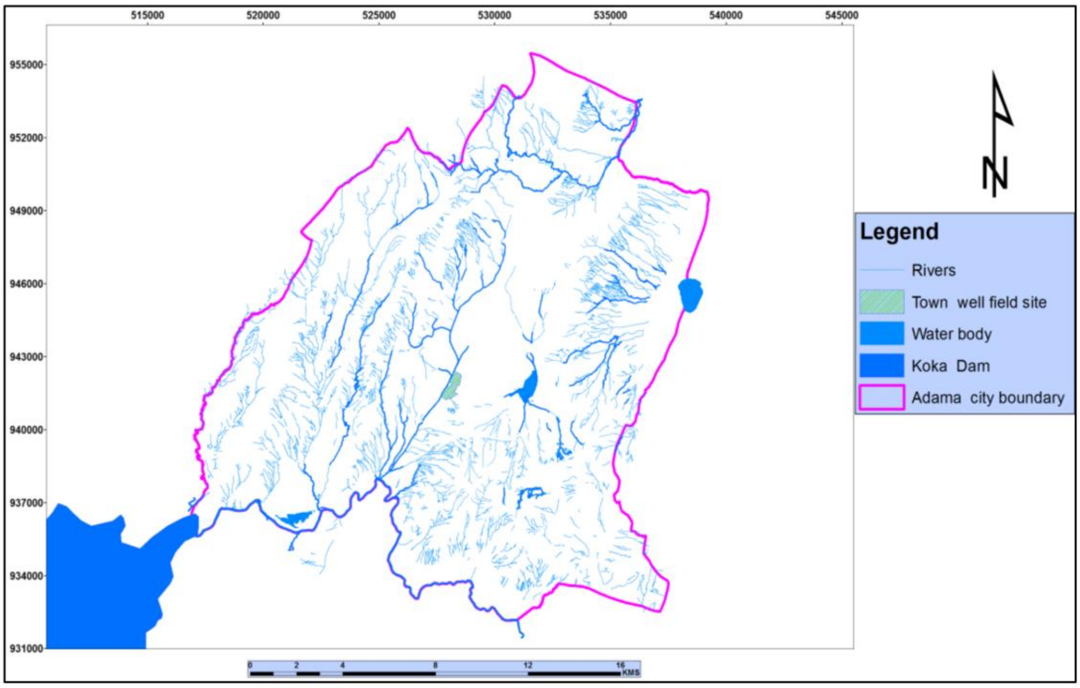

B. Adama Water Distribution Map

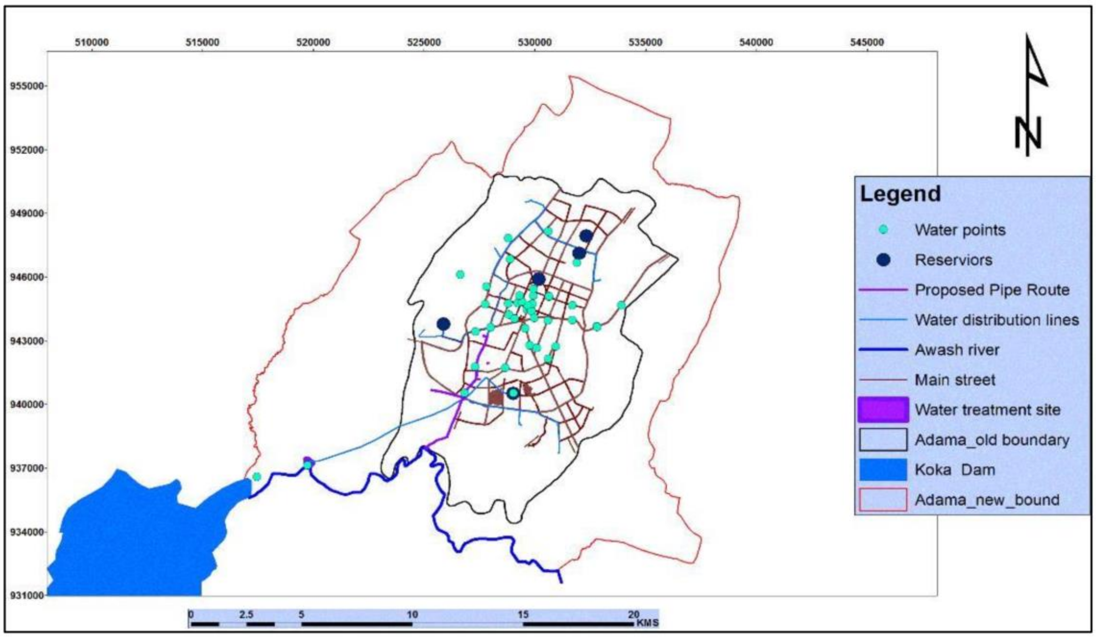

C. Adama Elevation Map

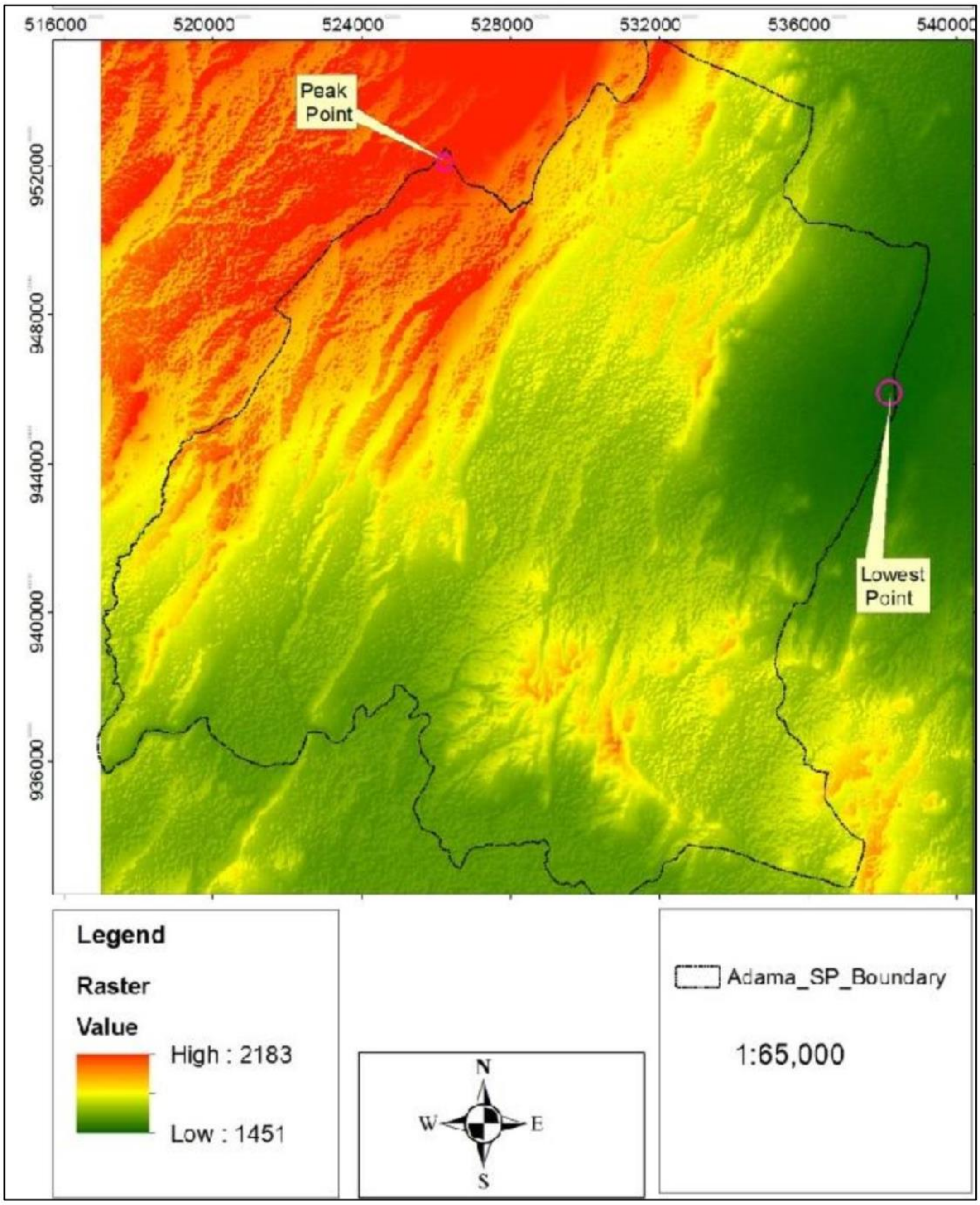

D. Adama Abbatoir Location

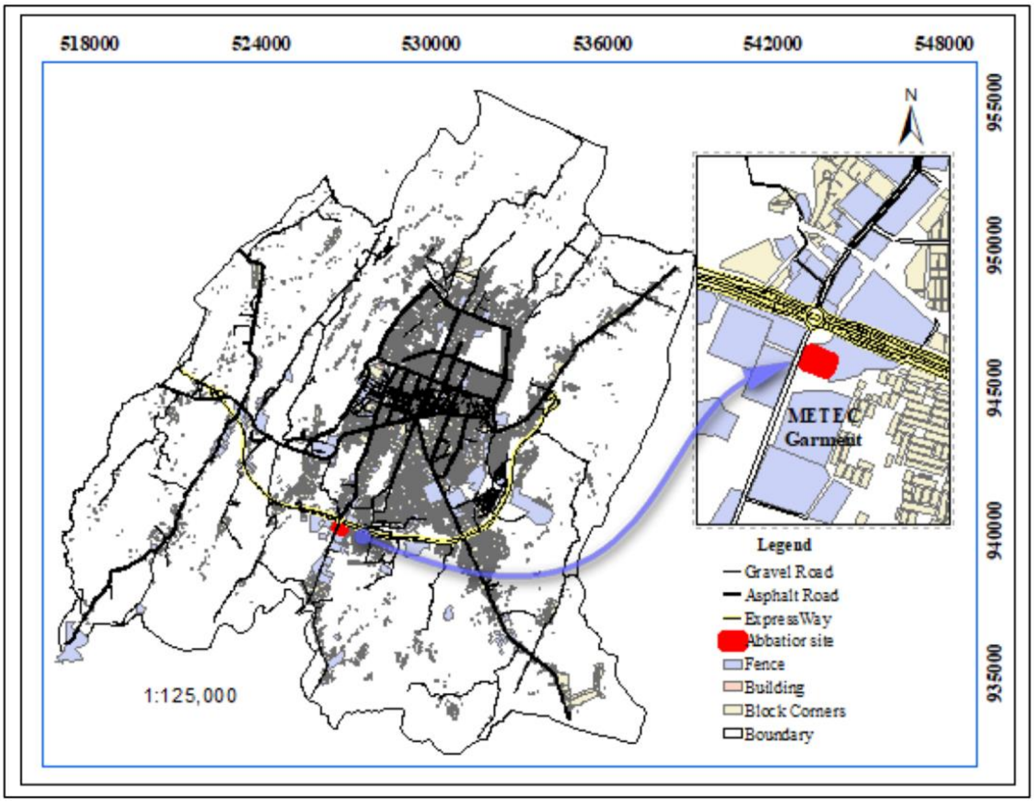

E. Adama Major Road Segments

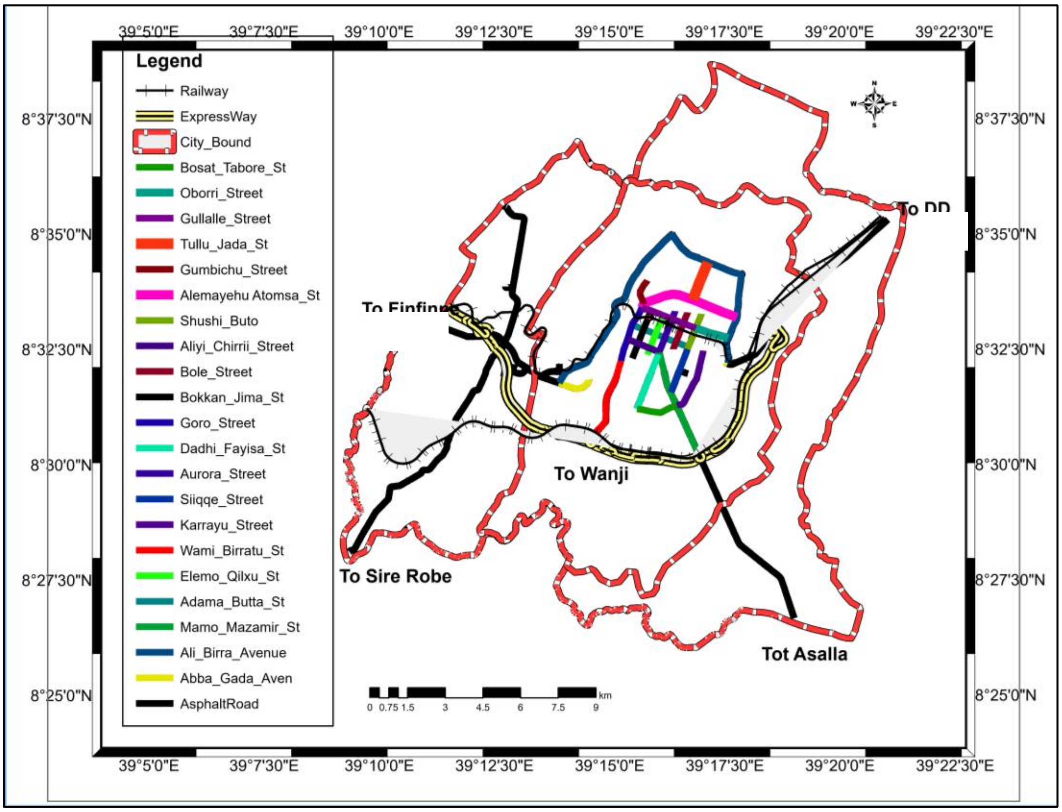

F. Published Articles